Analysis of ANSS Data for Stress Drop, Q(f), and Kappa

Utah Ground Motion Working Group

Ivan Wong
Seismic Hazards Group
URS Corporation
Oakland, CA

Jim Pechmann
Dept. of Geology and Geophysics
University of Utah
Salt Lake City, UT

Walt Silva and Bob Darragh
Pacific Engineering & Analysis
El Cerrito, CA

Tian Yu
Institute of Engineering Mechanics
China Earthquake Administration
Harbin, China

Salt Lake City, UT
14 February 2011

Introduction

- Objective: To evaluate the critical factors that control ground shaking hazard along the Wasatch Front: stress drop, kappa, and crustal attenuation.

- Some previous studies have suggested that ground motions in an extensional regime such as the Basin and Range Province may be lower than in California for the same magnitude and distance.

- The inference was that this difference may be due to the lower stress drops of extensional earthquakes compared to compressional earthquakes as first suggested by McGarr (1984).

Background

- No systematic evaluation of earthquake stress drops has been performed for earthquakes along the Wasatch Front.
- No studies have been performed to evaluate the variability in kappa in the central Wasatch Front. Kappa can have a very significant effect on high-frequency ground motions with lower values of kappa resulting in larger high-frequency ground motions.
- Only a few studies to estimate Q(f) for the Wasatch Front (Brockman and Bollinger, 1992; Jeon and Herrmann, 2004) have been performed.

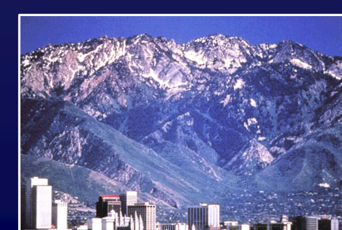

Scope of Work

- To analyze the available strong motion and broadband data from ANSS stations in the central Wasatch Front region for stress drop, kappa, and Q(f).

- The approach uses an inversion scheme developed by Walt Silva. In the inversion scheme, earthquake source, path and site parameters are obtained by using a nonlinear least-squares inversion of Fourier amplitude spectra.

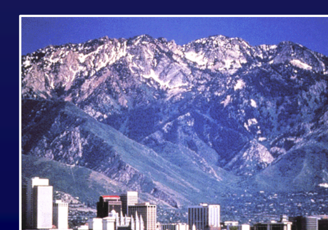

Earthquakes to be Analyzed

- Total of 17 events
- Period: May 2001 to November 2007
- Magnitude Range: **M** 3.0 to 4.2
- Number of stations recording events: 18 to 68

Scope of Work

- Steps involved in analyses are:
  1) Inversions with rock amp factors using rock recordings.
  2) Results from Step 1 used to invert soil recordings to obtain an average set of amp factors for soil sites.
  3) Rock and soil amp factors are used to invert both rock and soil recordings.
  4) Inversions were performed fixing Q_0 and R0 fixed to values in Step 3 and rock and soil amp factors to obtain station κ and stress drop.

Hard Rock V_S and V_P Profiles

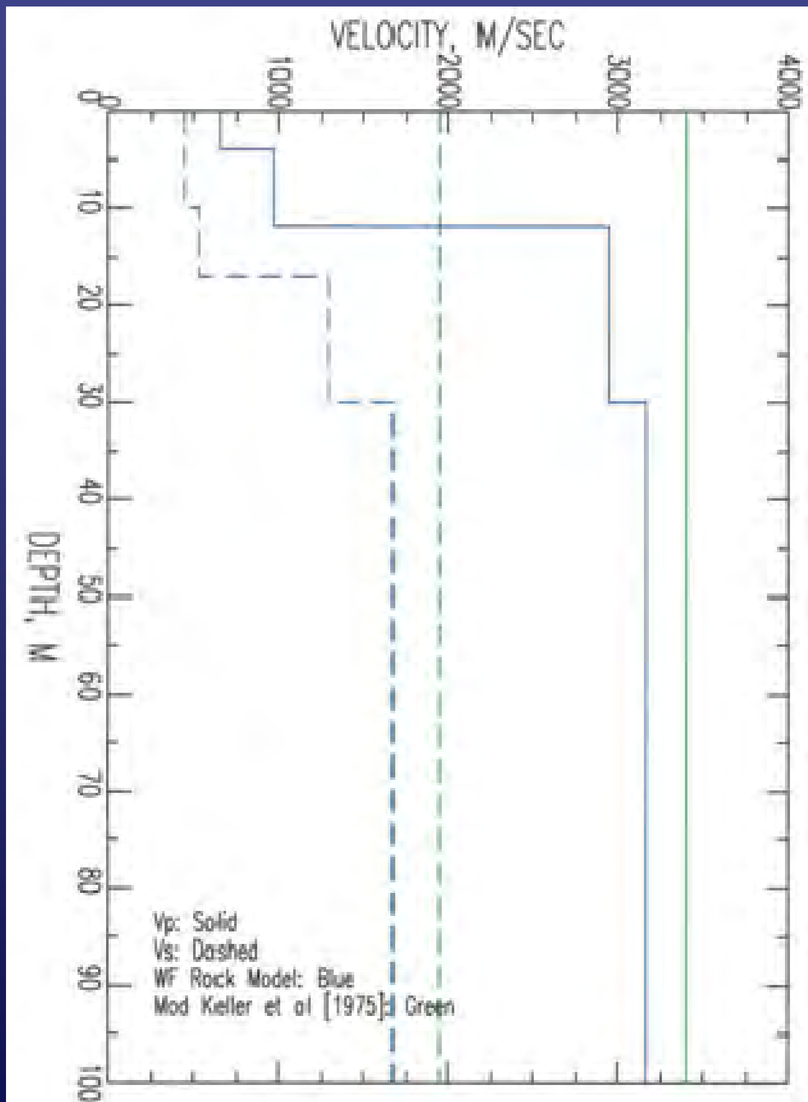

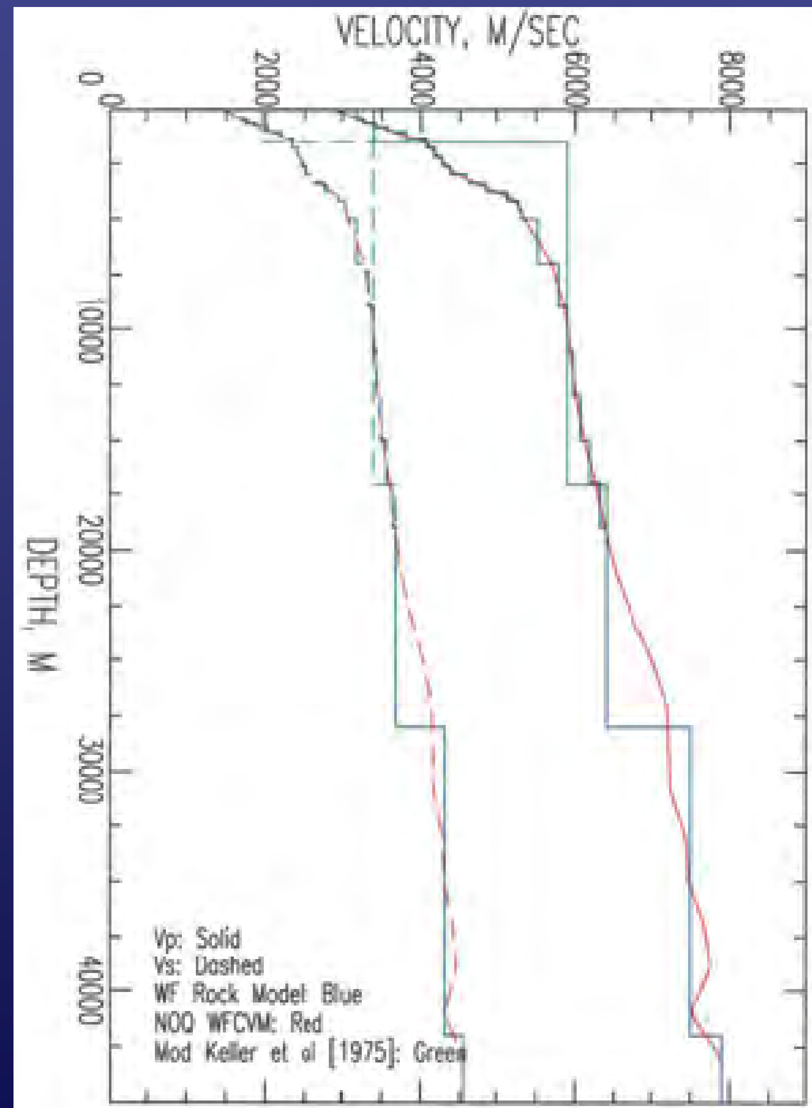

Frequency-Dependent Amplification Factors

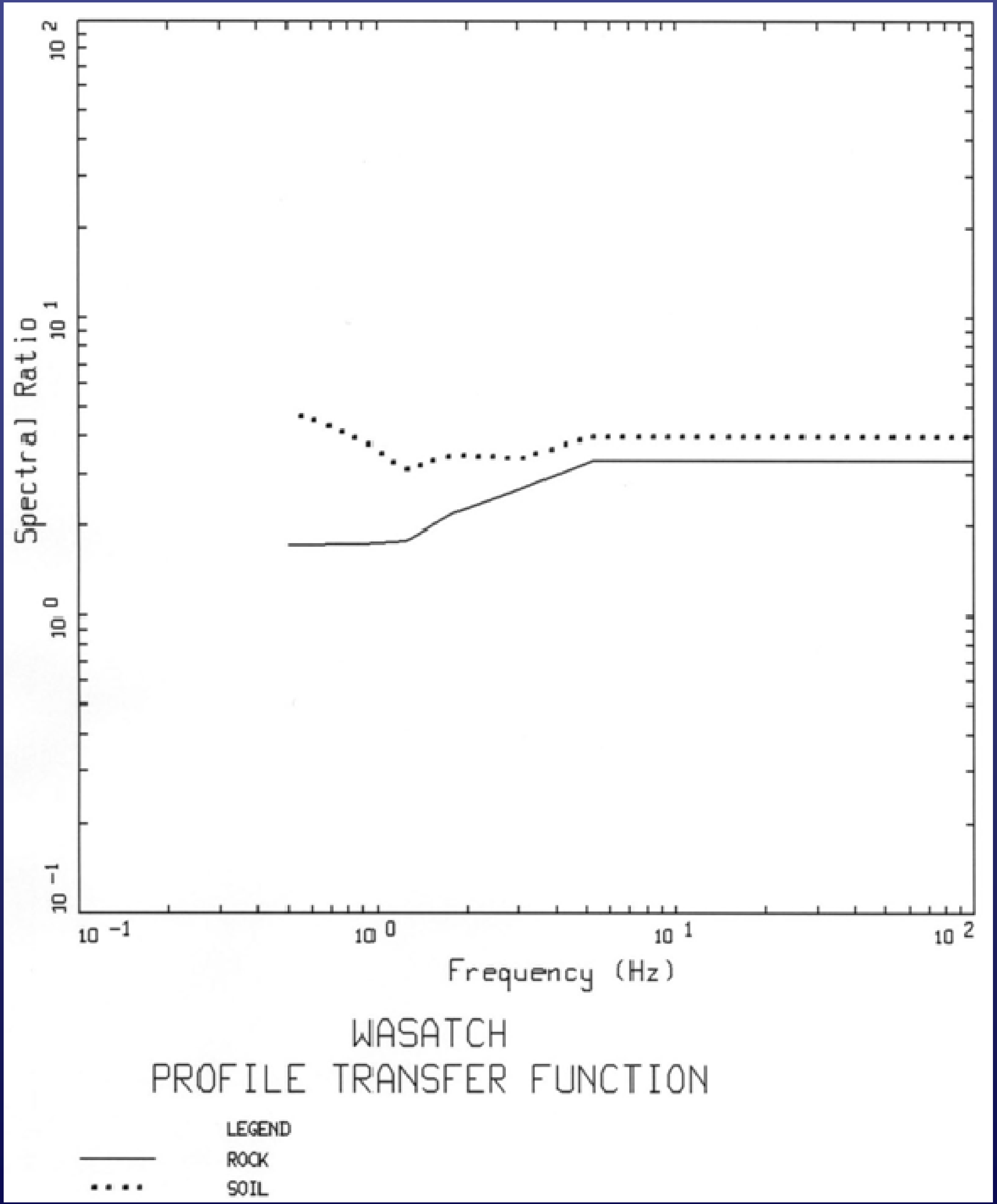

Spectral Inversion Results for Event #2

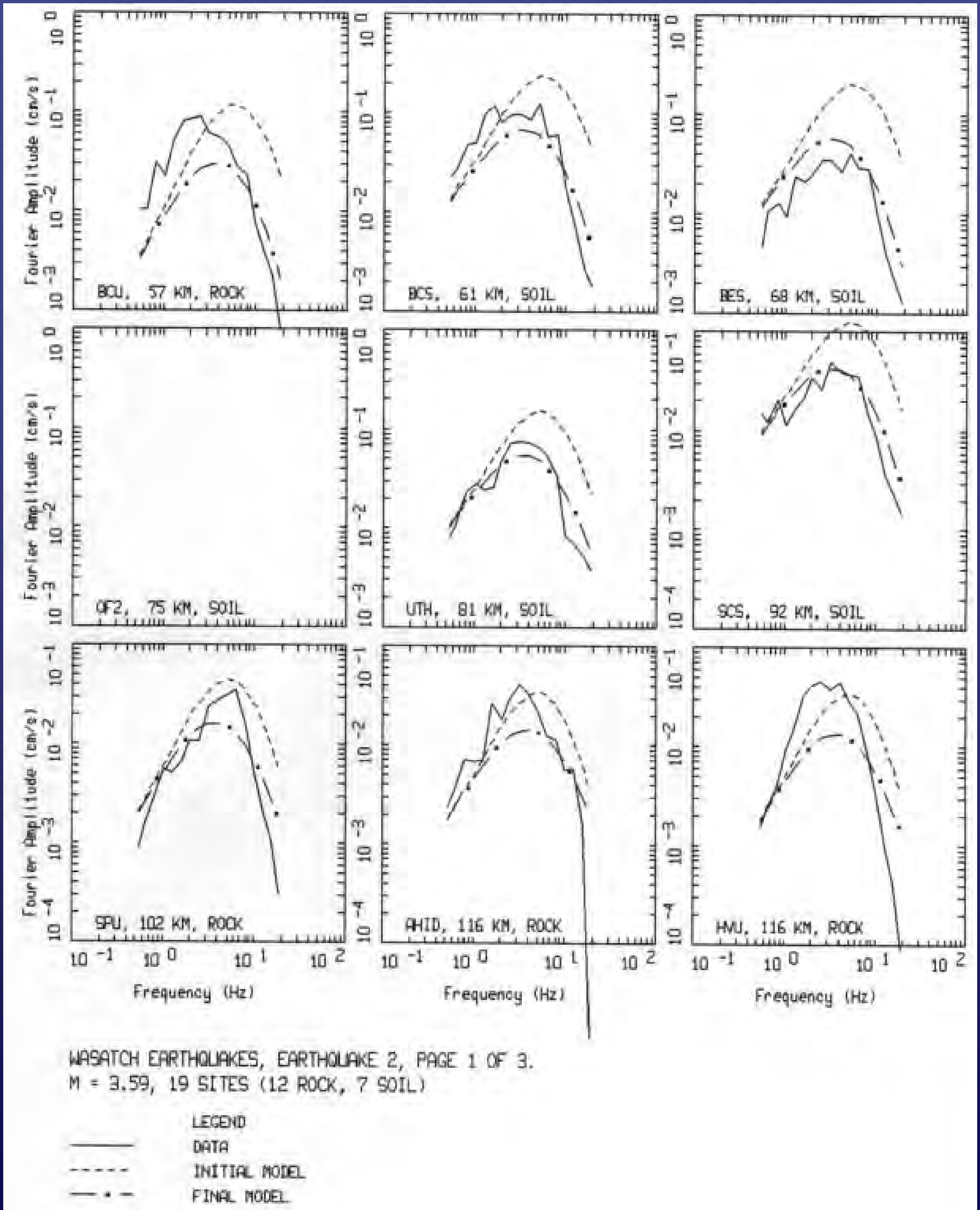

Spectral Inversion Results for Event #2

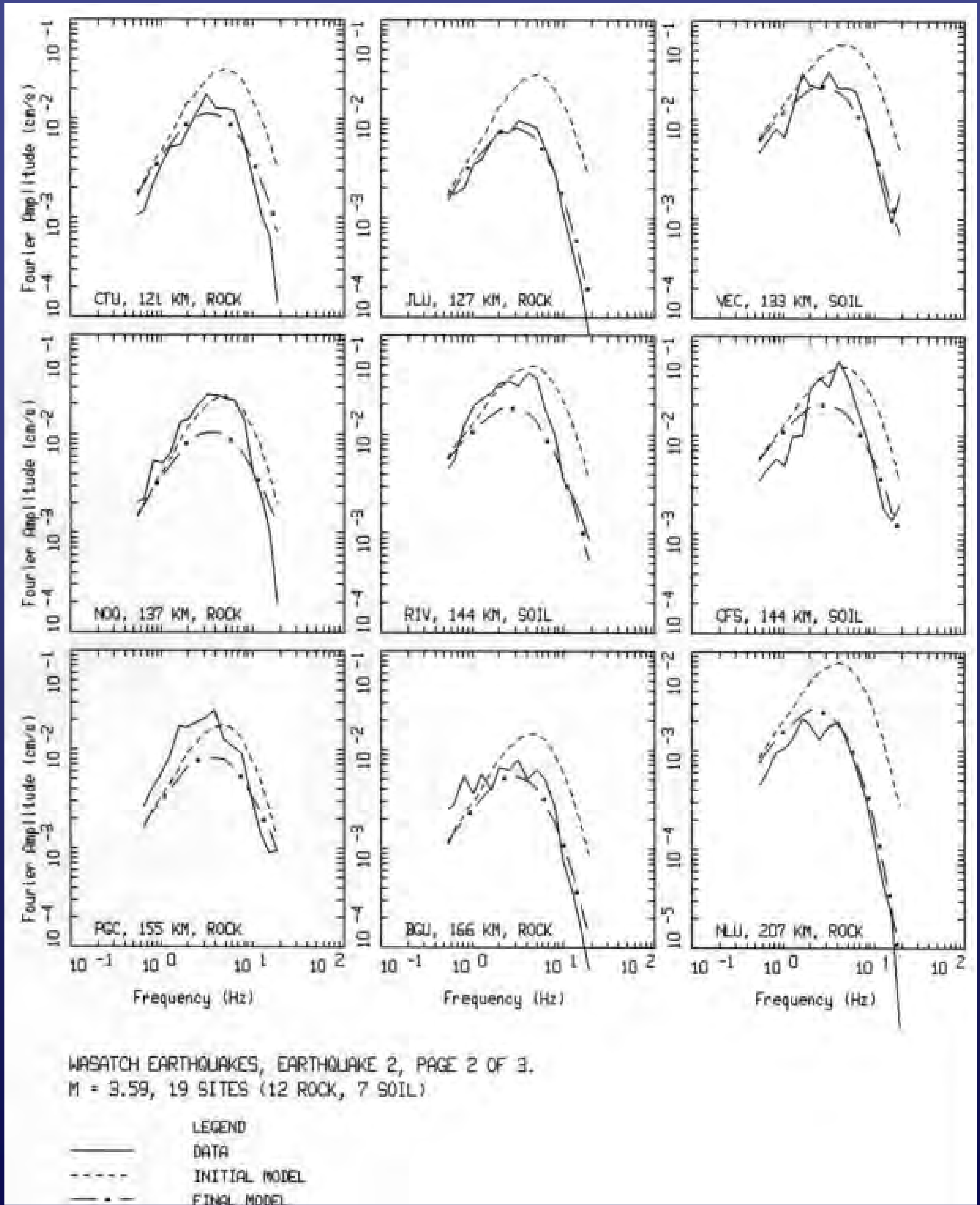

Spectral Inversion Results for Event #4

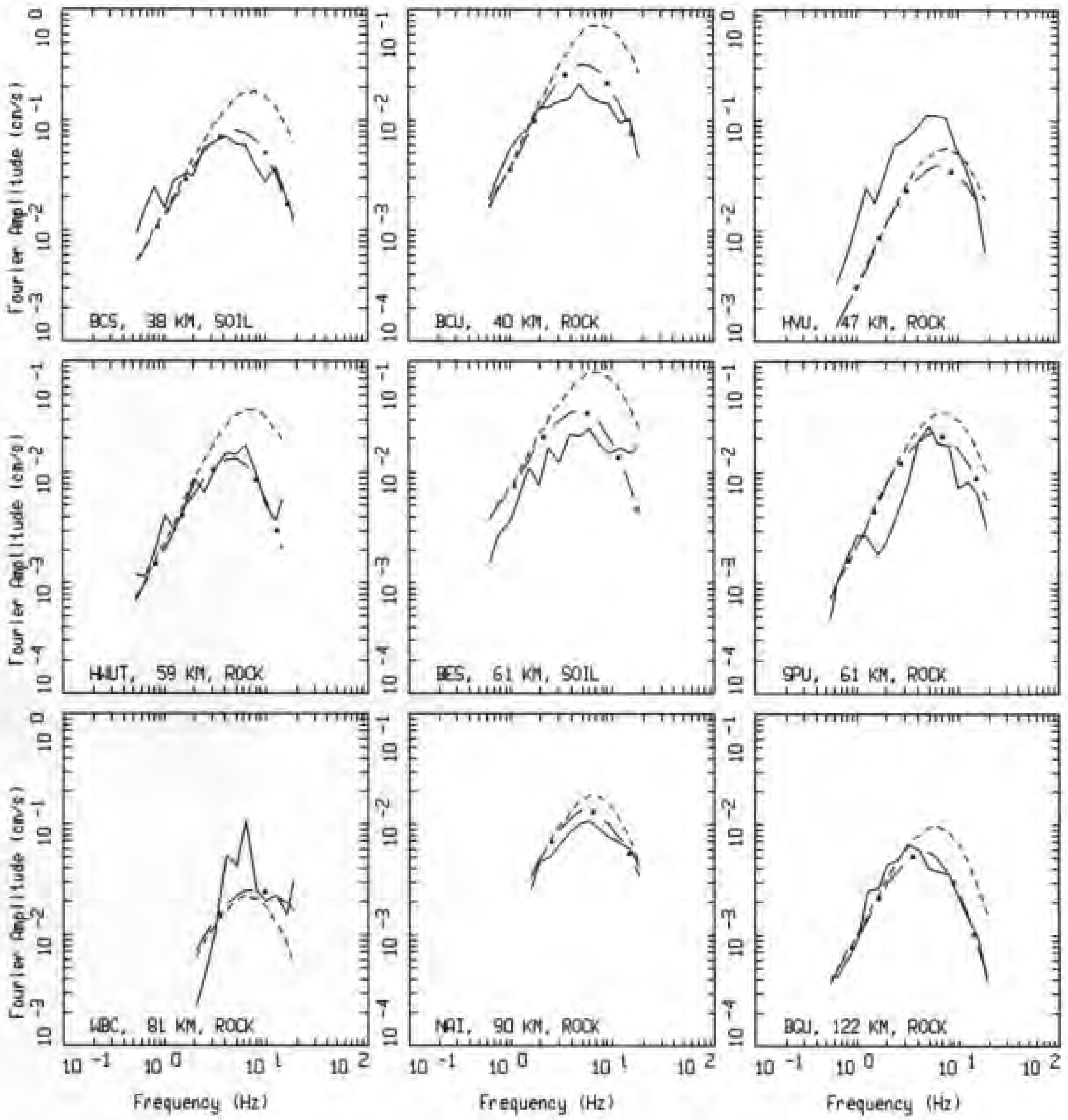

WASATCH EARTHQUAKES, EARTHQUAKE 4, PAGE 1 OF 2.
M = 3.15, 16 SITES (14 ROCK, 2 SOIL)

LEGEND
DATA
INITIAL MODEL
FINAL MODEL

Spectral Inversion Results for Event #4

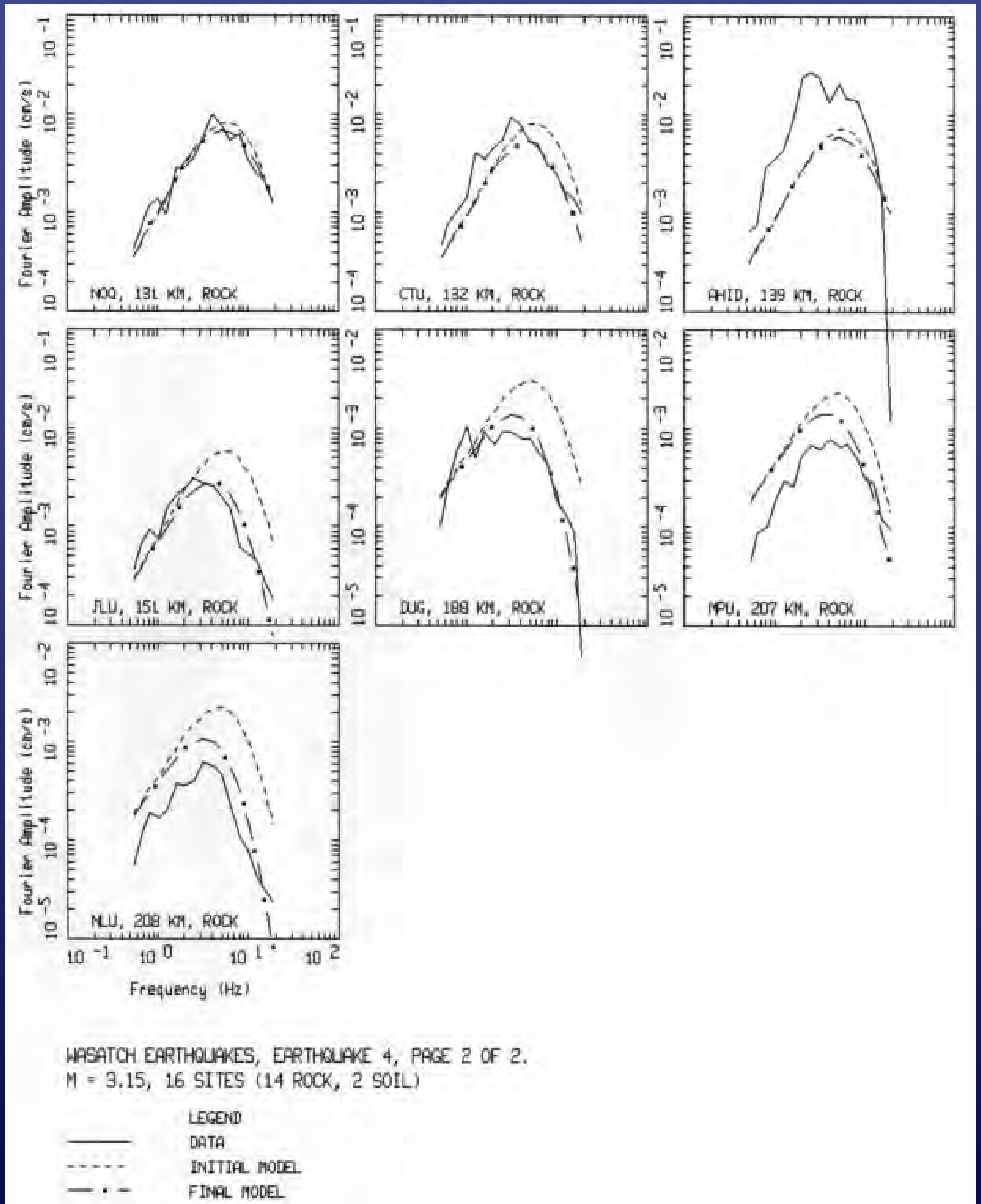

Model Bias for Soil Sites

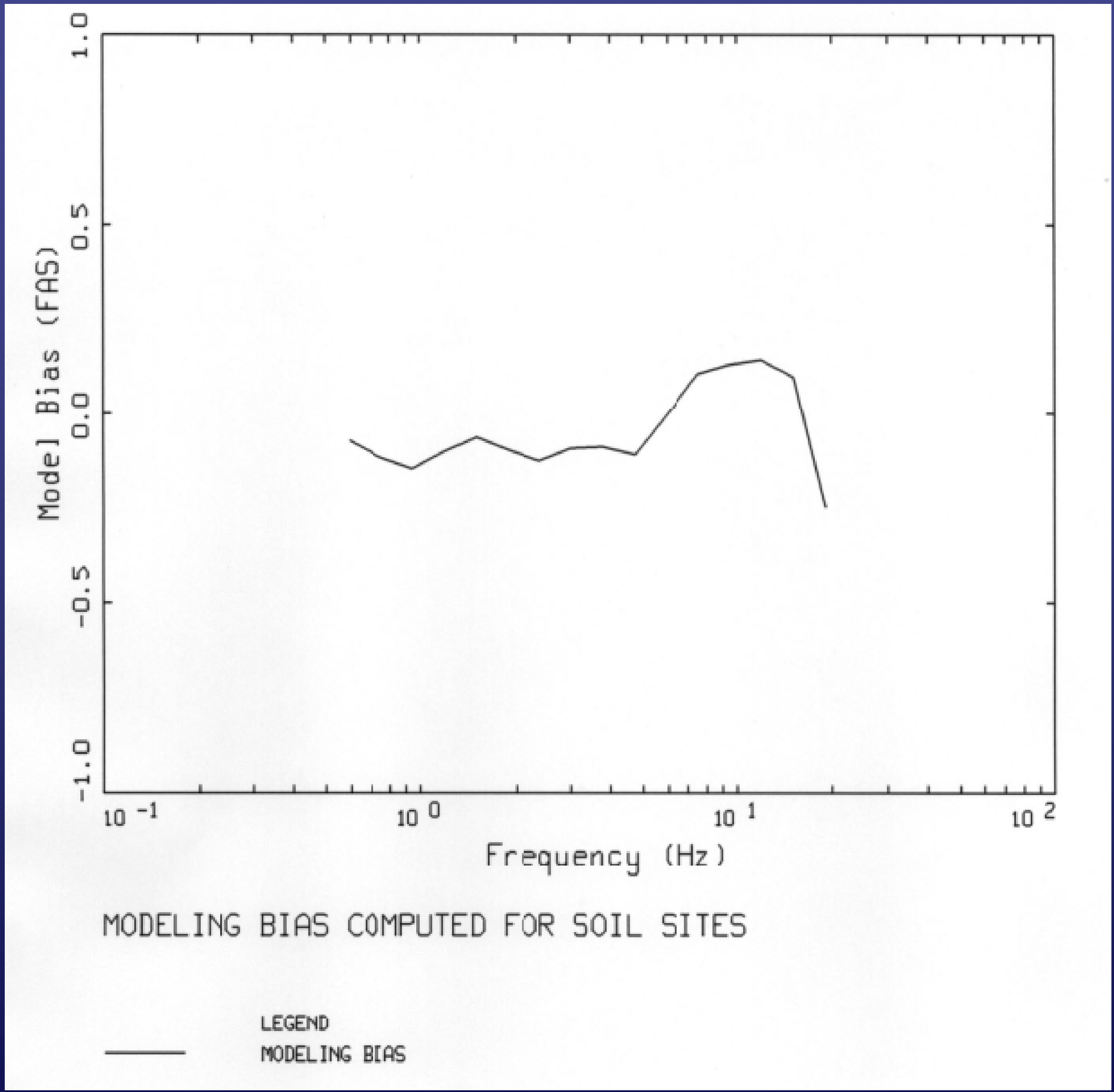

Model Bias for Rock Sites

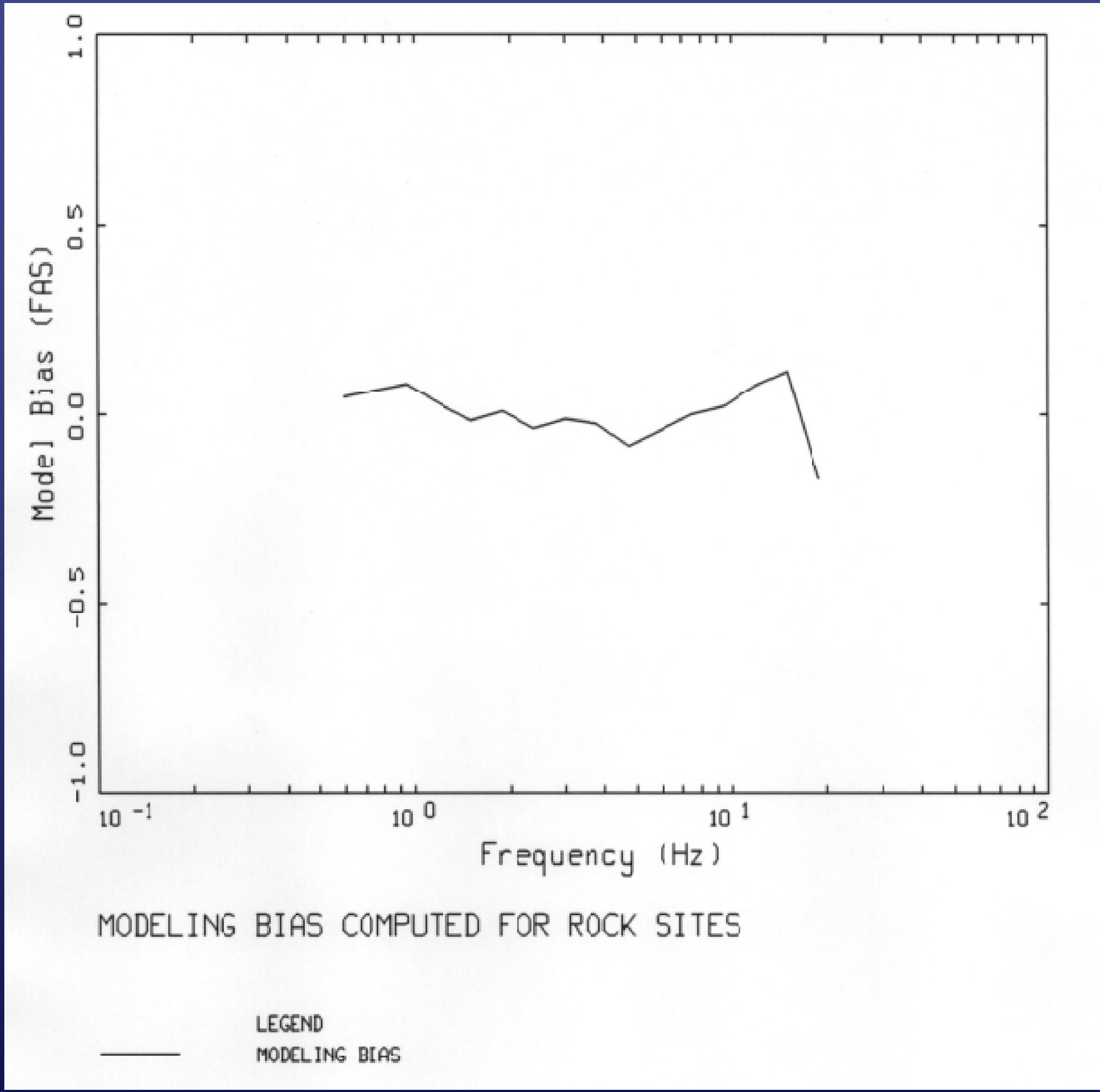

Model Bias for All Sites (Rock and Soil)

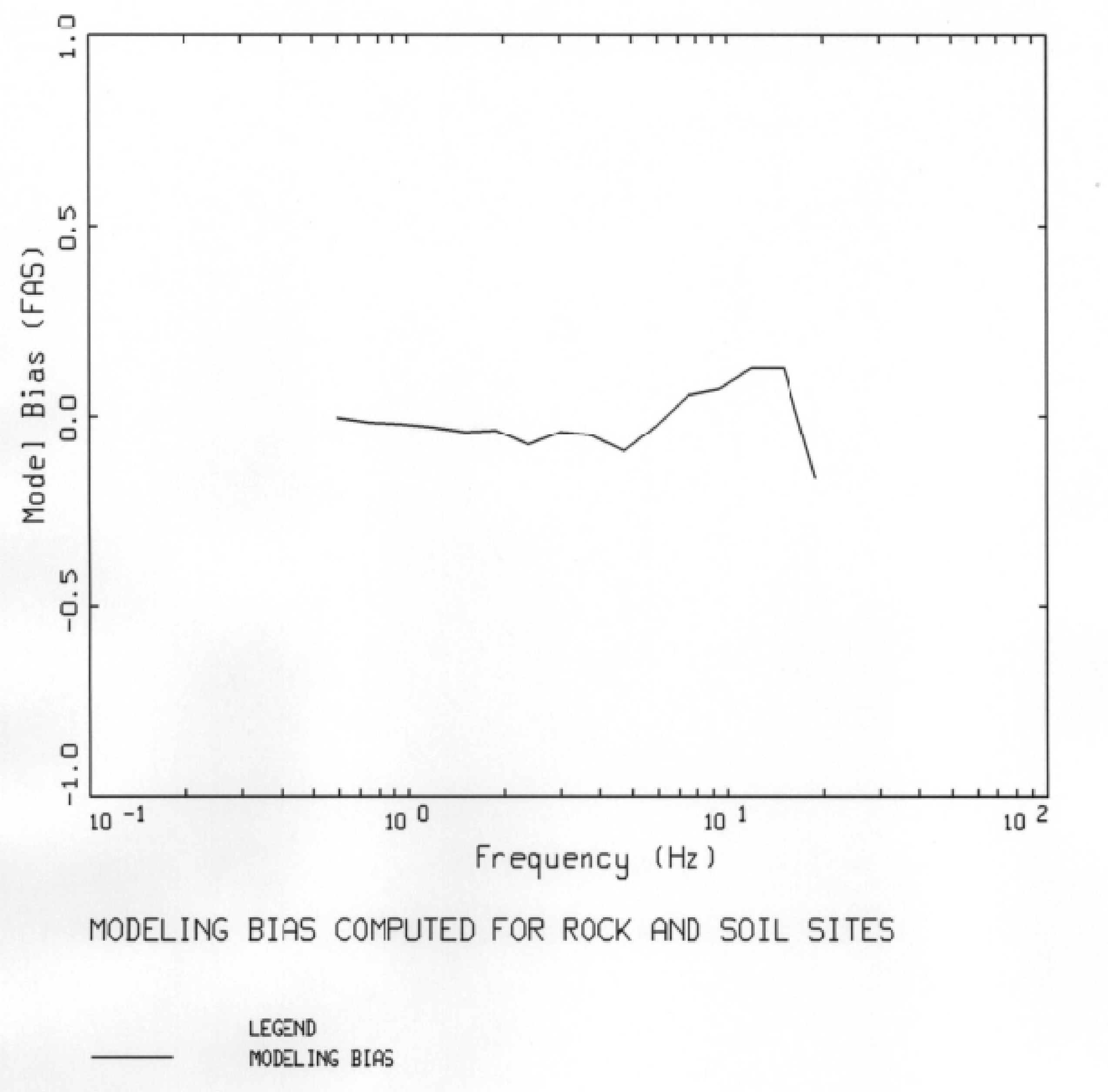

Final Preliminary Results

Event	Date	Event ID	Magnitude (M)	Latitude (degrees)	Longitude (degrees)	Depth (km)	Δσ (bars)
1	20010524	10224024041	3.30	40.3777	-111.9307	5.9	10.62
2	20020728	20728193840	3.59	41.7445	-111.3802	9.3	5.84
3	20030103	30103050212	3.62	41.2745	-111.8020	11.70	22.52
4	20030201	30201203731	3.15	41.8288	-112.2120	0.22	12.38
5	20030417	30417010419	4.24	39.5095	-111.8962	0.08	2.83
6	20030712	30712015440	3.50	41.2855	-111.6148	8.97	38.98
7	20031227	31227003924	3.64	39.6480	-111.9430	0.88	15.43
8	20040225	40225004104	3.38	41.9977	-111.8182	1.68	44.00
9	20040313	40313130447	3.17	39.6572	-111.9377	1.77	13.19
10	20050518	50518192147	3.29	41.4245	-111.0898	1.56	11.43
11	20050723	50723053748	3.30	41.8835	-111.6325	11.07	147.27
12	20050905	50905093155	3.00	41.0222	-111.3568	7.41	27.26
13	20051120	51120102429	2.62	41.3672	-111.6910	2.77	132.13
14	20060611	60611100150	3.41	40.2468	-111.0733	10.37	15.11
15	20061220	61220181536	3.35	41.1270	-111.5745	7.94	89.78
16	20070901	70901183202	3.92	41.6423	-112.3185	5.61	6.07
17	20071105	71105214801	3.91	39.3458	-111.6475	5.50	16.81

Final Inversion Results

Q_0	137.05
η	0.56
$\overline{\Delta\sigma}$ (bars)	20.1
$\overline{\kappa}$ (sec)	0.034
$\overline{\kappa}$ for rock sites (sec)	0.030
$\overline{\kappa}$ for soil sites (sec)	0.036
R0 (km)	59.88

Comparison of Stress Drops

Source	Region	Magnitude	Stress Drop
Becker and Abrahamson (1997)	Worldwide	5.1 – 6.9	16 – 93 bars 29 bars (median)
WCFS et al. (1996)	Basin and Range	2.8 – 6.0	8 – 114 bars 40 bars (mean)
This study	Wasatch Front	3.0 – 4.2	3 – 147 bars 20 bars (mean)
Silva et al. (1997)	California	5.7 – 7.3	59 bars (mean)

Wasatch Fault Central
Segments Logic Tree for Recurrence

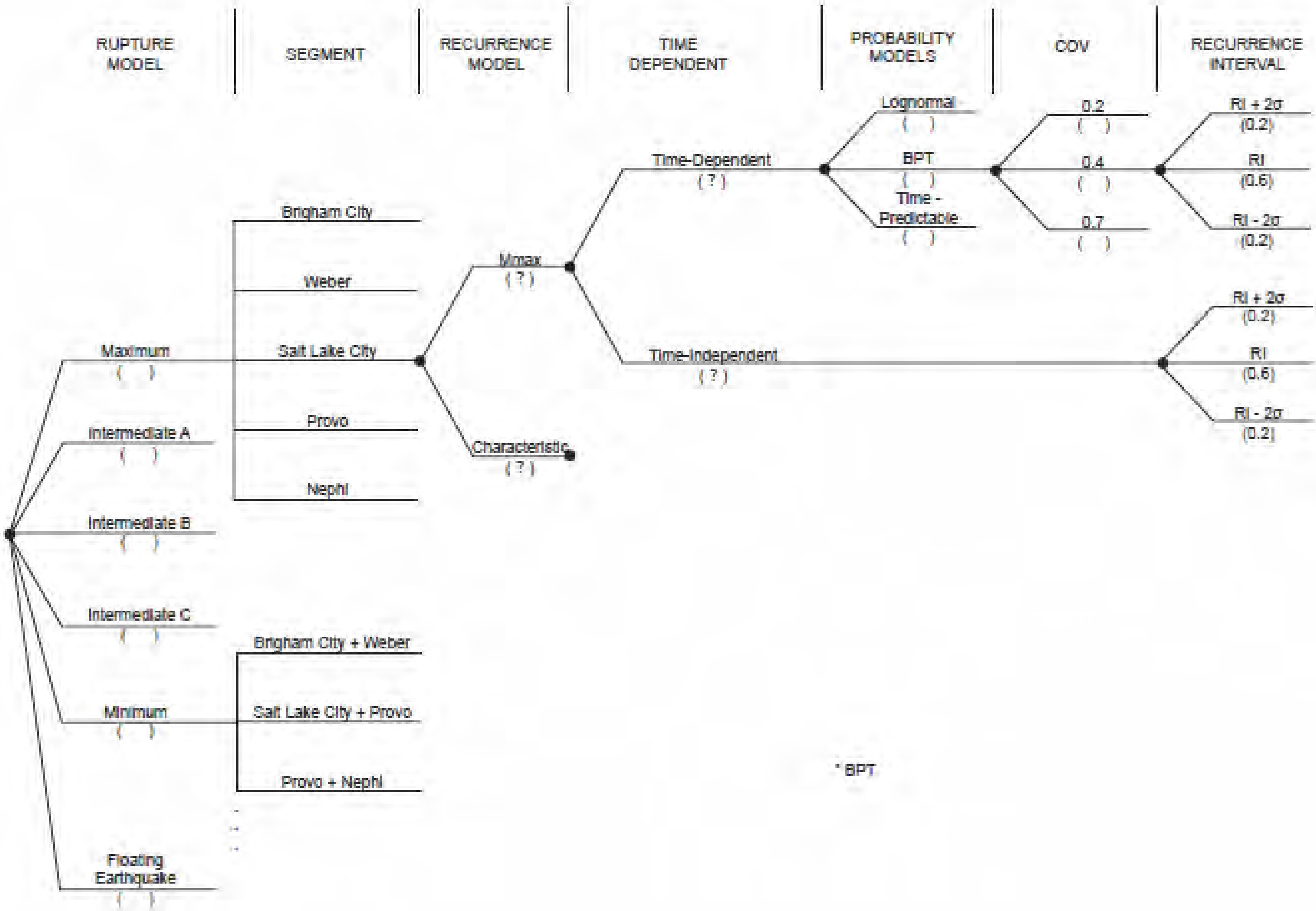

Wasatch Fault Central Segments Logic Tree for Mmax

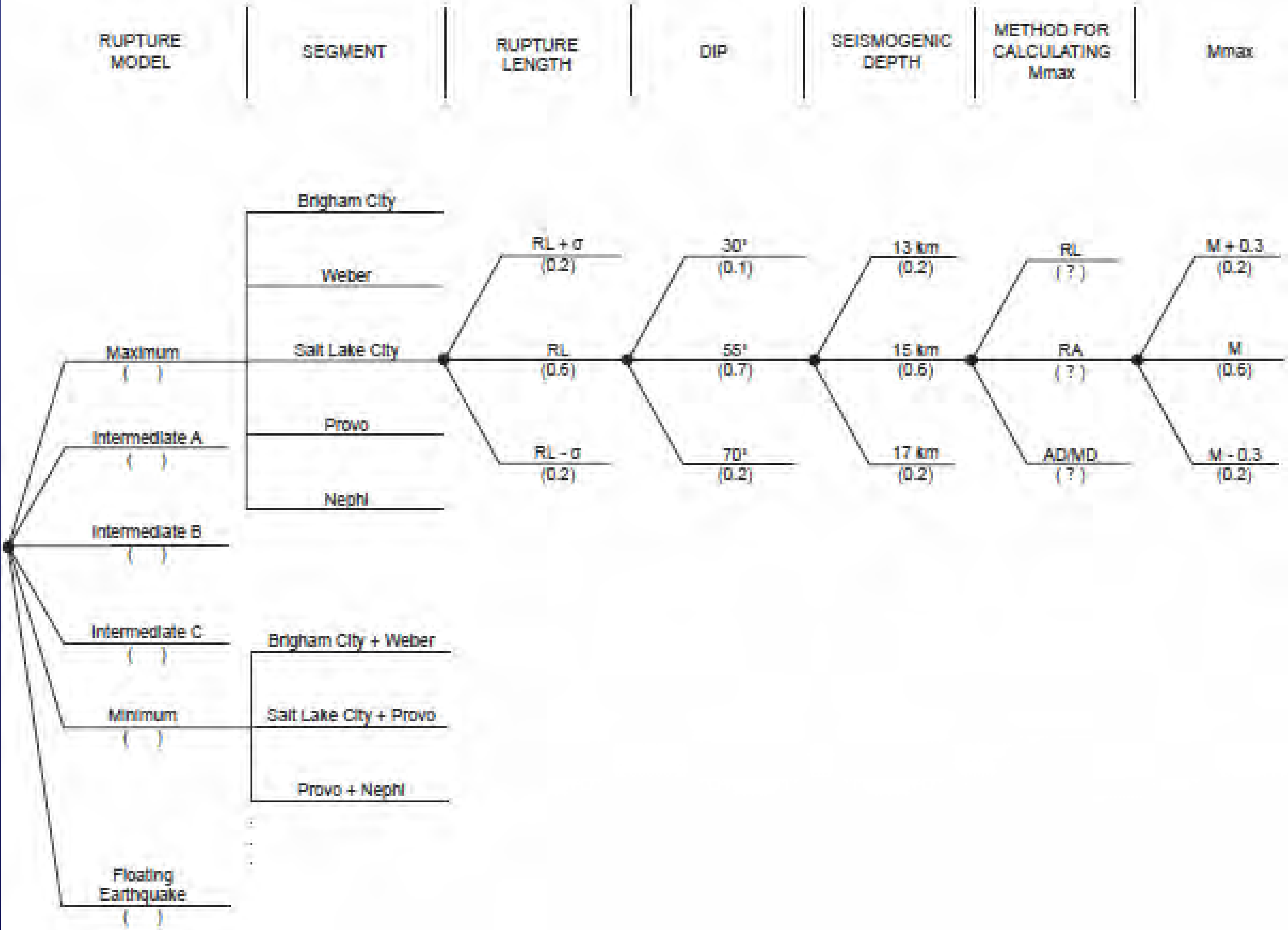

Three-Dimensional Nonlinear Earthquake Ground Motion Simulation in the Salt Lake basin

using the Wasatch Front Community Velocity Model

THE
QUAKE Group
AT Carnegie Mellon University

Ricardo Taborda and Jacobo Bielak
Computational Seismology Laboratory
Department of Civil and Environmental Engineering
Carnegie Mellon University

A research project sponsored by:

Region and Simulation Domain

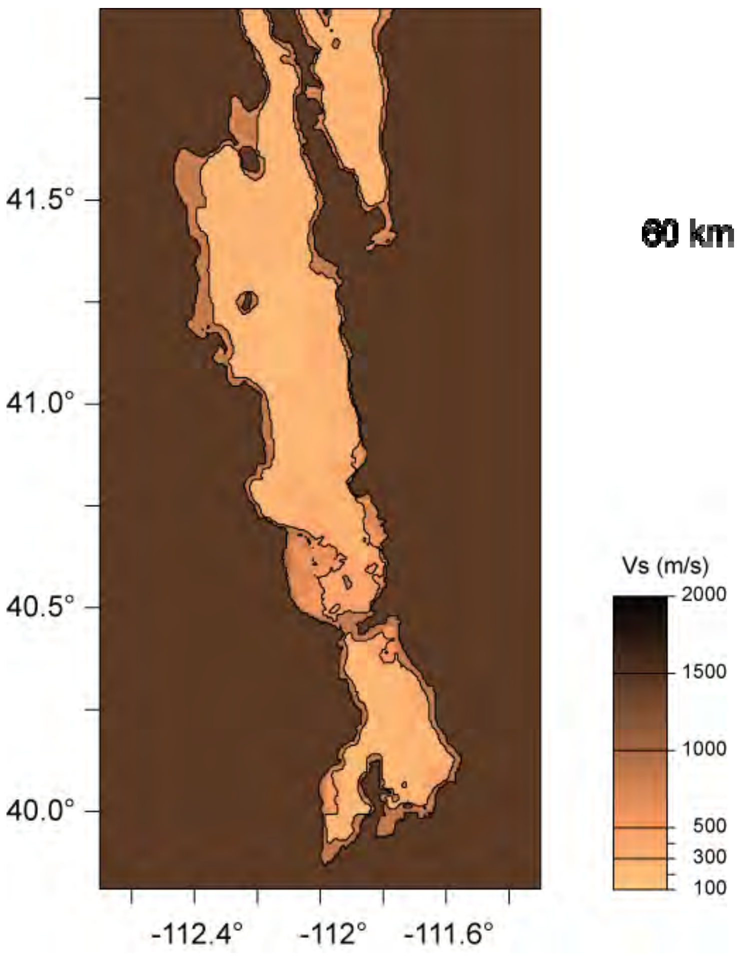

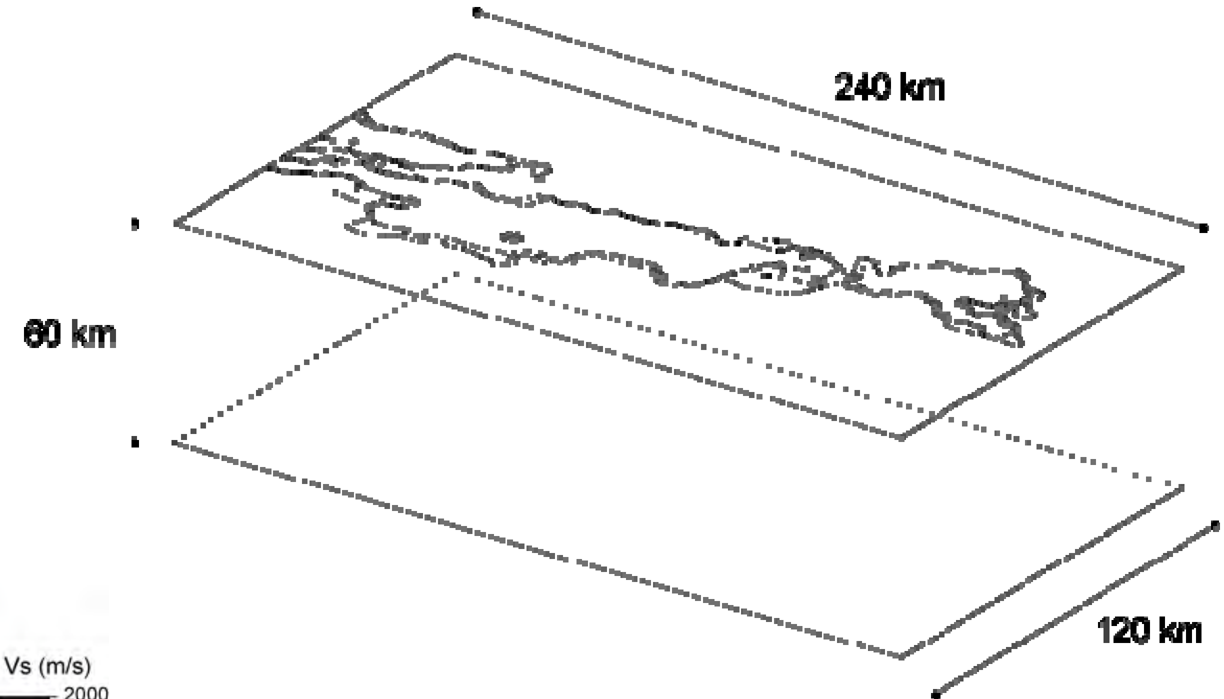

Source Models

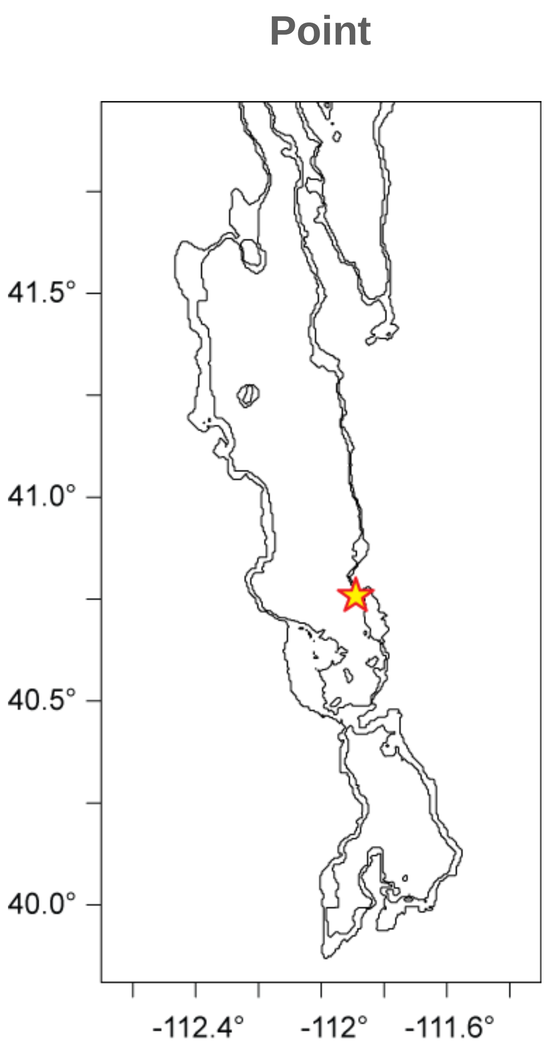

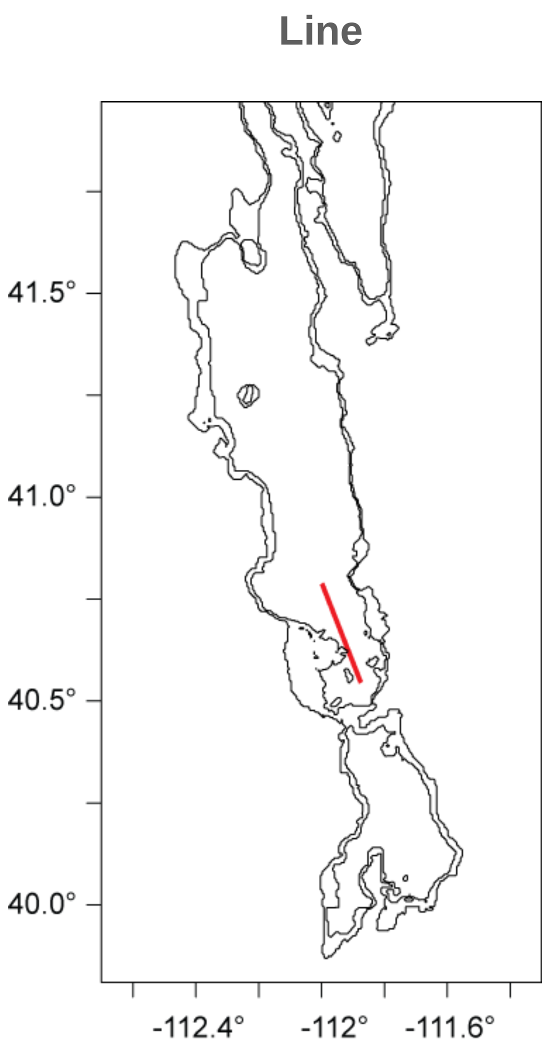

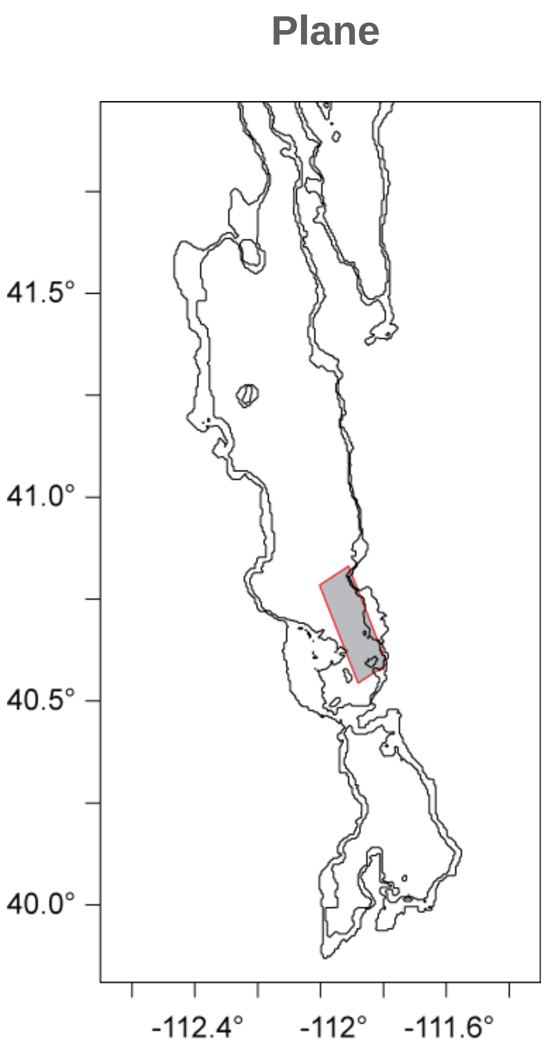

Point and Line

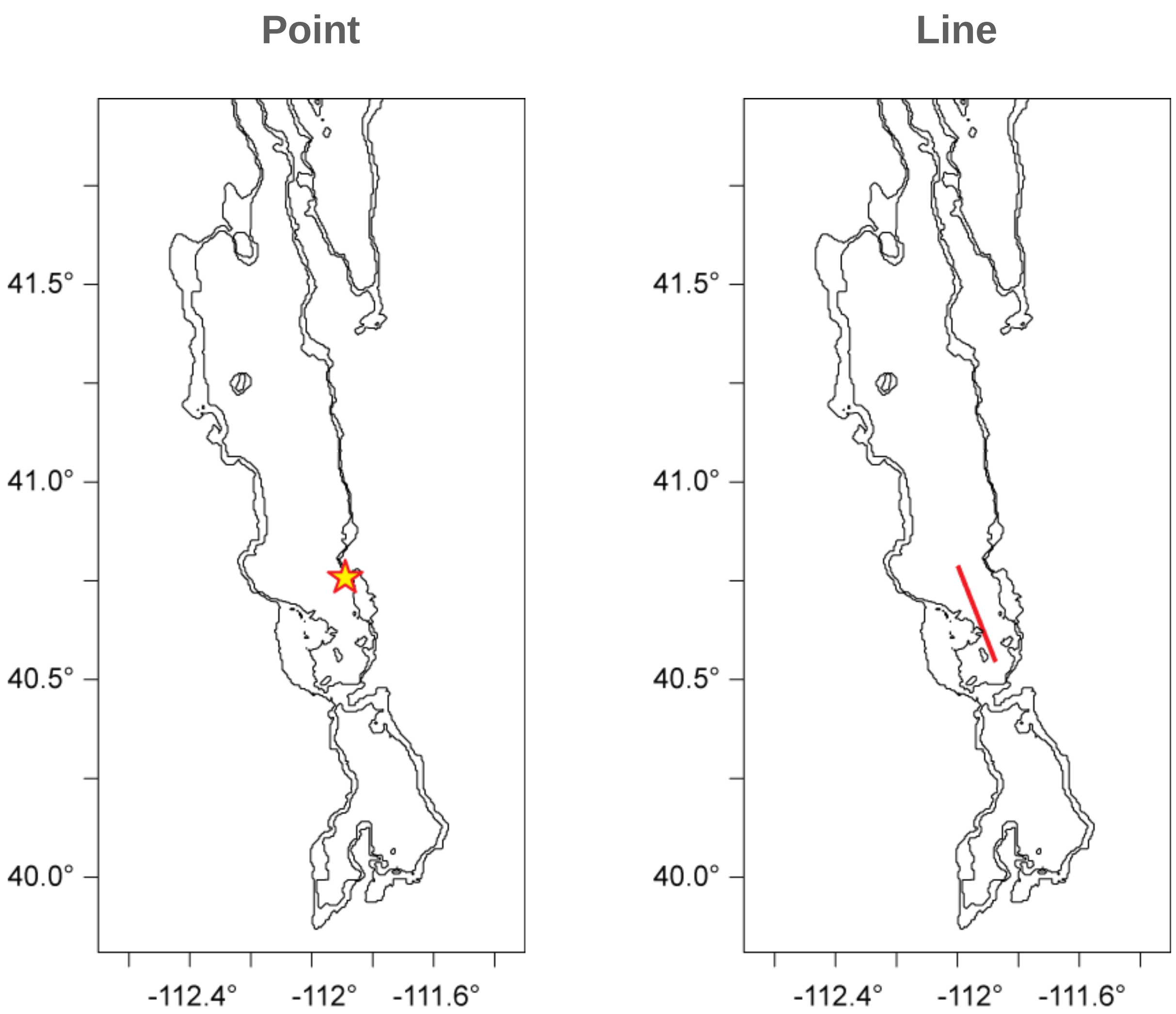

Mw	6.0 (point) 6.3 (line)
Strike	153º
Dip	50º
Rake	0º
Depth	13 km

Plane Source

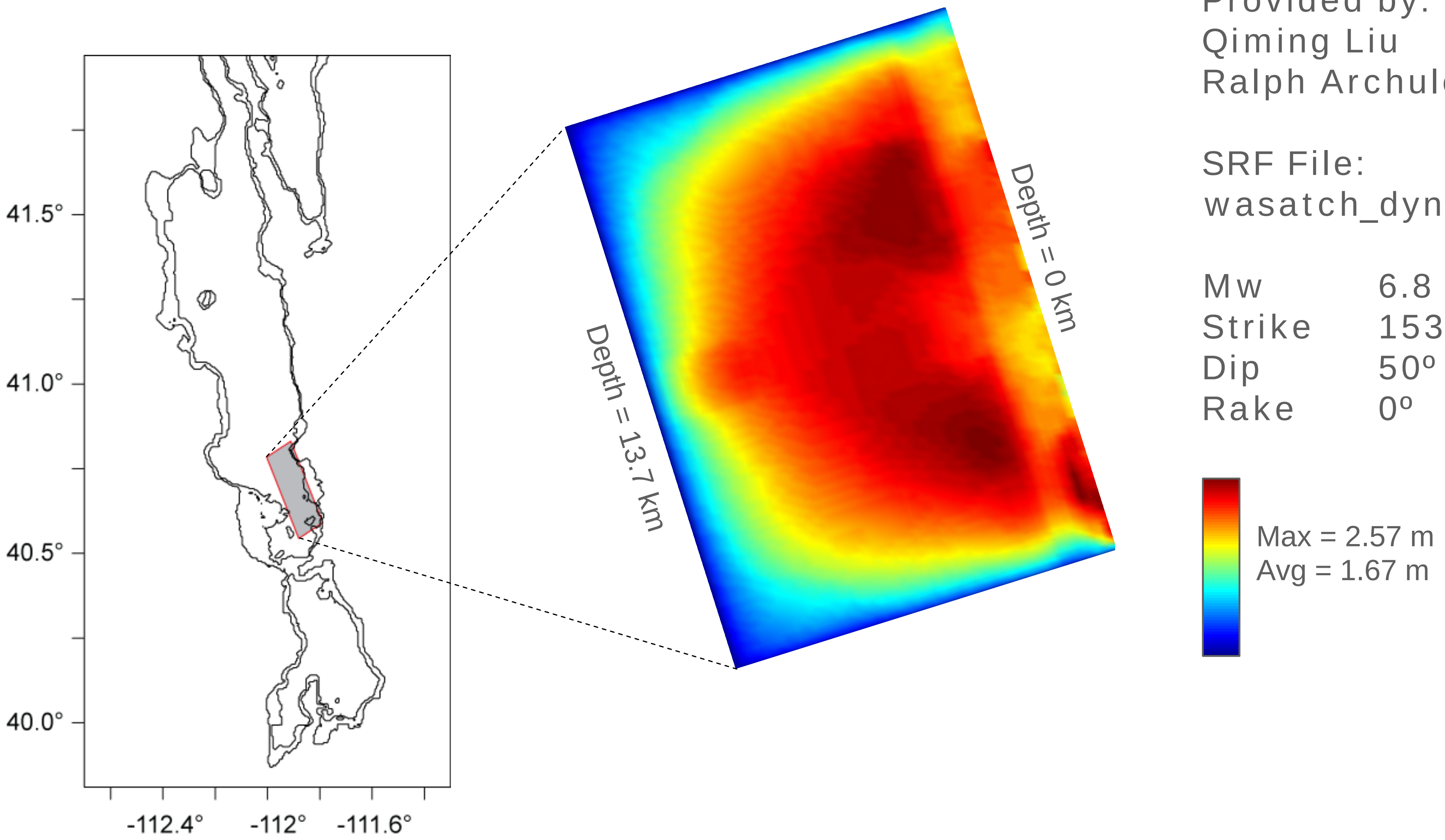

Provided by:
Qiming Liu
Ralph Archuleta

SRF File:
wasatch_dyna_vs.srf

Mw	6.8
Strike	153º
Dip	50º
Rake	0º

Simulation Parameters

Linear:

Vs_{min}	100 m/s	Source:	Plane
f_{max}	1.0 Hz	Sim. Time:	100 s
		Delta t:	0.0025 s
		Elements:	152,587,905
		Processors:	4,800
		Walltime:	4 hr 30 min

Linear & Nonlinear:

Vs_{min}	500 m/s	Source:	Point & Line
f_{max}	0.5 Hz	Sim. Time:	40 s
		Delta t:	0.001 – 0.01 s
		Elements:	10,859,318
		Processors:	480
		Walltime:	15 min (dt = 0.01 s) 1 hr 15 min (dt = 0.001 s)

Wave Propagation in Inelastic Media

Linear momentum equation

$$\sigma_{ij,j} + f_i = \rho \ddot{u}_i$$

Applying finite Elements but keep stress terms

$$\mathbf{M}\ddot{\mathbf{u}} + \mathbf{C}\dot{\mathbf{u}} + \sum_e \int_{\Omega_e} \mathbf{B}^{\mathrm{T}} \sigma_{ij} d\Omega_e = \mathbf{f}$$

Applying central differences in time and decoupling with respect to the mass matrix

Explicit

Forward solution of displacements

$$\begin{aligned} u^i_{n+1} &= \frac{\Delta t^2}{m^i} f^i_n + \left(2u^i_n - u^i_{n-1}\right) - \alpha \Delta t \left(u^i_n - u^i_{n-1}\right) \\ &- \frac{\Delta t}{m^i} \beta \left(\sum_{\mathbf{e}} \mathbf{K}^{\mathbf{e}} \left(\mathbf{u}^{\mathbf{e}}_n - \mathbf{u}^{\mathbf{e}}_{n-1}\right)\right)_i - \frac{\Delta t^2}{m^i} \left(\sum_e \int_{\Omega_e} \left(\mathbf{B}^{\mathrm{T}} \sigma_{ij}\right)_n d\Omega_e\right)_i \end{aligned}$$

Rate-Dependent Plasticity

Hooke's law and Strain Tensor decomposition

$$\epsilon_{ij}^{e} = \epsilon_{ij} - \epsilon_{ij}^{p}$$

$$\sigma_{ij} = C_{ijmn}\left(\epsilon_{mn} - \epsilon_{mn}^{p}\right)$$

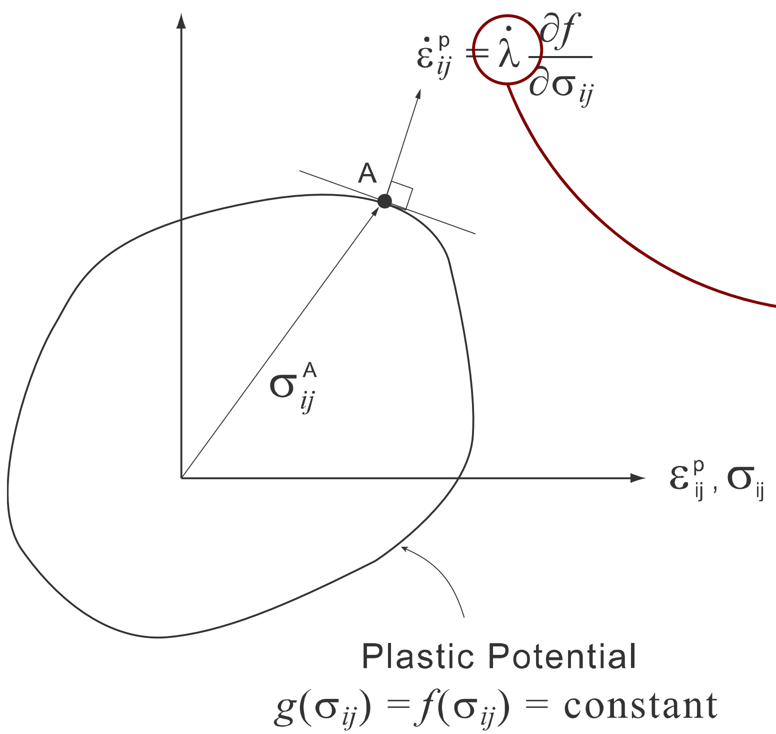

Power Law (Perzyna, 1963, 1966)

$$\dot{\lambda} = \dot{\lambda}_0 \left\langle \frac{F\left(\sigma_{ij}\right)}{k\left(\sigma_{ij}, k_n\right)} \right\rangle^{\frac{1}{m}}$$

m strain rate sensitivity

$\dot{\lambda}_0$ material strain rate

Plane Source — Linear

Vs_{min} = 100 m/s, f_{max} = 1.0 Hz

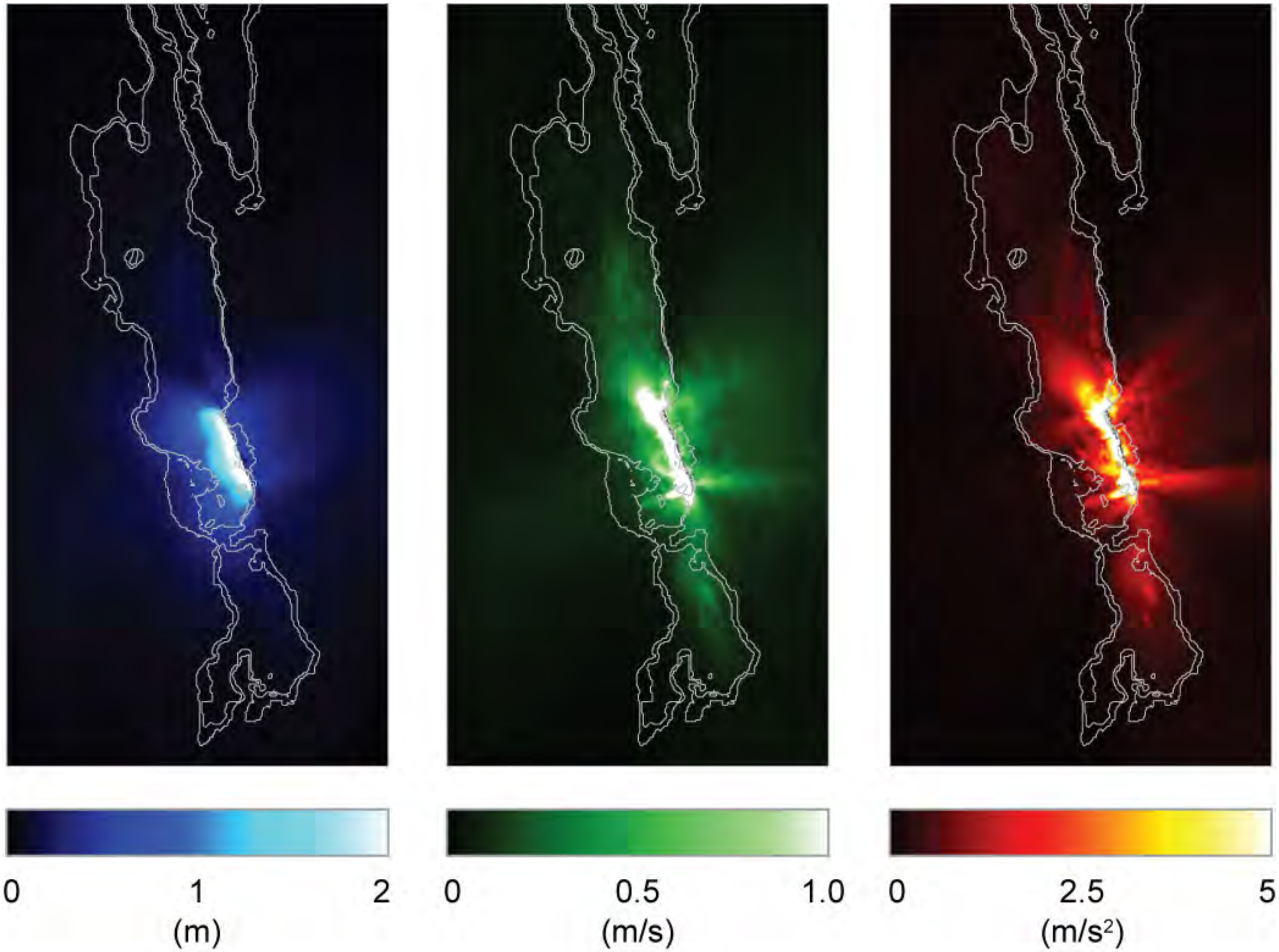

Nonlinear Properties Criteria

Yield Function Histories

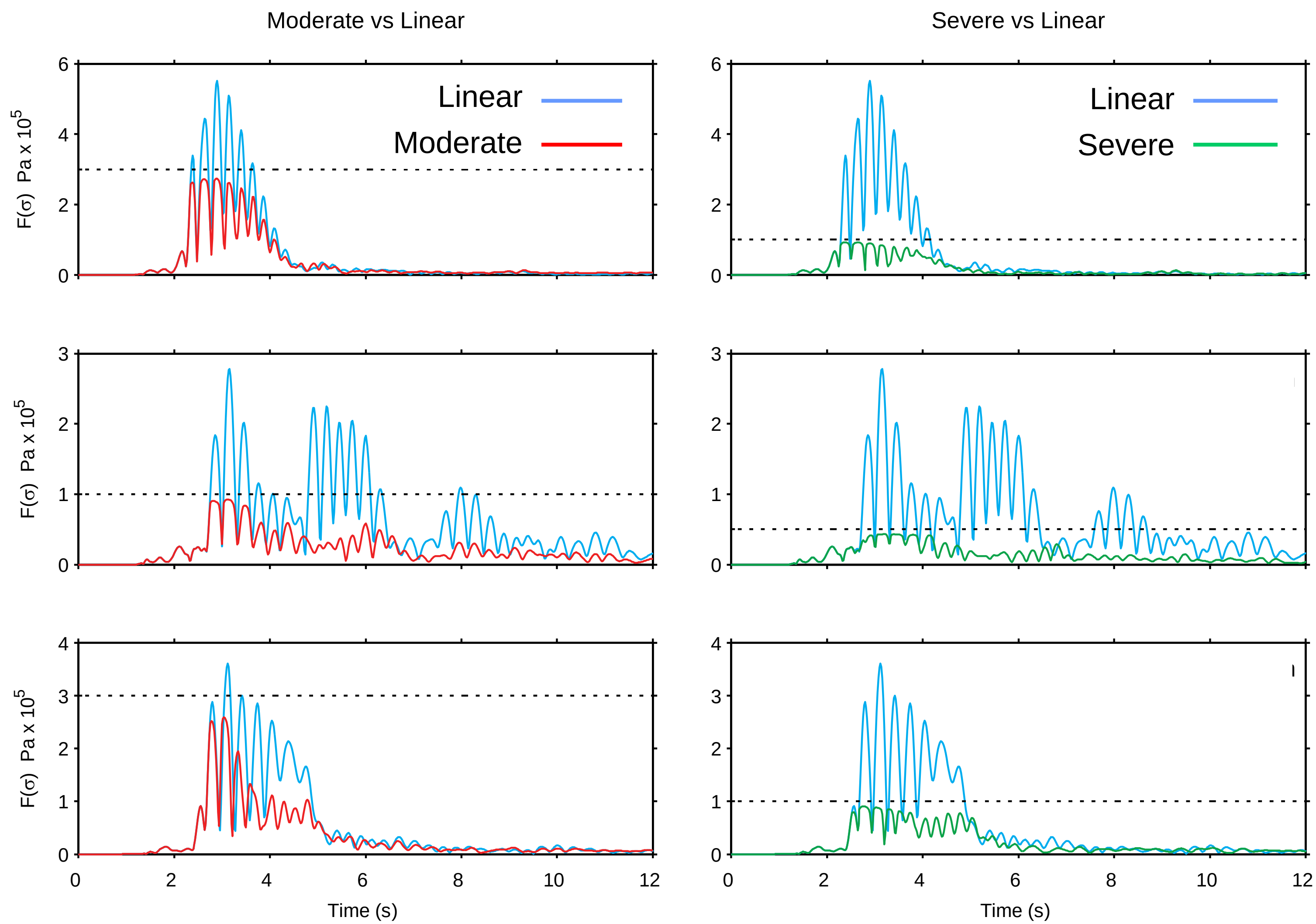

Nonlinear Properties Criteria

Point Source:

	Fs_{avg} (Pa)	Fs_{max} (Pa)	
Linear	4.31E+03	2.28E+05	
Nonlinear	4.33E+03	6.82E+04	(30% of Peak)

Line Source:

Linear	1.73E+03	5.24E+04	
Nonlinear A	1.68E+03	1.73E+04	(33% of Peak)
Nonlinear B	1.22E+03	6.05E+03	(11% of Peak)
Nonlinear C	9.39E+02	3.69E+03	(7% of Peak)

Point Source — Linear vs Nonlinear

Displacement

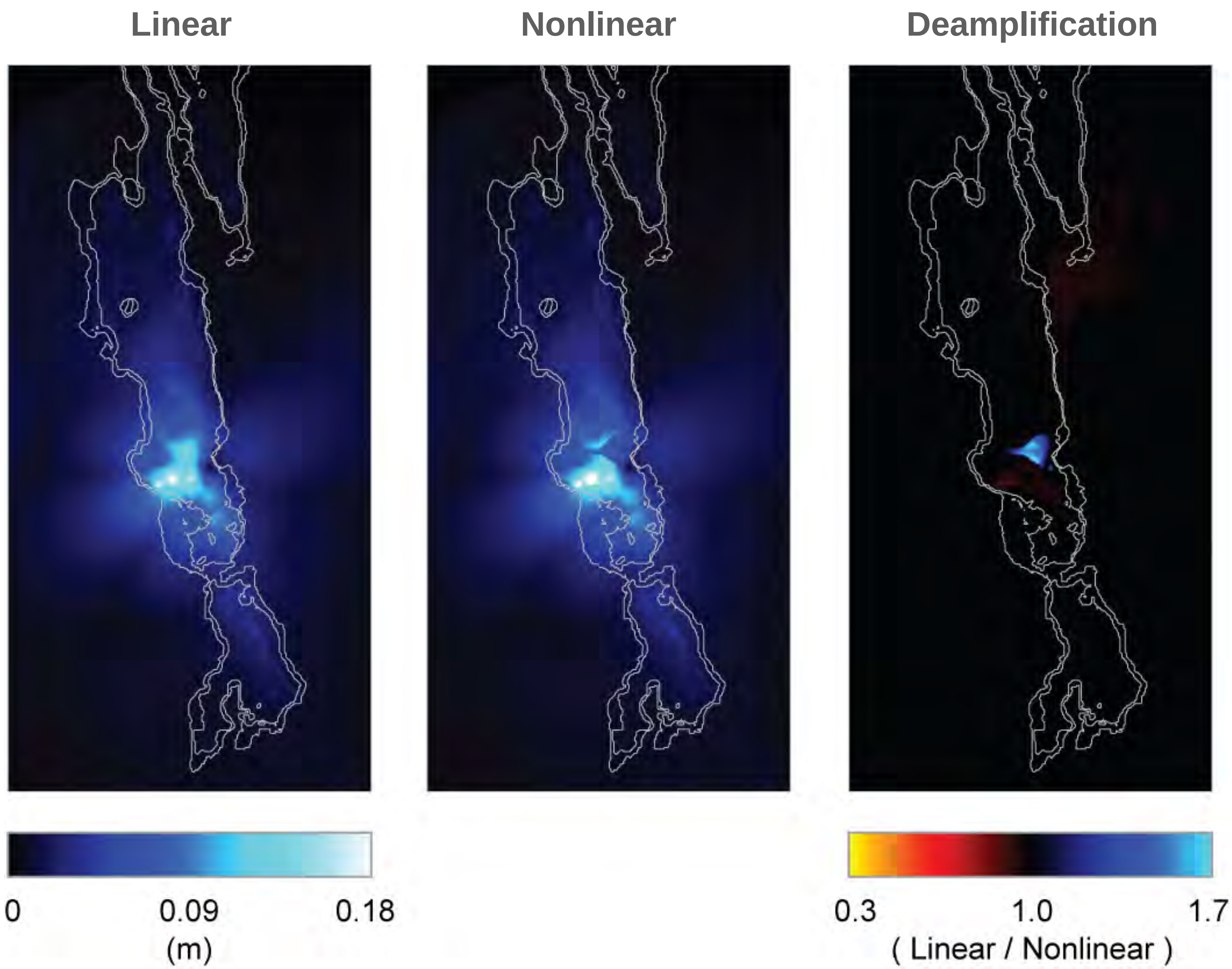

Point Source — Linear vs Nonlinear

Velocity

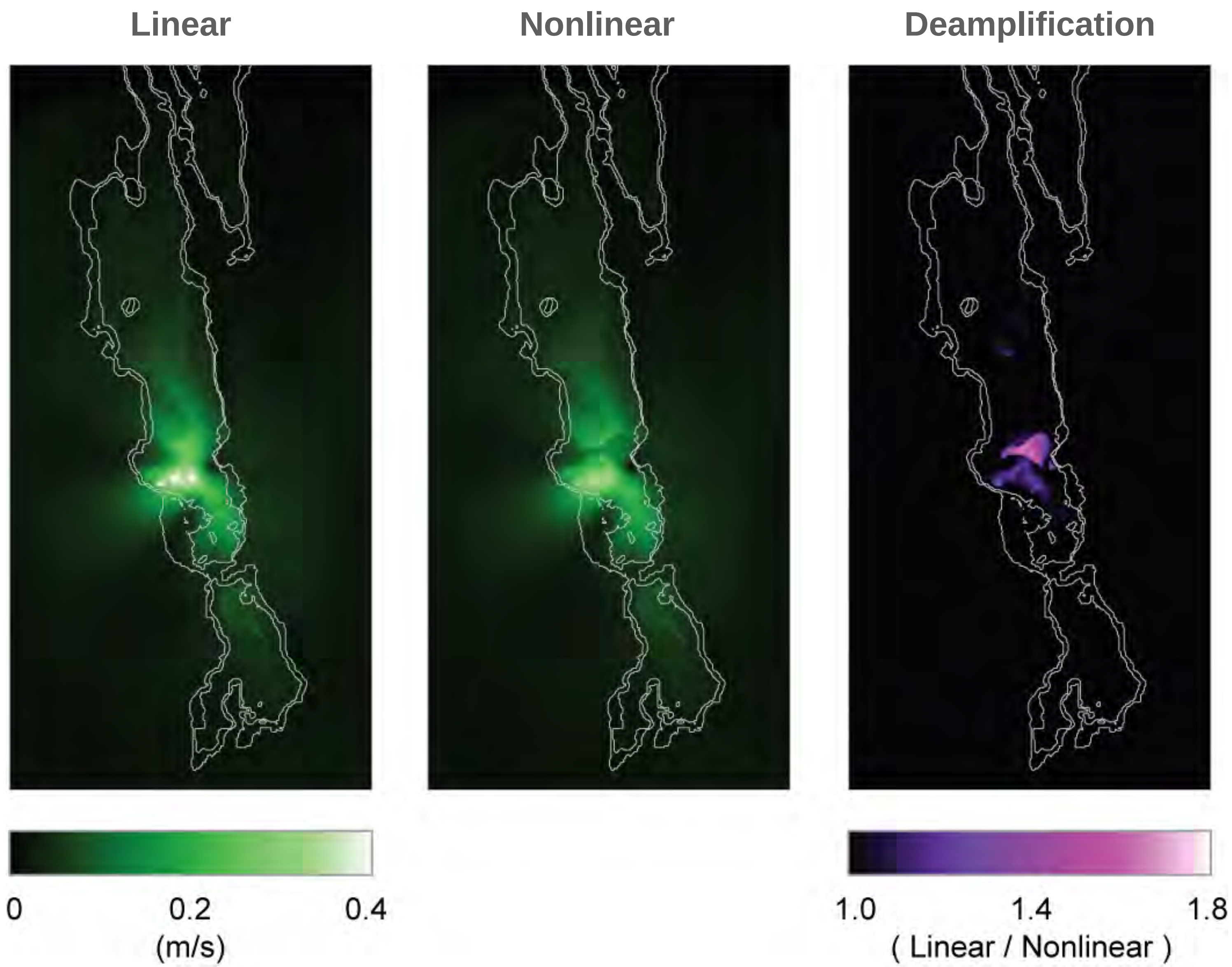

Point Source — Linear vs Nonlinear

Acceleration

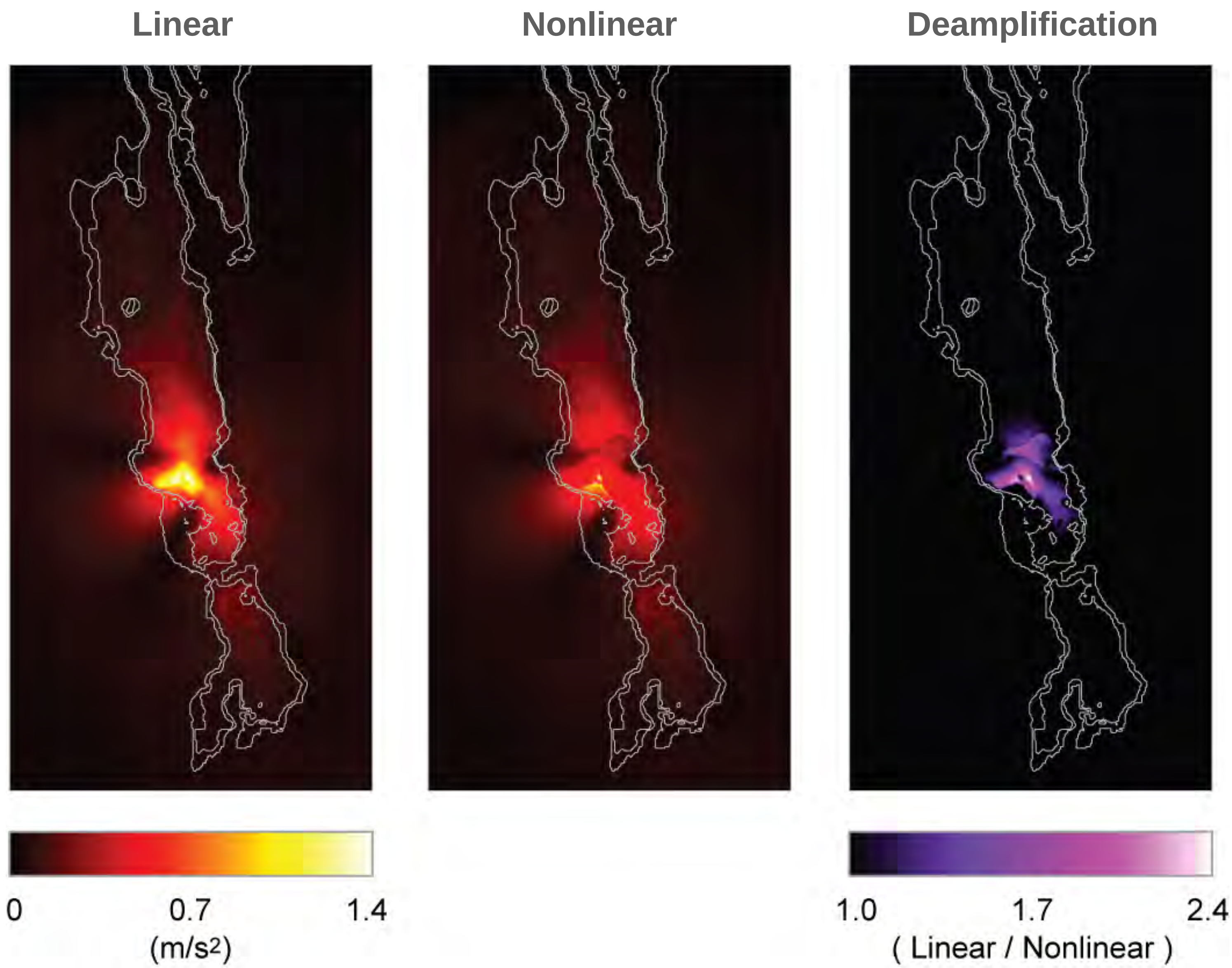

'Line' Source — Linear vs Nonlinear A

Displacement

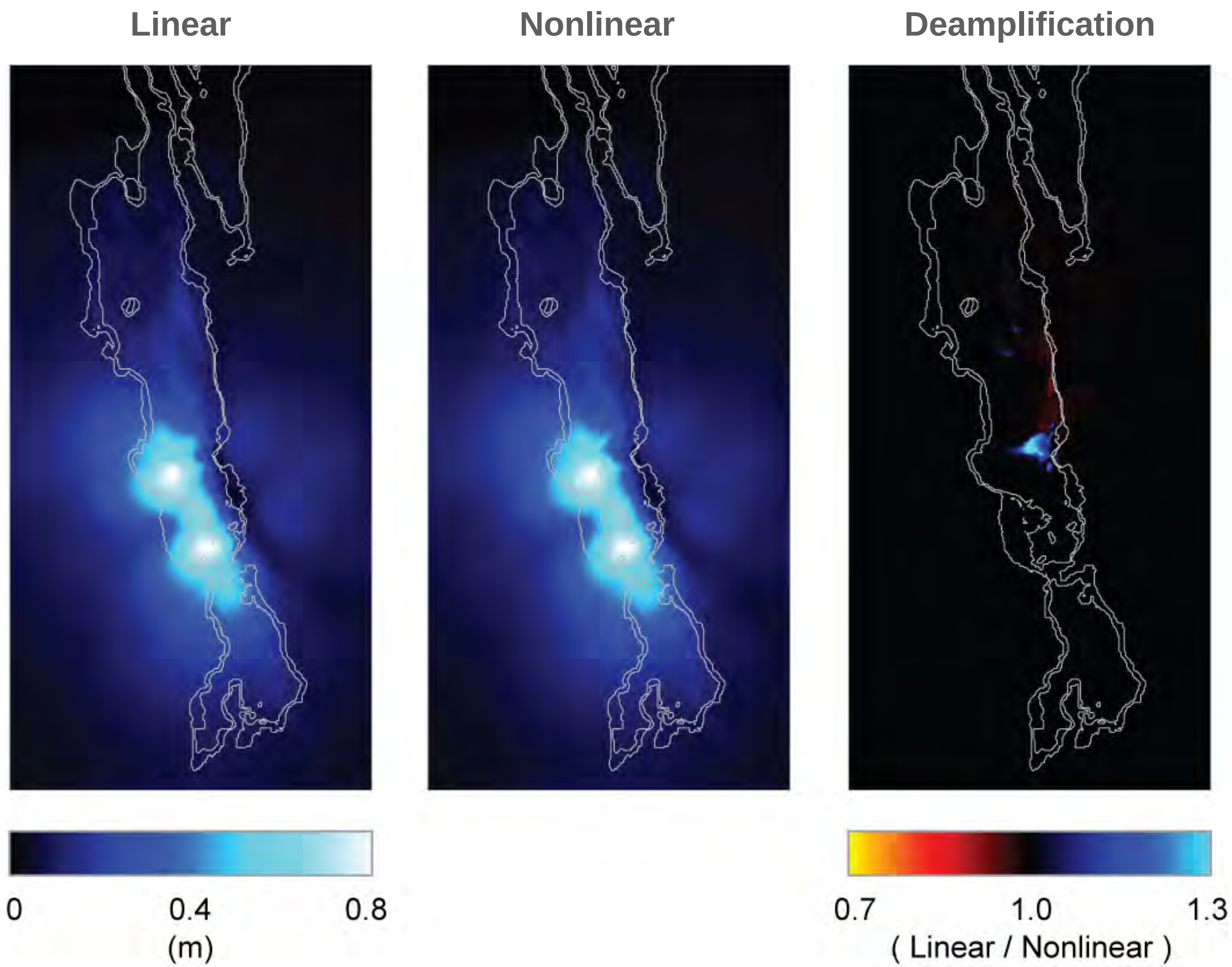

‘Line’ Source — Linear vs Nonlinear A

Velocity

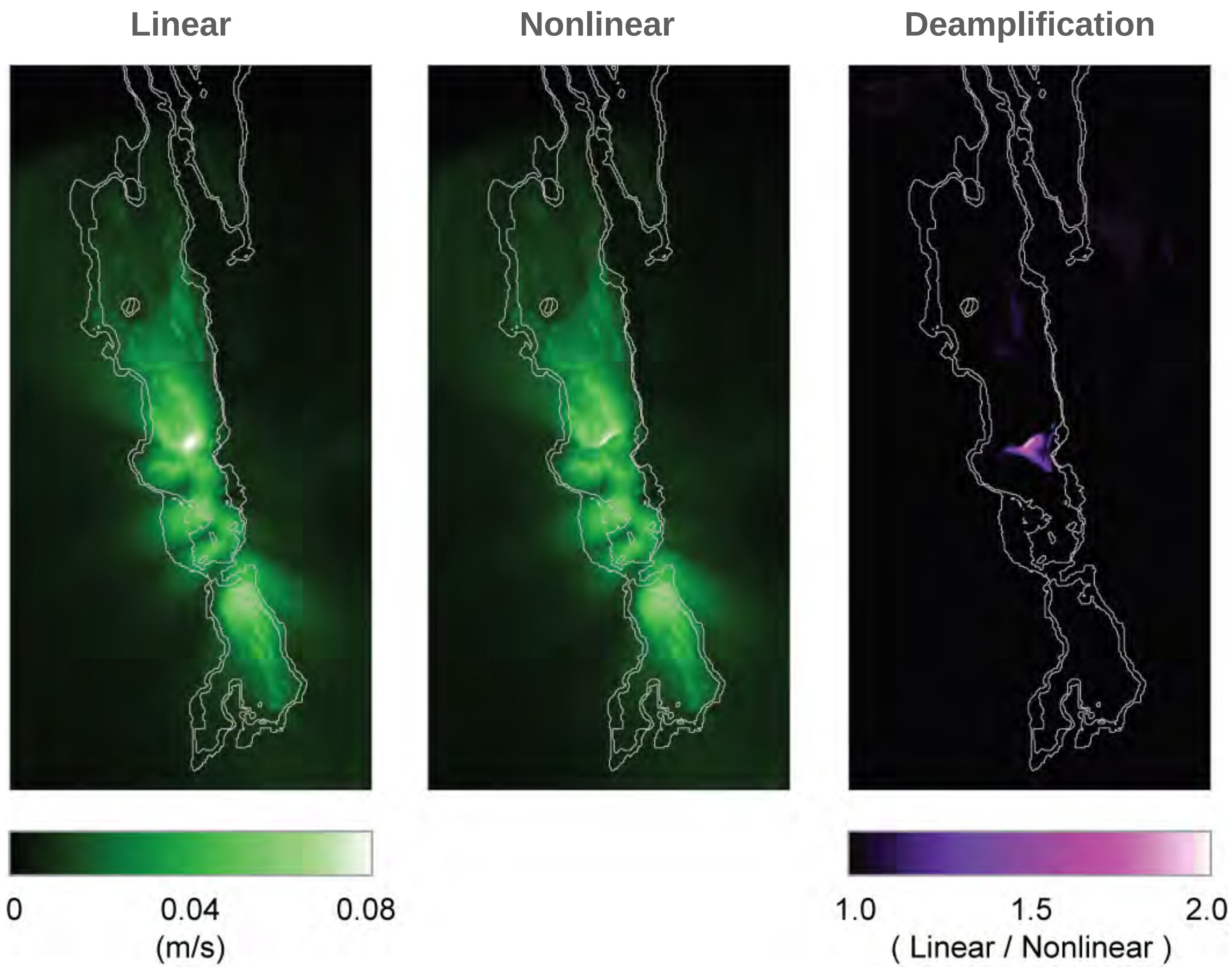

‘Line’ Source — Linear vs Nonlinear A

Acceleration

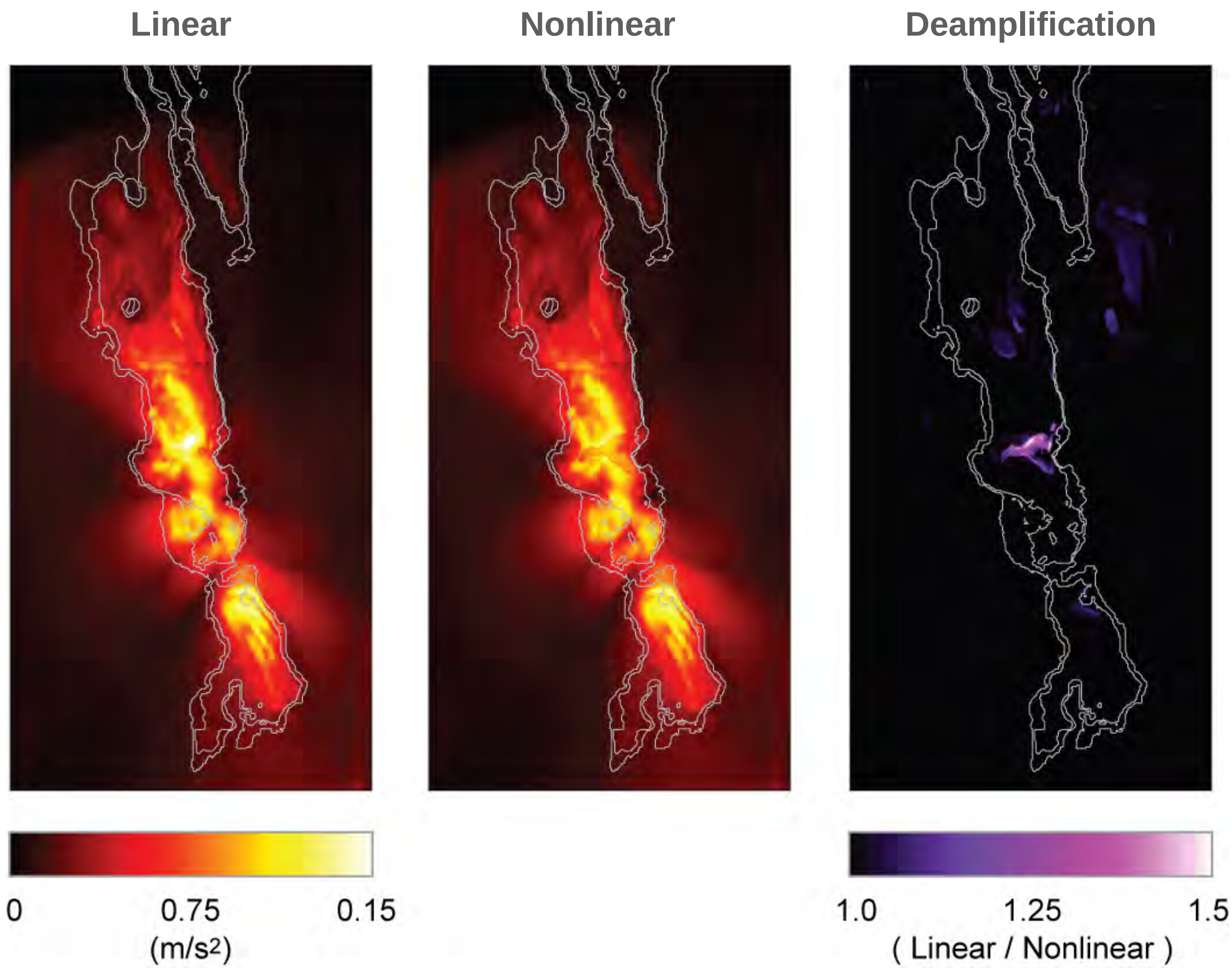

‘Line’ Source — Linear vs Nonlinear B

Displacement

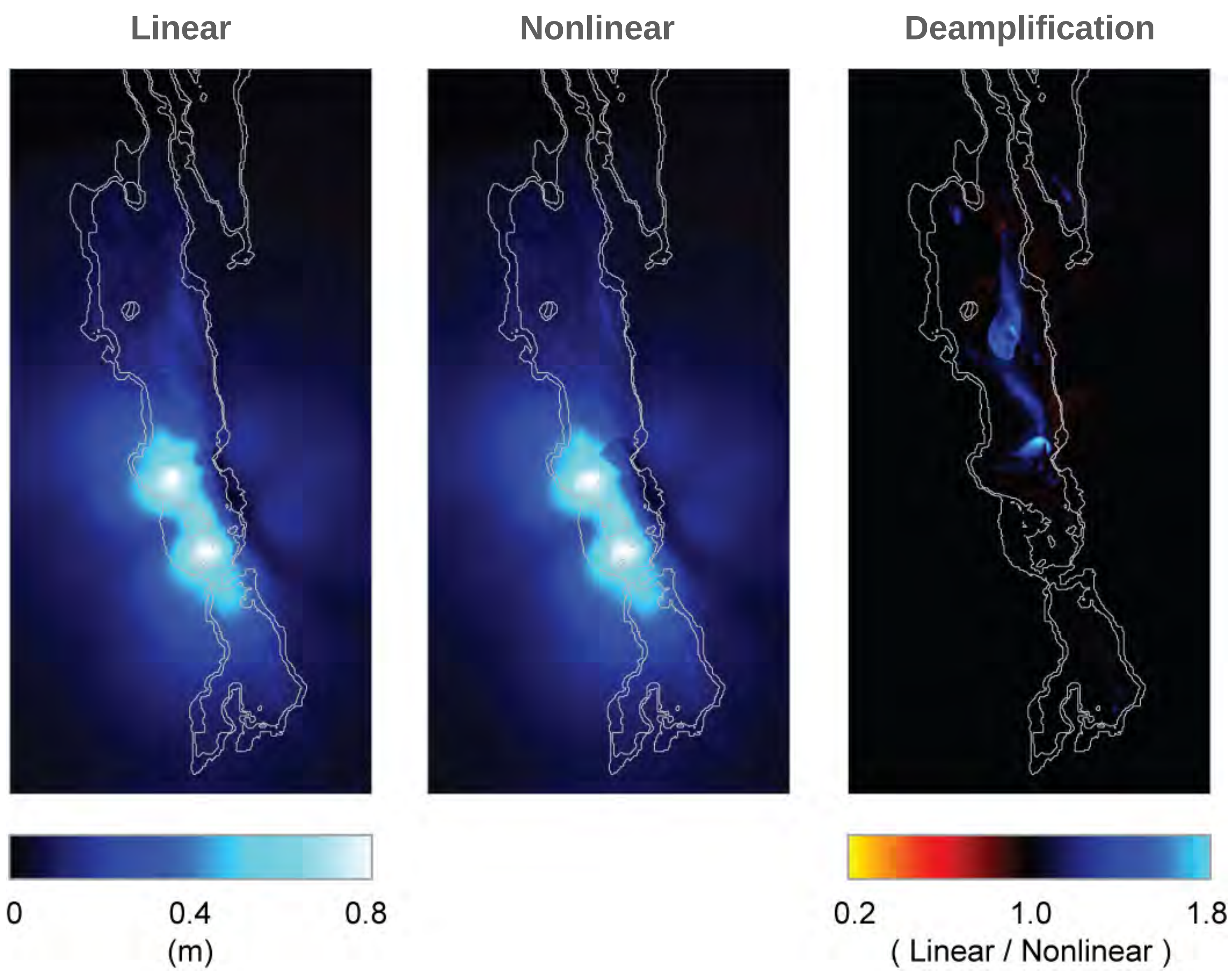

‘Line’ Source — Linear vs Nonlinear B

Velocity

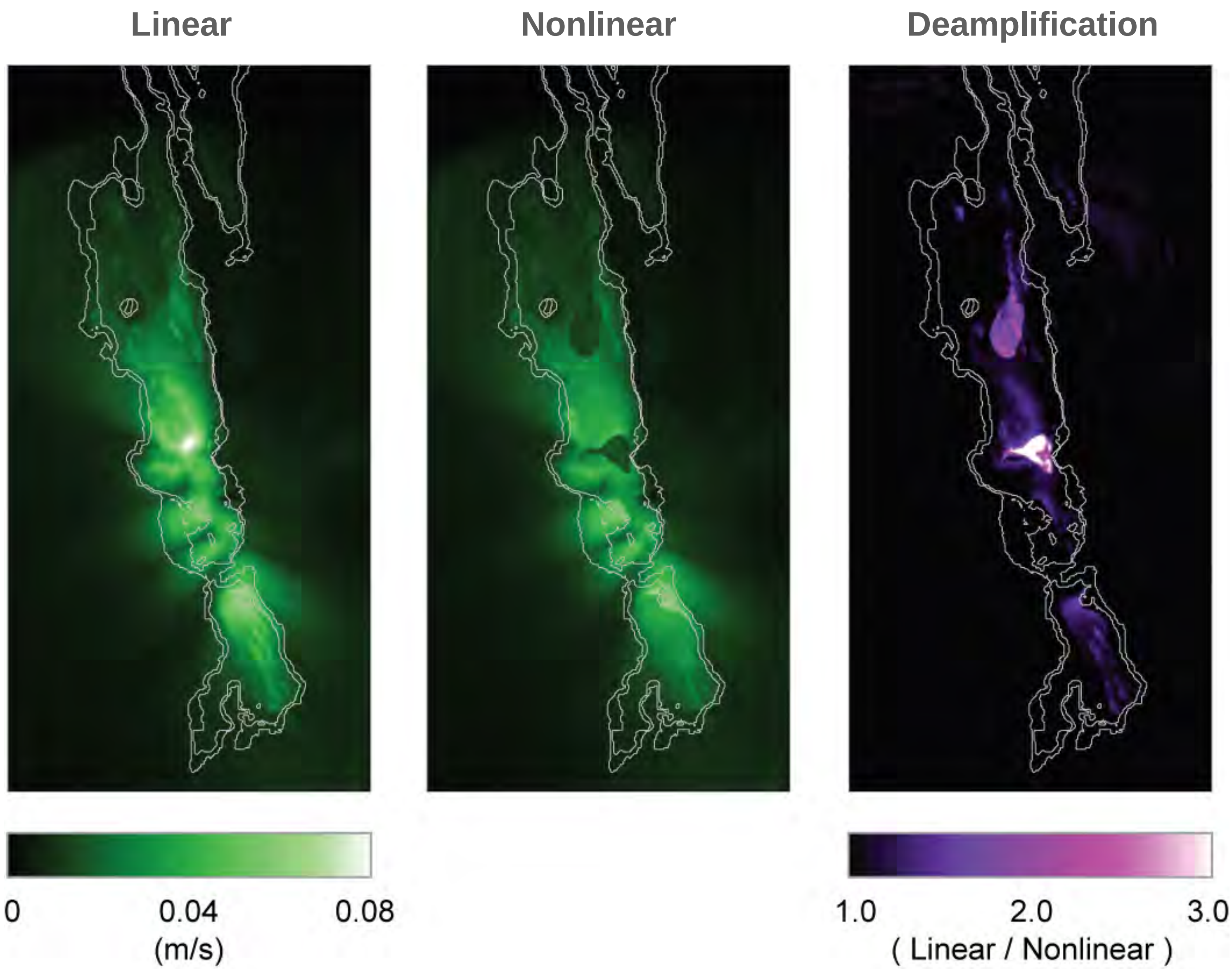

‘Line’ Source — Linear vs Nonlinear B

Acceleration

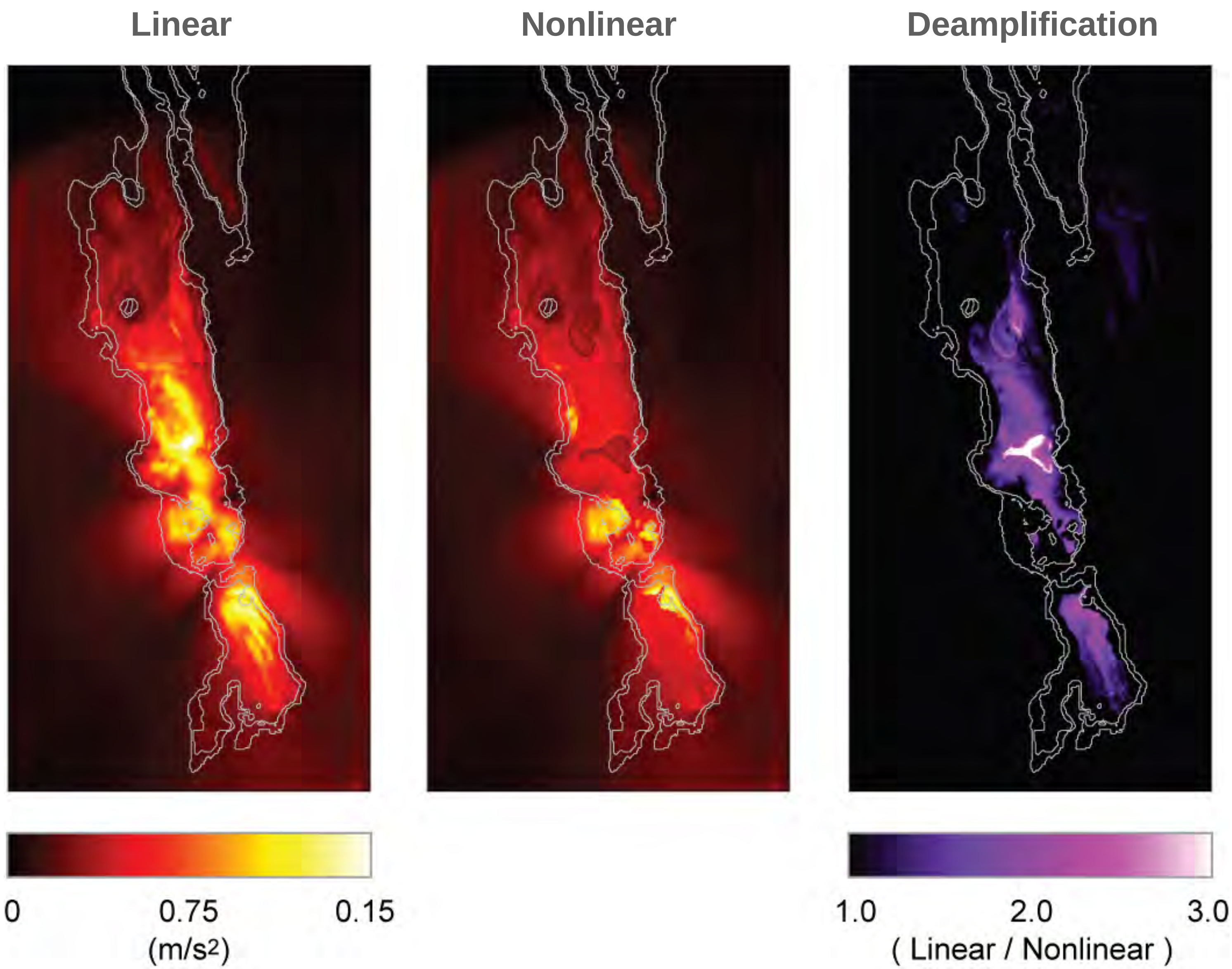

‘Line’ Source — Linear vs Nonlinear C

Displacement

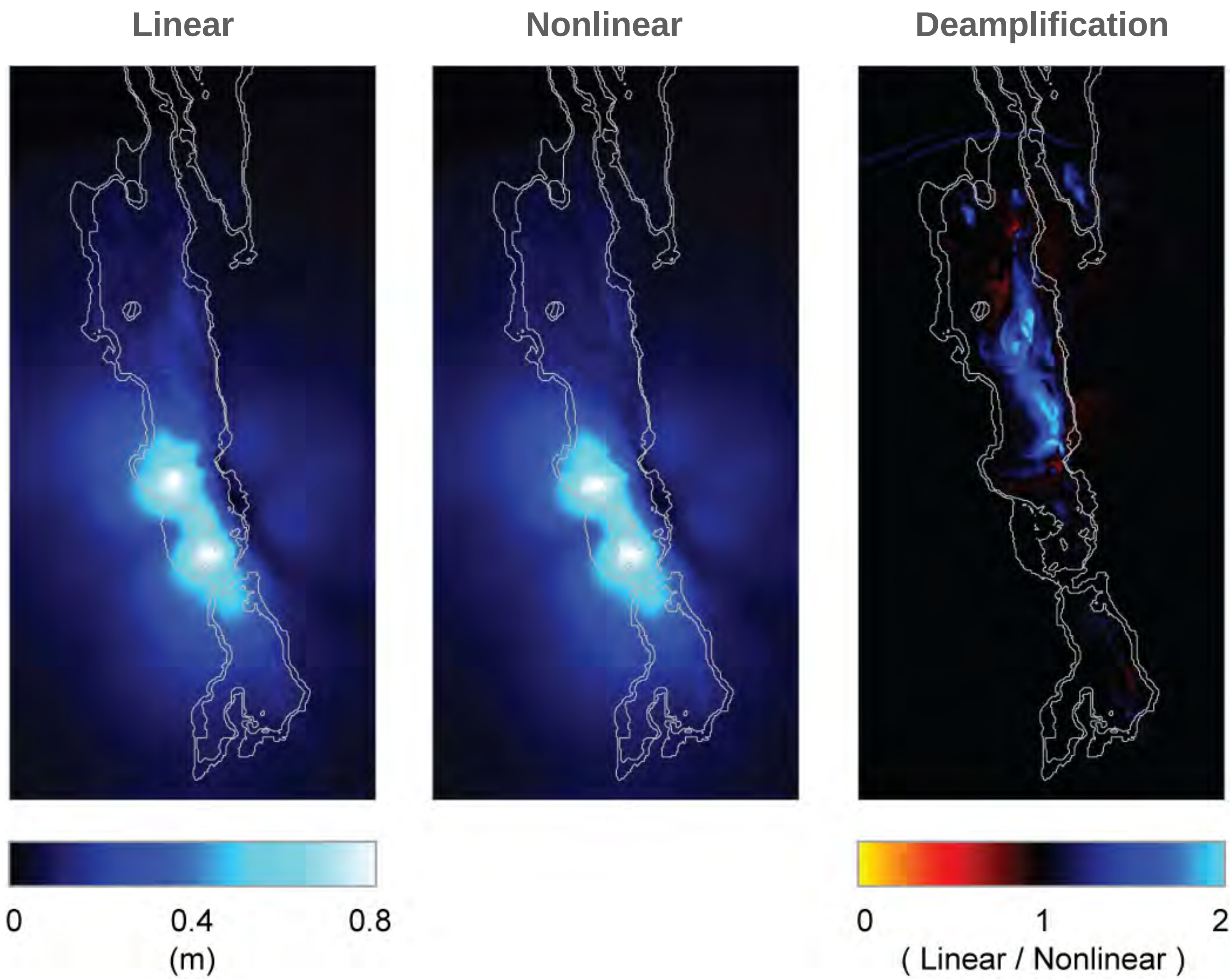

‘Line’ Source — Linear vs Nonlinear C

Velocity

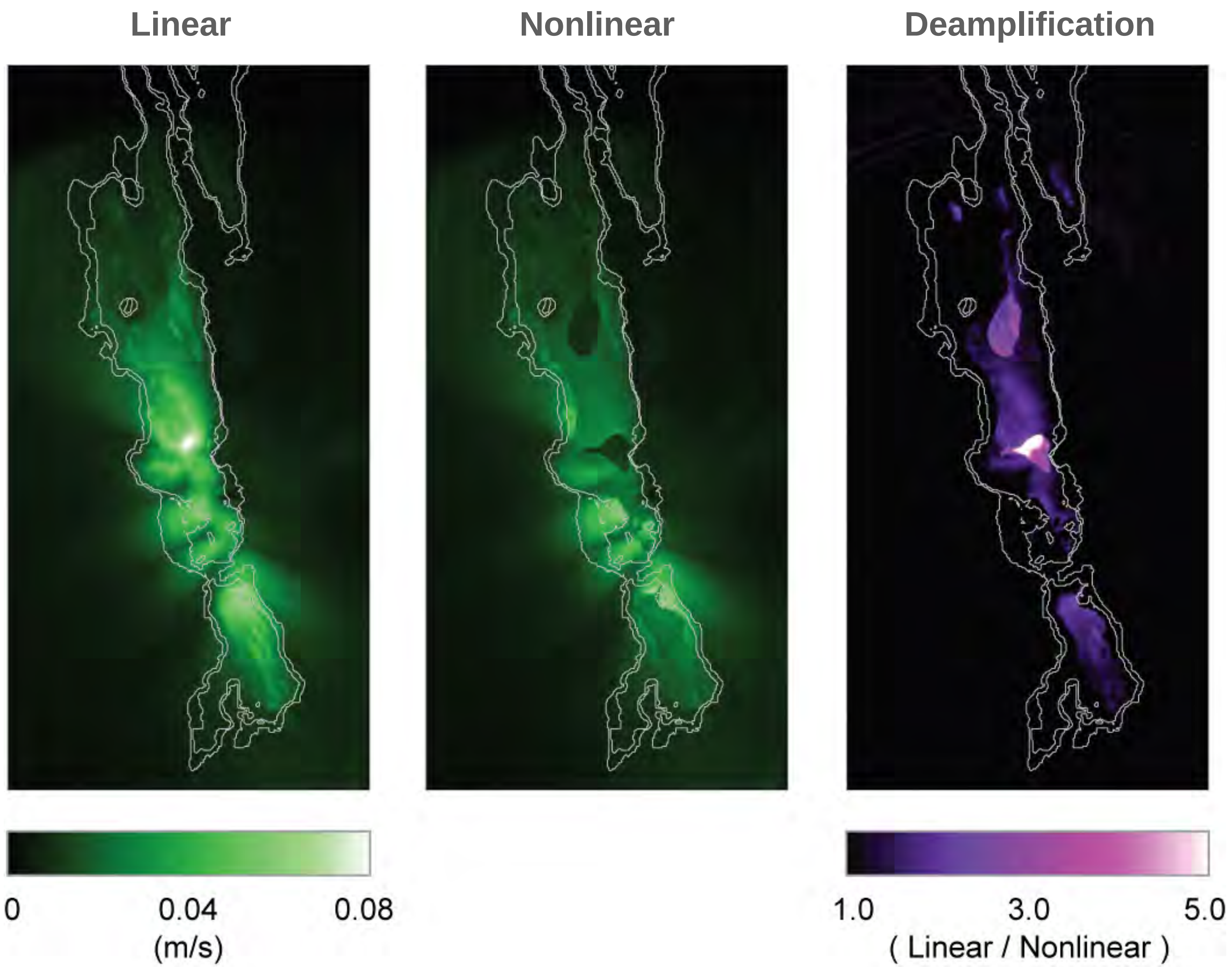

‘Line’ Source — Linear vs Nonlinear C

Acceleration

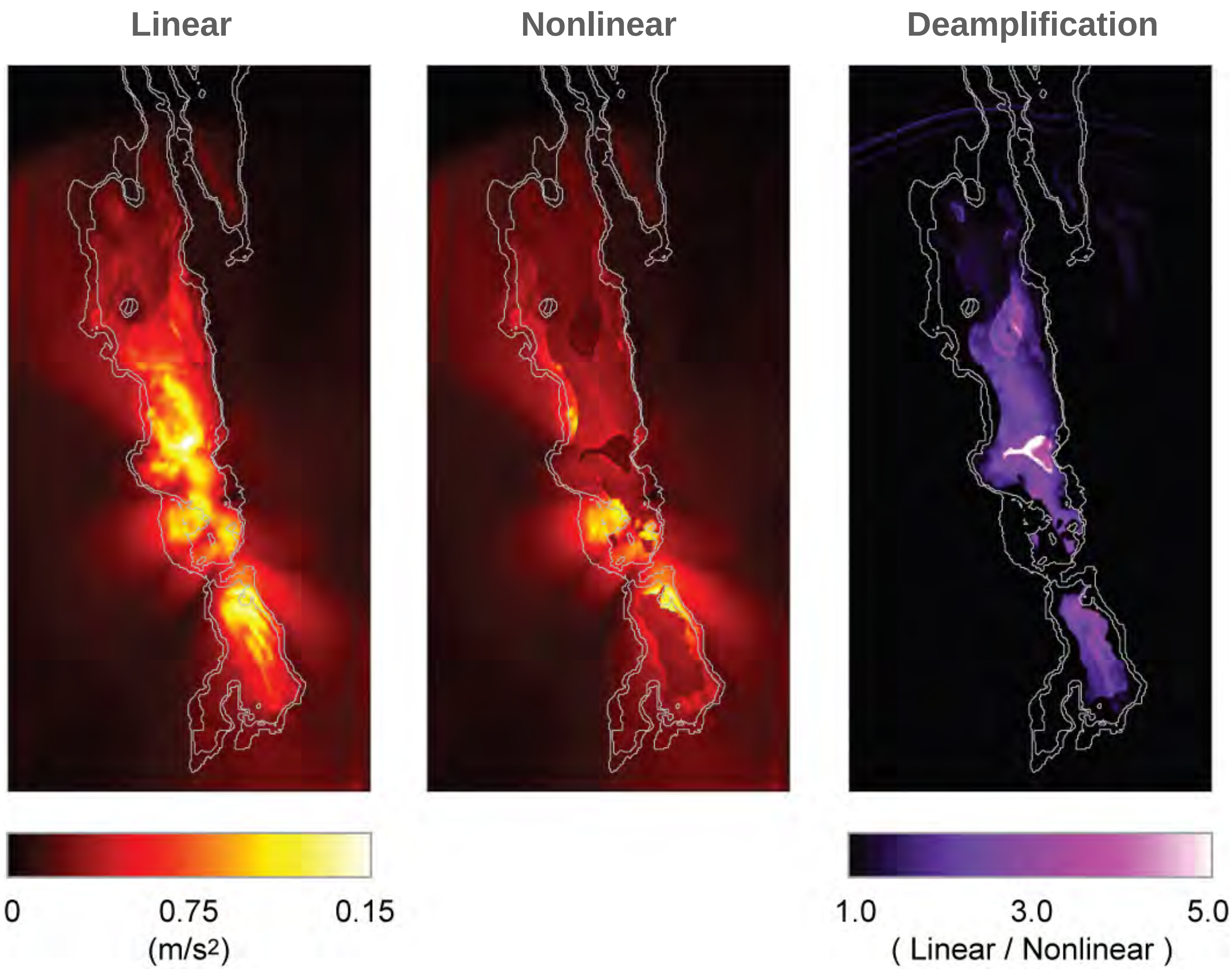

‘Line’ Source — Linear vs Nonlinear A,B,C

Displacement

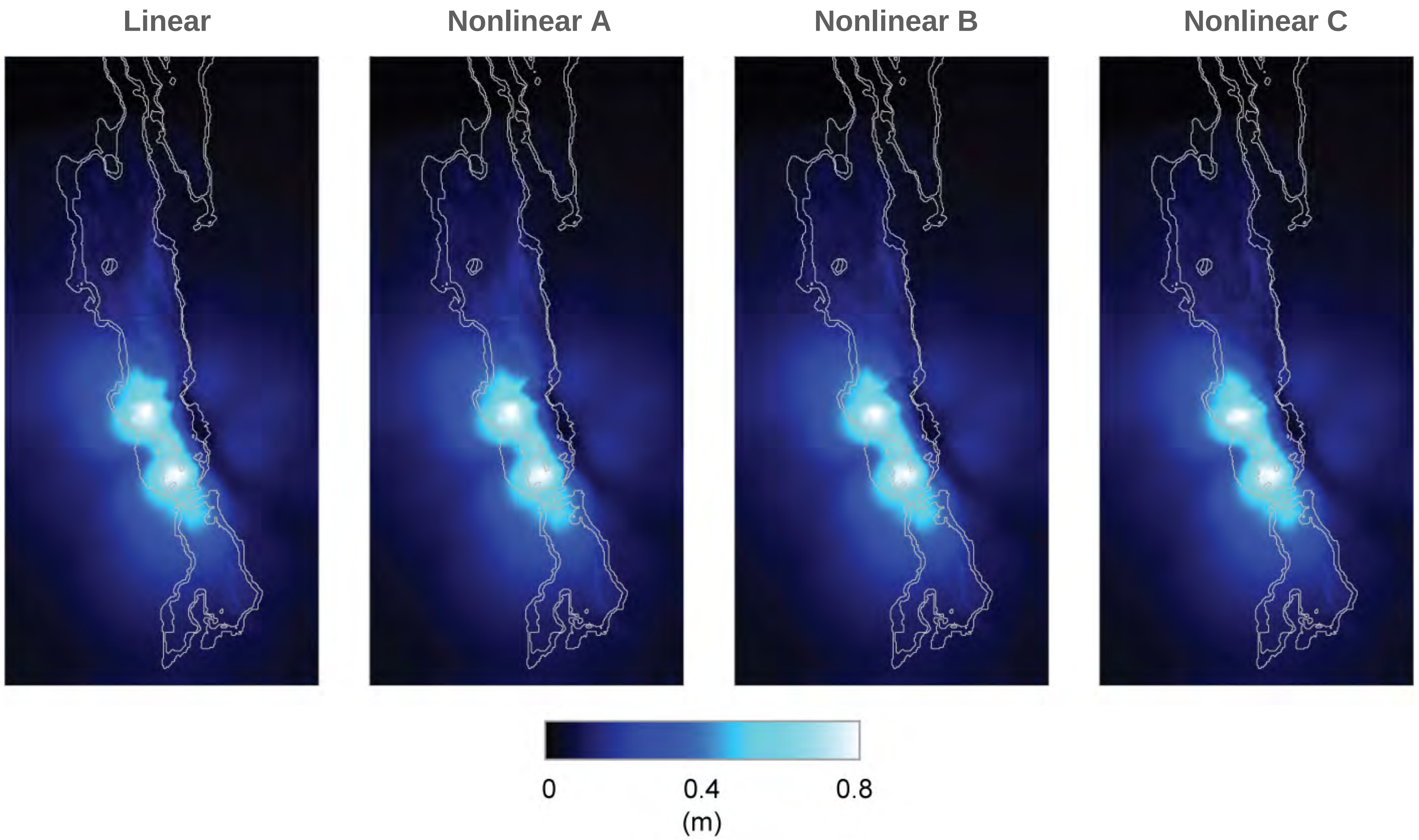

‘Line’ Source — Linear vs Nonlinear A,B,C

Velocity

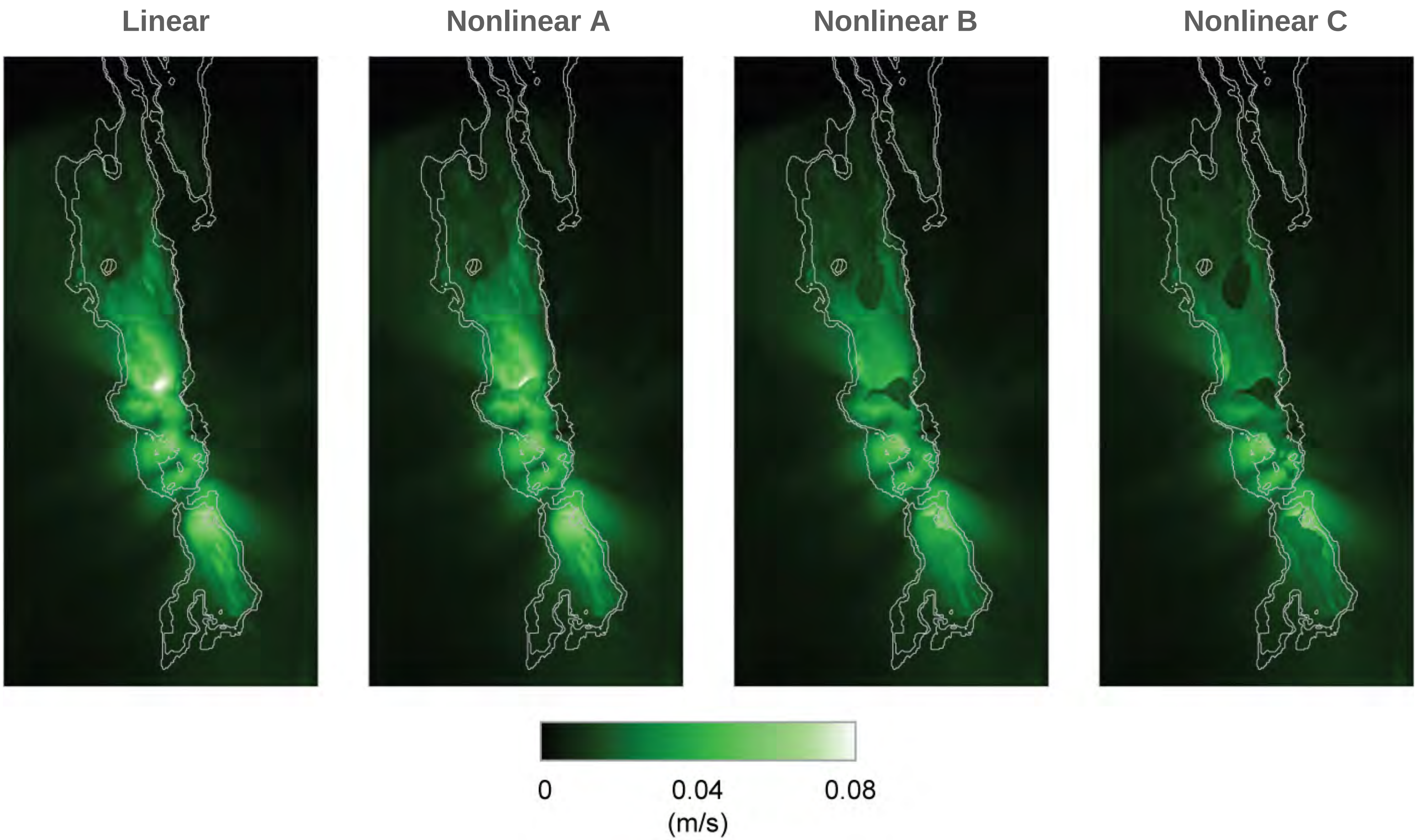

‘Line’ Source — Linear vs Nonlinear A,B,C

Acceleration

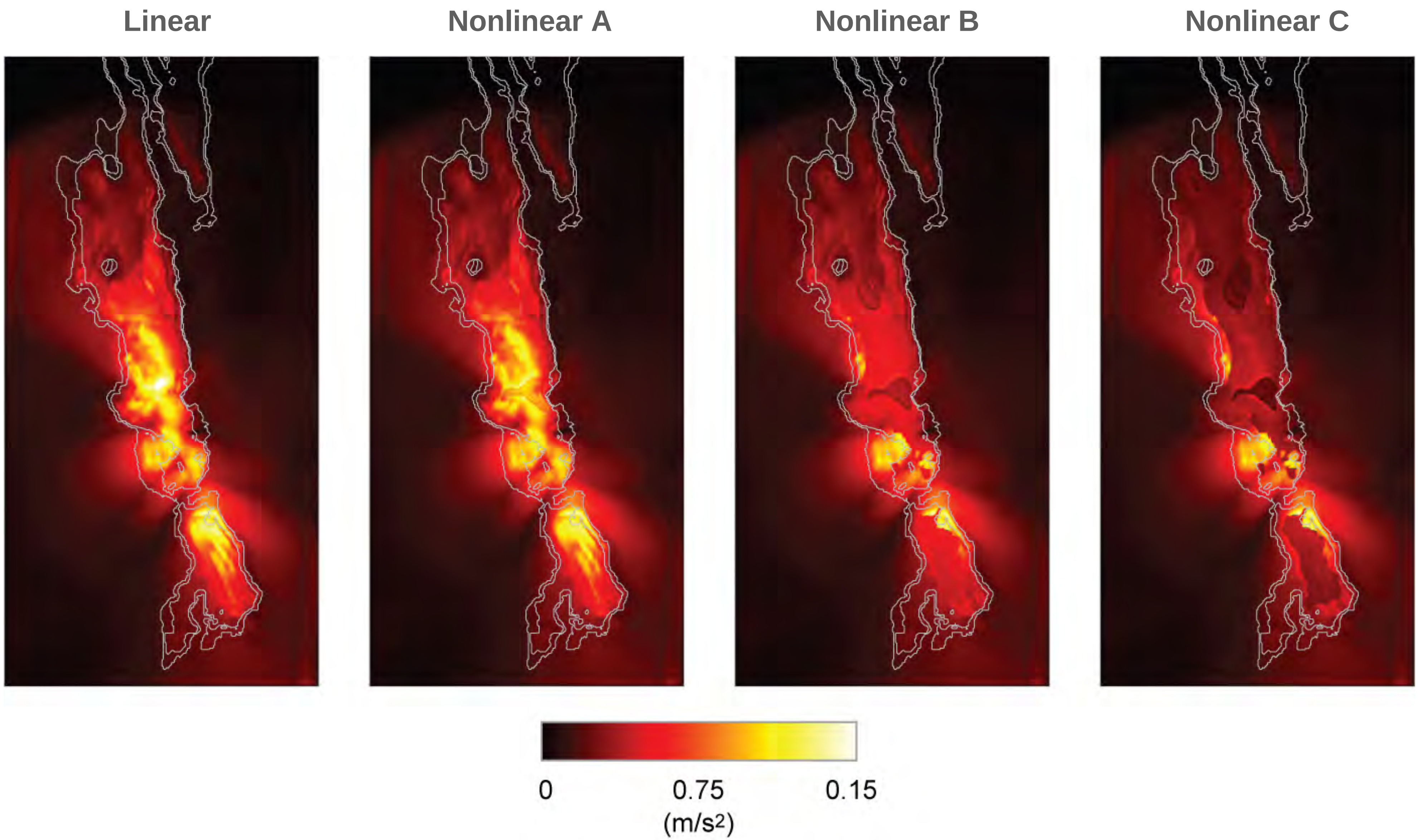

Recording Stations

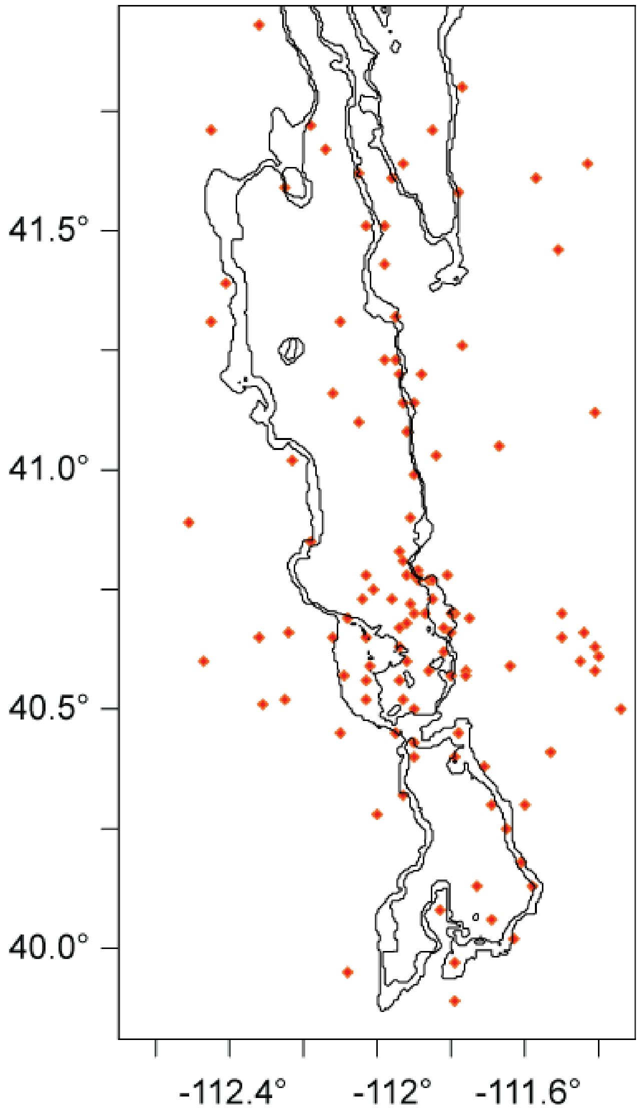

University of Utah
Regional/Urban Seismic Network
(http://www.quake.utah.edu)

119 stations

Synthetic Time Histories

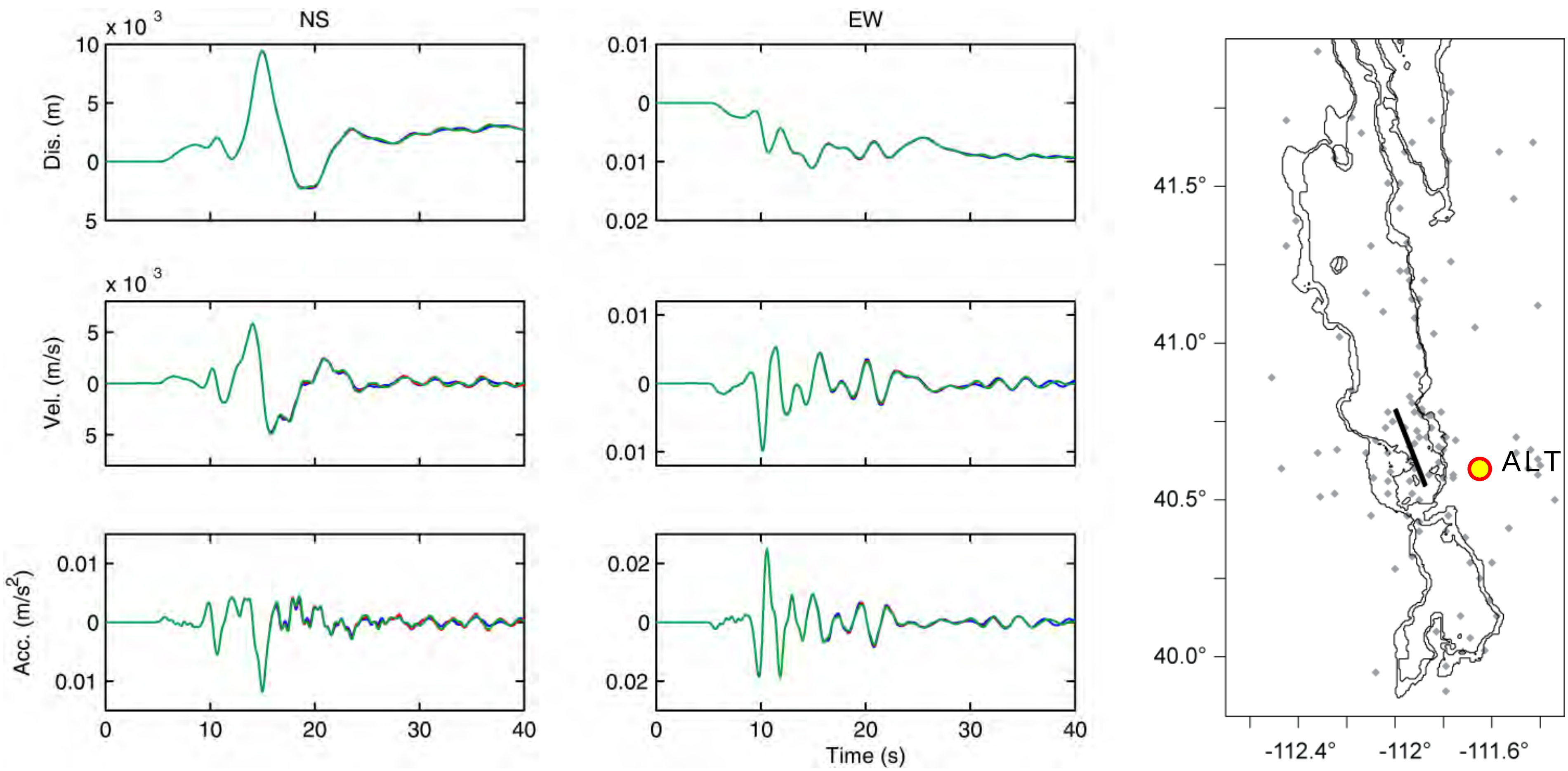

Linear

Nonlinear B

Nonlinear C

Synthetic Time Histories

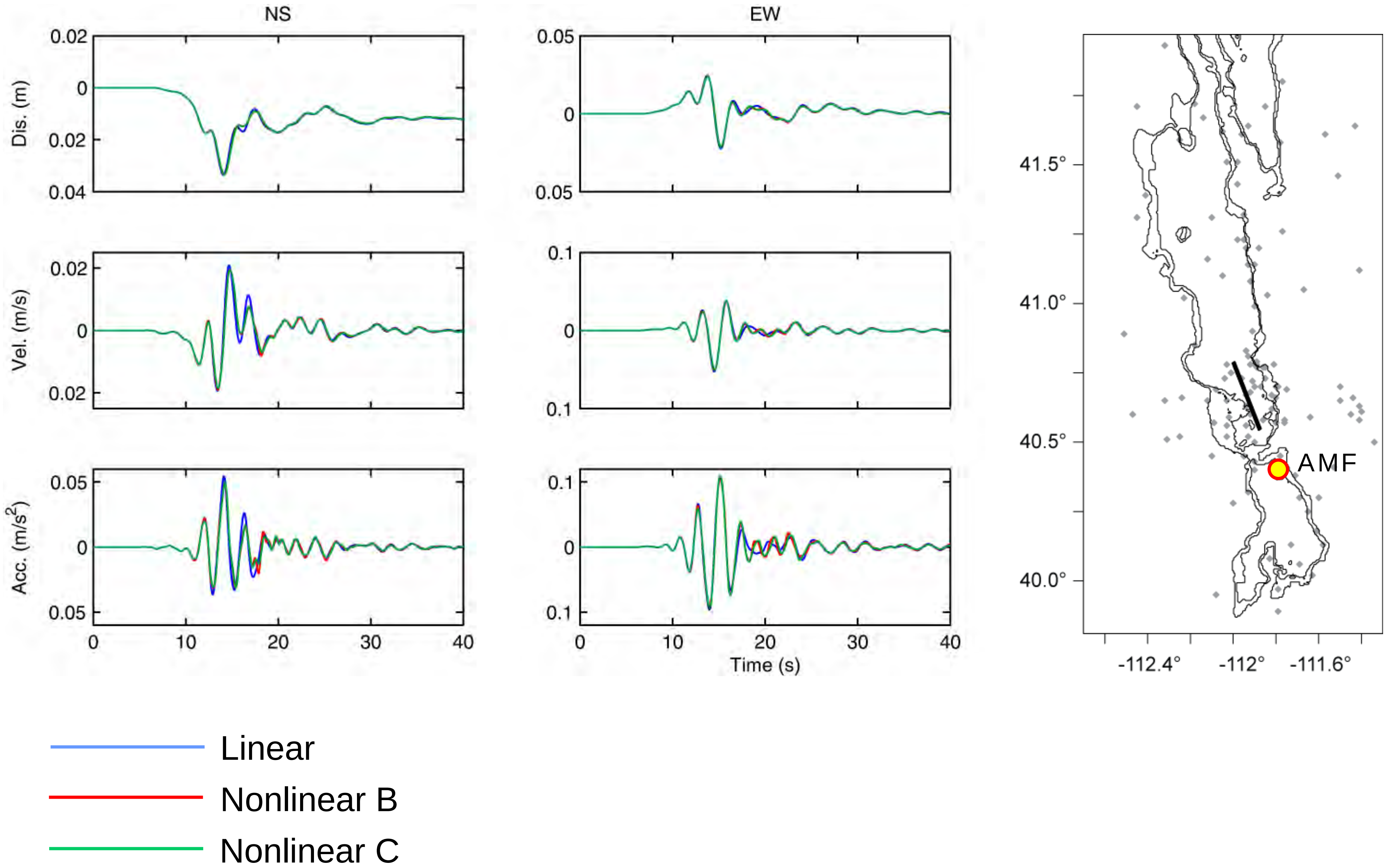

Synthetic Time Histories

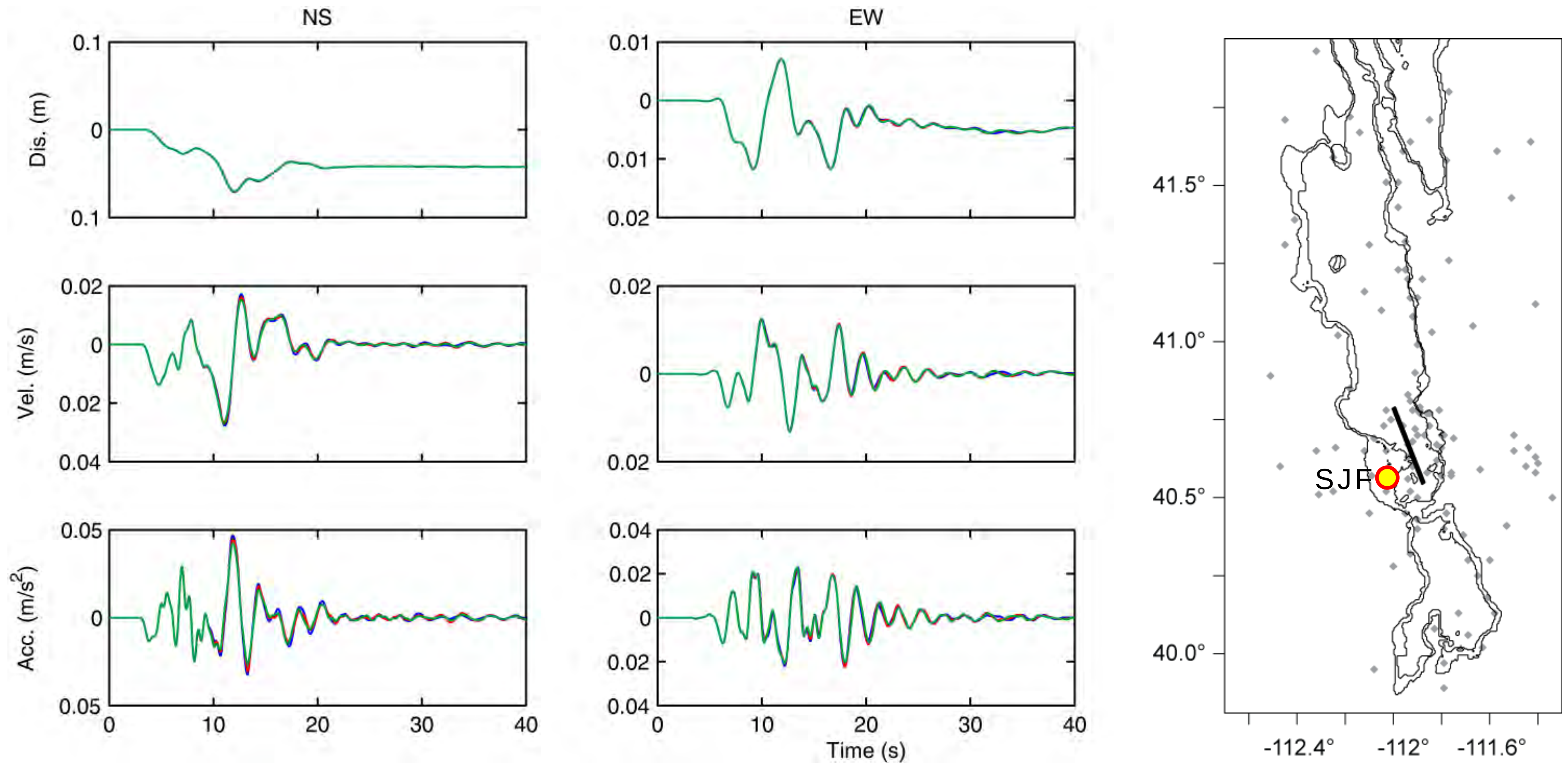

Linear

Nonlinear B

Nonlinear C

Synthetic Time Histories

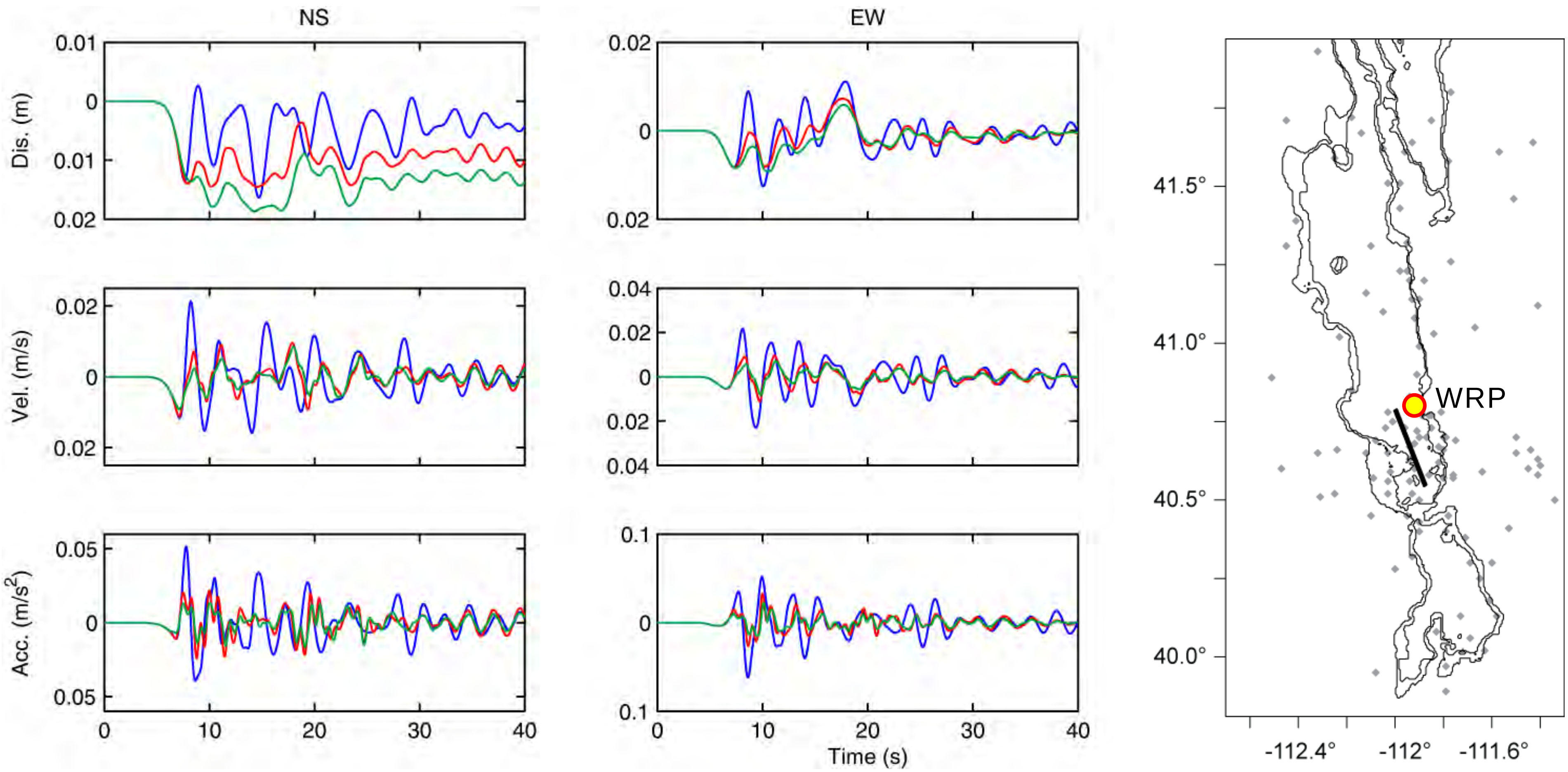

Linear

Nonlinear B

Nonlinear C

Synthetic Time Histories

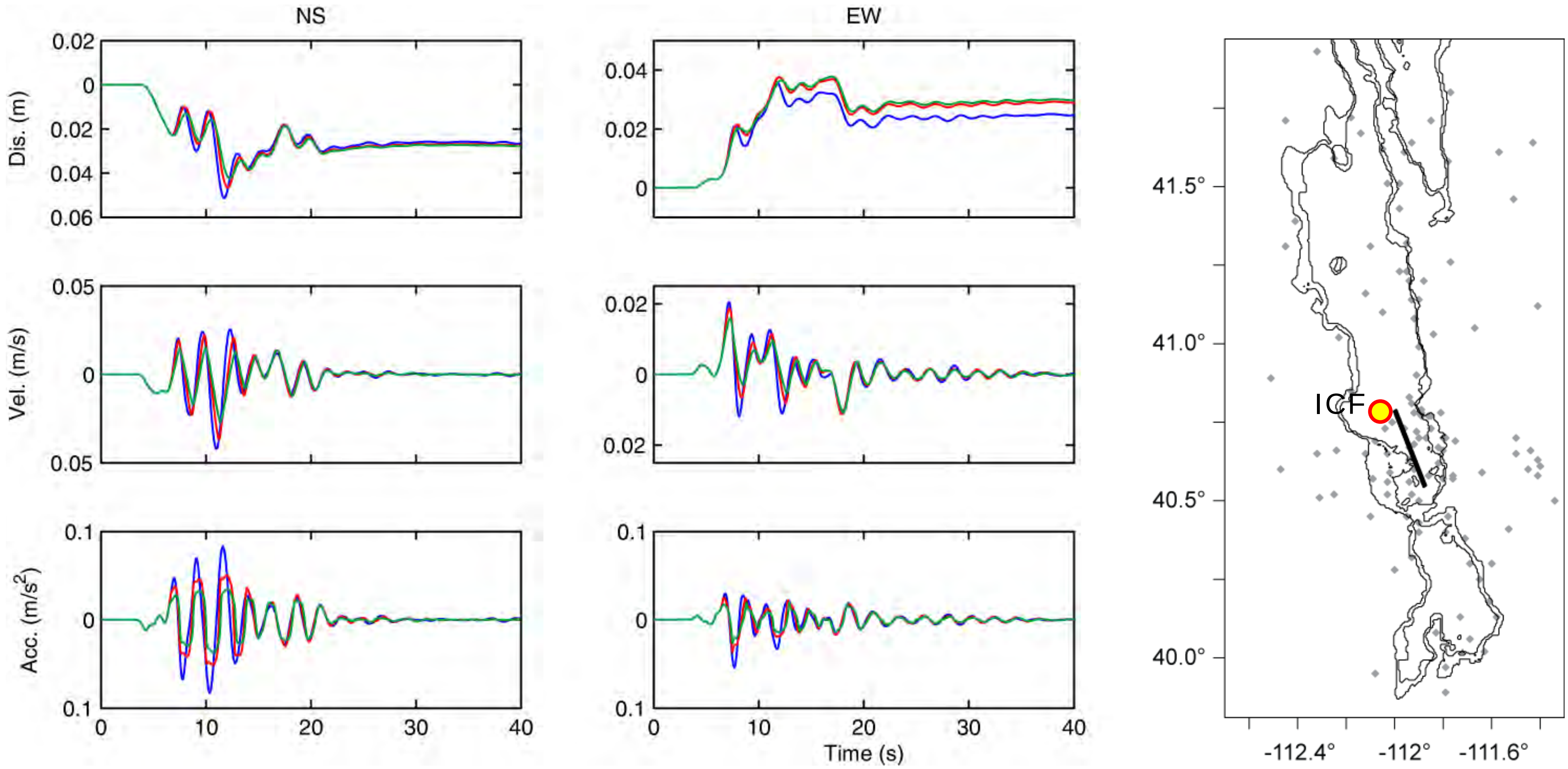

Linear

Nonlinear B

Nonlinear C

Synthetics Fourier Amplitude

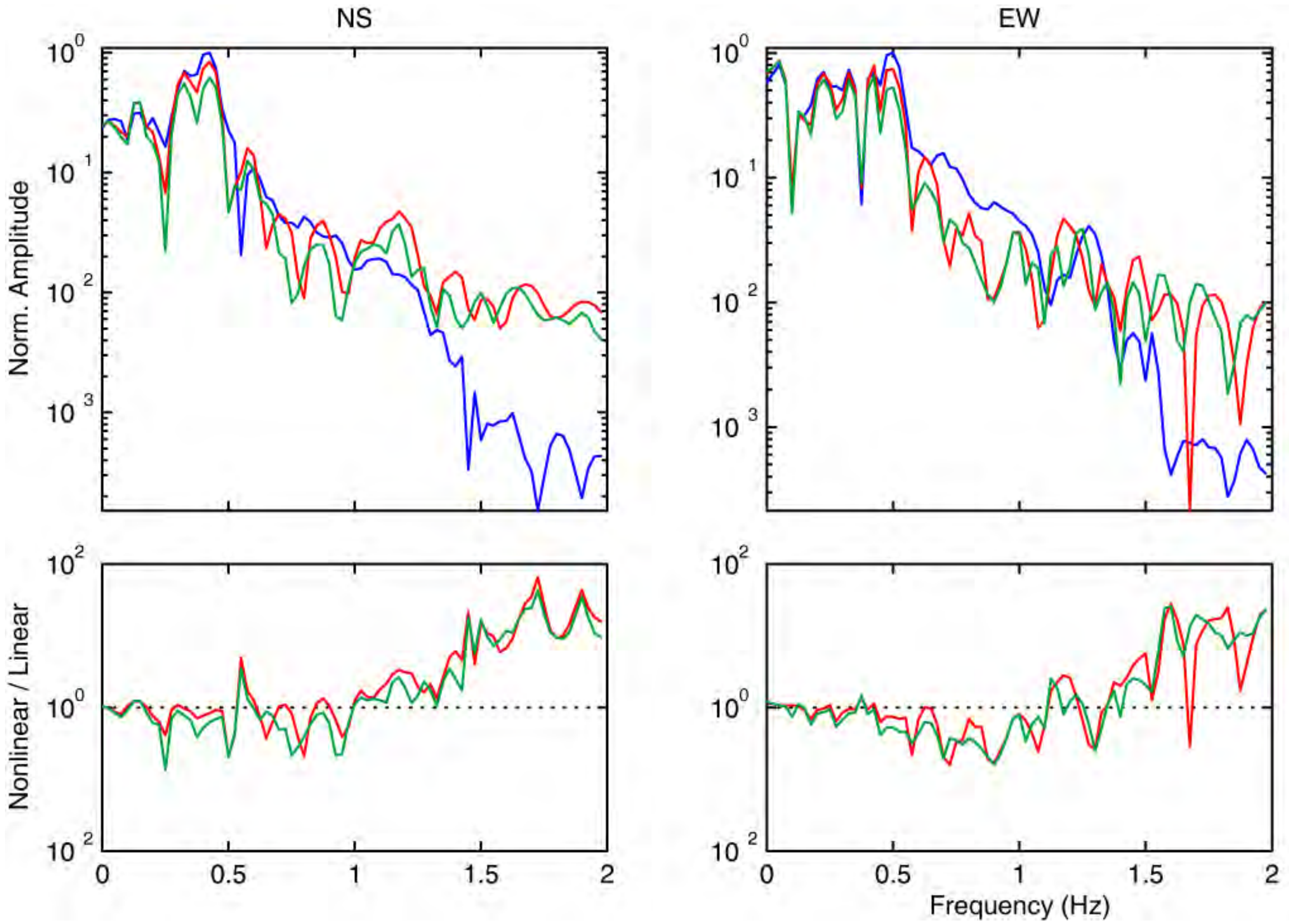

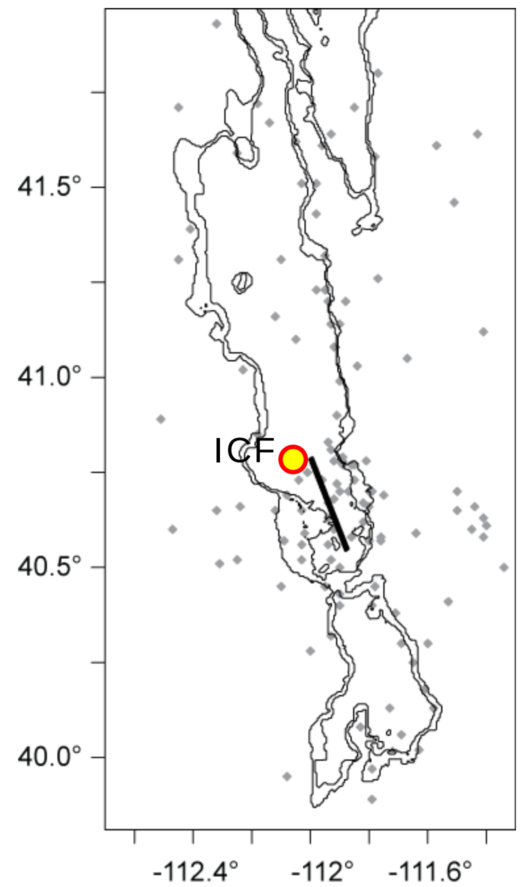

Linear

Nonlinear B

Nonlinear C

Stress-Strain Relationship

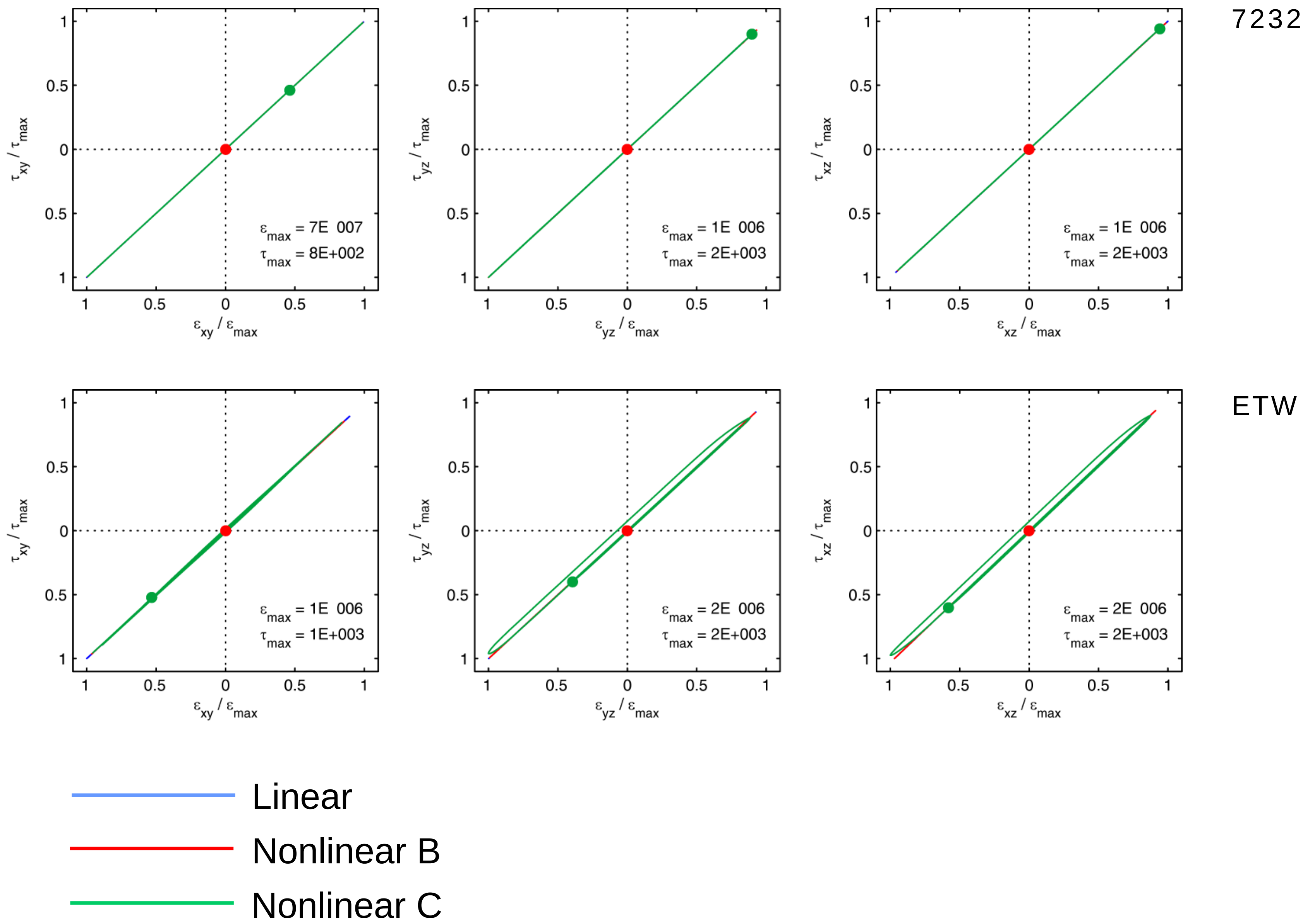

Stress-Strain Relationship

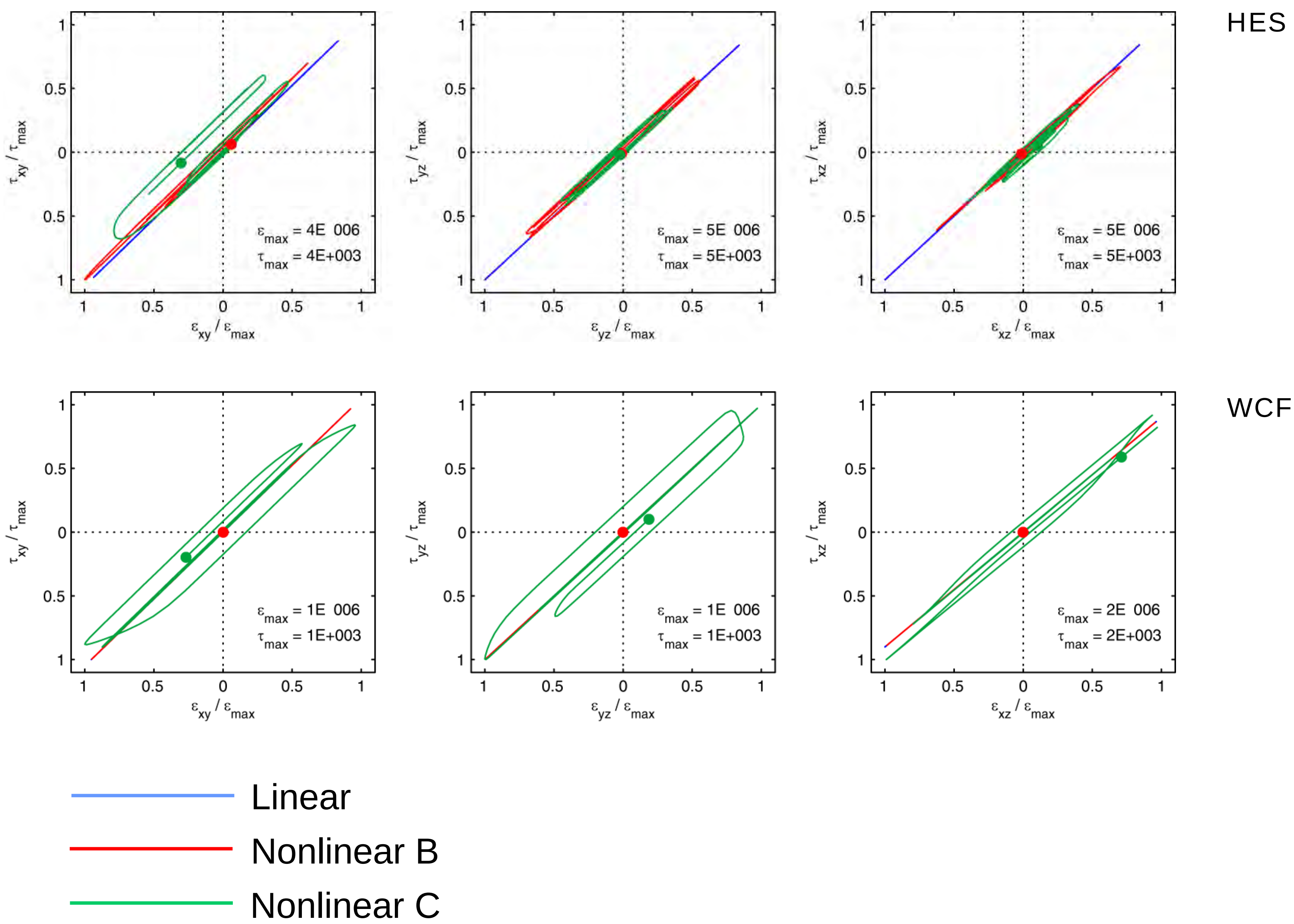

Stress-Strain Relationship

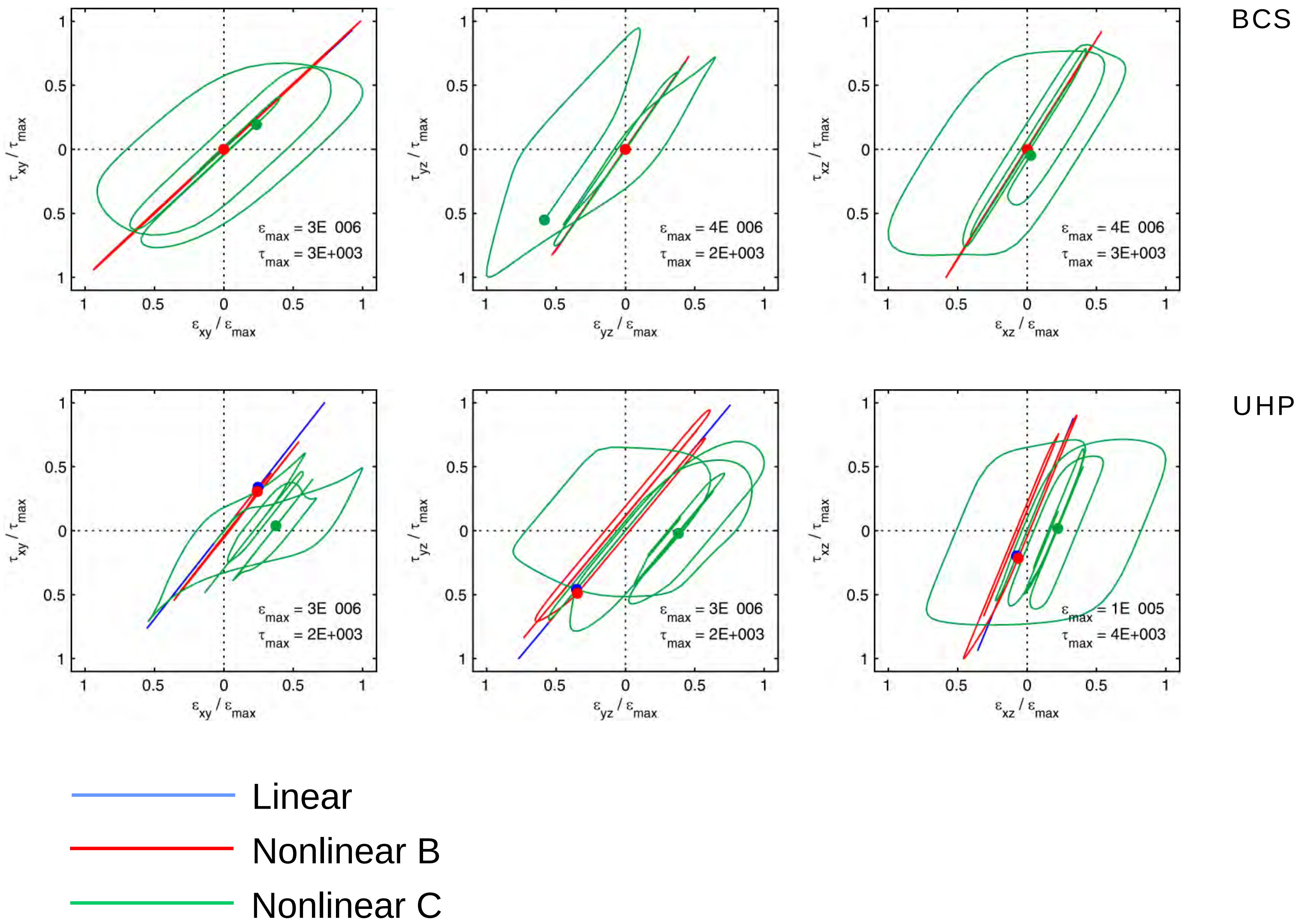

Stress-Strain Relationship

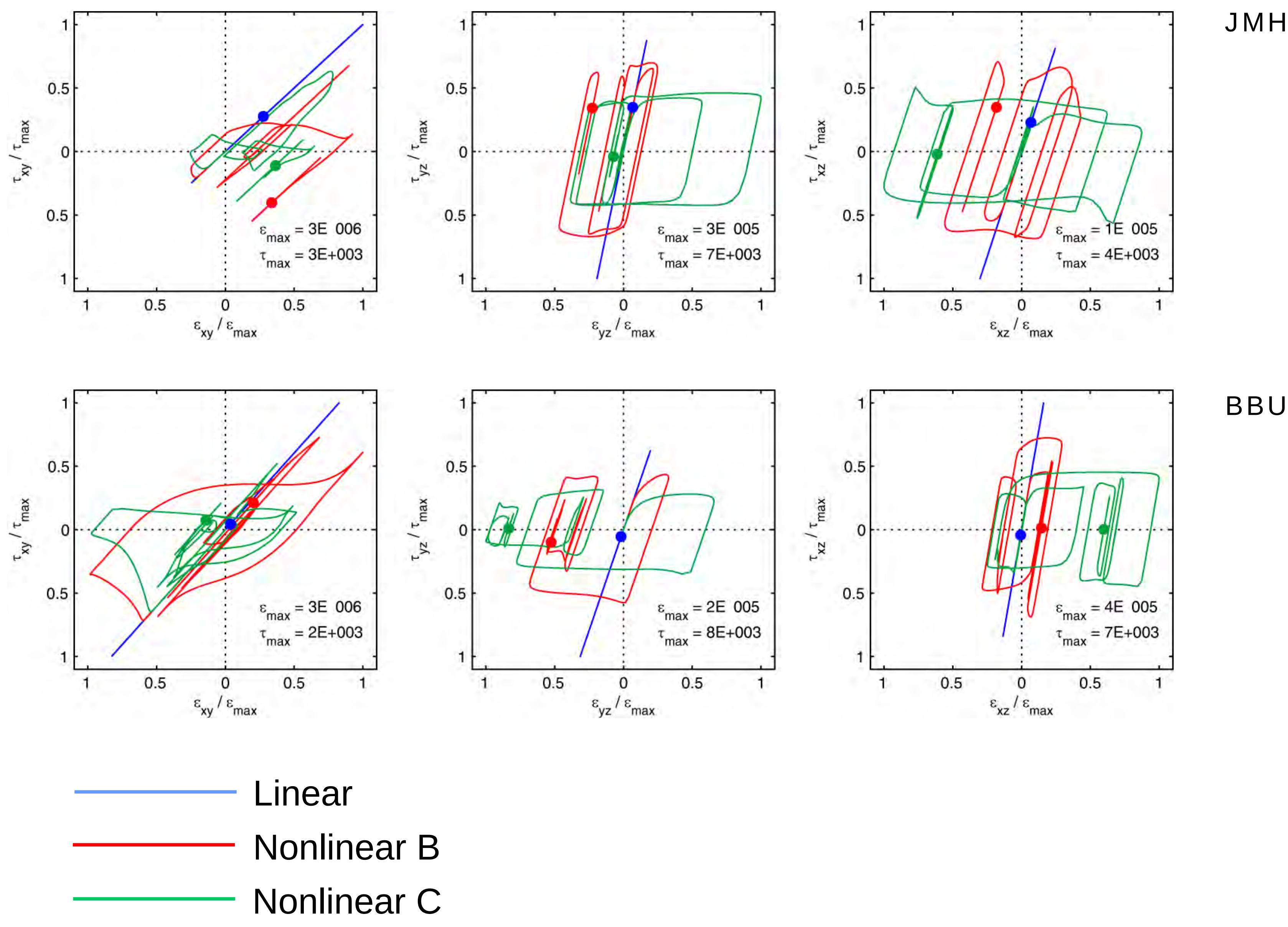

Status Recap and Plan Ahead

- Started in late September 2010
- Large scale model 120 km x 240 km x 60 km
- Linear simulation at 1Hz and 100 m/s
- Multiple nonlinear simulations at 0.5 Hz and 500 m/s
- Thus far, results suggest that the largest nonlinear behavior is well localized near the fault, but peak velocities and accelerations are substantially reduced throughout the entire basin.

- Need to define a smaller model 80 km x 80 km x 40 km for nonlinear simulations at higher frequencies (2 Hz) and have all material with Vs = 100–500 m/s be nonlinear
- Need alternative source models
- Will need several runs to adjust soil parameters
- 6 months to finish and produce final report.

Three-Dimensional Nonlinear Earthquake Ground Motion Simulation in the Salt Lake basin

using the Wasatch Front Community Velocity Model

THE
QUAKE Group
AT **Carnegie Mellon University**

Ricardo Taborda and Jacobo Bielak
Computational Seismology Laboratory
Department of Civil and Environmental Engineering
Carnegie Mellon University

A research project sponsored by:
USGS
science for a changing world

Characterization of Shallow S-Wave Velocity Structures in Southwestern Utah

Simin Huang, Kris Pankow, Michael Thorne, and Bill Stephenson

Special thanks to Bill Lund, Tyler Knudsen, and Gary Christenson

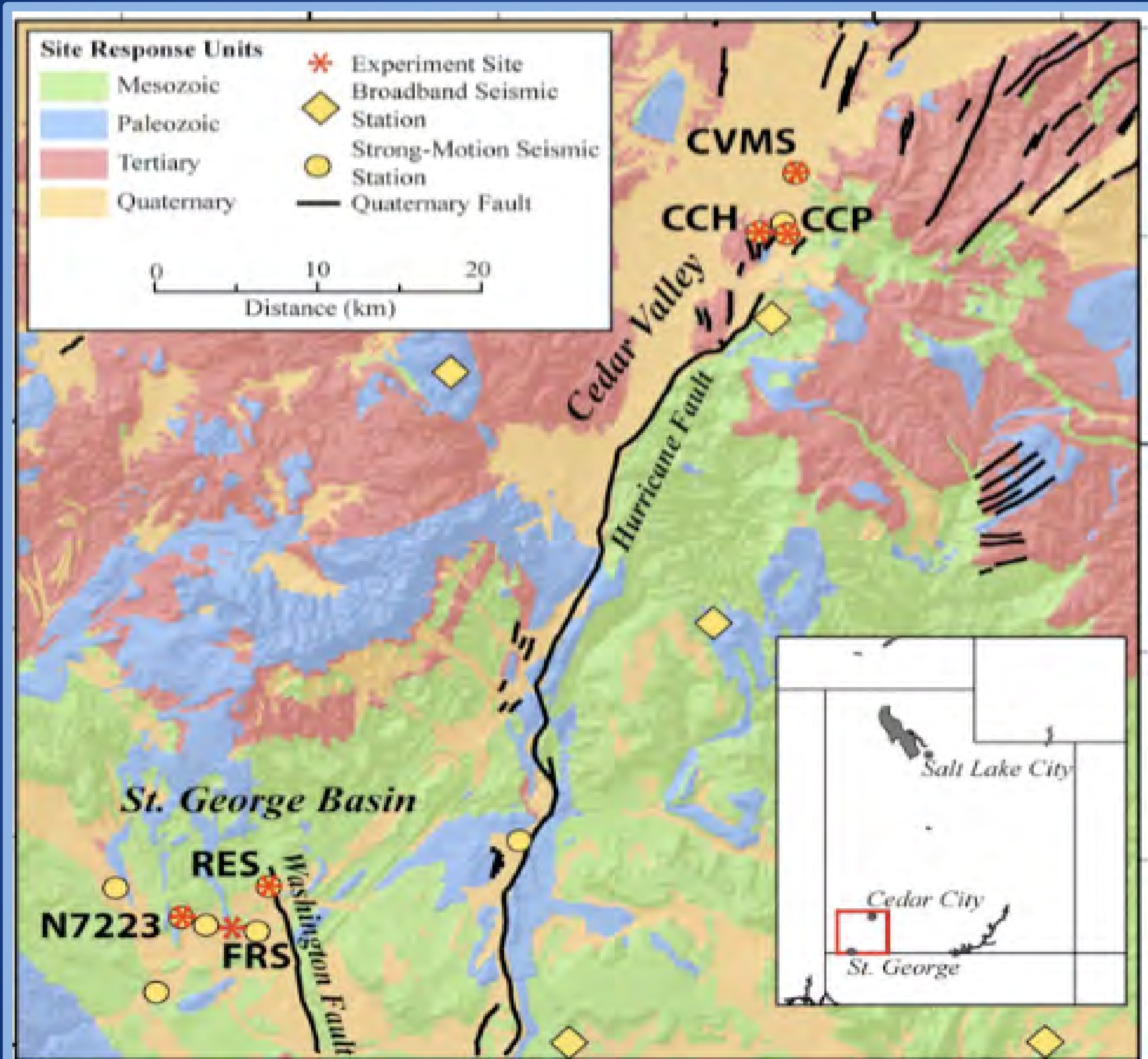

Site Response Units
Mesozoic
Paleozoic
Tertiary
Quaternary
Experiment Site
Broadband Seismic Station
Strong-Motion Seismic Station
Quaternary Fault
0
10
20
Distance (km)
CVMS
CCH
CCP
Cedar Valley
Hurricane Fault
St. George Basin
RES
N7223
FRS
Washington Fault
Salt Lake City
Cedar City
St. George

Table 1. Station Locations

Site		Location Lat	Location Lon	Geologic Description
CCH	Cedar City Church	37.66°	-113.09°	Tertiary conglomerate with interbedded basalt flows[1]
CCP	Cedar City High School	37.66°	-113.07°	Quaternary piedmont-slope alluvium—silt, sand, and gravel[1]
CVMS	Canyon View Middle School	37.71°	-113.06°	Quaternary piedmont-slope alluvium—silt, sand, and gravel[1]
FRS	Fossil Track Intermediate School	37.10°	-113.54°	Shallow Jurassic siltstone and sandstone[2]
N7223	Dixie State College	37.10°	-113.57°	Quaternary mixed alluvial and eolian deposits—clay to sand[2]
RES	Riverside Elementary School	37.10°	-113.52°	Quaternary alluvial-stream deposits—clay to small gravel[2]

[1]Rowley *et al.* (2006)
[2]Higgins and Willis (1995)

Data Processing

- Four – station equilateral triangle array

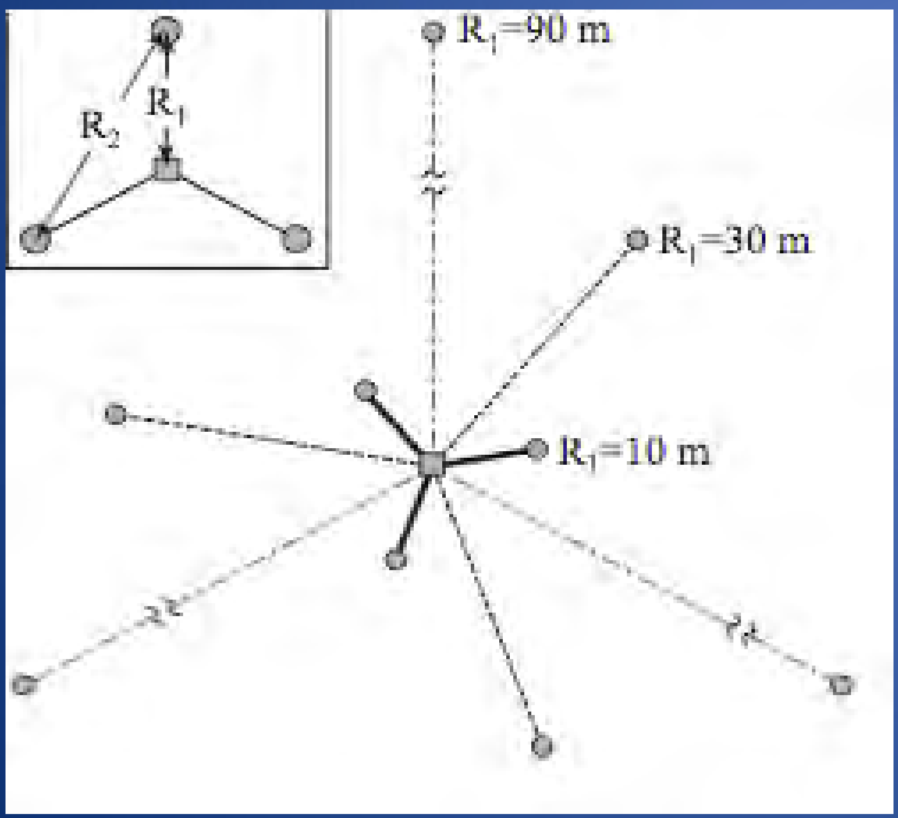

Data Processing

1. Coherency

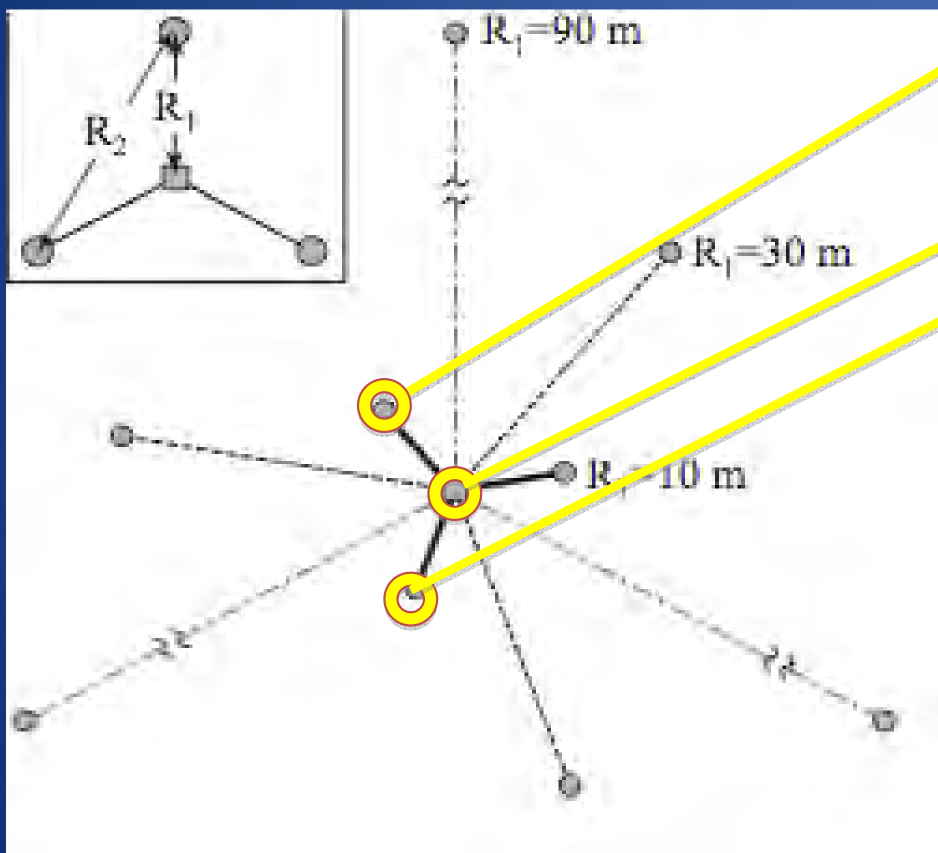

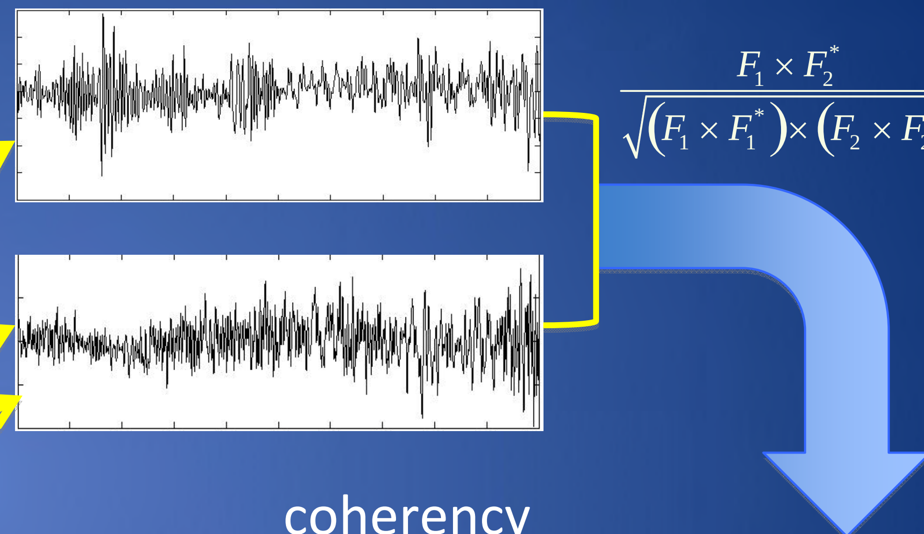

$$\frac{F_1 \times F_2^*}{\sqrt{\left(F_1 \times F_1^*\right) \times \left(F_2 \times F_2^*\right)}}$$

coherency

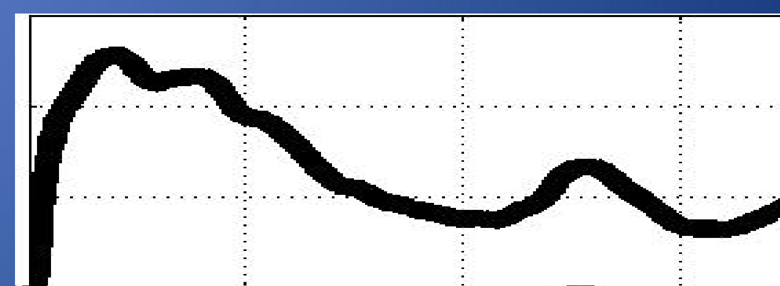

Jo Bessel Function

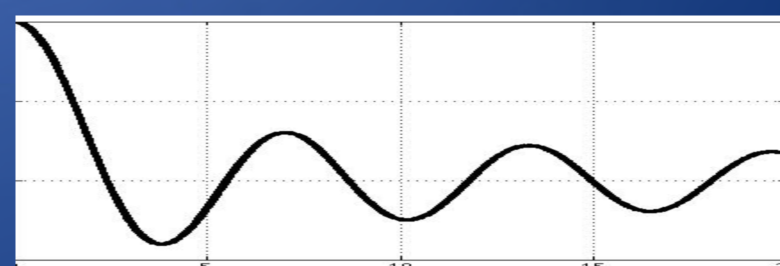

Data Processing

2. Phase Velocity Dispersion curve

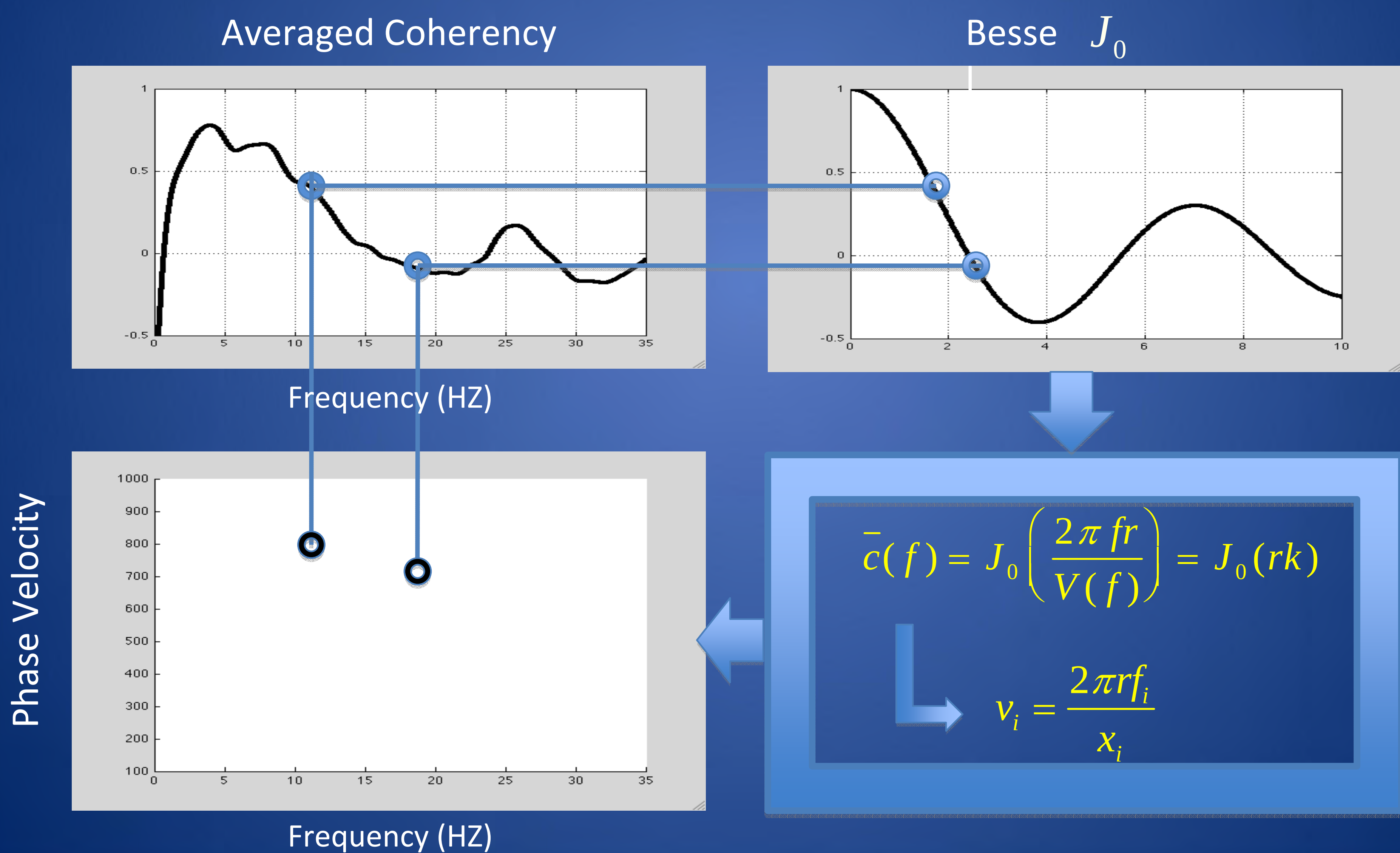

Data Processing

3. HVSR (Horizontal over Vertical Spectral Ratio)

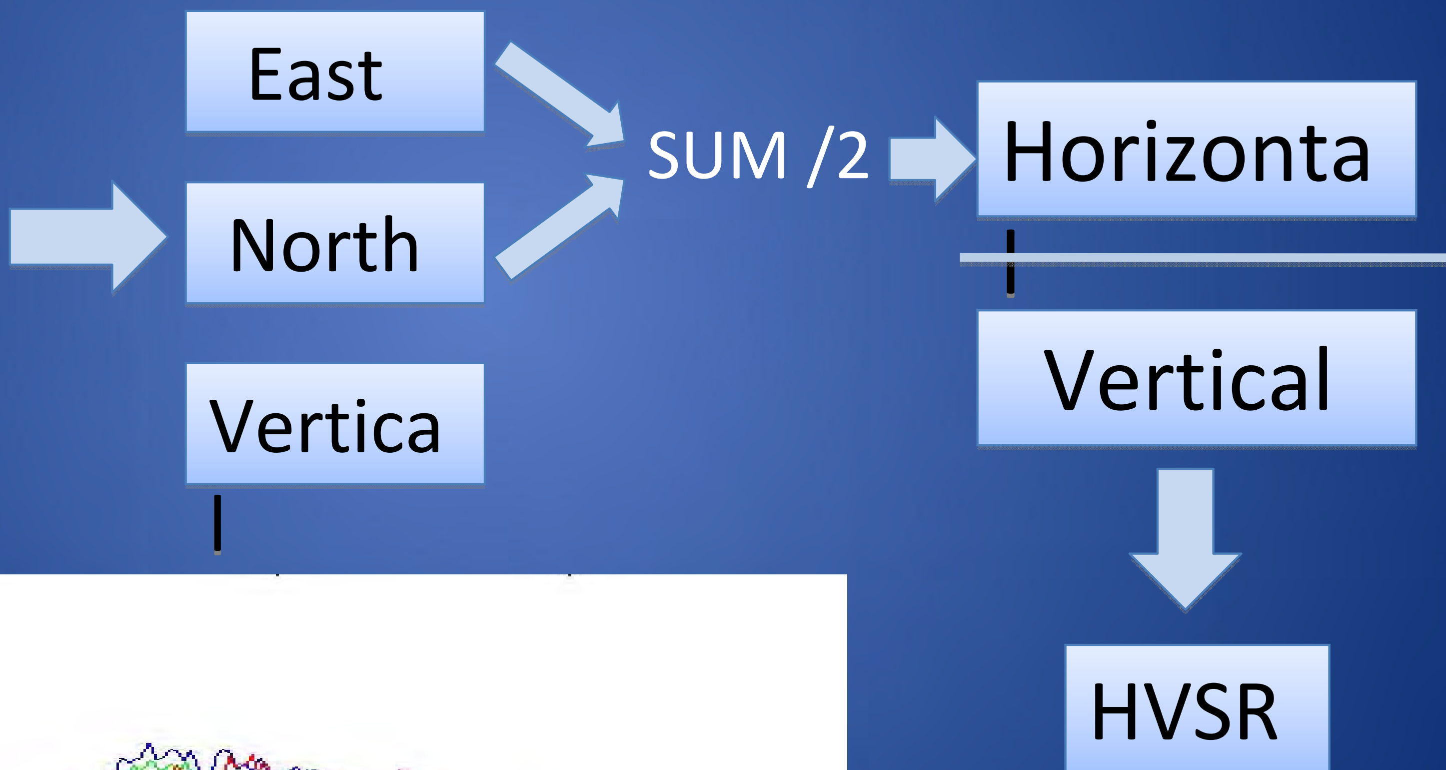

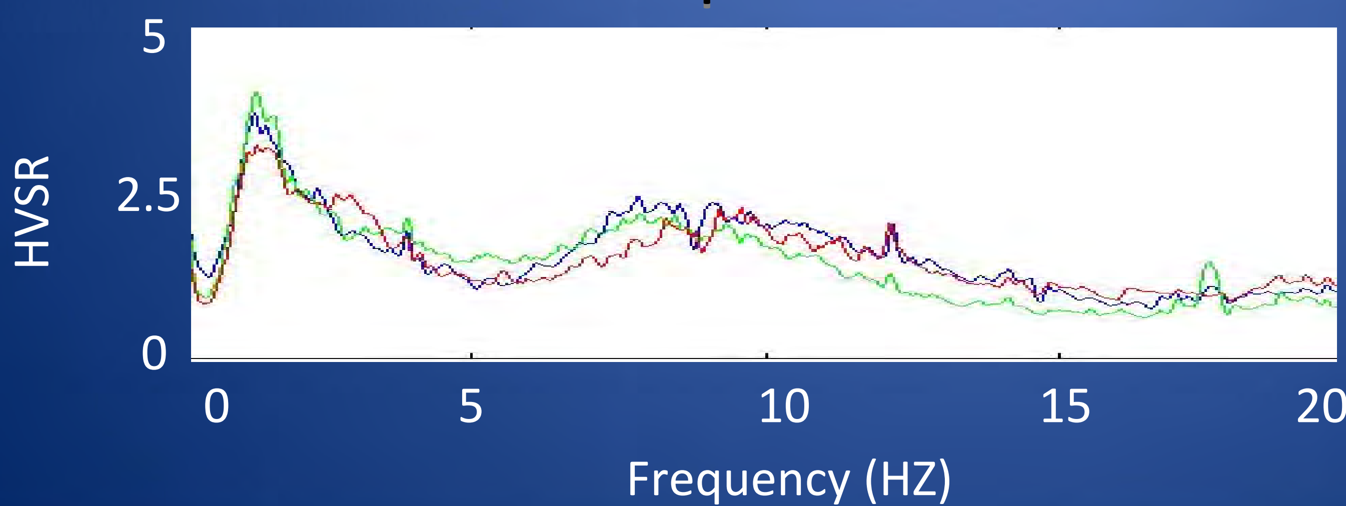

Modeling

- MMSPAC (Multi-mode SPAC , Asten, 2004)

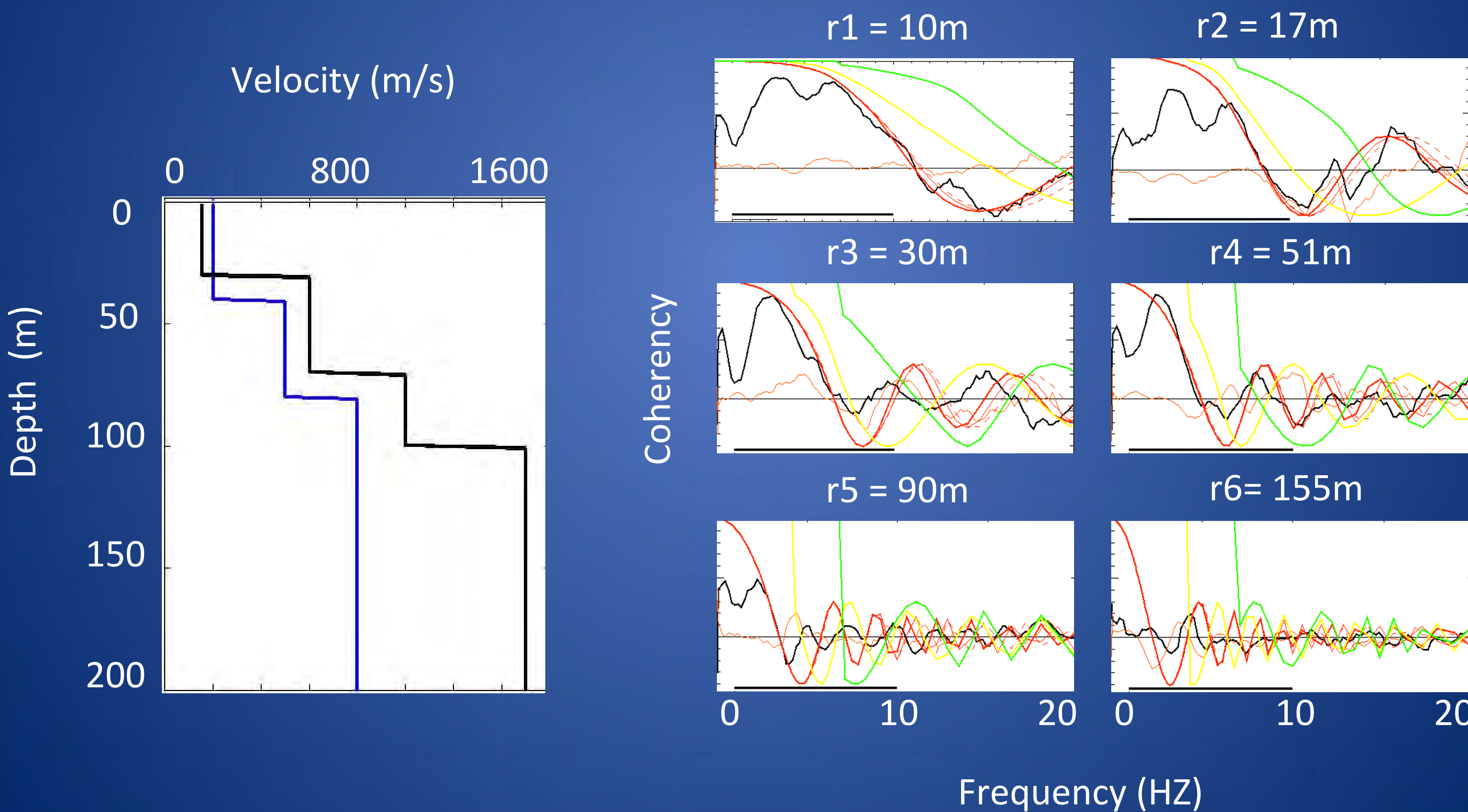

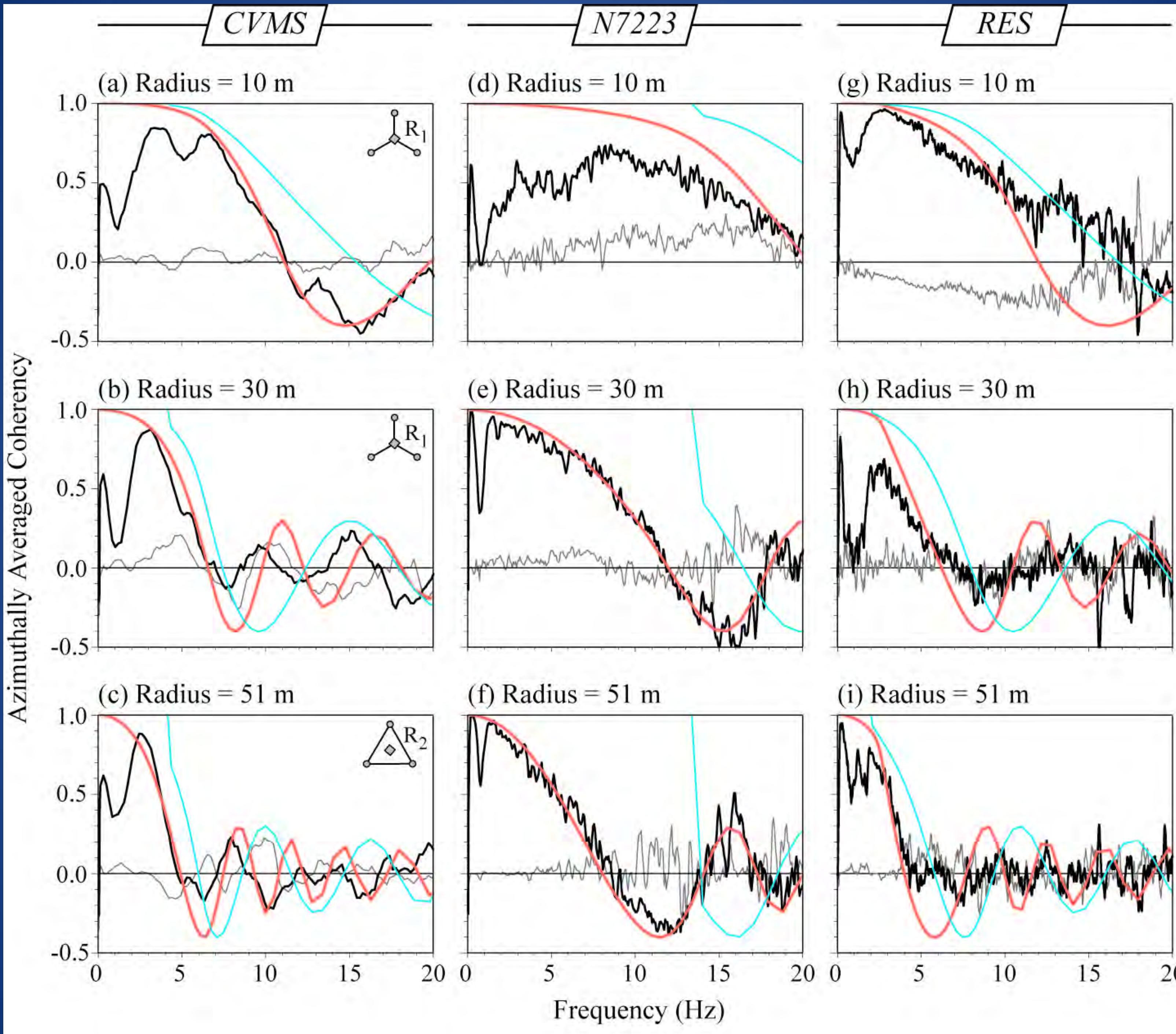
CVMS
N7223
RES
(a) Radius = 10 m
(d) Radius = 10 m
(g) Radius = 10 m
(b) Radius = 30 m
(e) Radius = 30 m
(h) Radius = 30 m
(c) Radius = 51 m
(f) Radius = 51 m
(i) Radius = 51 m
R1
R1
R2
Azimuthally Averaged Coherency
1.0
0.5
0.0
-0.5
0
5
10
15
20
Frequency (Hz)

Modeling

Geopsy

Université Joseph Fourier (Grenoble, France)

Université Potsdam (Potsdam, Germany)

Ellipticity

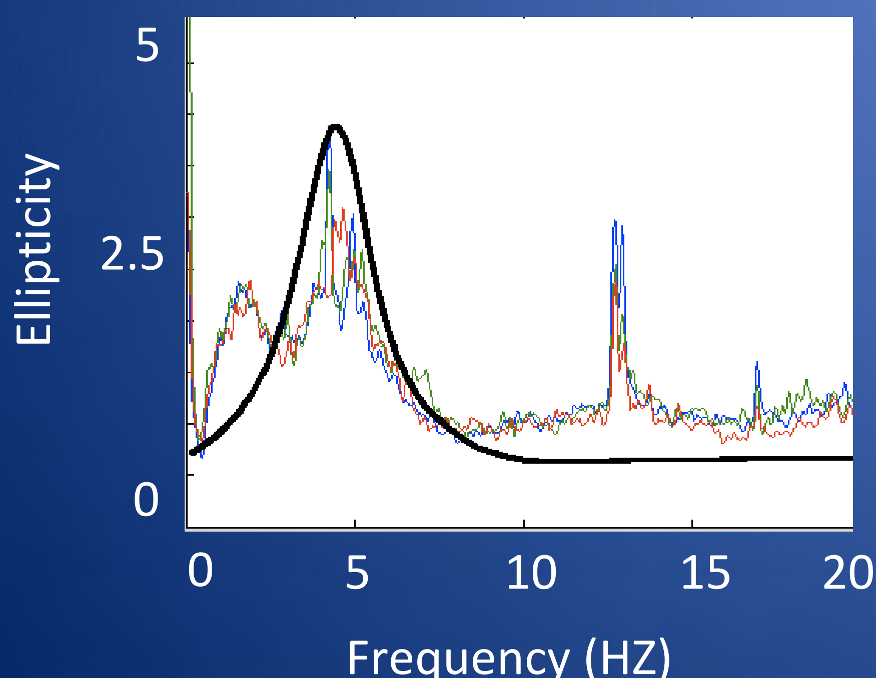

Phase Velocity

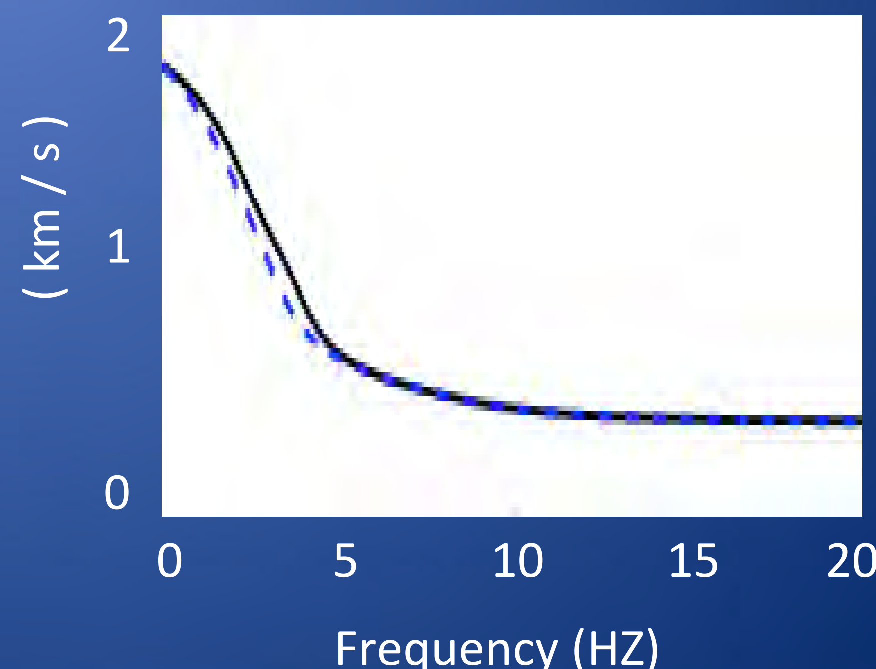

HVSR and Ellipticity

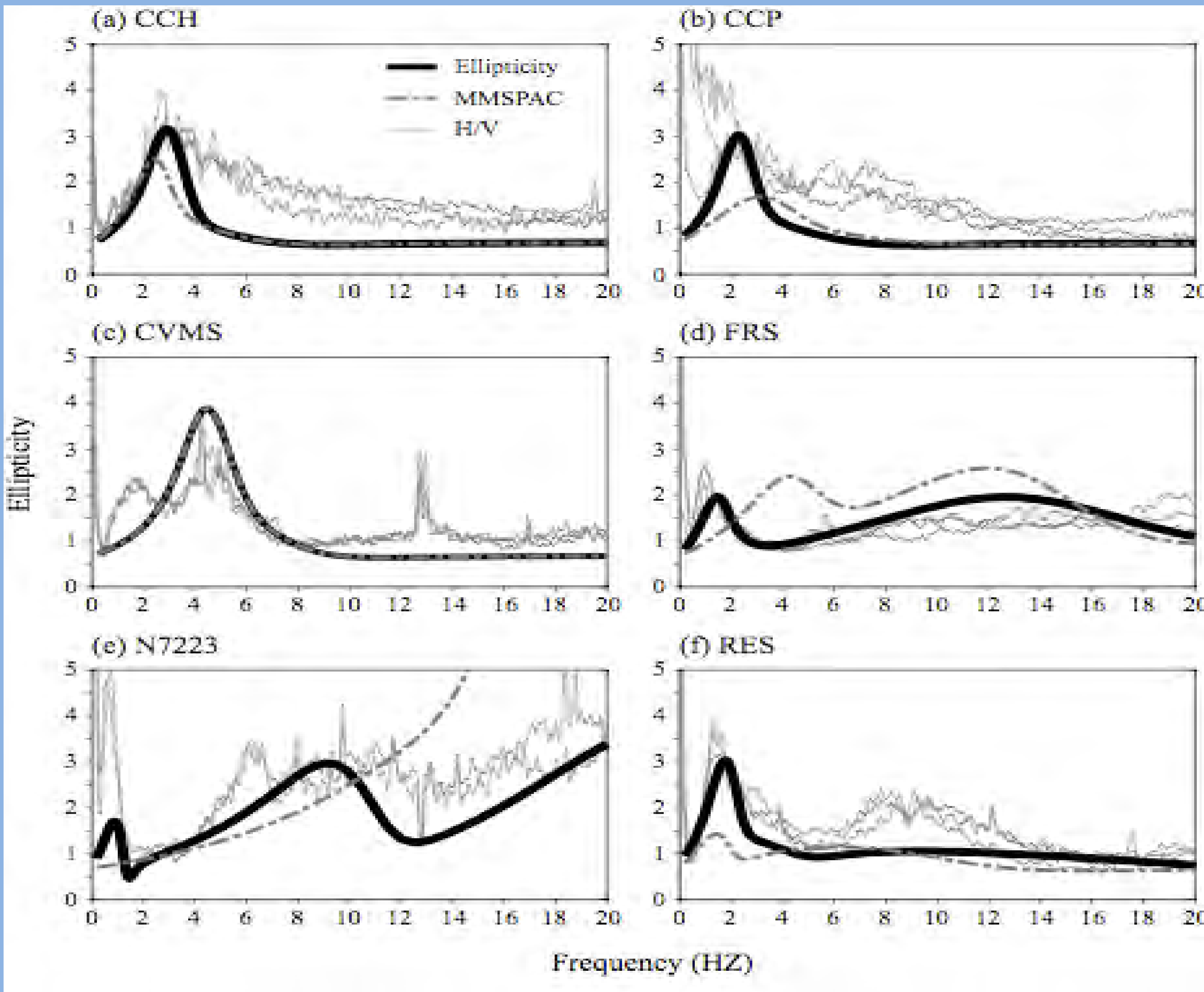

Gray thin lines:
HVSR of data

Gray dash lines:
Ellipticity of models determined from MMSPAC

Gray lines:
Ellipticity of modified models

Phase velocity dispersion curves

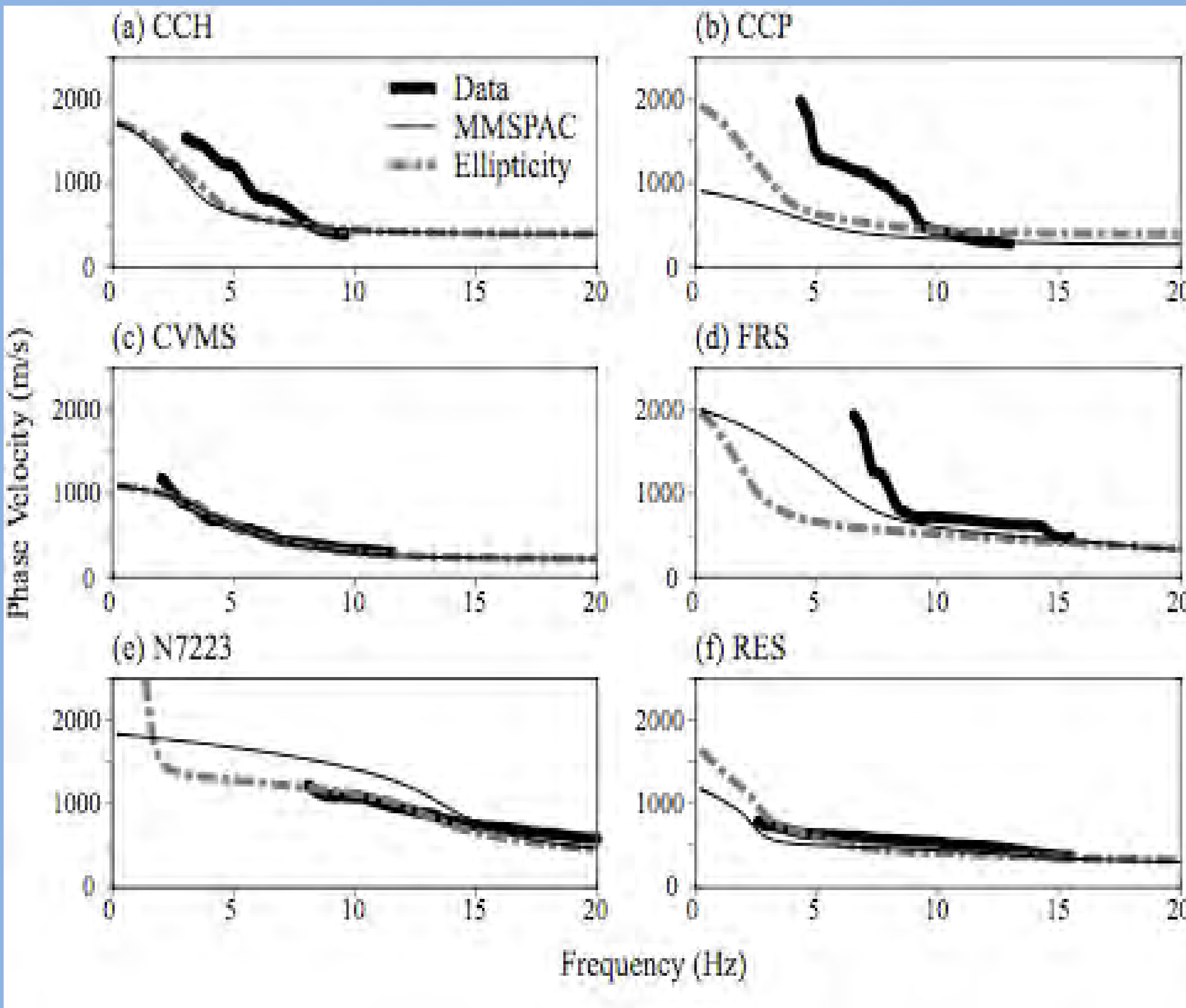

Black thick lines: Phase velocity of data

Black thin lines: Phase velocity of models determined from MMSPAC

Gray dash lines: Phase velocity of modified models

Results

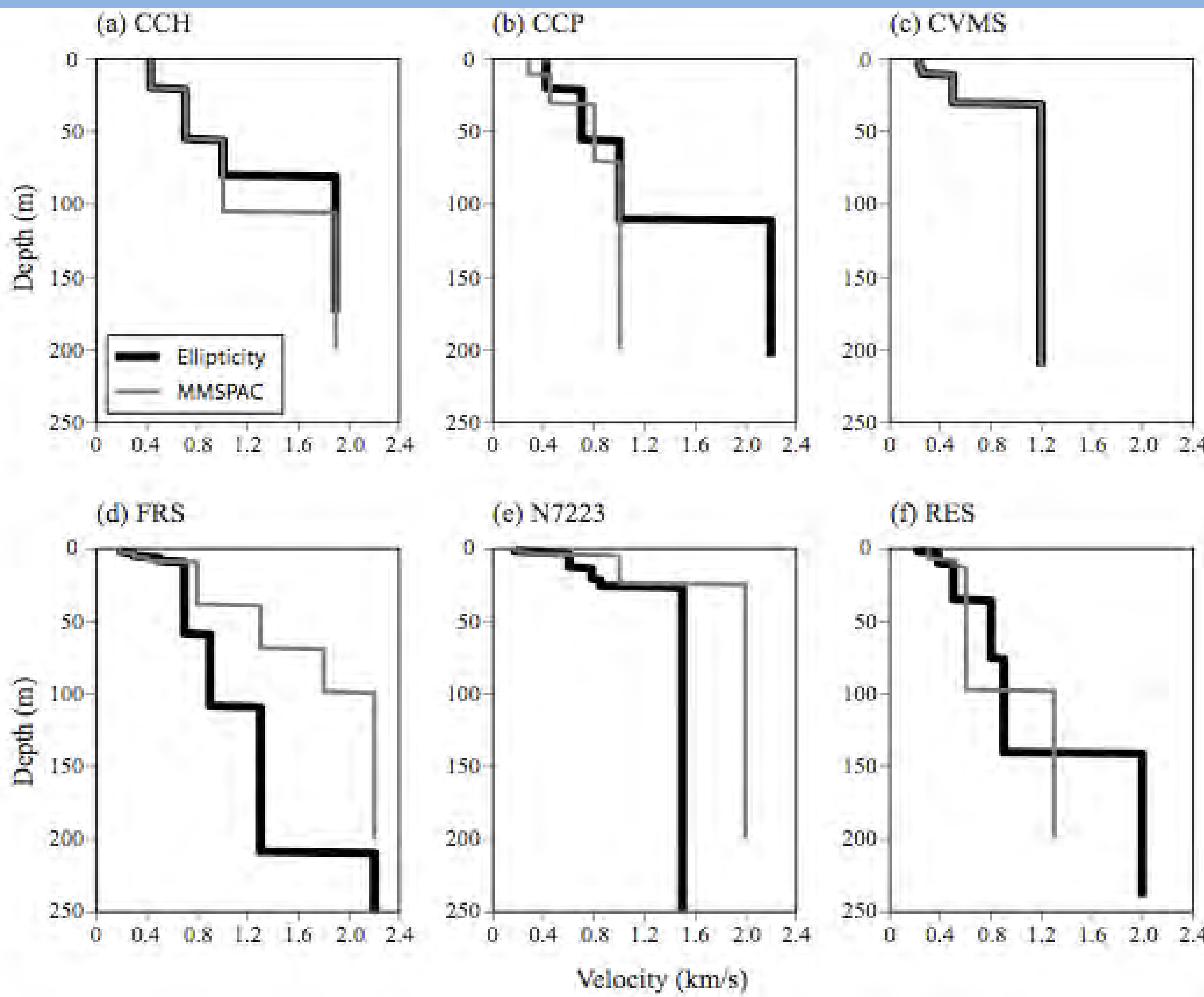

(a) CCH
(b) CCP
(c) CVMS
(d) FRS
(e) N7223
(f) RES
Depth (m)
Velocity (km/s)
Ellipticity
MMSPAC
0
50
100
150
200
250
0
0.4
0.8
1.2
1.6
2.0
2.4

Table 2. Results

	MMSPAC Model				Ellipticity Model			
Site	**V_S30 (m/s)**	**Bedrock Depth (m)**	**Velocity Jump (m/s)**	**NEHRP Code**	**V_S30 (m/s)**	**Bedrock Depth (m)**	**Velocity Jump (m/s)**	**NEHRP Code**
CCH	485	105	1000-1900	C	485	80	1000-1900	C
CCP	374	60	800-1000	C	485	120	1000-2200	C
CVMS	367	30	500-1200	C	367	30	500-1200	C
FRS	545	*	1800-2200	C	522	*	1300-2200	C
N7223	736	24	1000-2000	C	529	30	850-1300	C
RES	462	98	600-1300	C	413	141	900-2000	C

* Bedrock exposed at surface

Conclusions

- We consider the models refined using HVSR to provide the best fit to the data for all the sites except for FRS.
- All models except that for CVMS seem reasonable given what is known of the geology. At CVMS the models are well constrained by the data.

Conclusions

- The average shear-wave velocity in the upper 30 meters (V_S30) is between 360 and 760 m/s for all six sites, corresponding to NEHRP site class unit C. Little strong-ground motion amplification is expected for average shear velocities in this range.

Ground Motion in the Salt Lake Valley from Multi-Segment Faults

Qiming Liu (UC Santa Barbara)

Ralph Archuleta (UC Santa Barbara)

Robert Smith (University of Utah)

Modeling Area

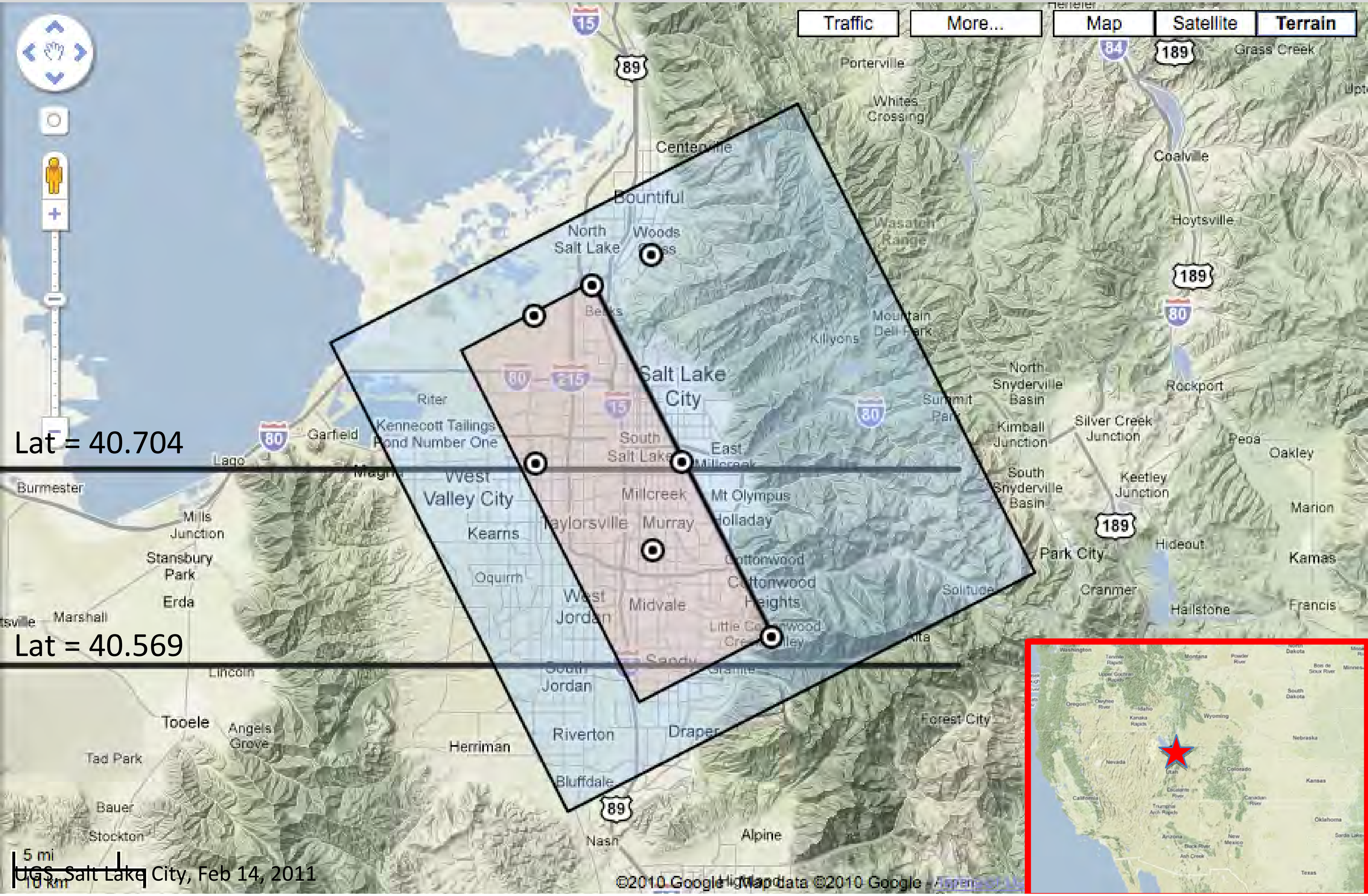

Meshing

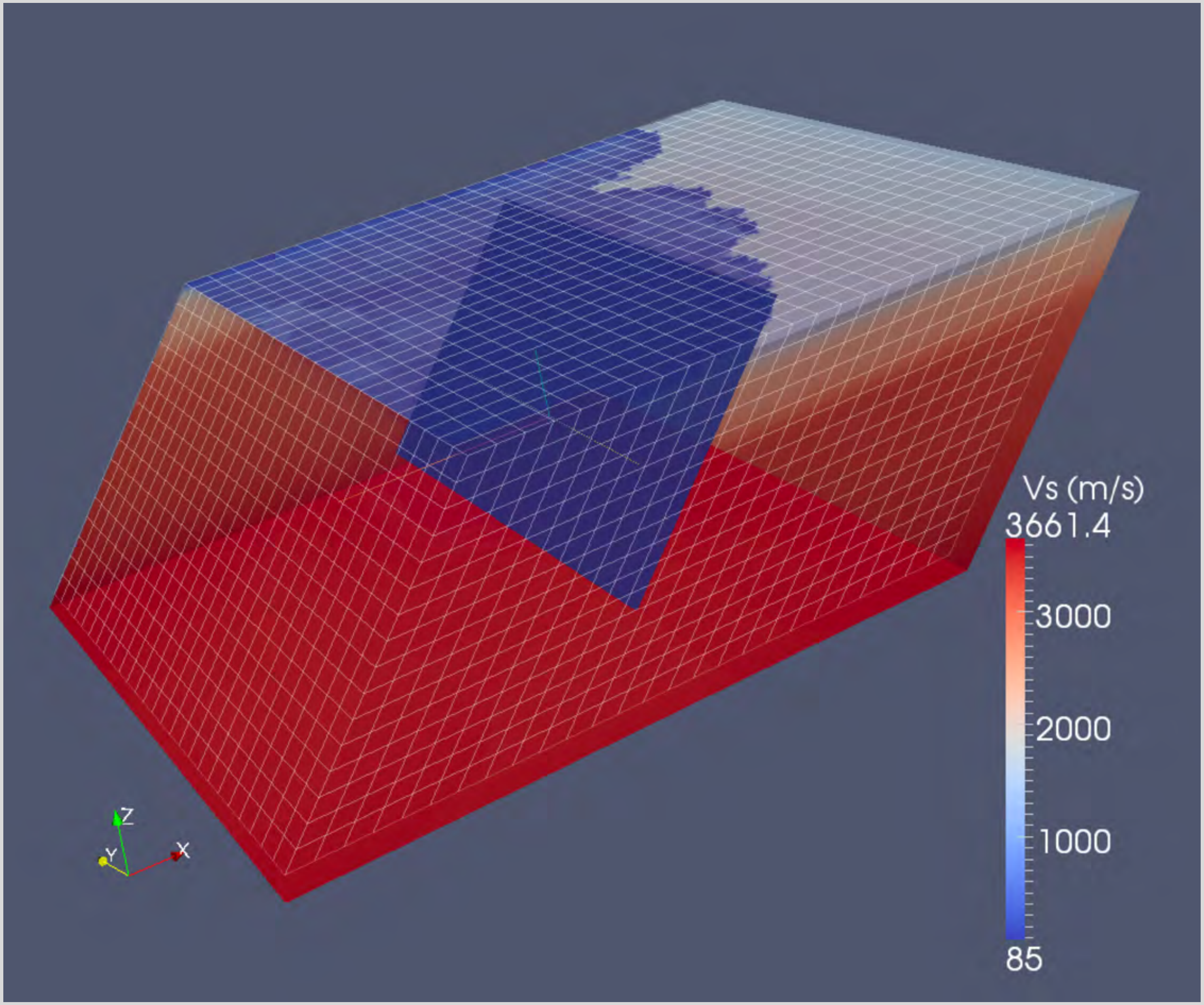

Case Study (cont.)

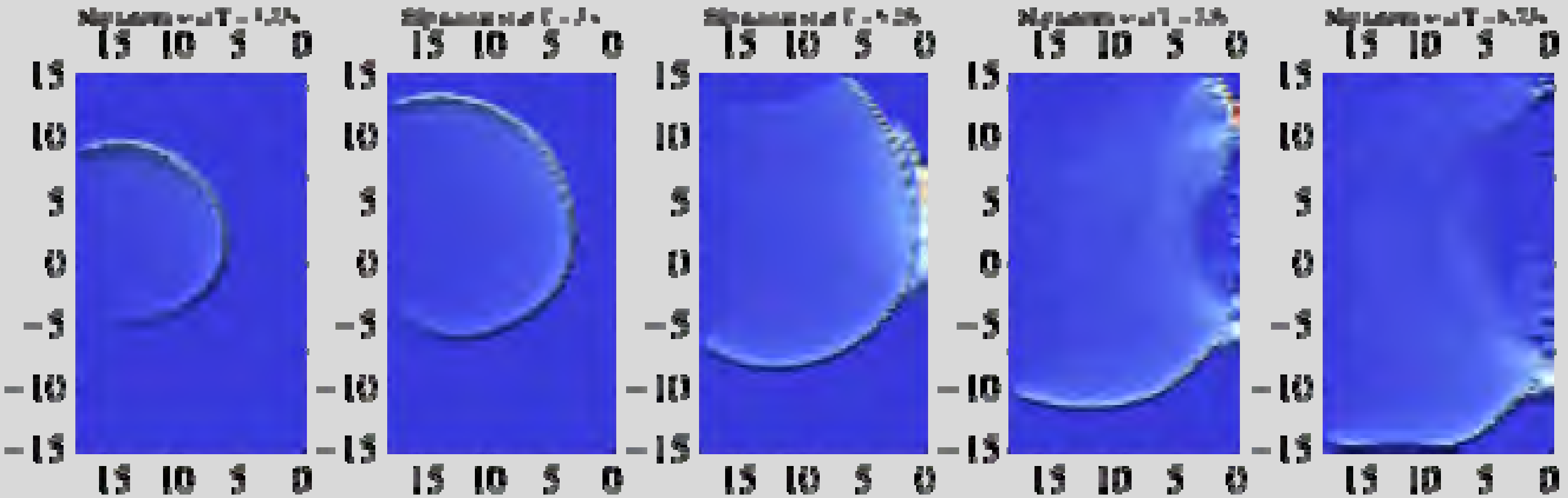

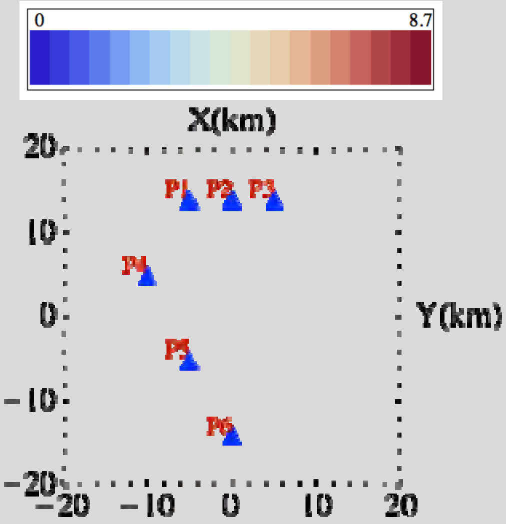

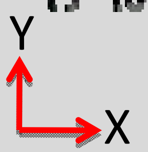

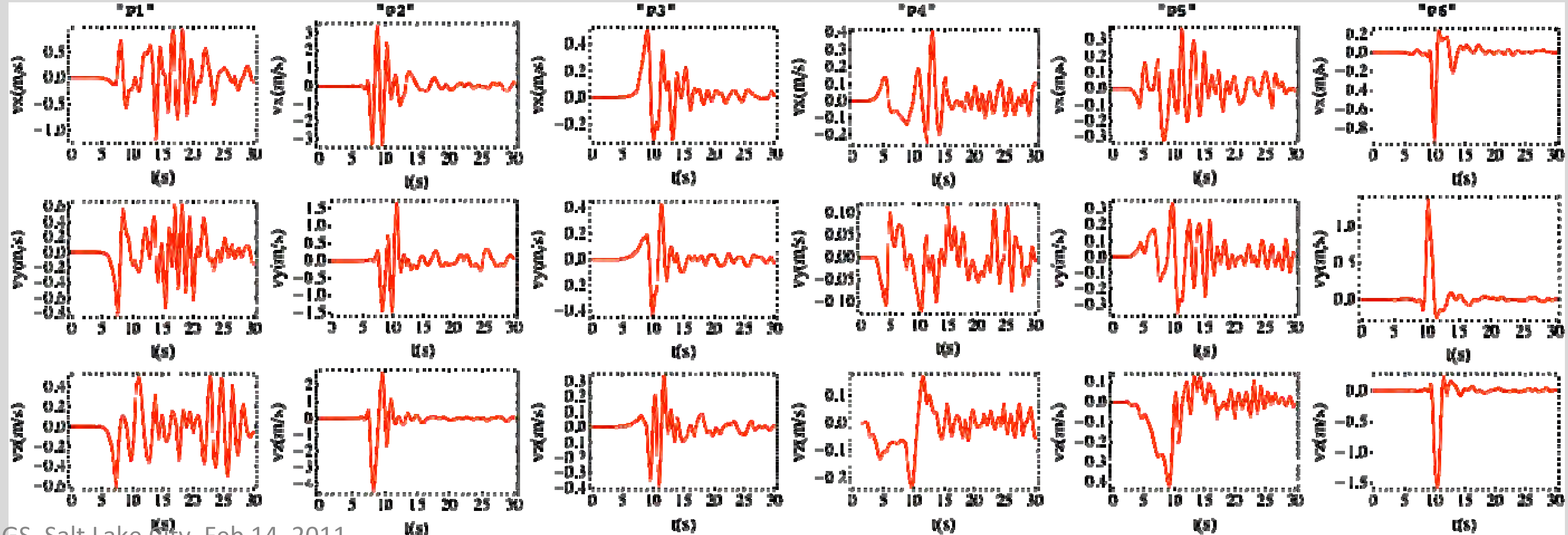

Case Study (cont.)

$$CAV = \int_0^T |\ddot{u}(t)| dt$$

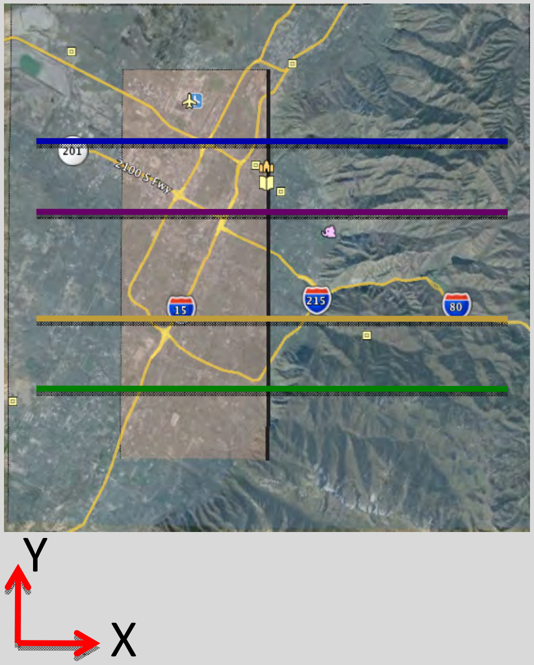

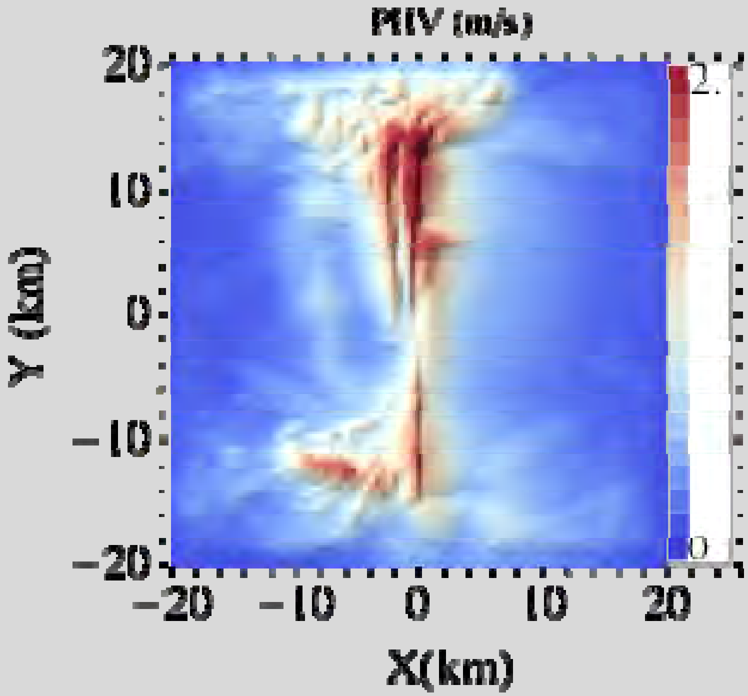

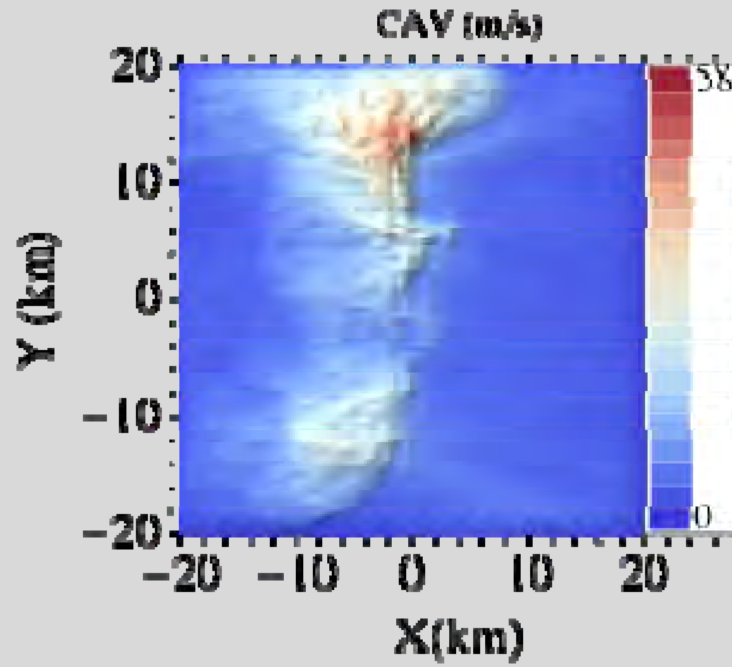

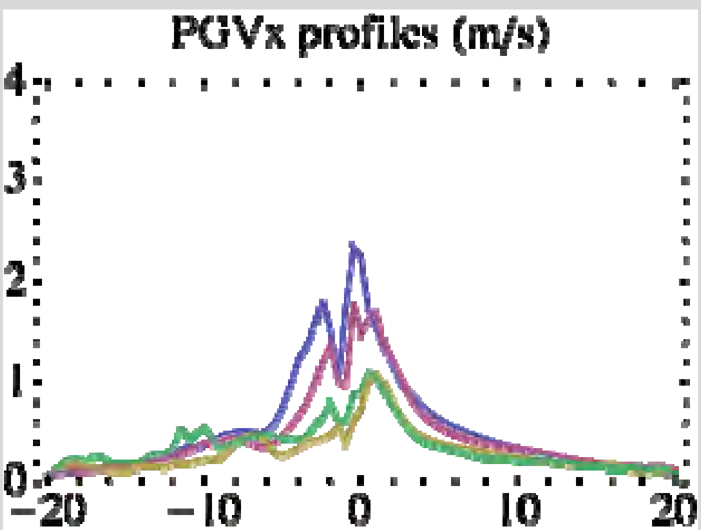

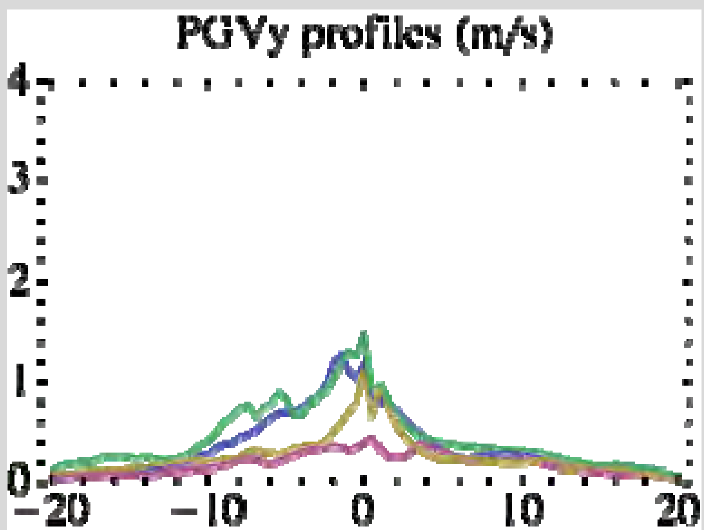

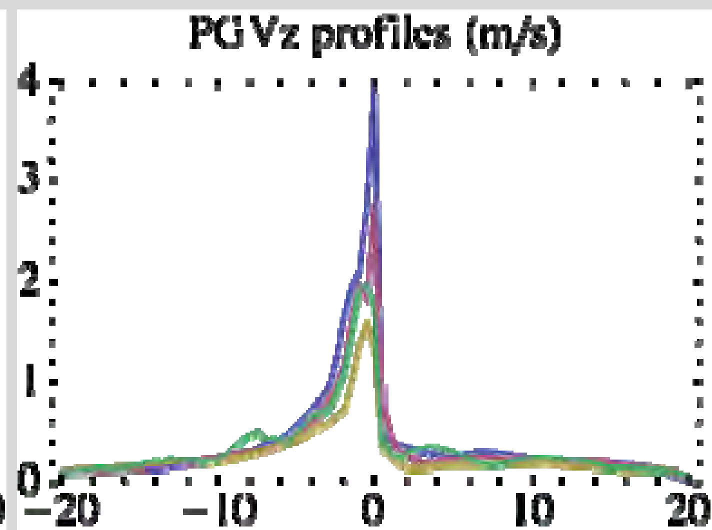

Comparing with NGA Prediction

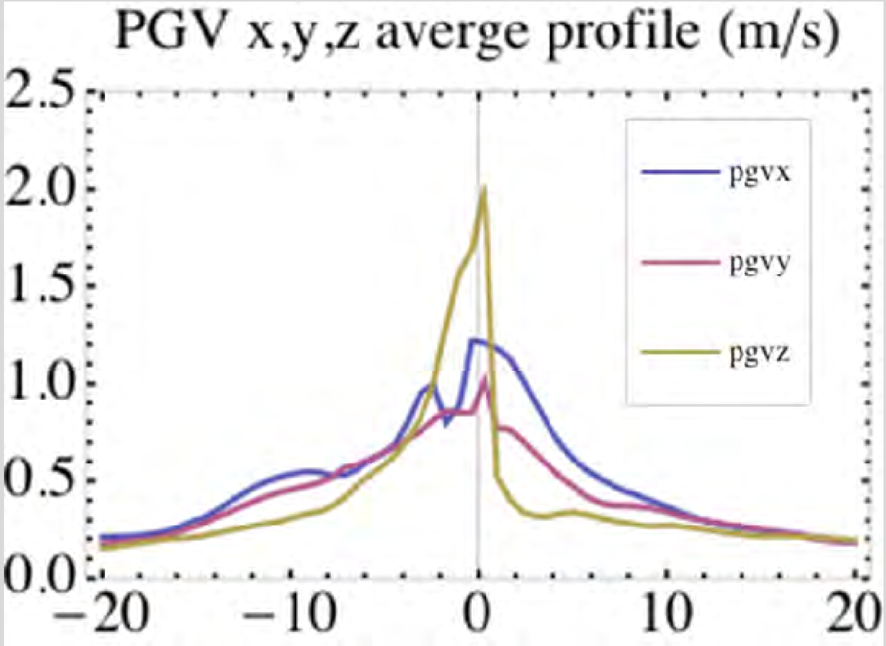

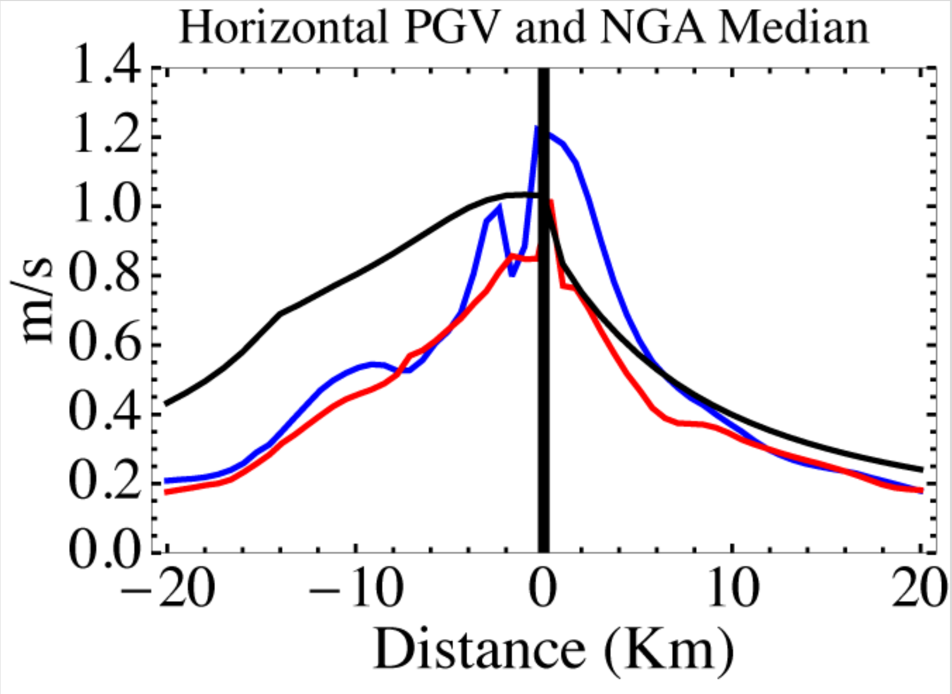

Behavior of Shear Stress at a Point on the Fault

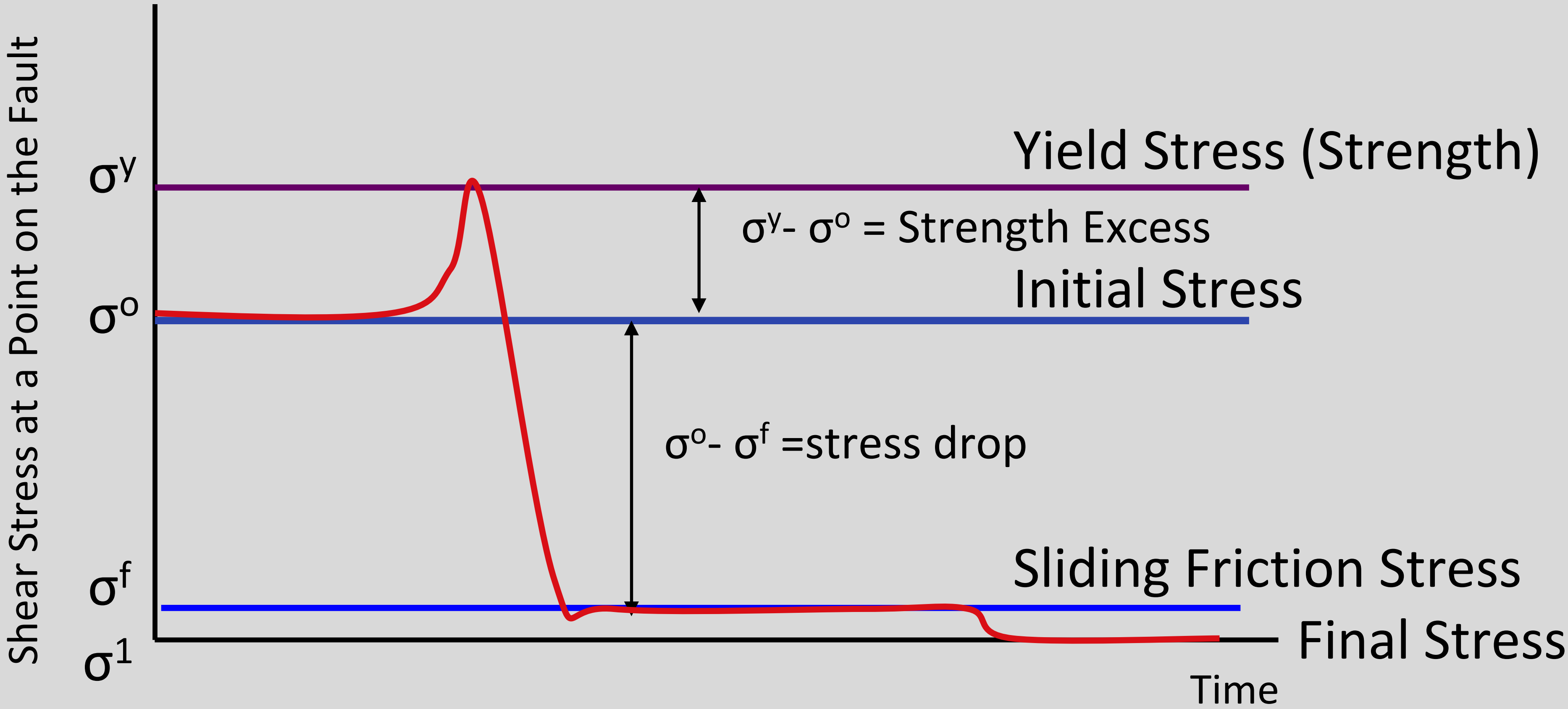

S= Strength Excess/Stress Drop=$(\sigma^y - \sigma^o)/(\sigma^o - \sigma^f)$

Schematic of Friction, Seismicity, Slip

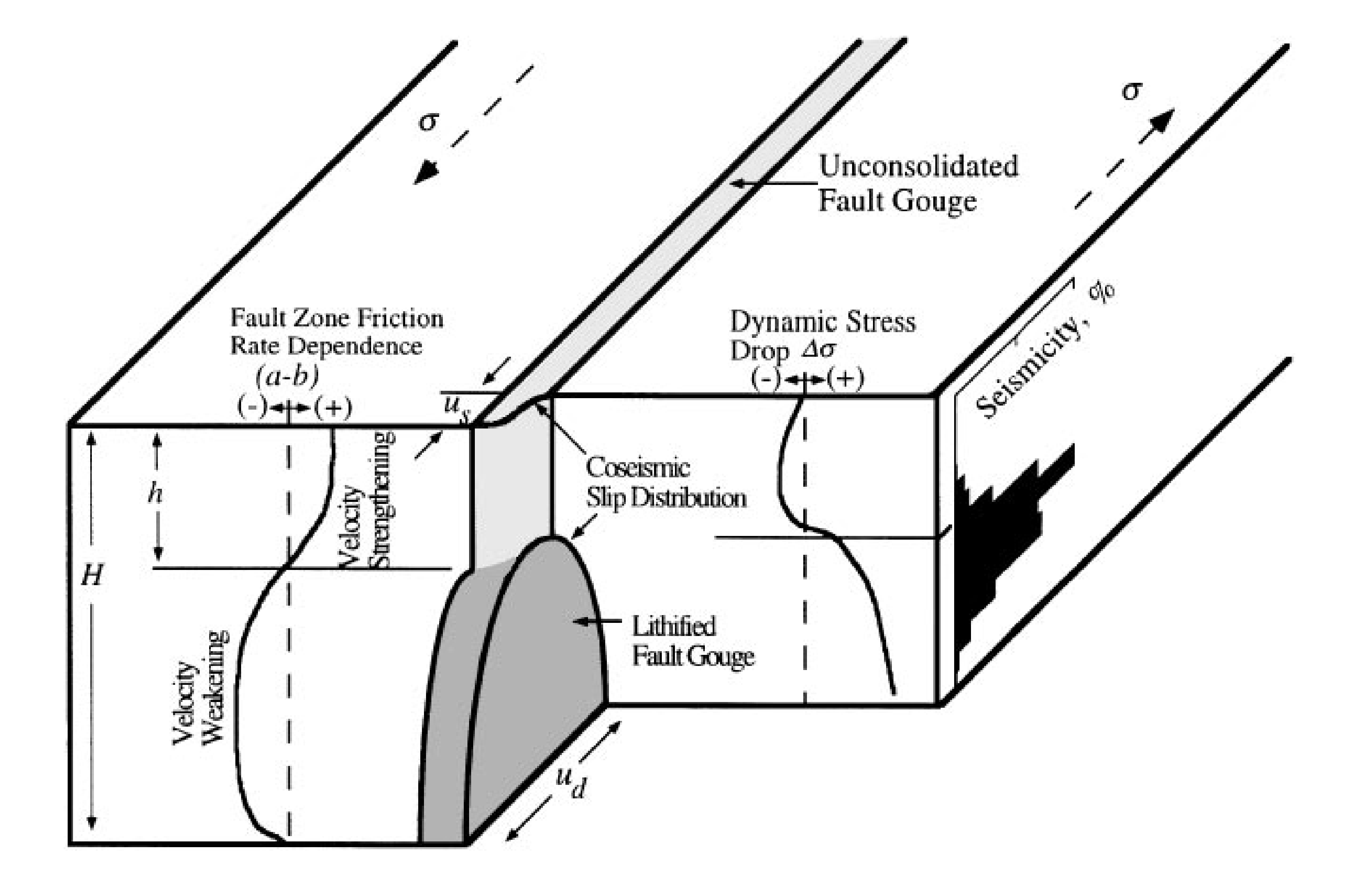

From Chris Marone, Laboratory-Derived Friction Laws and Their Application to Seismic Faulting, Annual Reviews Earth Planetary Science, vol. 26, 1998, 643–96.

Behavior of Shear Stress at a Point on the Fault: Negative Stress Drop

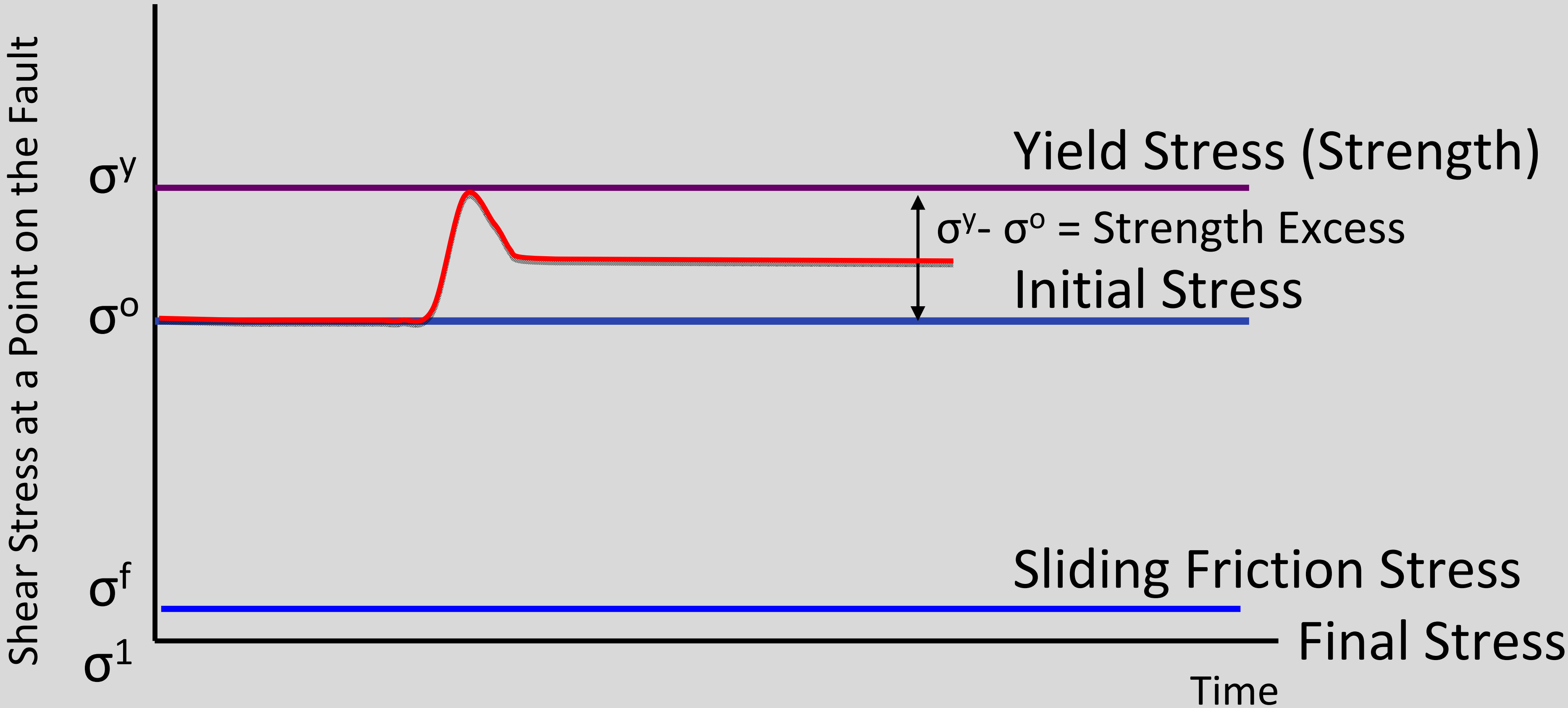

S= Strength Excess/Stress Drop=$(\sigma^y - \sigma^o)/(\sigma^o - \sigma^f)$

Comparison of slip snapshots: With and without velocity strengthening

timestamps: (1.875s, 5.625s, 7.5s, 10.0s), slip in meters

No velocity strengthening

With velocity strengthening

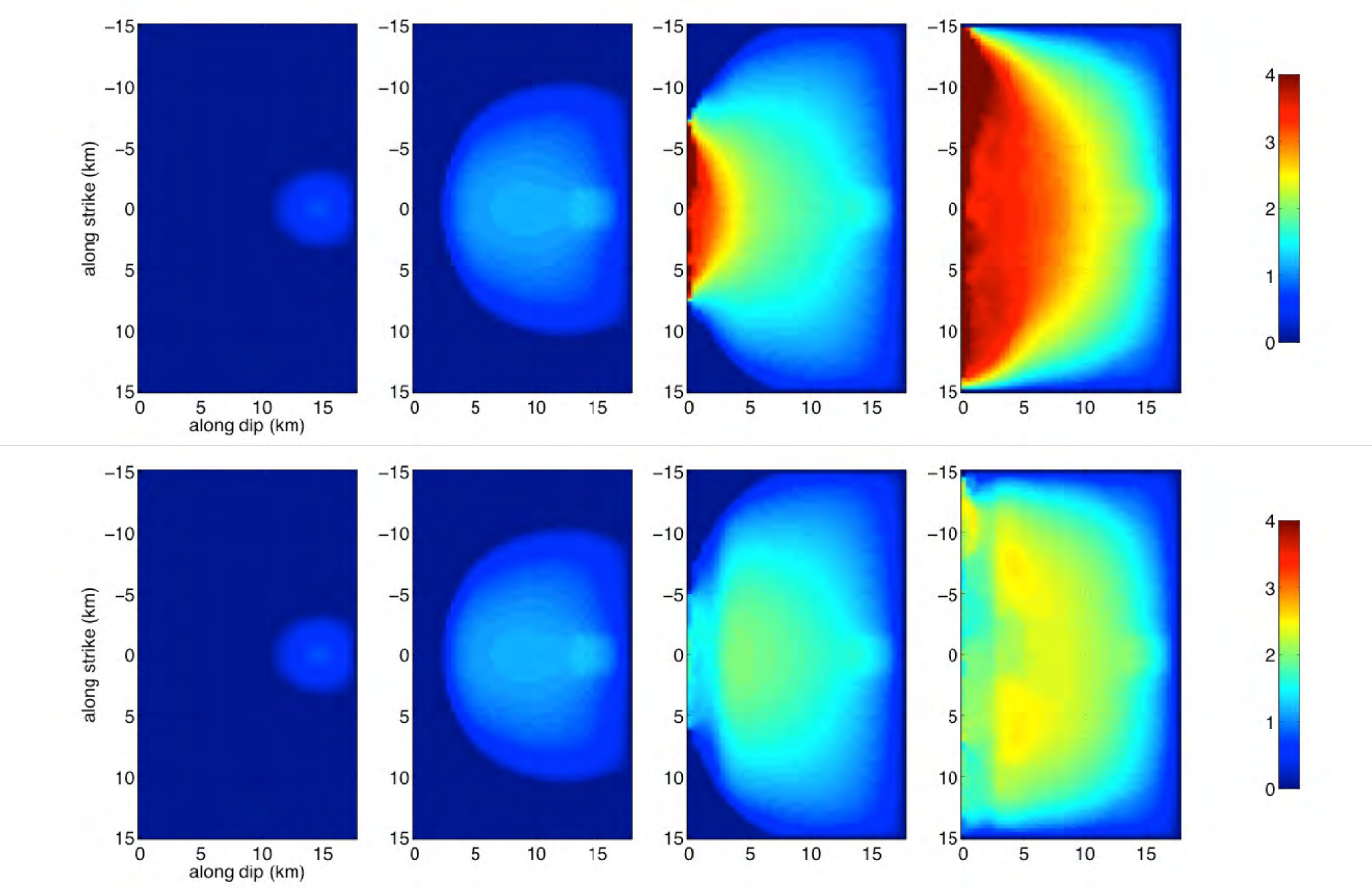

C. B. DuRoss (2008). Holocene Vertical Displacement on the Central Segments of the Wasatch Fault Zone, Utah, Bull. Seismol. Soc. Am., 98, 2918-2933.

PGV Surface Maps: X, Y, Z components

With No velocity strengthening

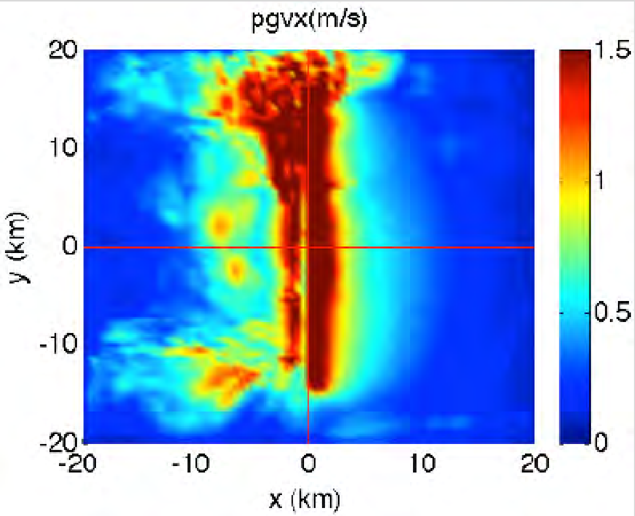

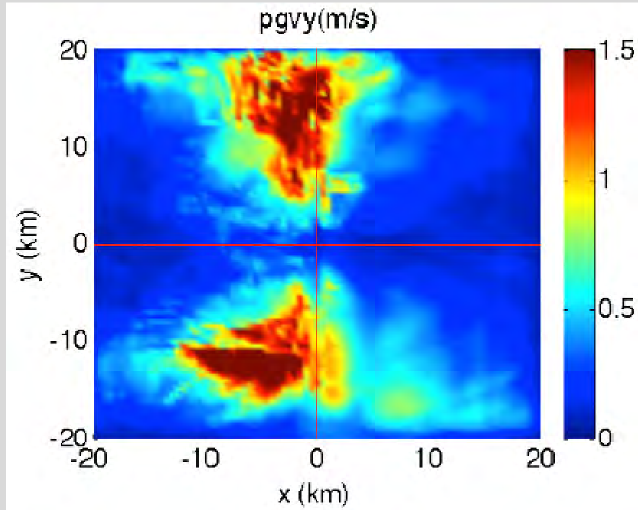

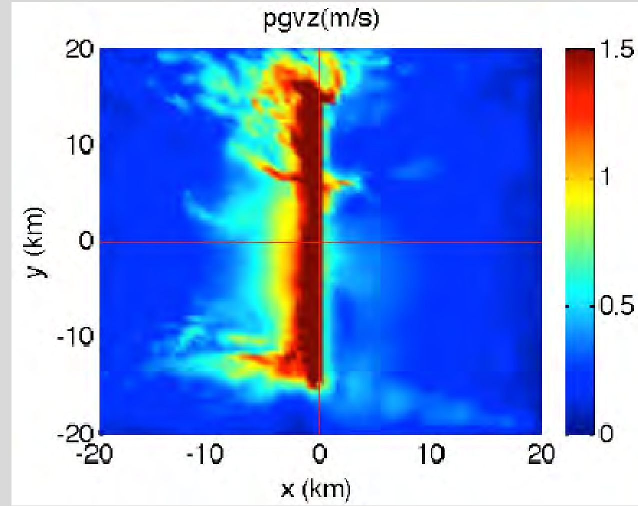

With velocity strengthening

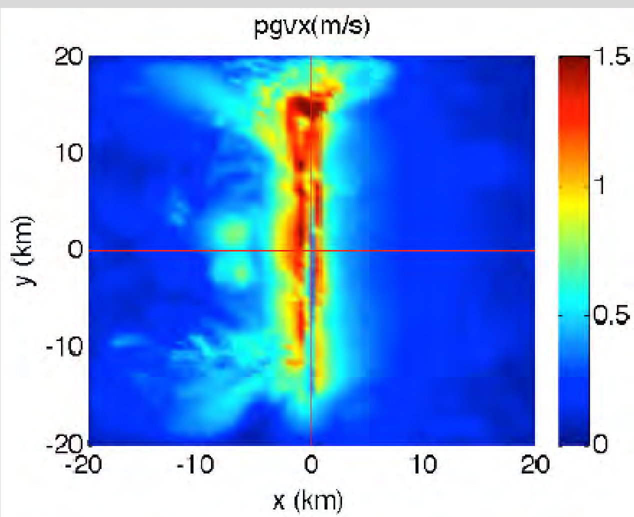

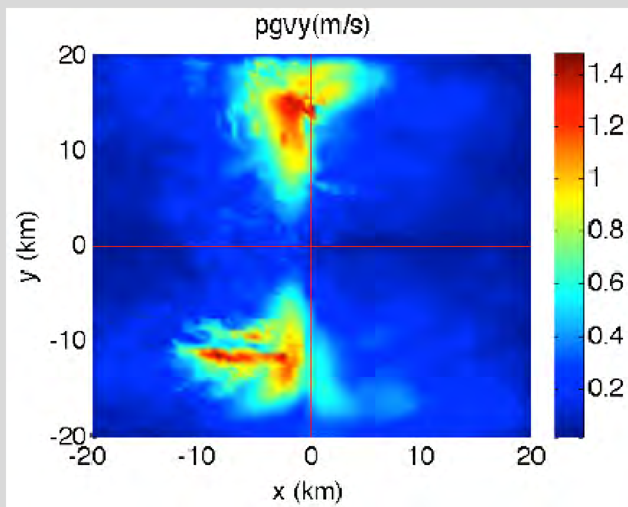

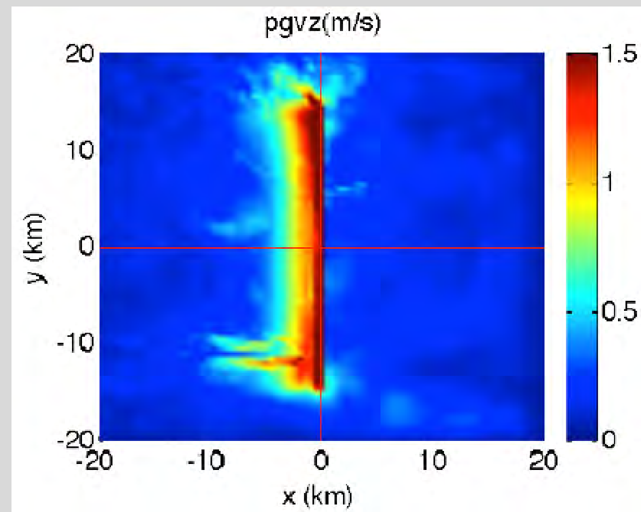

Prediction of Peak Velocity on East-West Profiles

Black: No Velocity Strengthening
Red: Velocity Strengthening

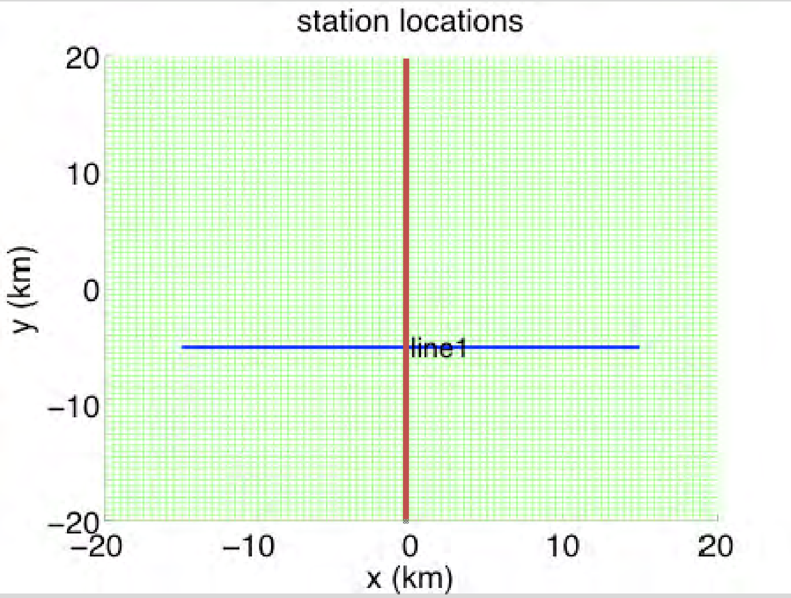

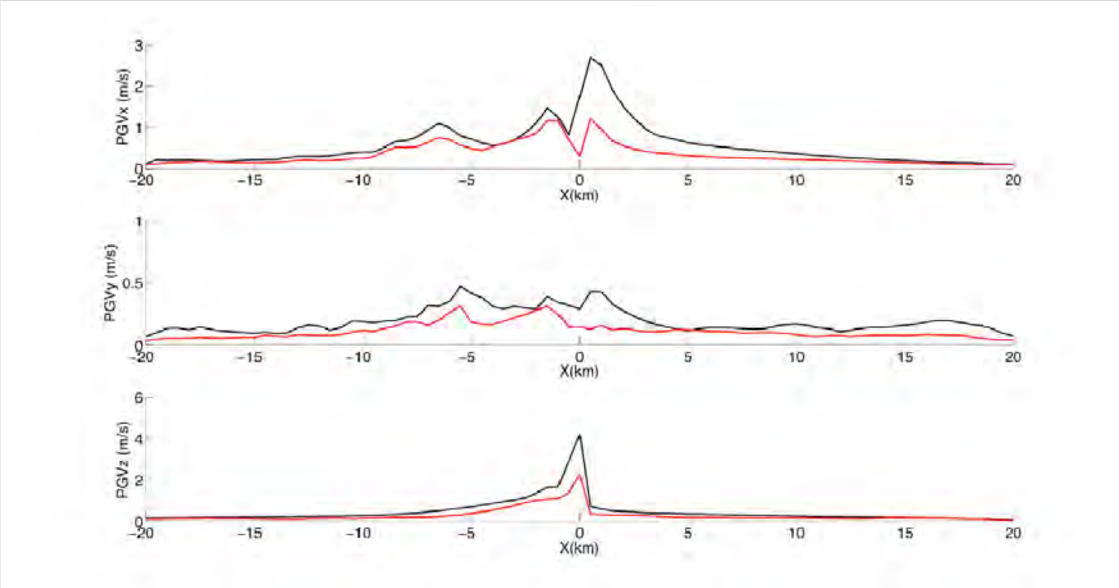

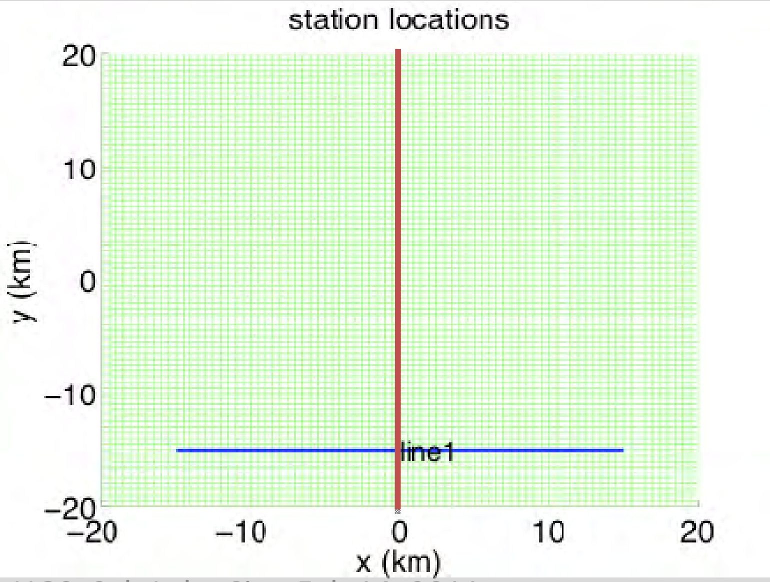

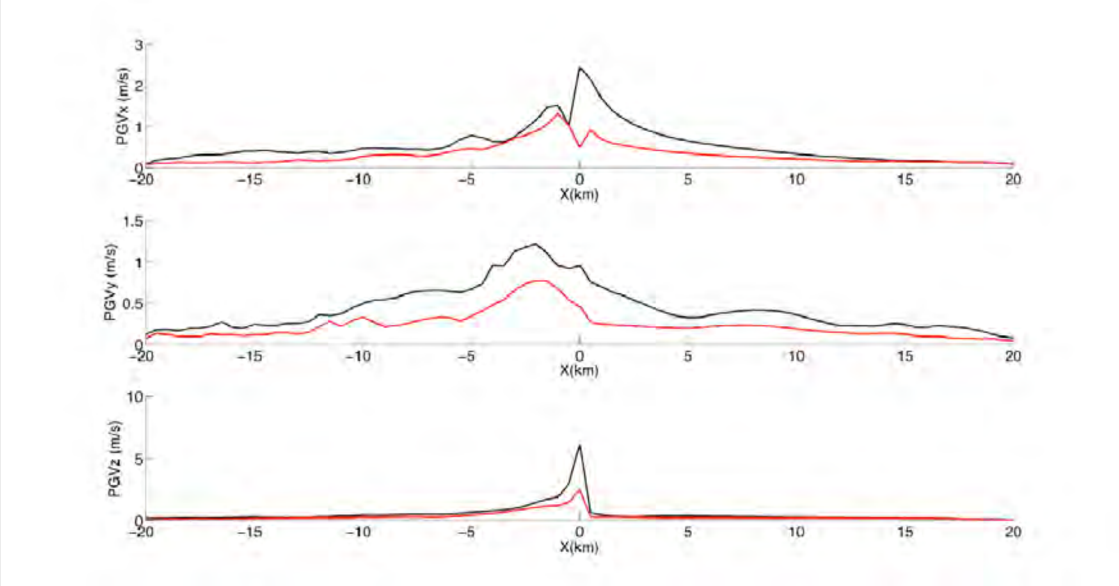

Particle Velocity Time Histories

Black: No Velocity Strengthening
Red: Velocity Strengthening

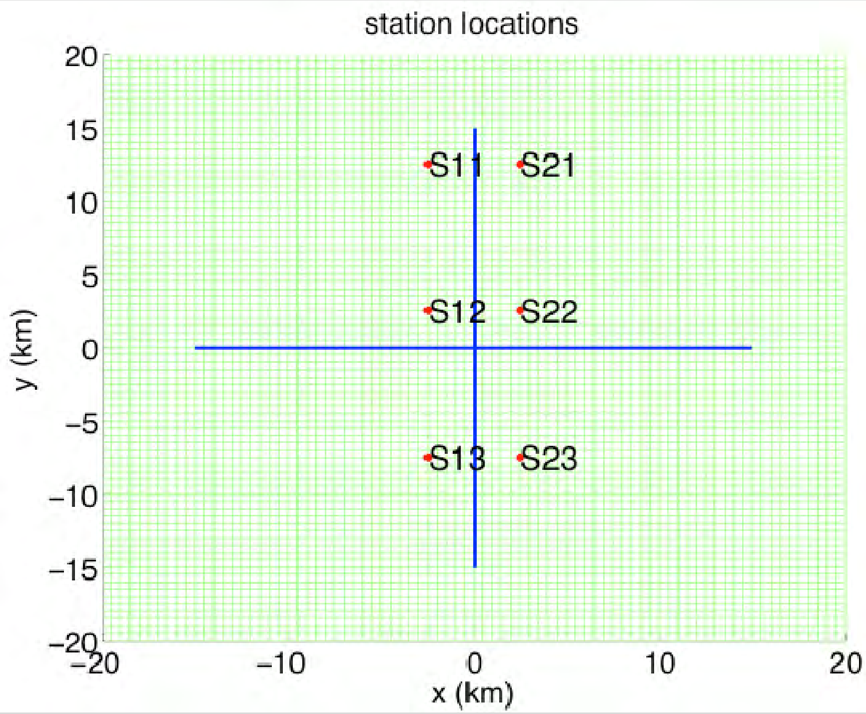

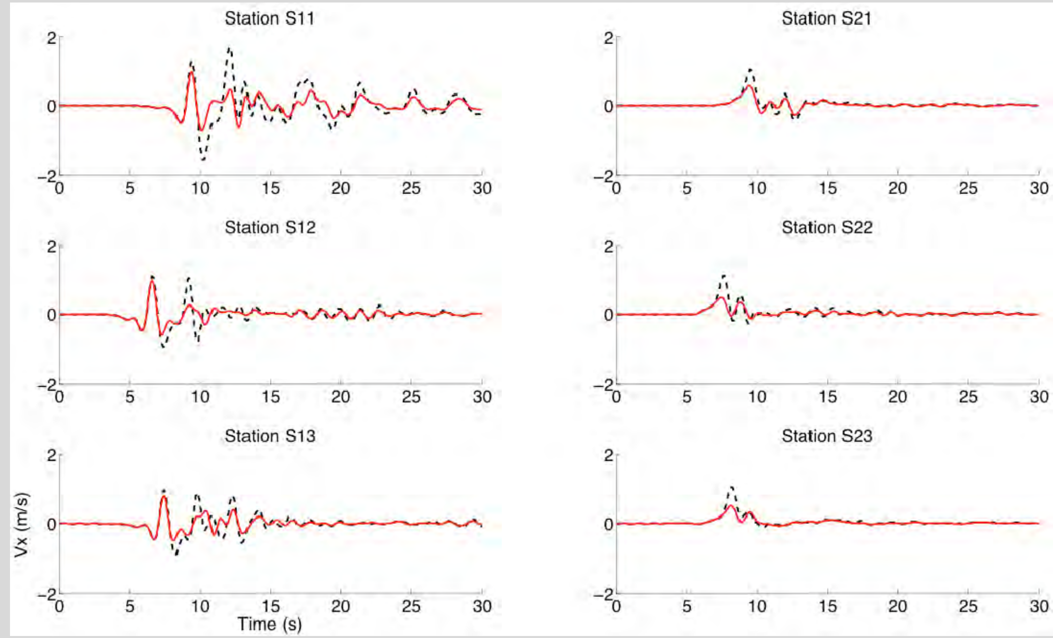

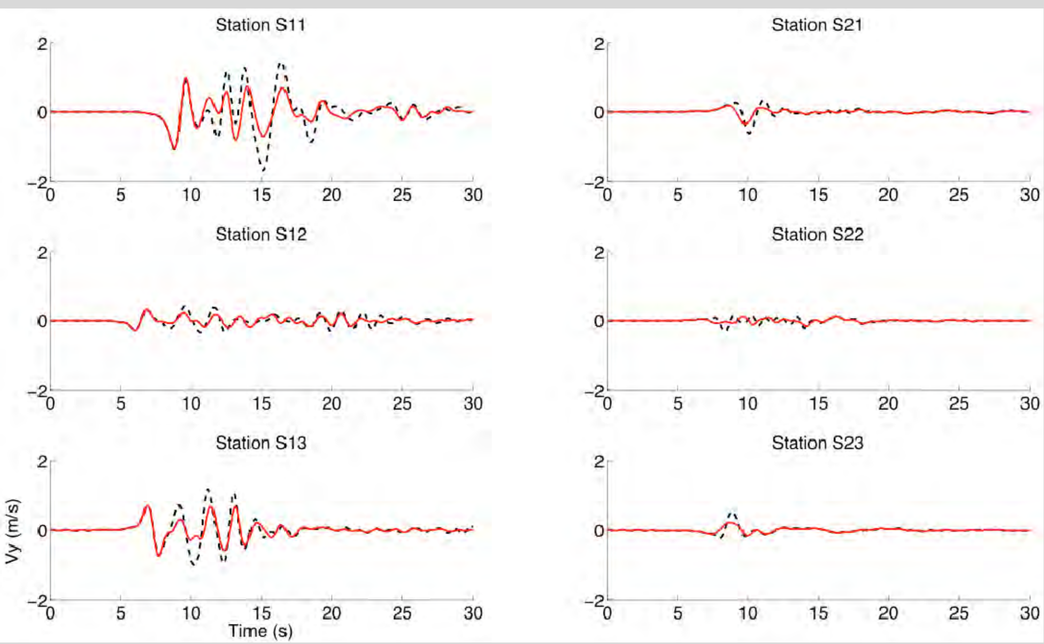

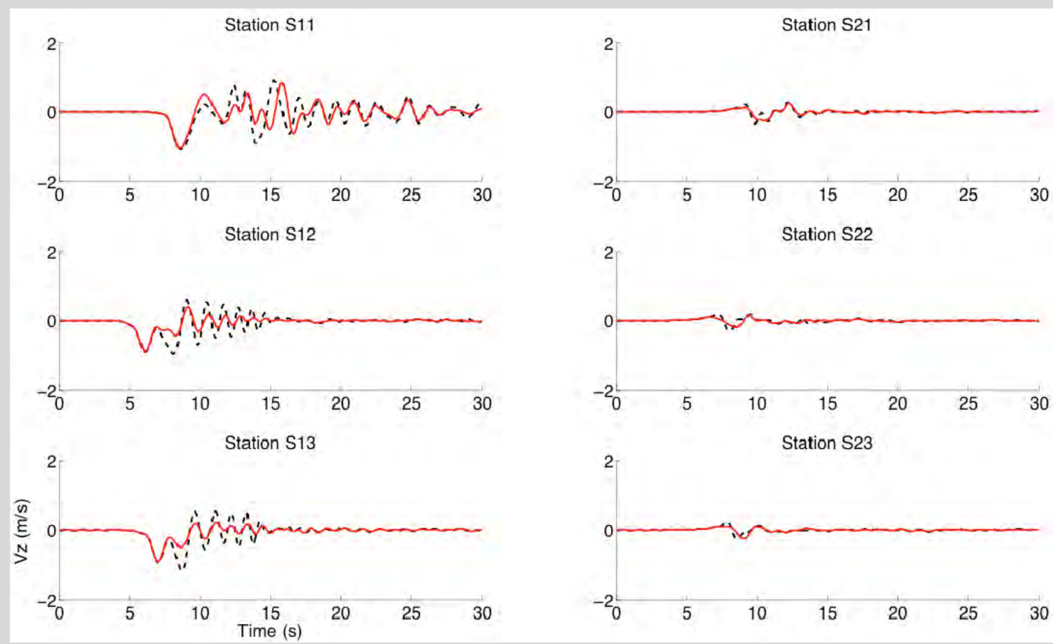

Particle Velocity Time Histories

Black: No Velocity Strengthening
Red: Velocity Strengthening

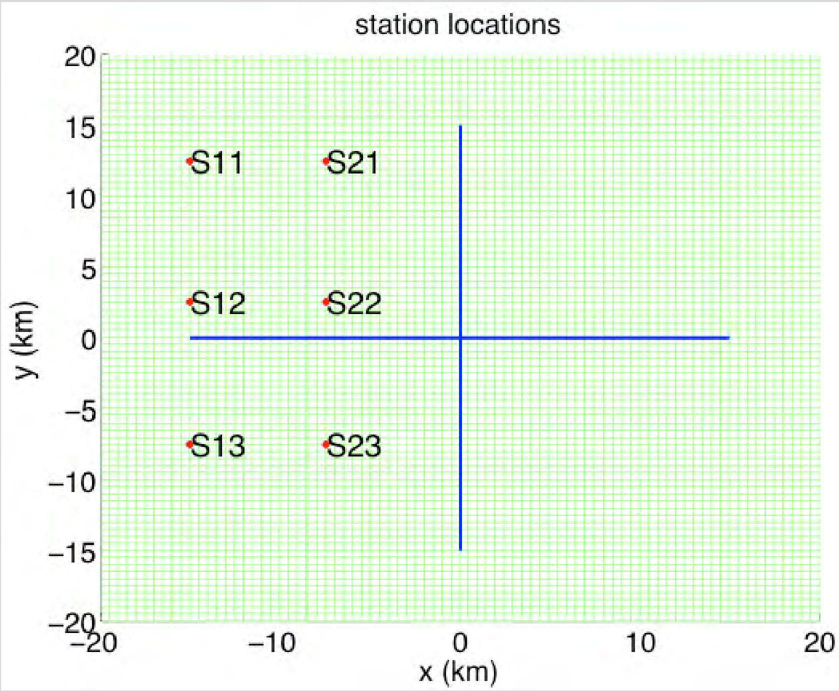

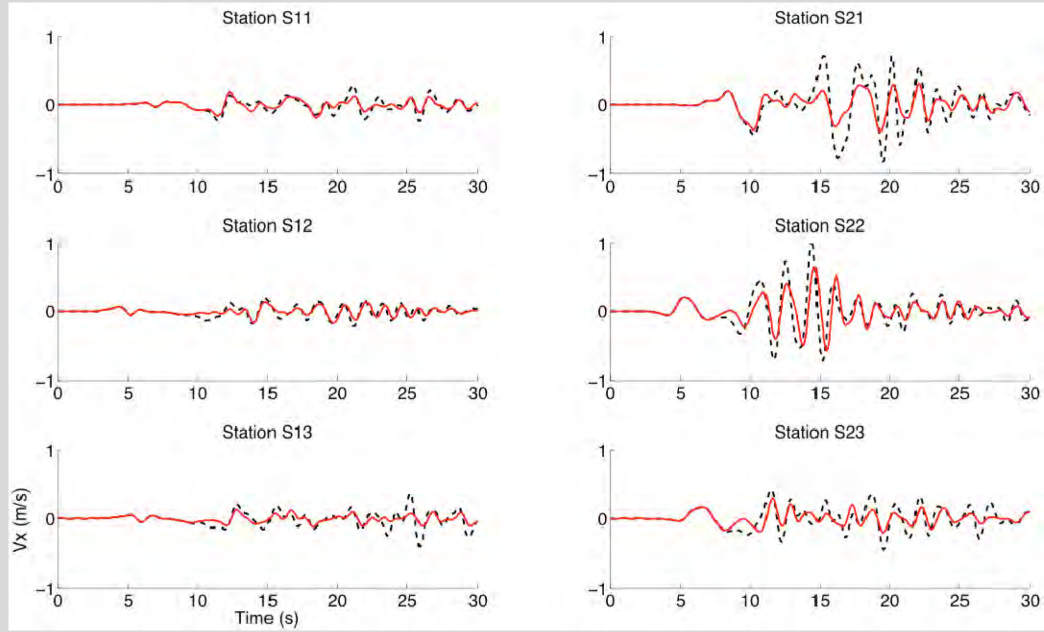

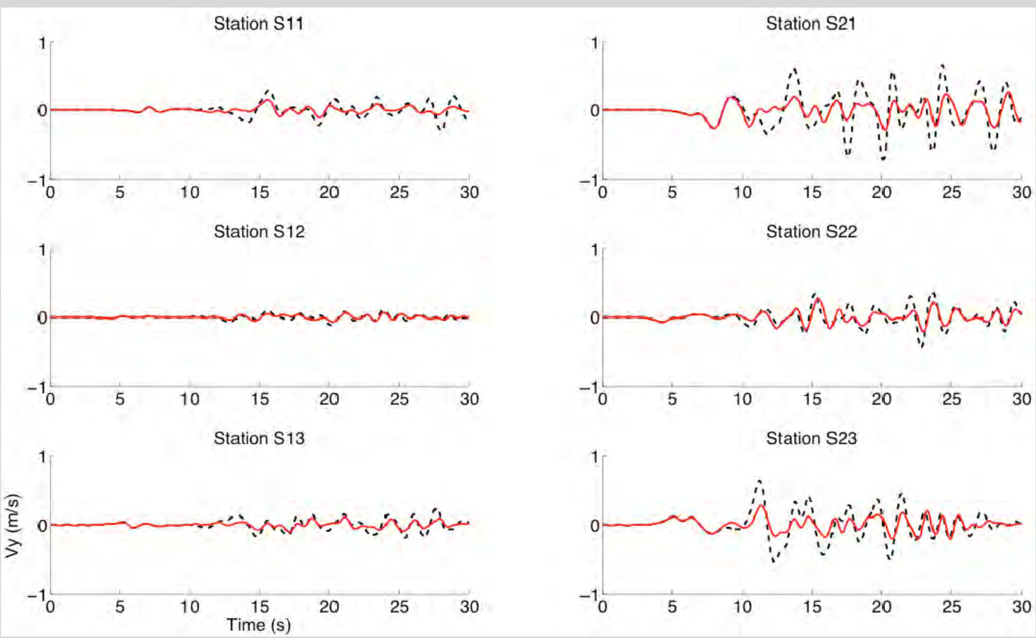

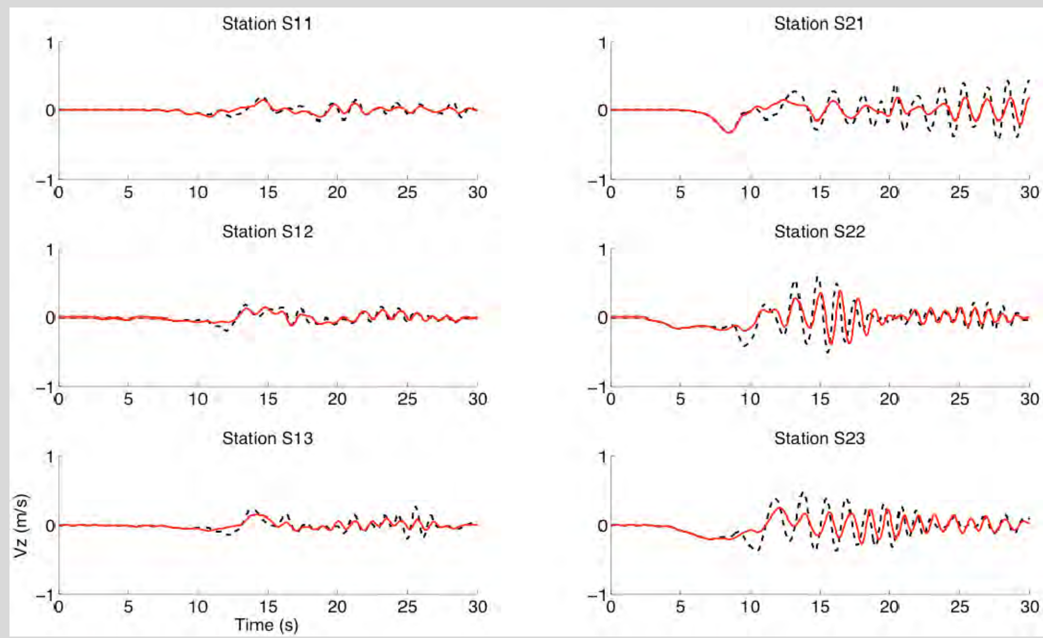

Multiple Segments

- Faults are not single planar features but complex in shape, connectivity, etc.
- Fault jumping and dynamic triggering can significantly change the seismic moment.
- Limited quantitative results on dynamic triggering
    1. Parallel strike-slip faults (Harris et al. 1991)
    2. Parallel thrust faults (Magistrale & Day 1999)

Multiple Segments

UGS, Salt Lake City, Feb 14, 2011

Computing model

Keyword	Value
Lx, Ly, Lz	40km,40km,17km
dx,dy,dz	100m,100m,100m
Strike,dip	180°, 50°
Friction Law	Slip-weakening
Initial normal stress	• Uniform (36MPa) • Depth dependent
μ_{0}, μ_{d}, μ_{s}, S	0.536, 0.448, 0.66, 1.16
D_c	0.25m
dt, Tmax	0.01, 20.0
V_p, V_s, ρ	5712m/s,3298m/s,2700kg/m^3

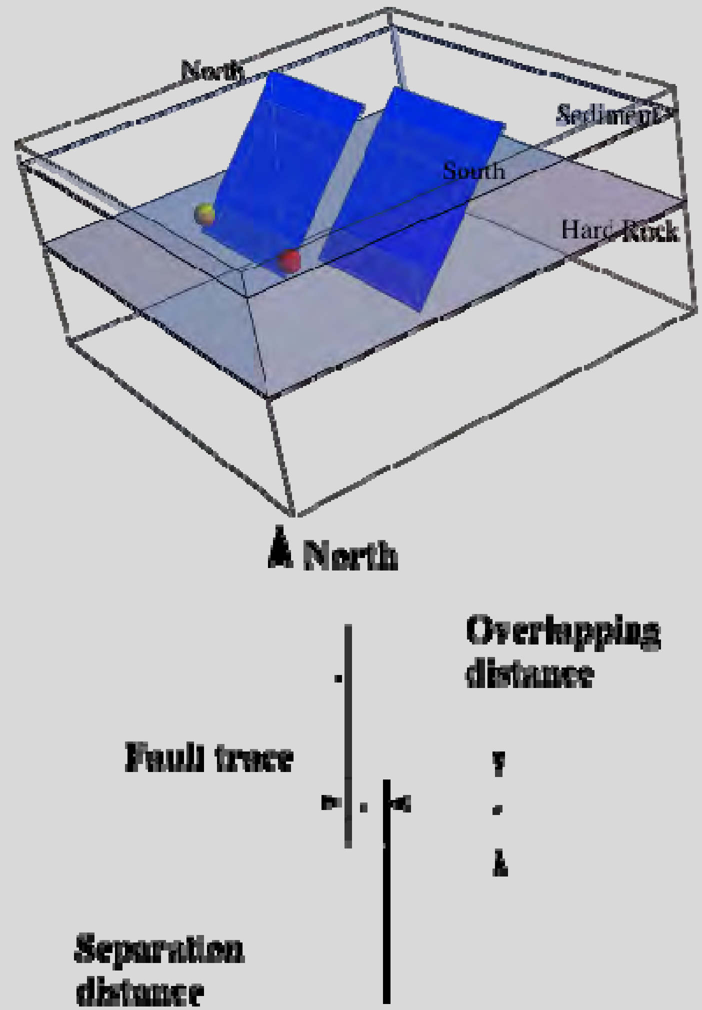

3D Fault geometry model (top)
Map view of the fault segments and key terminology

Comparison of Slip Snapshots between a Single Fault and a Two-Segment Fault

snapshots of the fault: (1.875s 5.625s 13.0s 20.0s), slip in meters

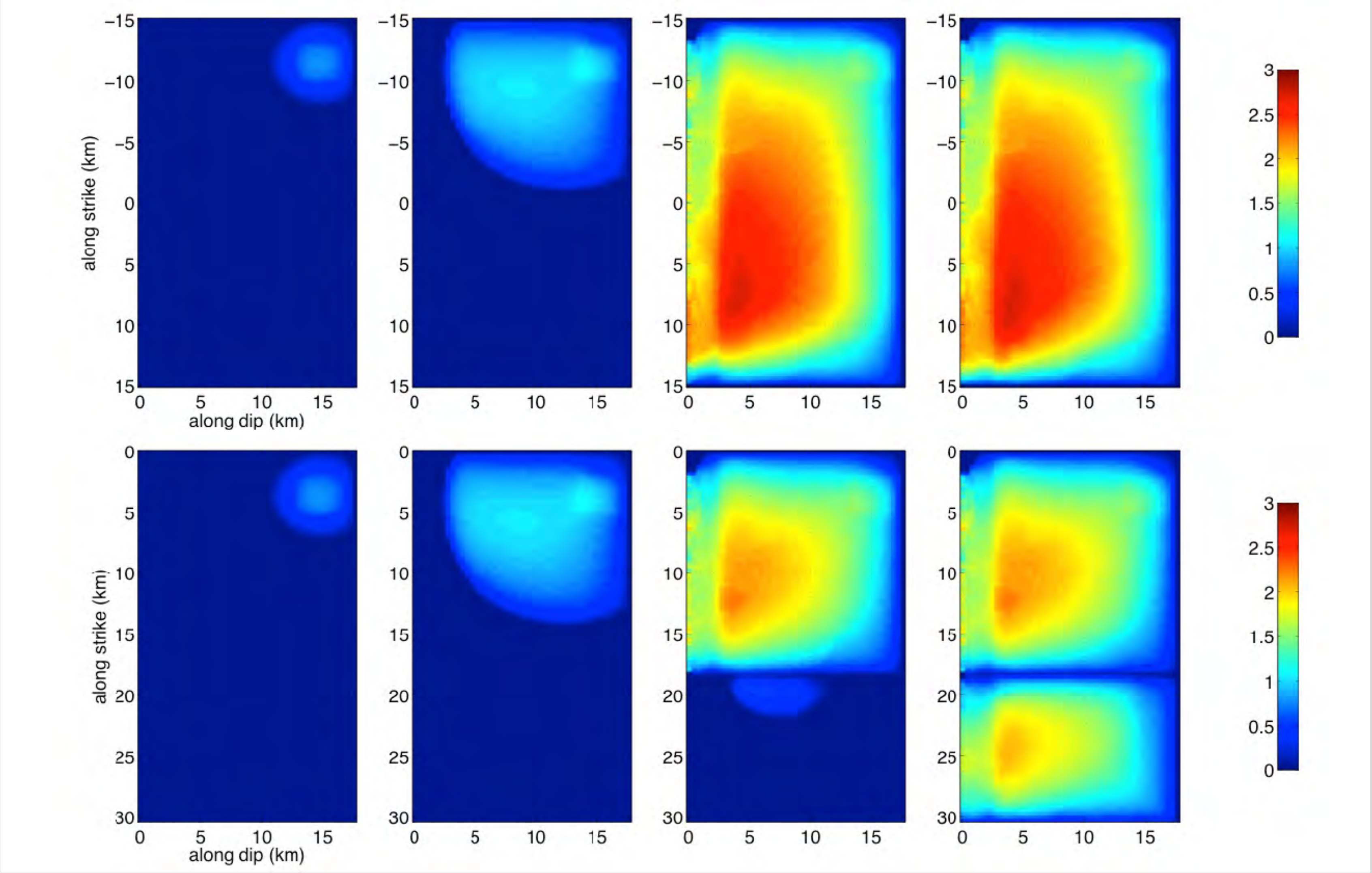

PGV Surface Maps: X, Y, Z components

Single Fault Plane

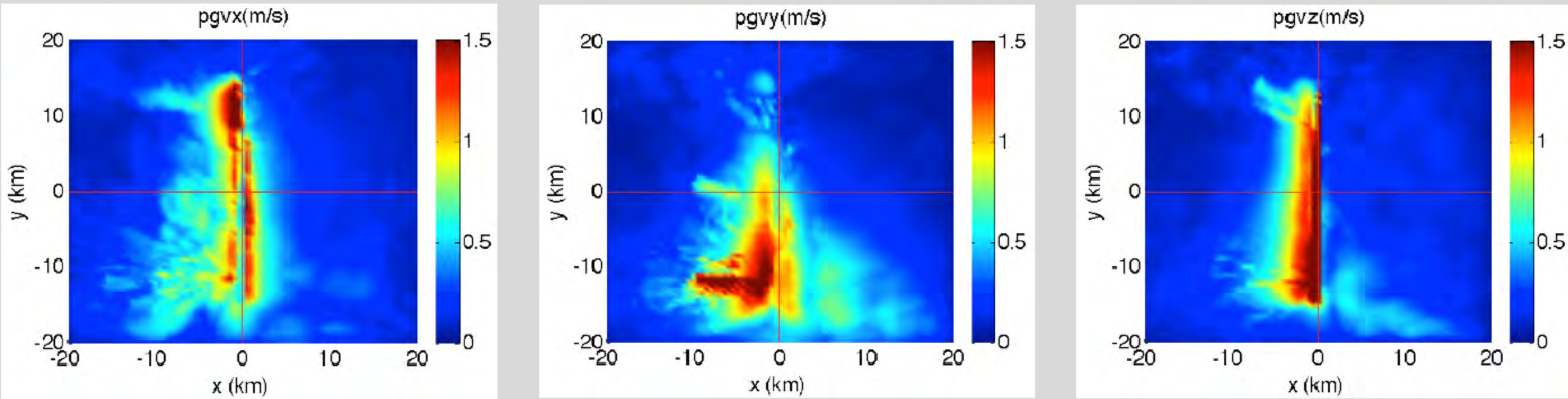

Two-Segment Fault Plane

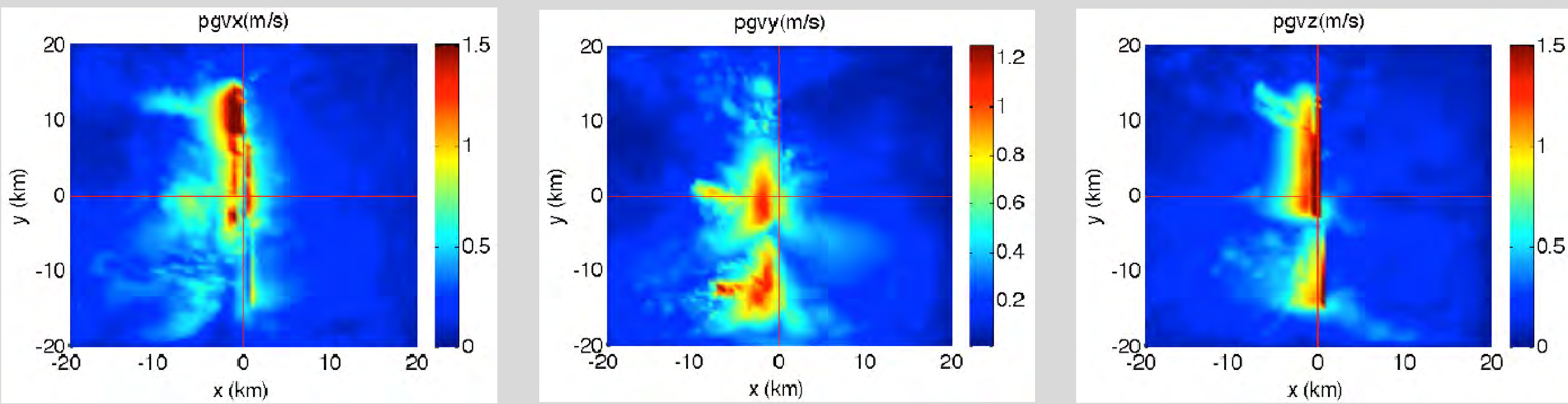

Prediction of Peak Velocity on East-West Profile

Black: Single Fault Plane
Red: Two-Segment Fault

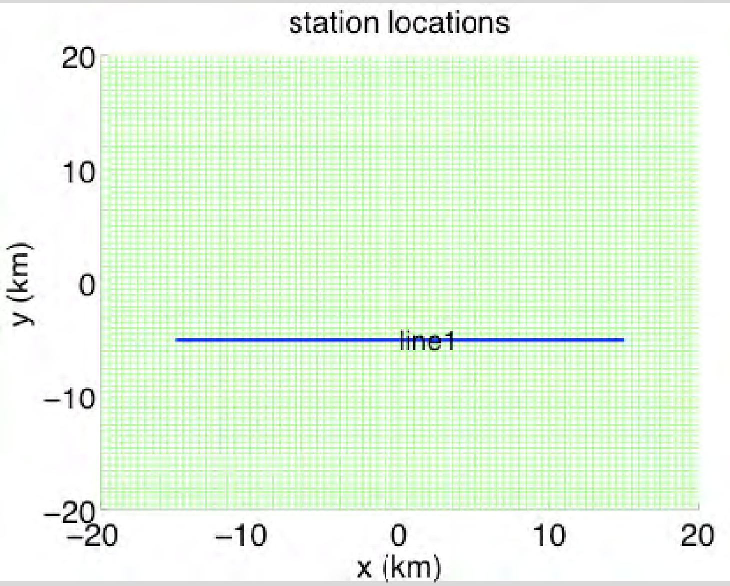

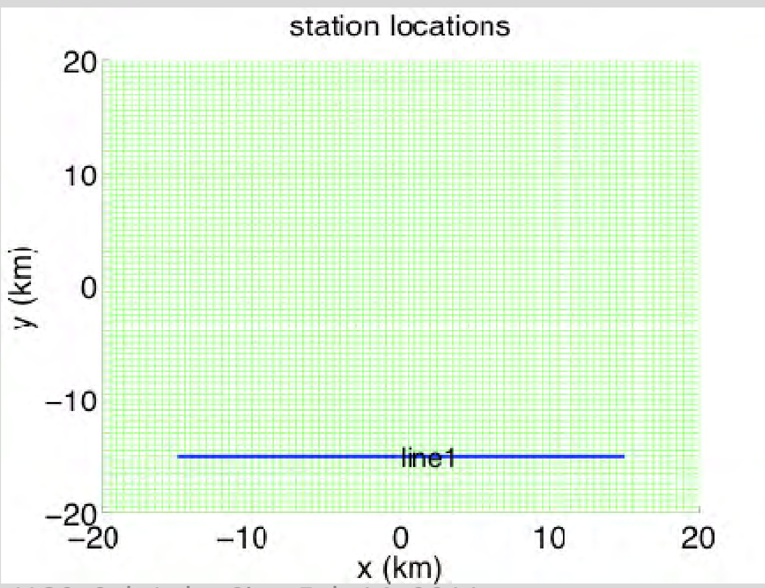

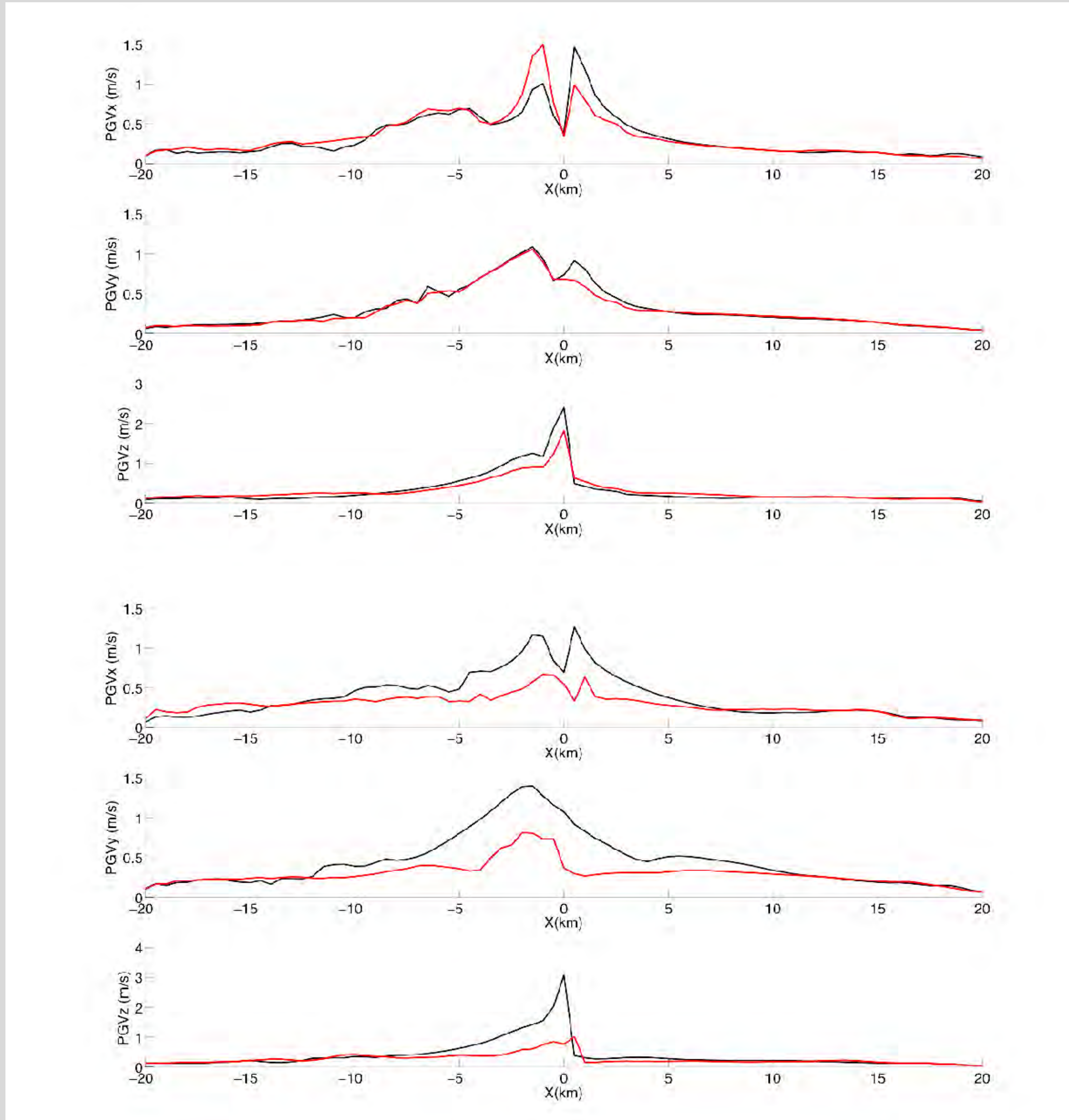

Particle Velocity Time Histories

Black: Single Fault Plane
Red: Two-Segment Fault

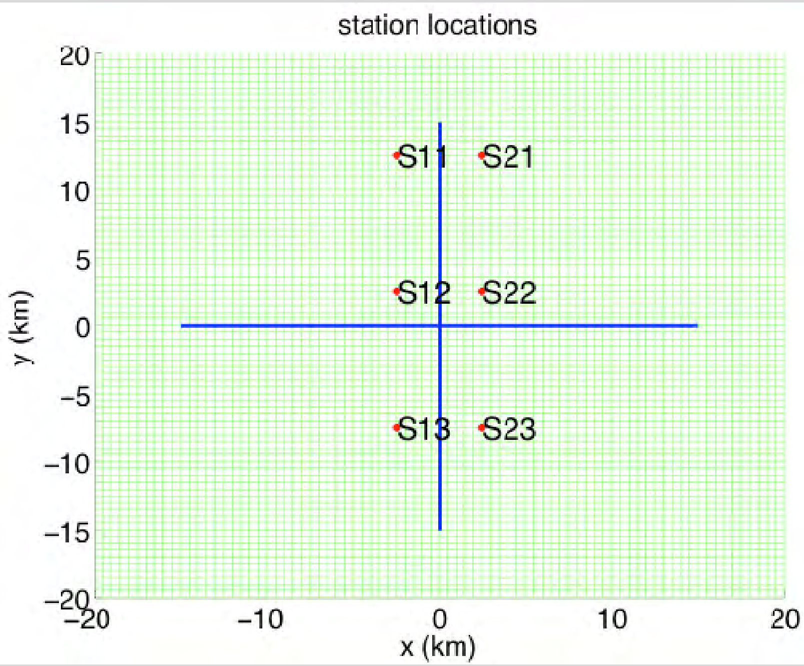

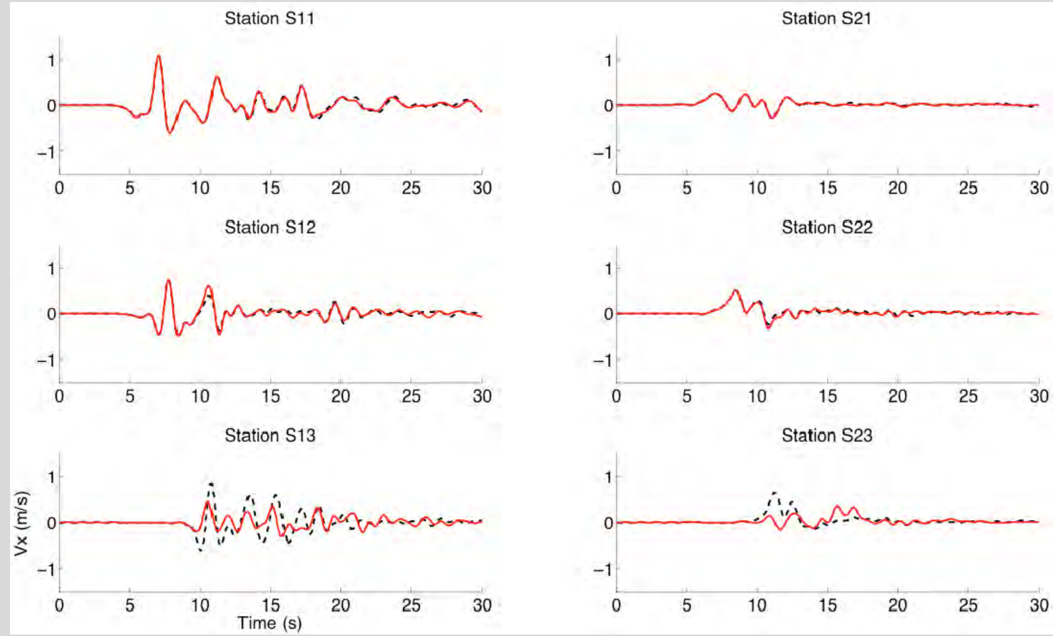

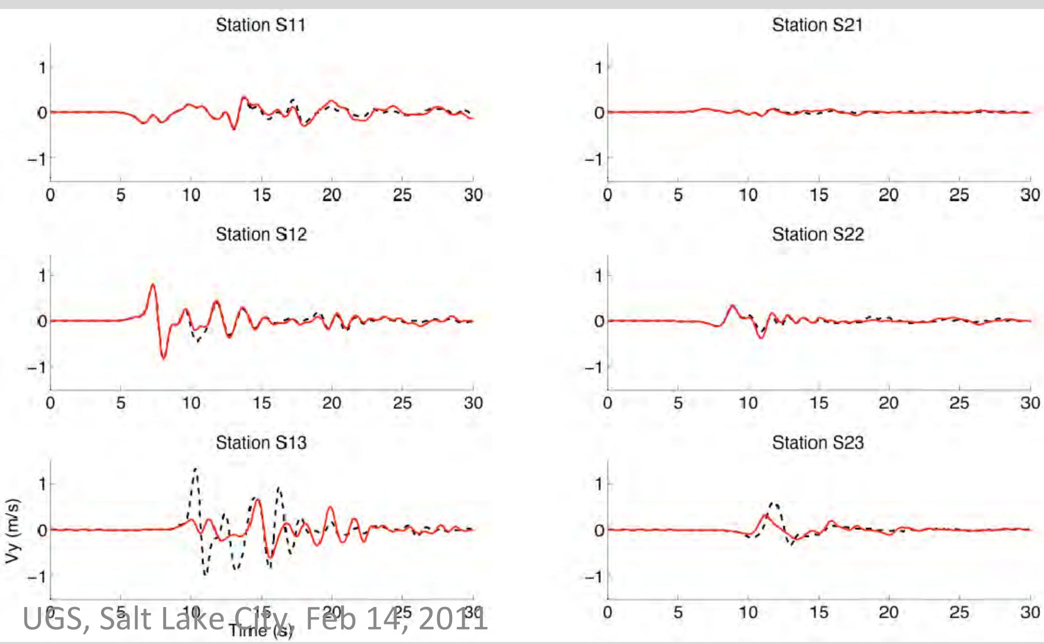

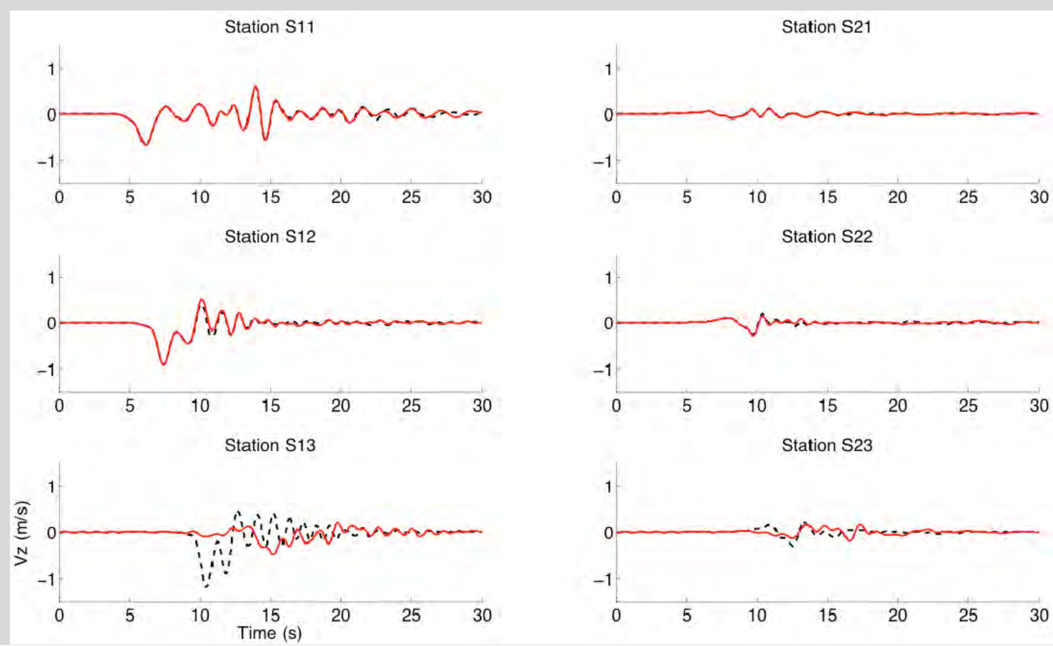

Particle Velocity Time Histories

Black: Single Fault Plane
Red: Two-Segment Fault

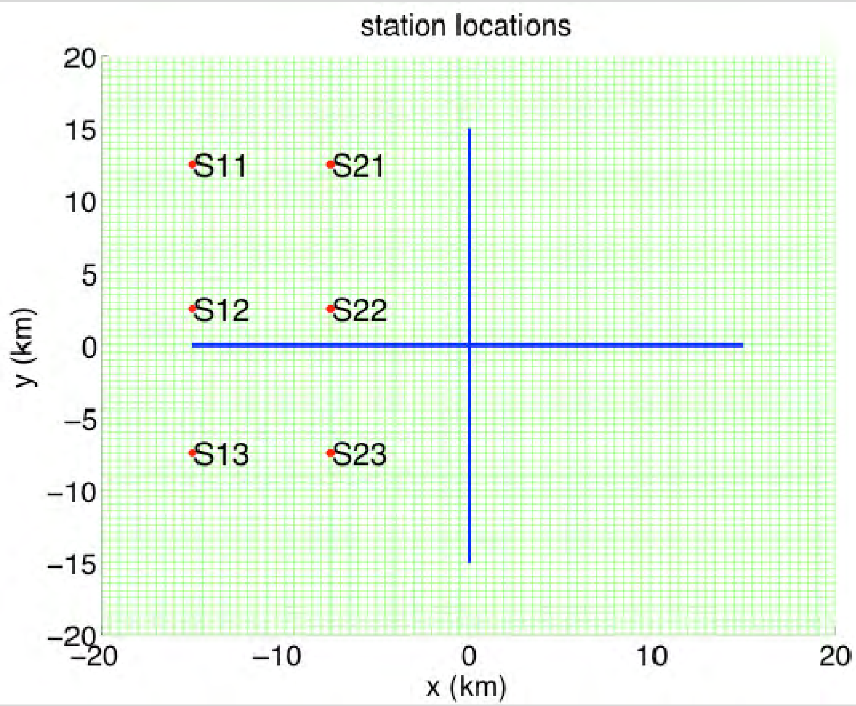

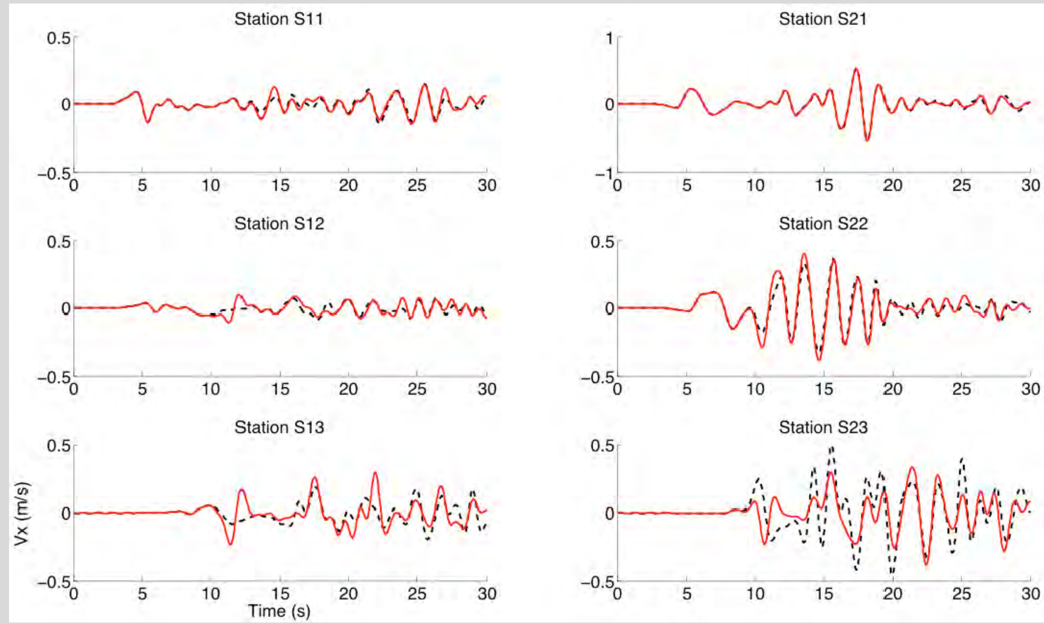

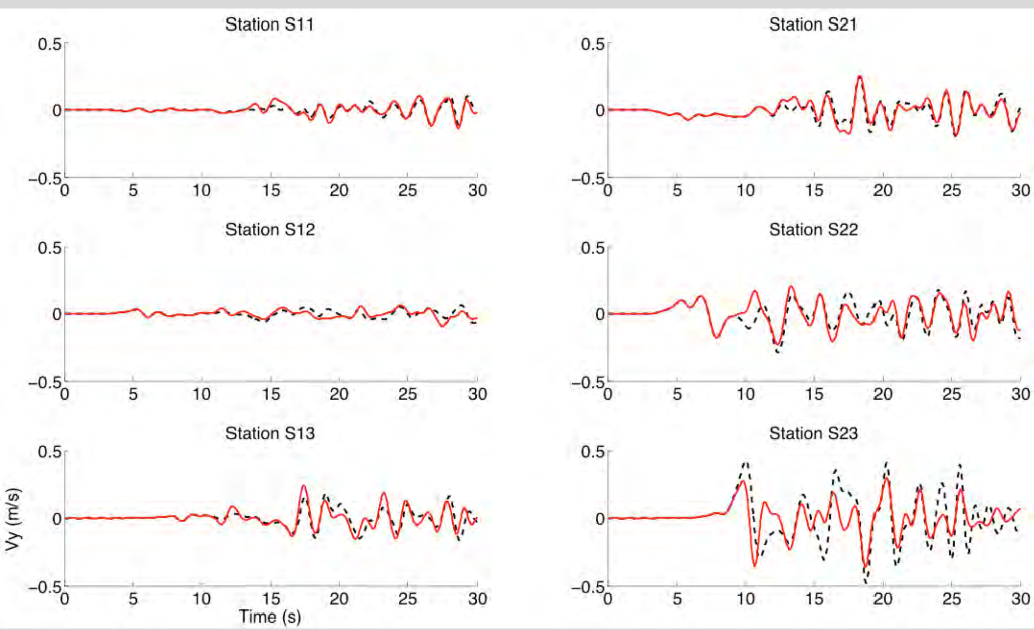

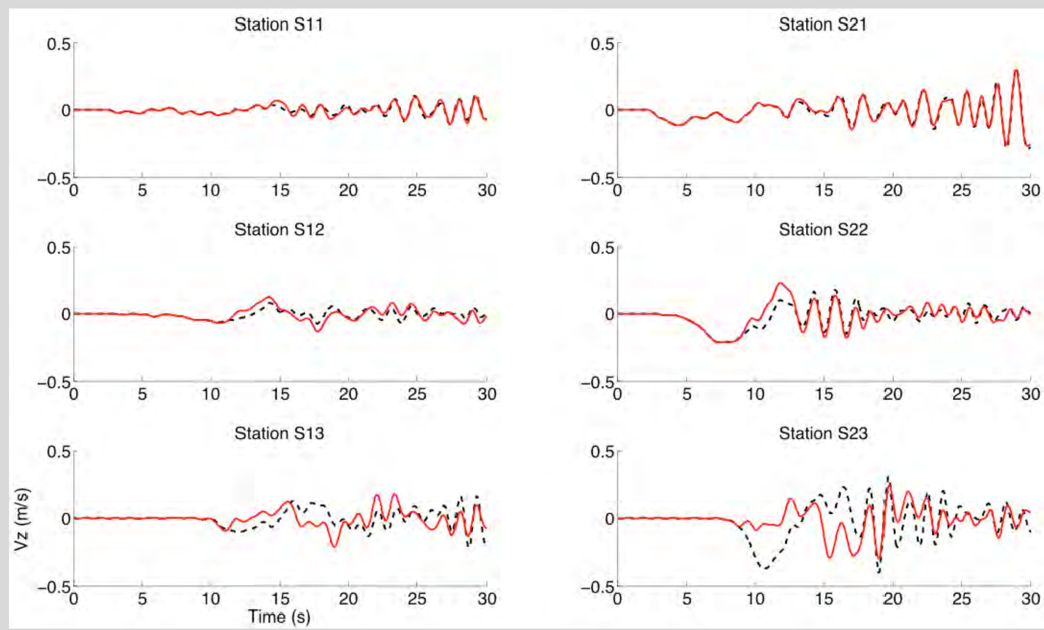

Development of Coulomb stress on planes sub-parallel to the main fault

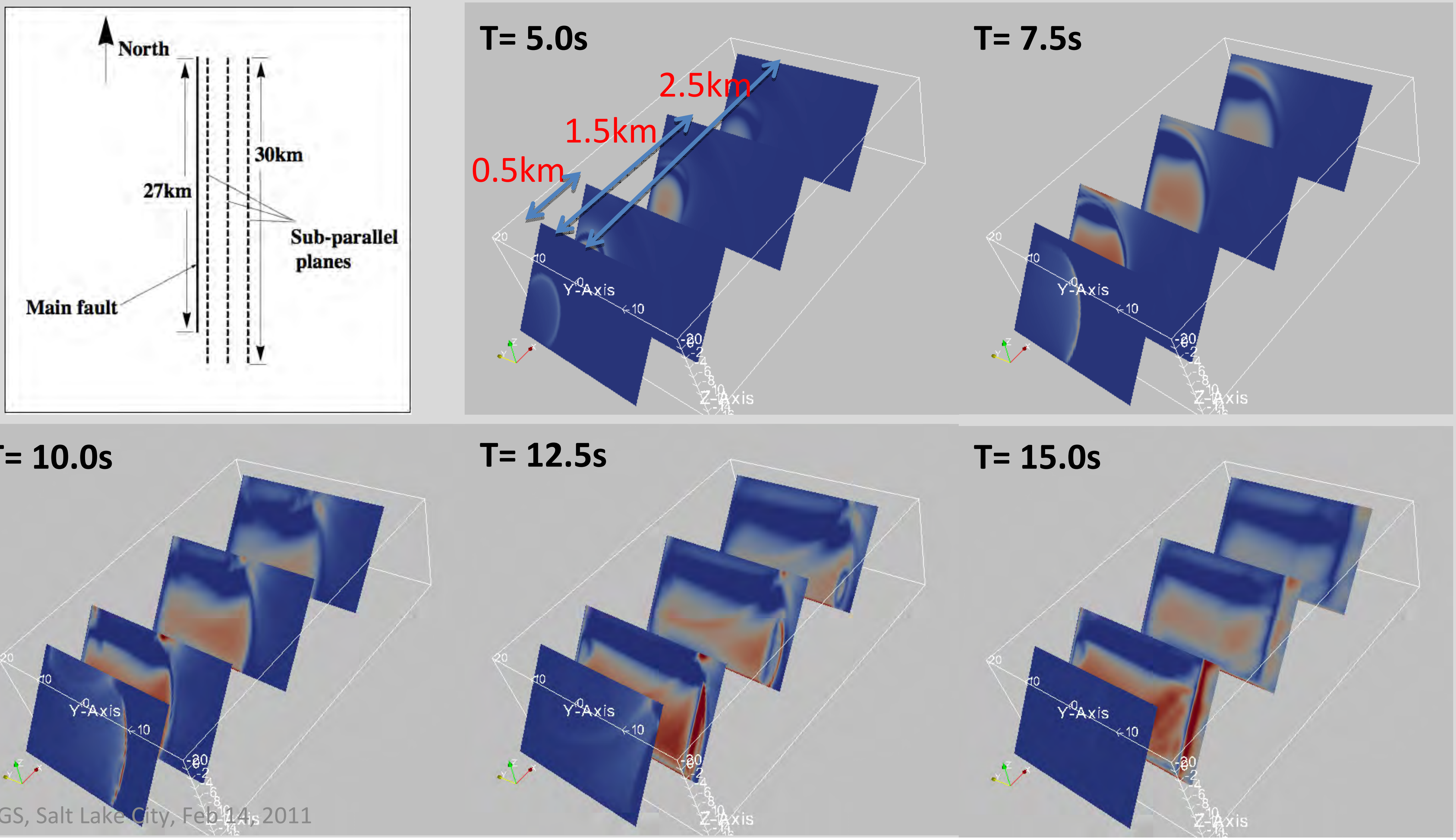

Thank You

Ground Motion Predictions from 0-10 HZ for M7 Earthquakes on the Salt Lake City Segment of the Wasatch Fault, Utah

Daniel Roten
Kim B. Olsen
Harold W. Magistrale
SDSU

James C. Pechmann
University of Utah

Victor M. Cruz-Atienza
UNAM

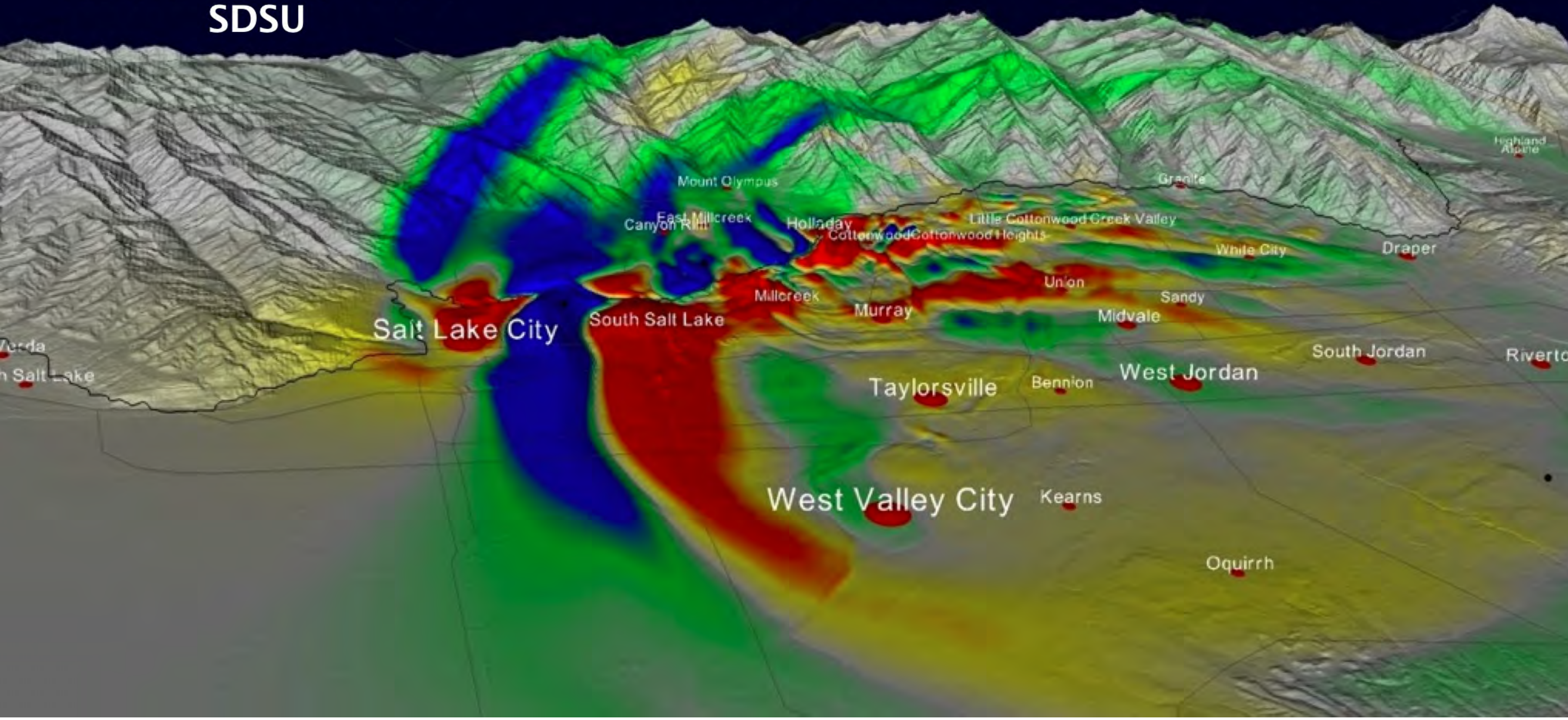

Introduction

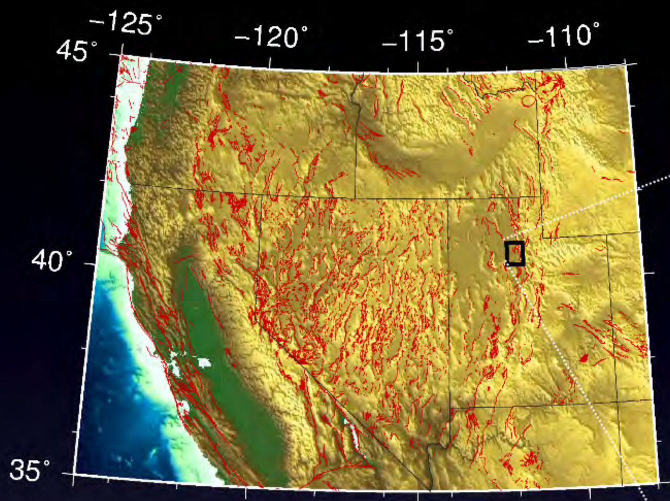

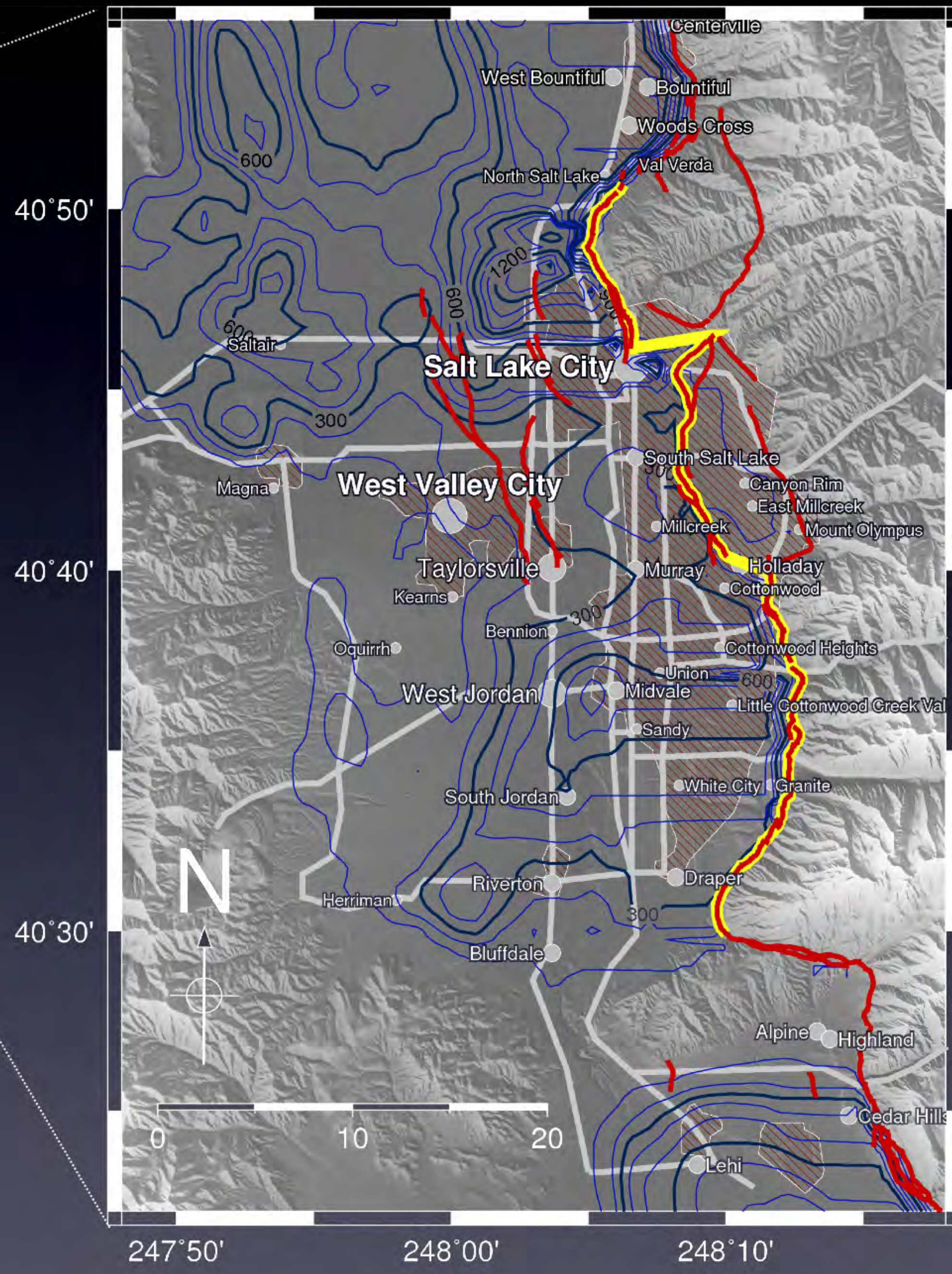

Introduction

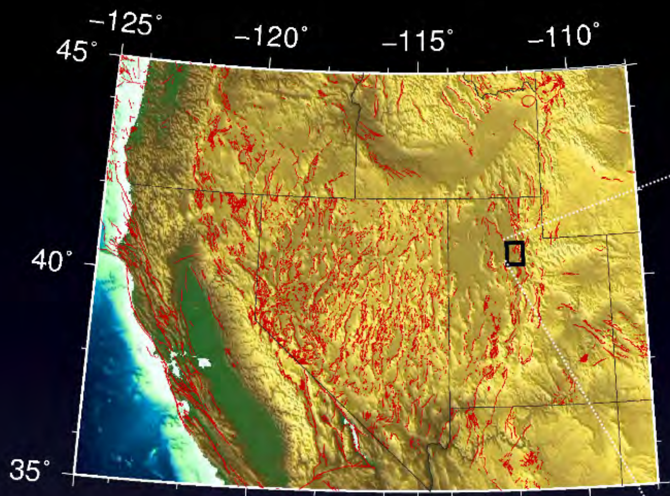

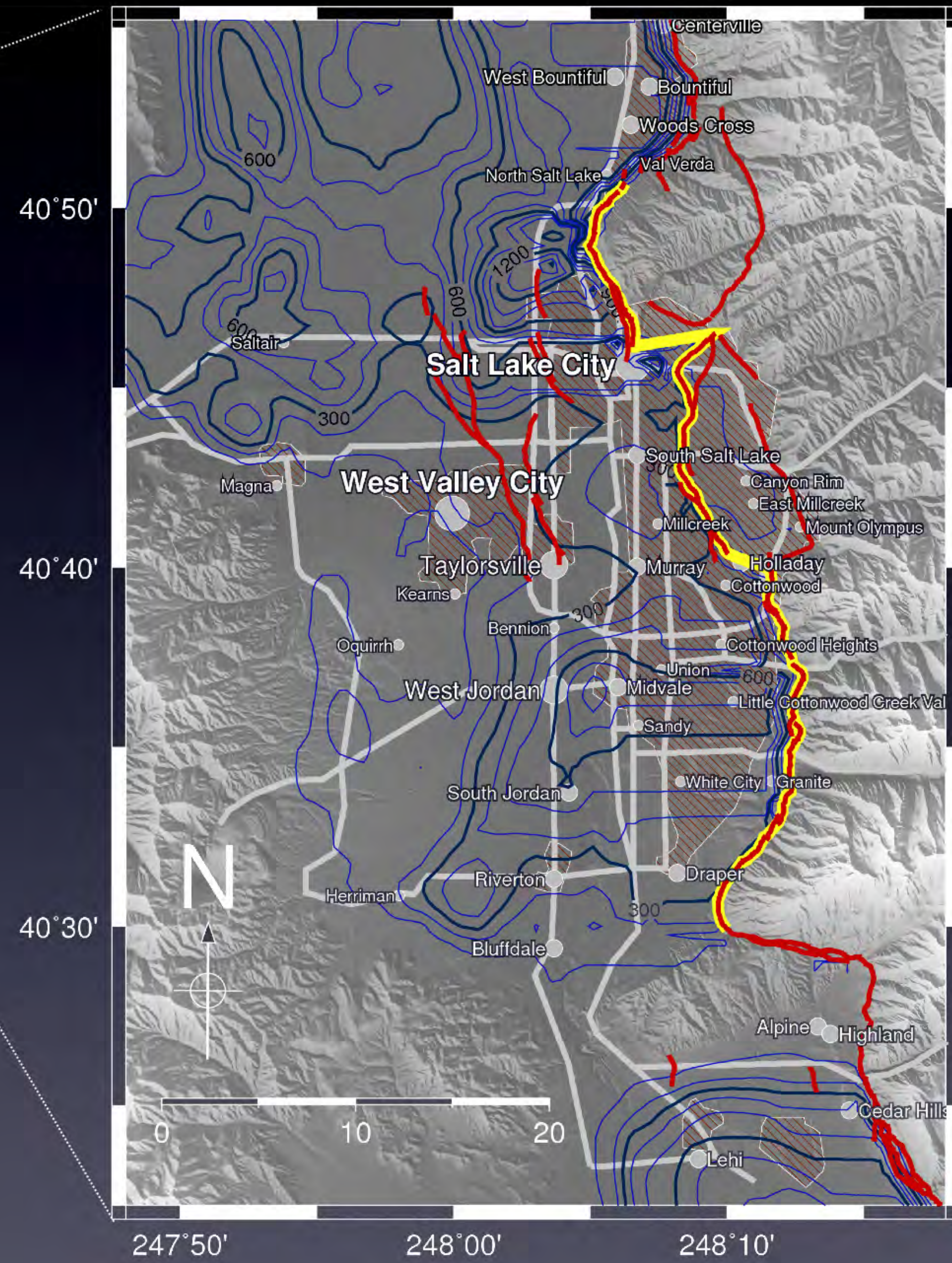

Salt Lake City segment of Wasatch Fault:

- M~7 every 1350 ± 200 years
- 16% probability of M7 event in next 100 yrs (McCalpin and Nelson, 2000)
- 6-9% probability for next 50 yrs (Wong et al., 2002)

Four-Step Method

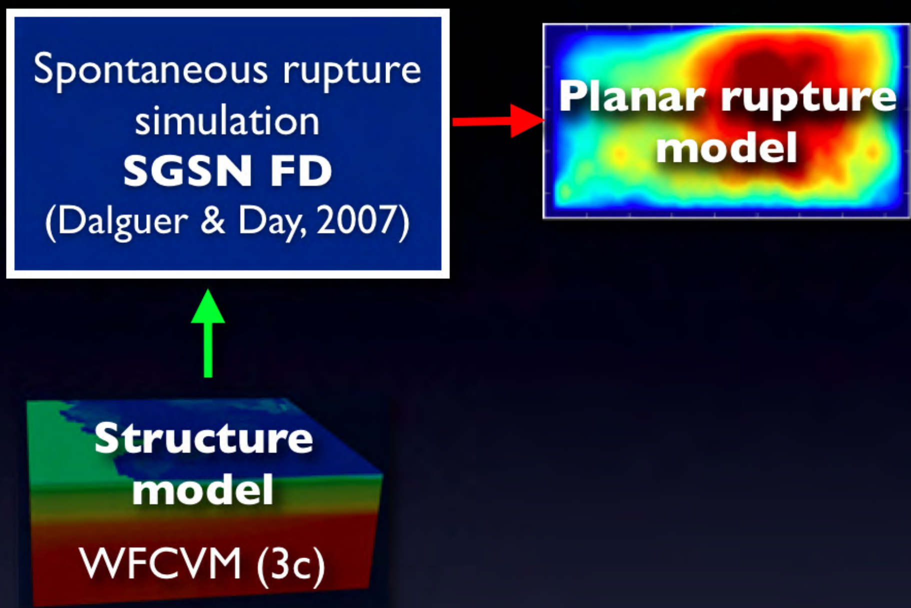

Four-Step Method

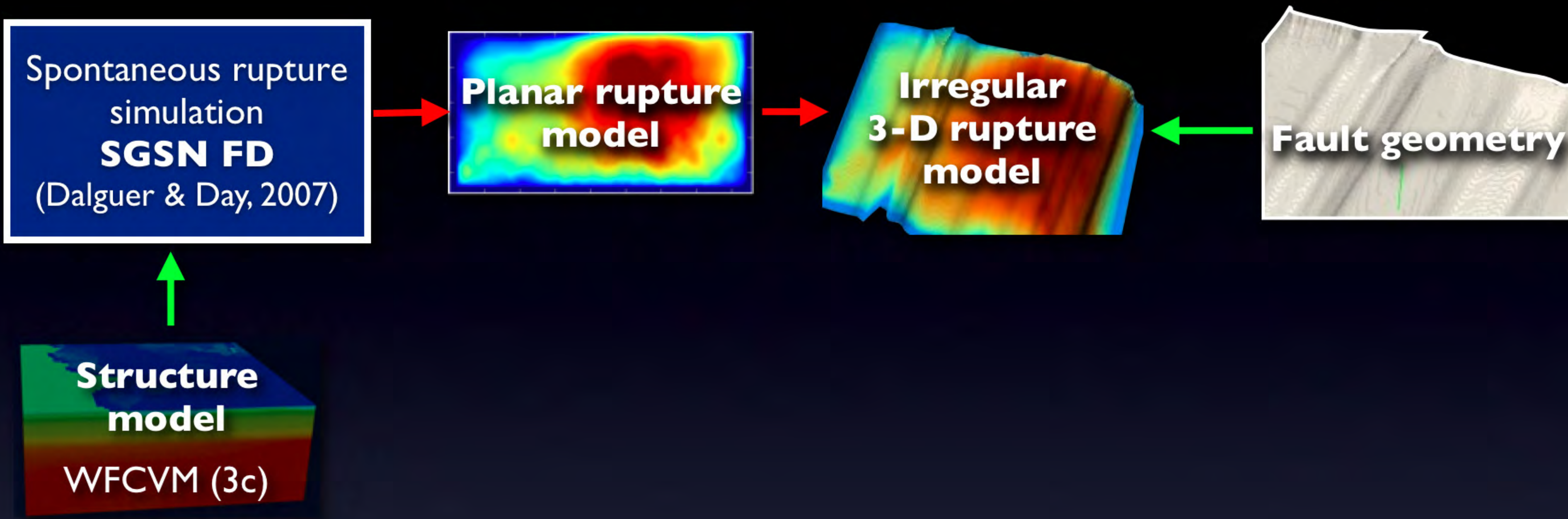

Four-Step Method

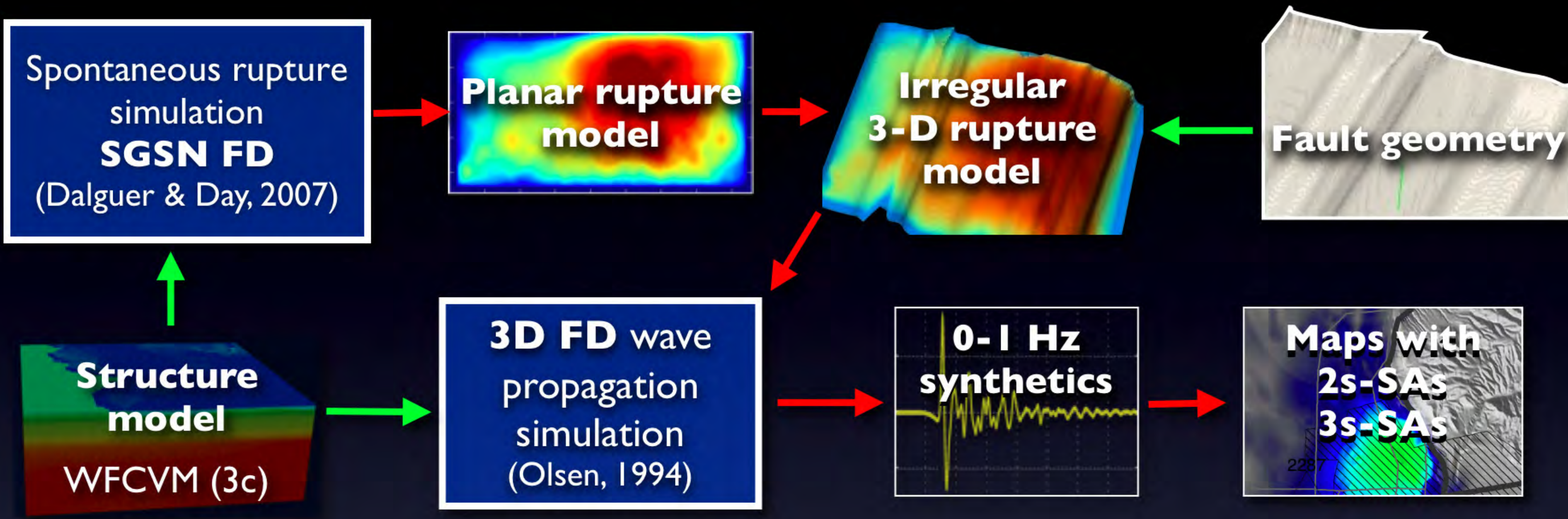

Four-Step Method

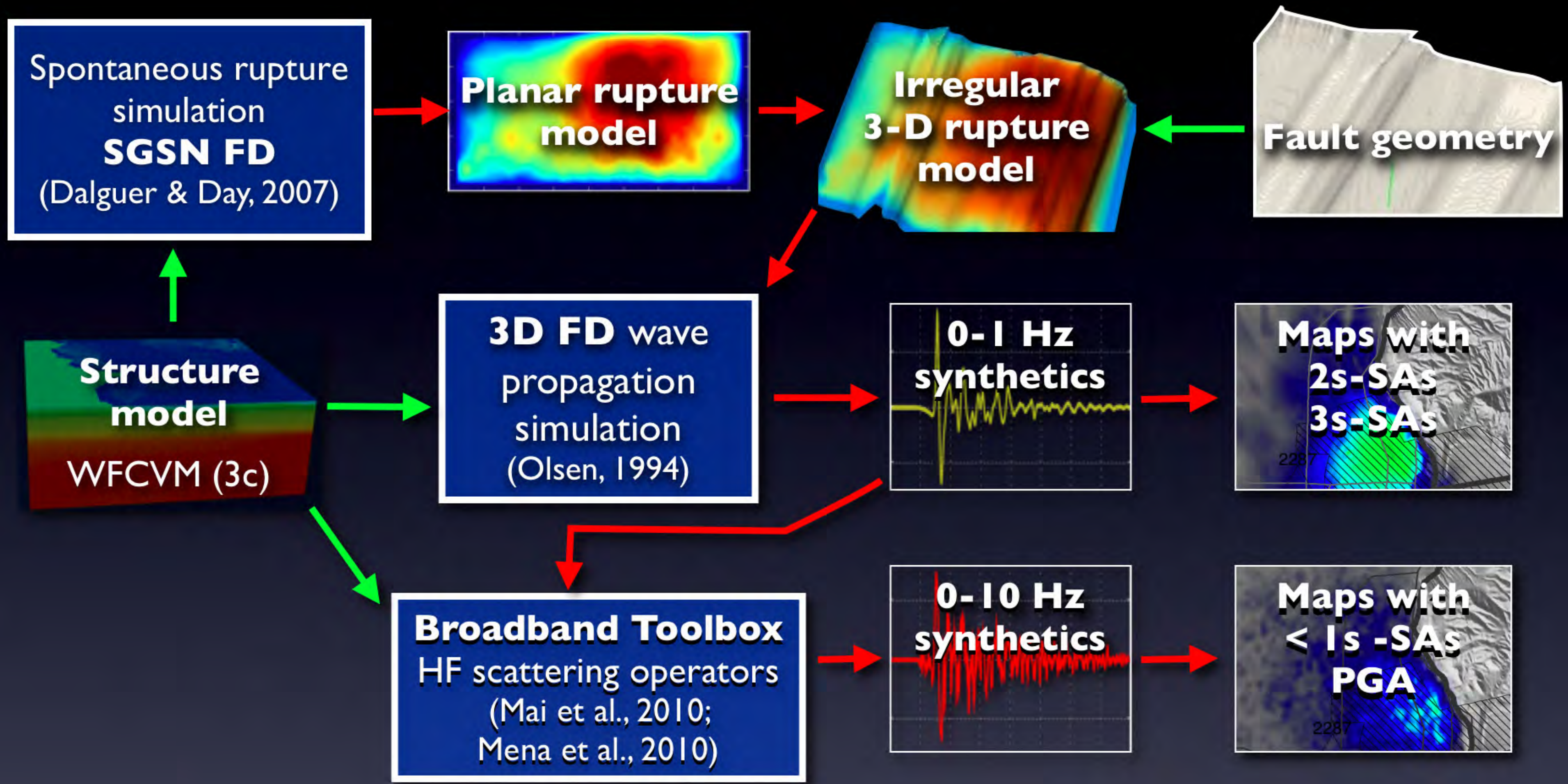

Four-Step Method

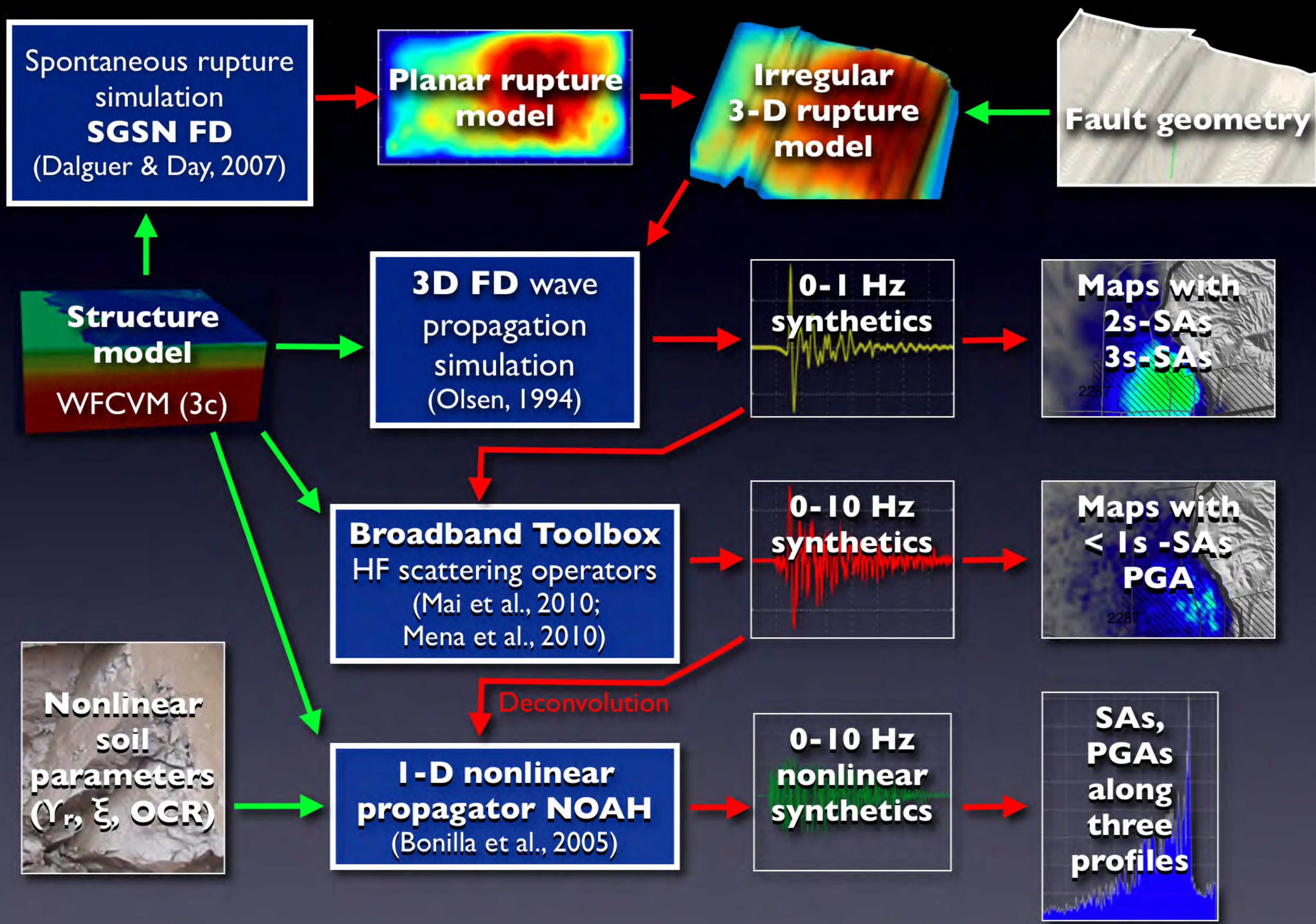

Four-Step Method

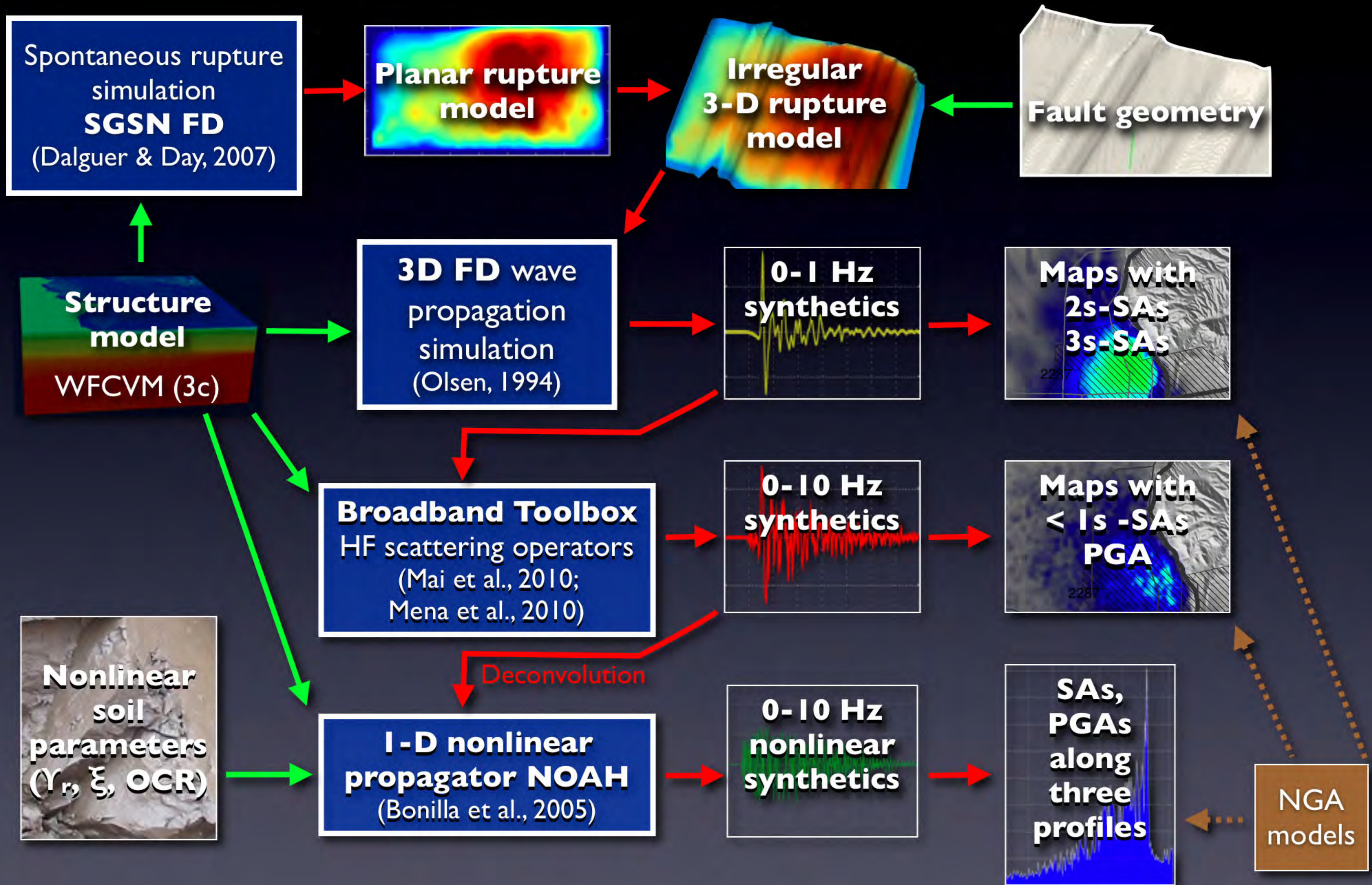

3D model of the WFSLC segment

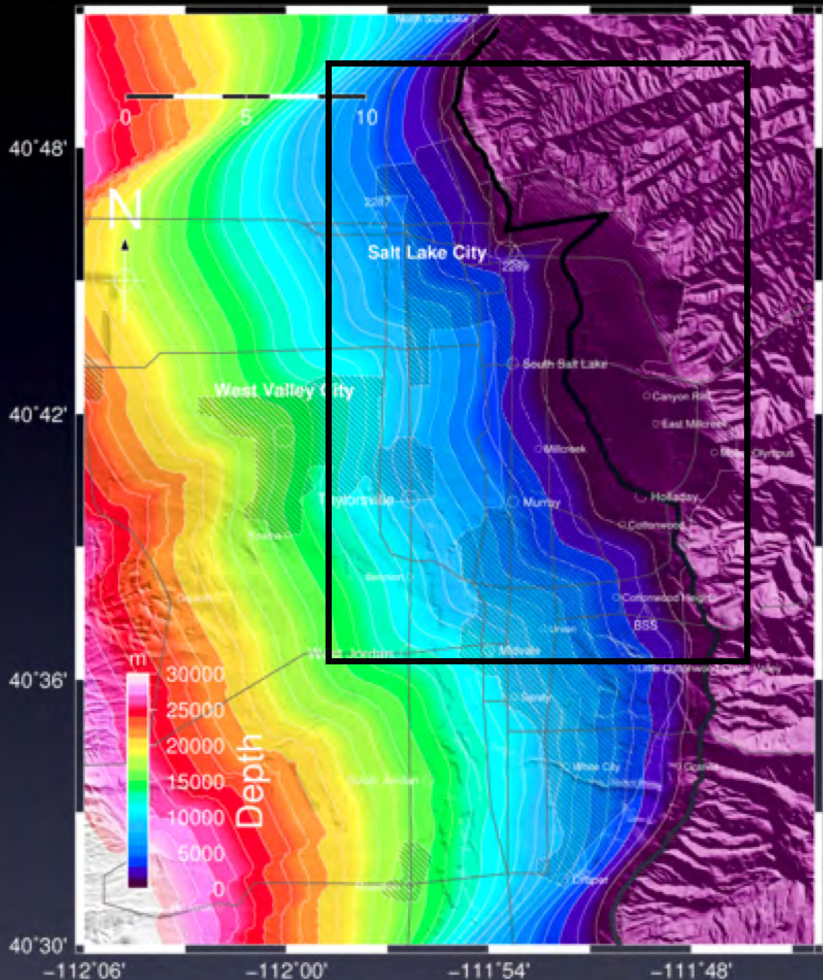

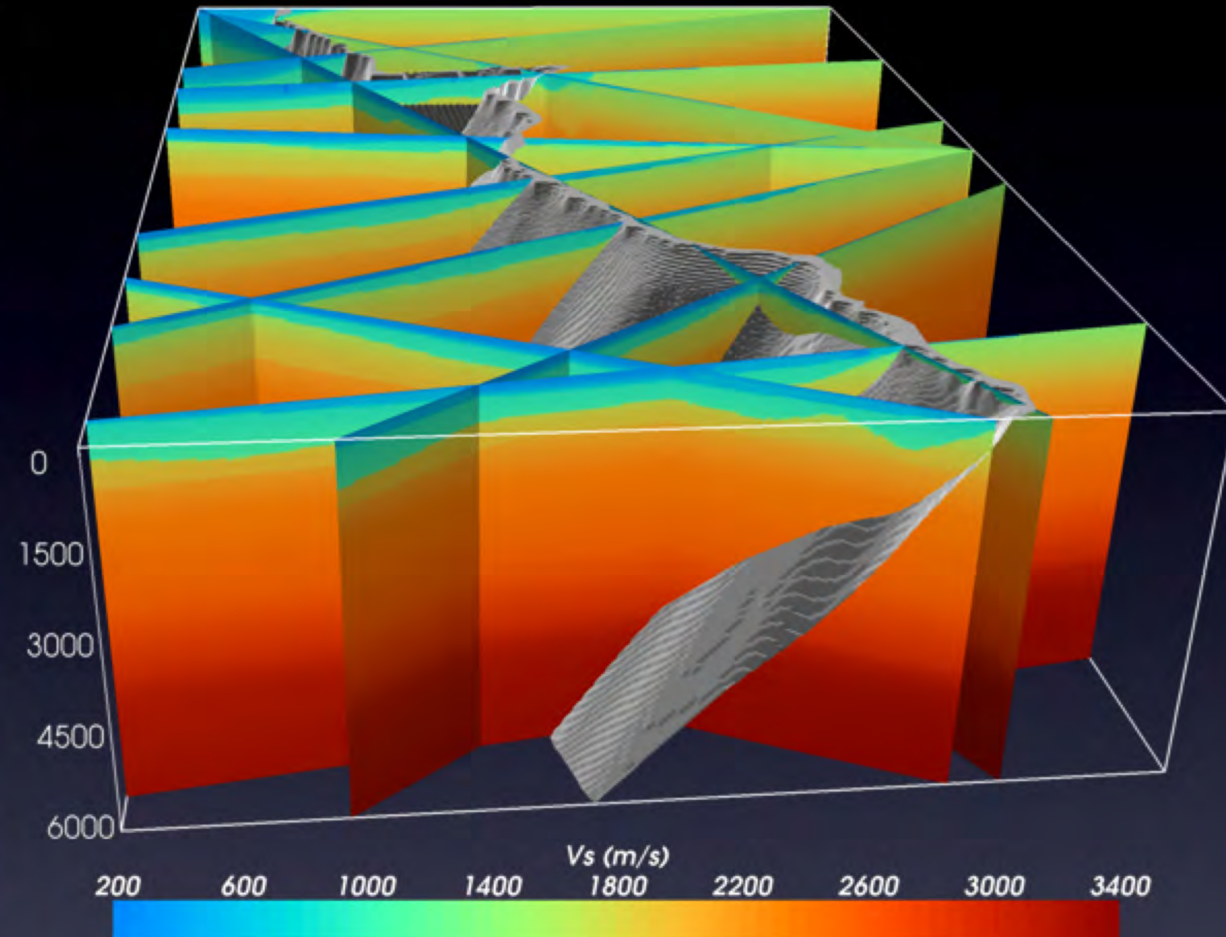

- Final model of the SLC segment of the WF used for M7 scenario simulations
- Fault geometry mostly consistent with eastern boundaries of the Salt Lake Valley basin

Spontaneous Rupture Models

- Simulation of dynamic rupture process on a planar vertical fault
- Staggered-grid split node finite difference method (Dalguer & Day, 2007)
- Depth-dependent normal stress (Dalguer & Mai, 2008)
- Simulated velocity strengthening near the free surface (reduce τ_0, increase d_0, $\mu_d > \mu_s$)
- Four rupture models with different hypocenter locations

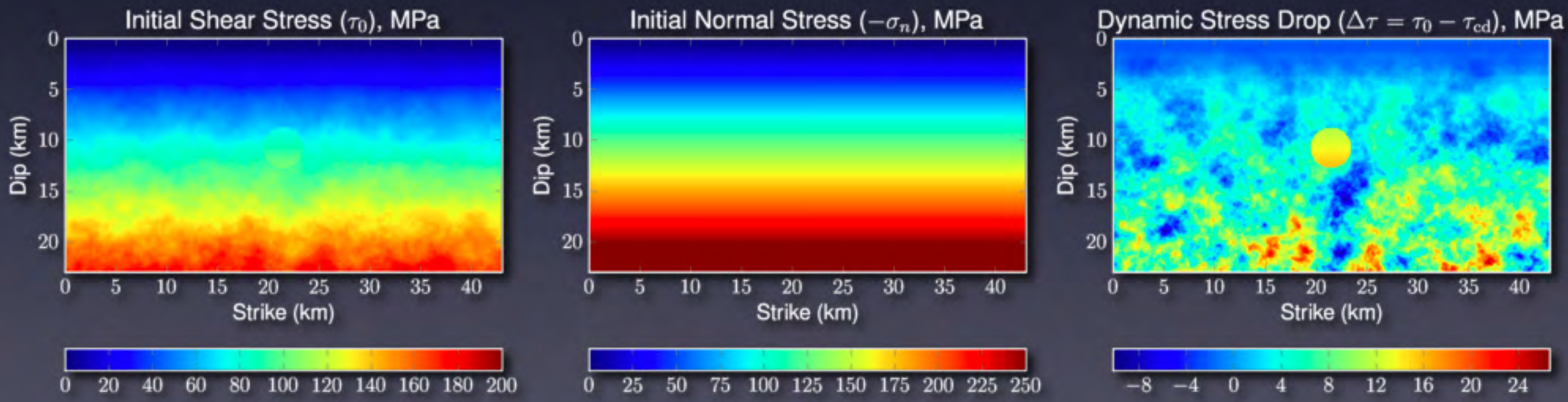

Spontaneous Rupture Models

- Simulation of dynamic rupture process on a planar vertical fault
- Staggered-grid split node finite difference method (Dalguer & Day, 2007)
- Depth-dependent normal stress (Dalguer & Mai, 2008)
- Simulated velocity strengthening near the free surface (reduce τ_0, increase d_0, $\mu_d > \mu_s$)
- Four rupture models with different hypocenter locations

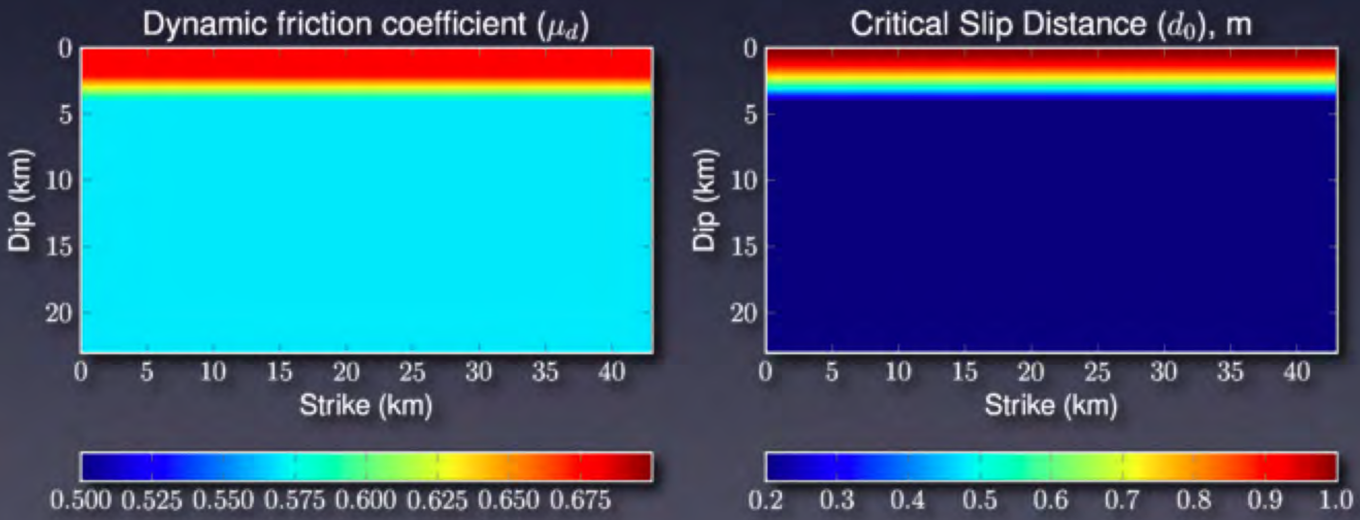

Spontaneous Rupture Models

Scenario A

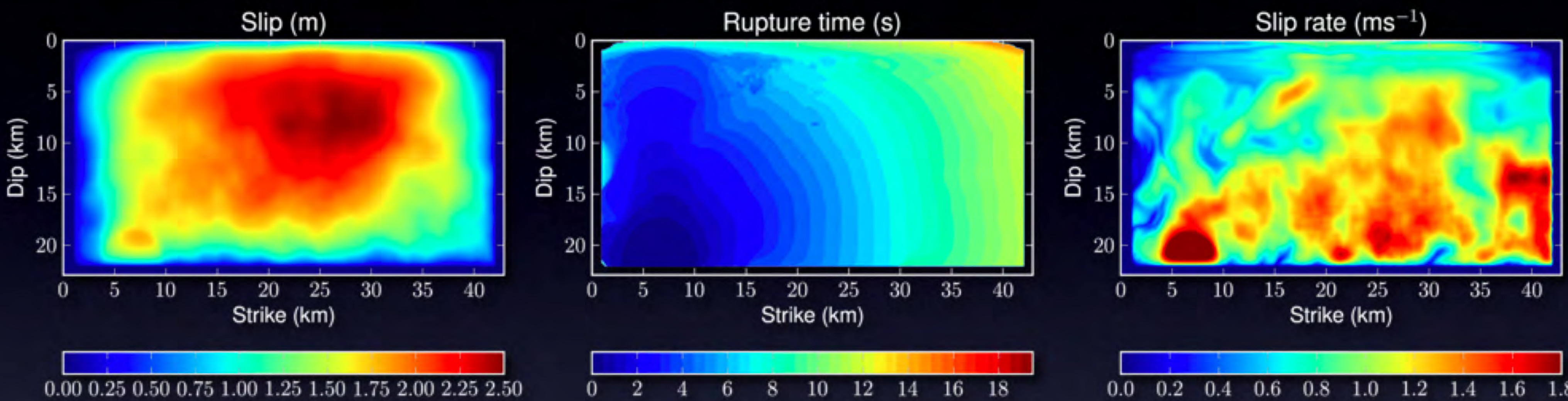

Scenario B

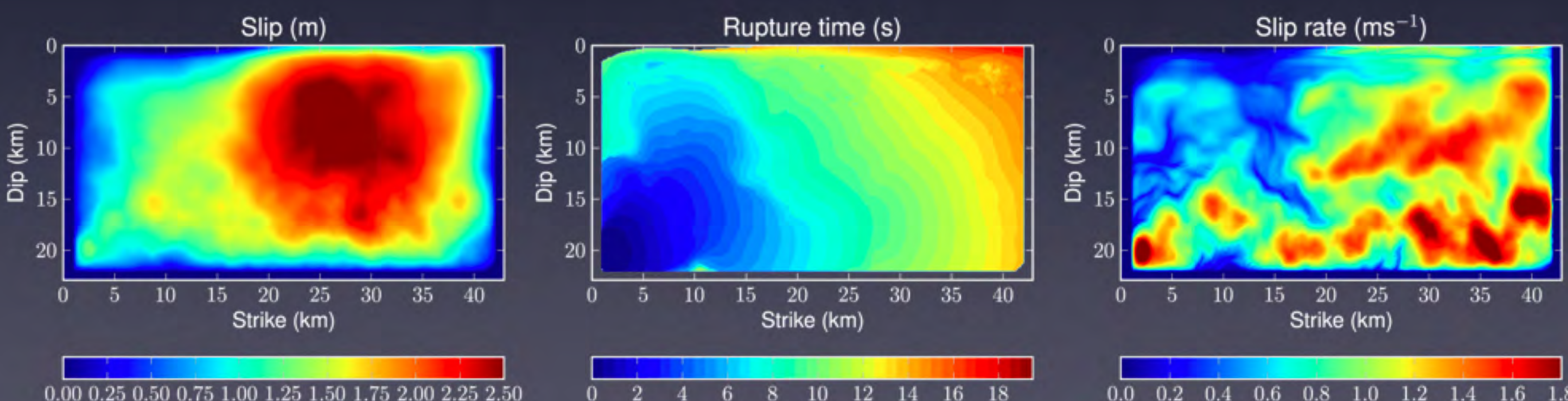

Spontaneous Rupture Models

Scenario C

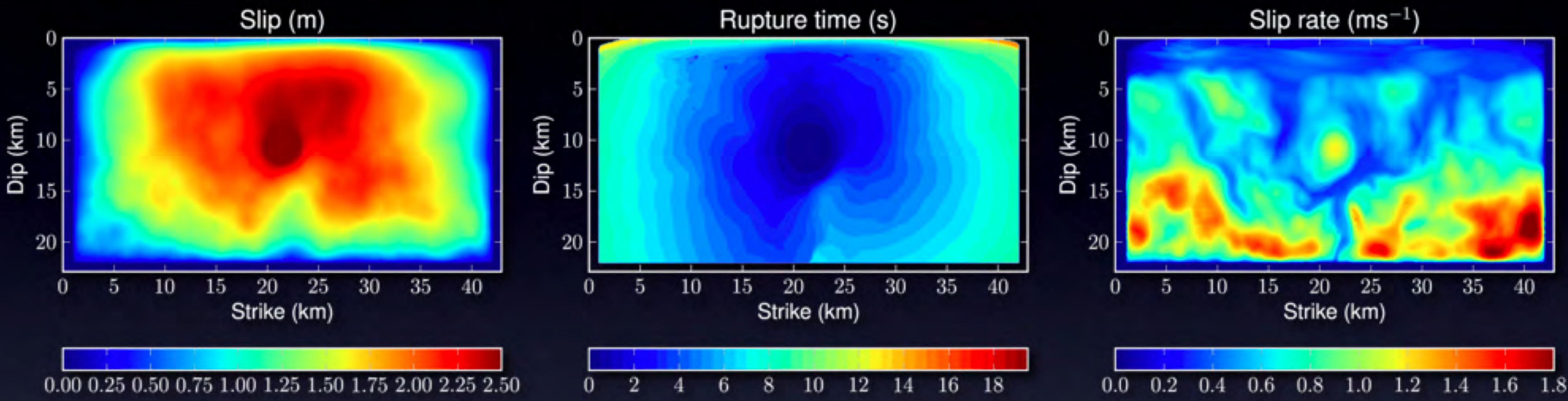

Scenario D

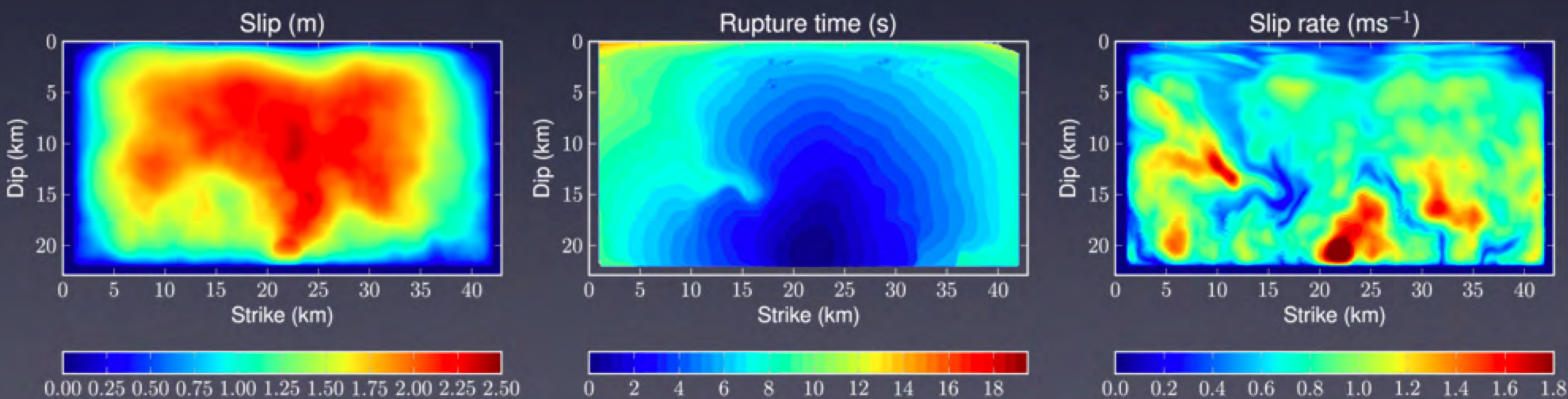

Six scenario EQs

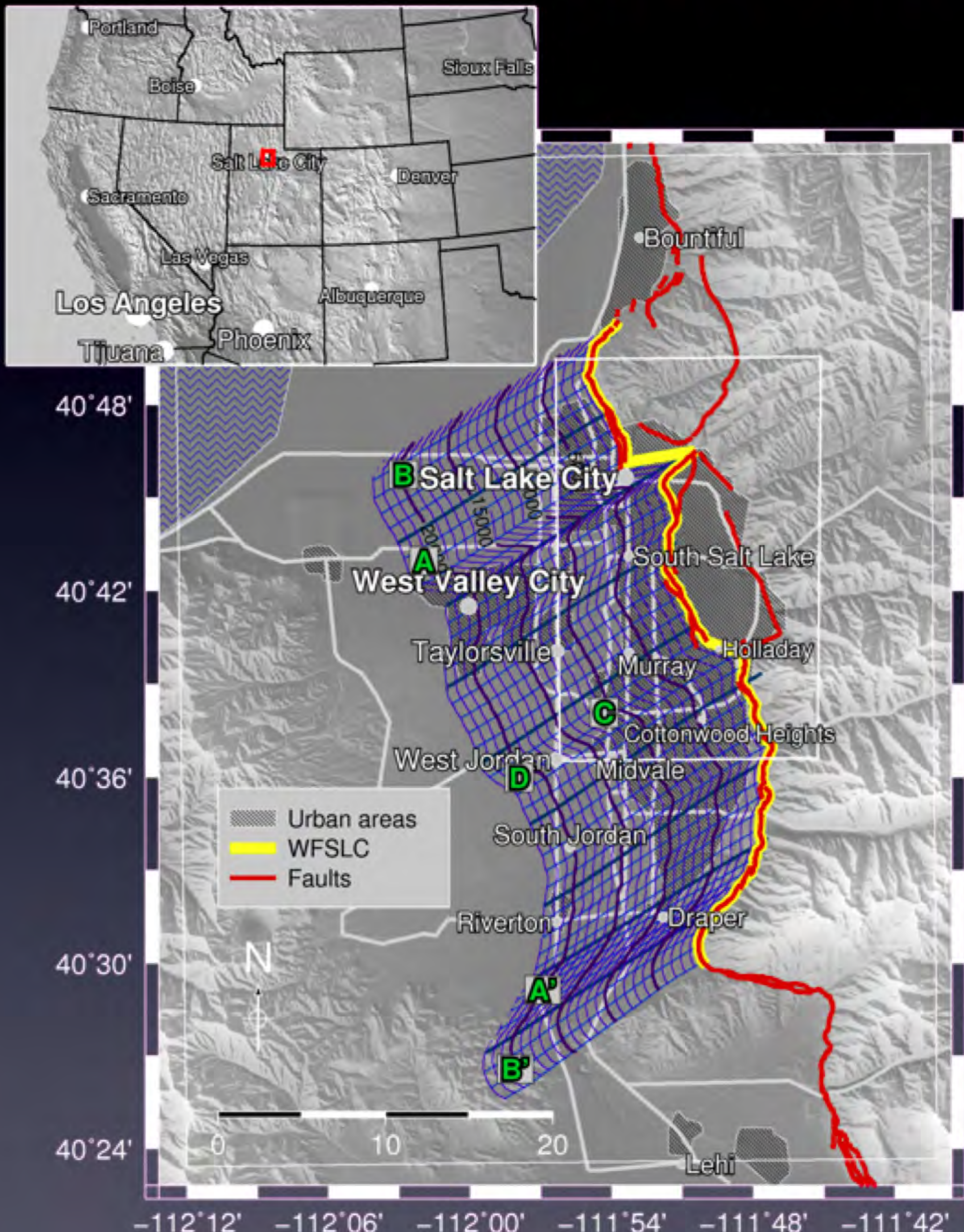

Representative distribution of hypocenter locations:

Normal faulting EQs tend to originate near brittle-ductile transition zone (~15 km depth):

- 5 deep hypocenters (20 km down-dip)
- 1 shallower hypocenter (10 km down-dip)

Rupture tends to start near non-conservative barriers:

- near northern end (A, B)
- near southern end (A', B')
- near bifurcation near Holladay stepover (C, D)

(Bruhn et al. ,1992)

FD Simulation of Wave Propagation

- Planar rupture models are projected onto irregular 3-D model of the WF and the moment rate time histories are inserted into grid nodes
- Two of the four rupture models are mirrored laterally, yielding six source models
- Wave propagation of these source models is simulated with velocity-stress staggered-grid finite difference method (Olsen, 1994)

FD3D parameters	
Model dimensions	1500 x 1125 x 500
Simulation length	60s (24,000 iter.)
Discretization	40m / 0.0025 s
Minimum V_S	200 ms^{-1}
Highest frequency	1 Hz
# of CPU cores	1875
Wall-clock runtime	2.5 hrs (NICS Kraken)

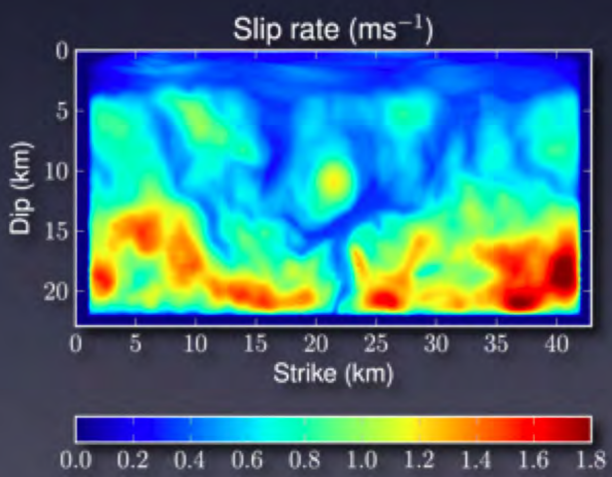

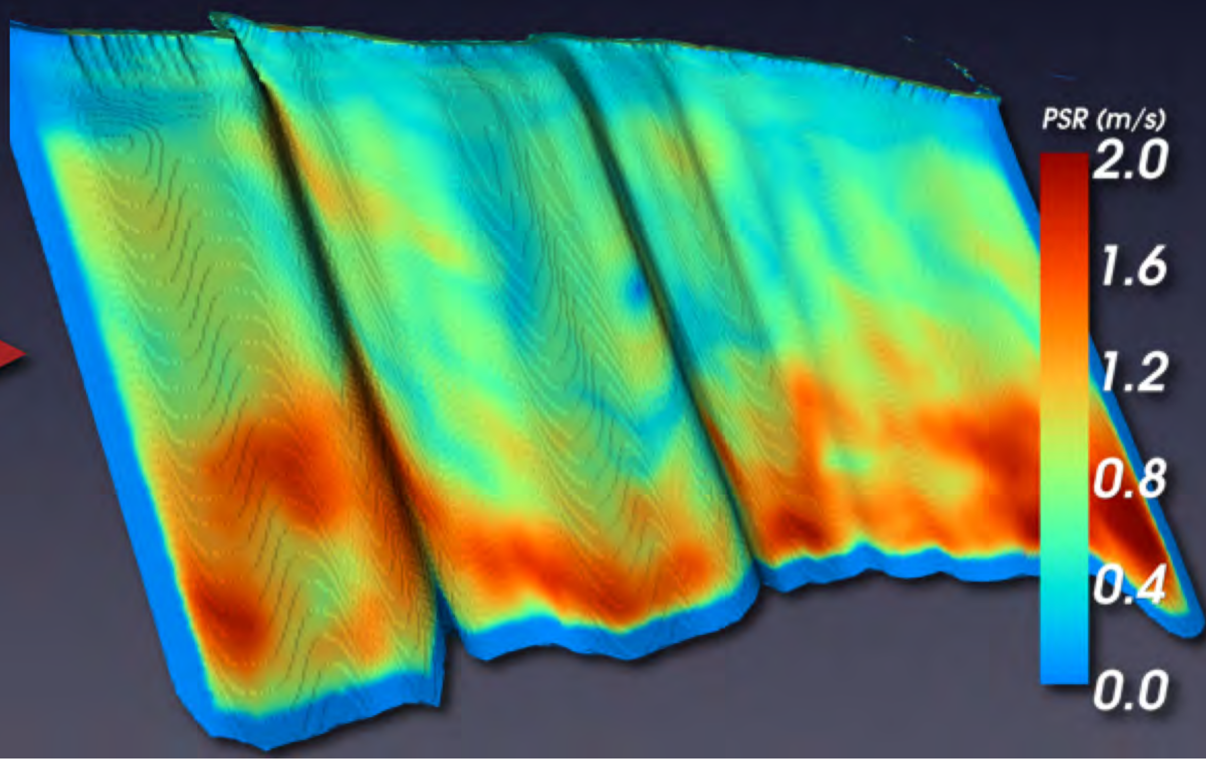

Spectral Accelerations at 2s (2s-SAs)

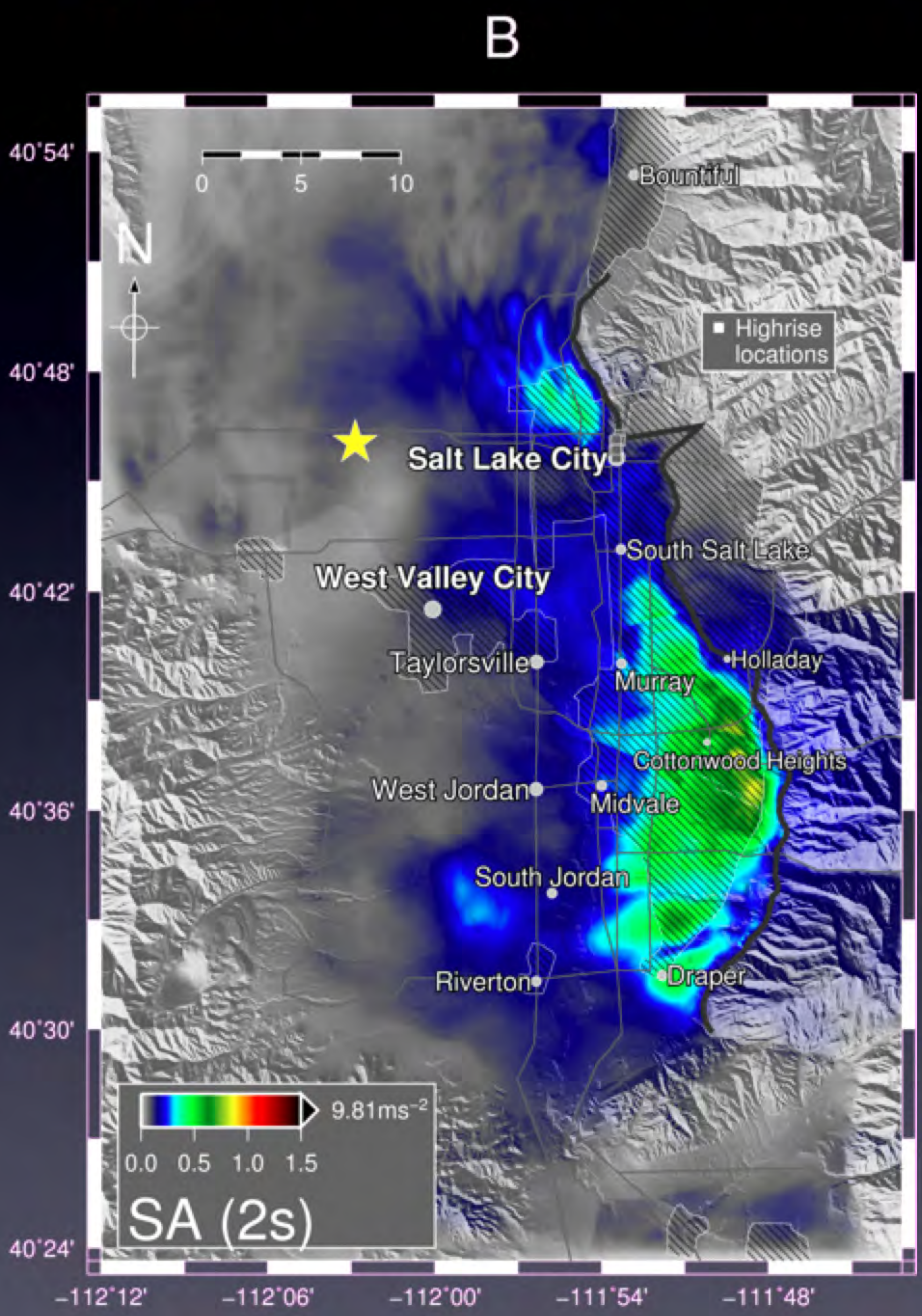

Spectral Accelerations at 2s (2s-SAs)

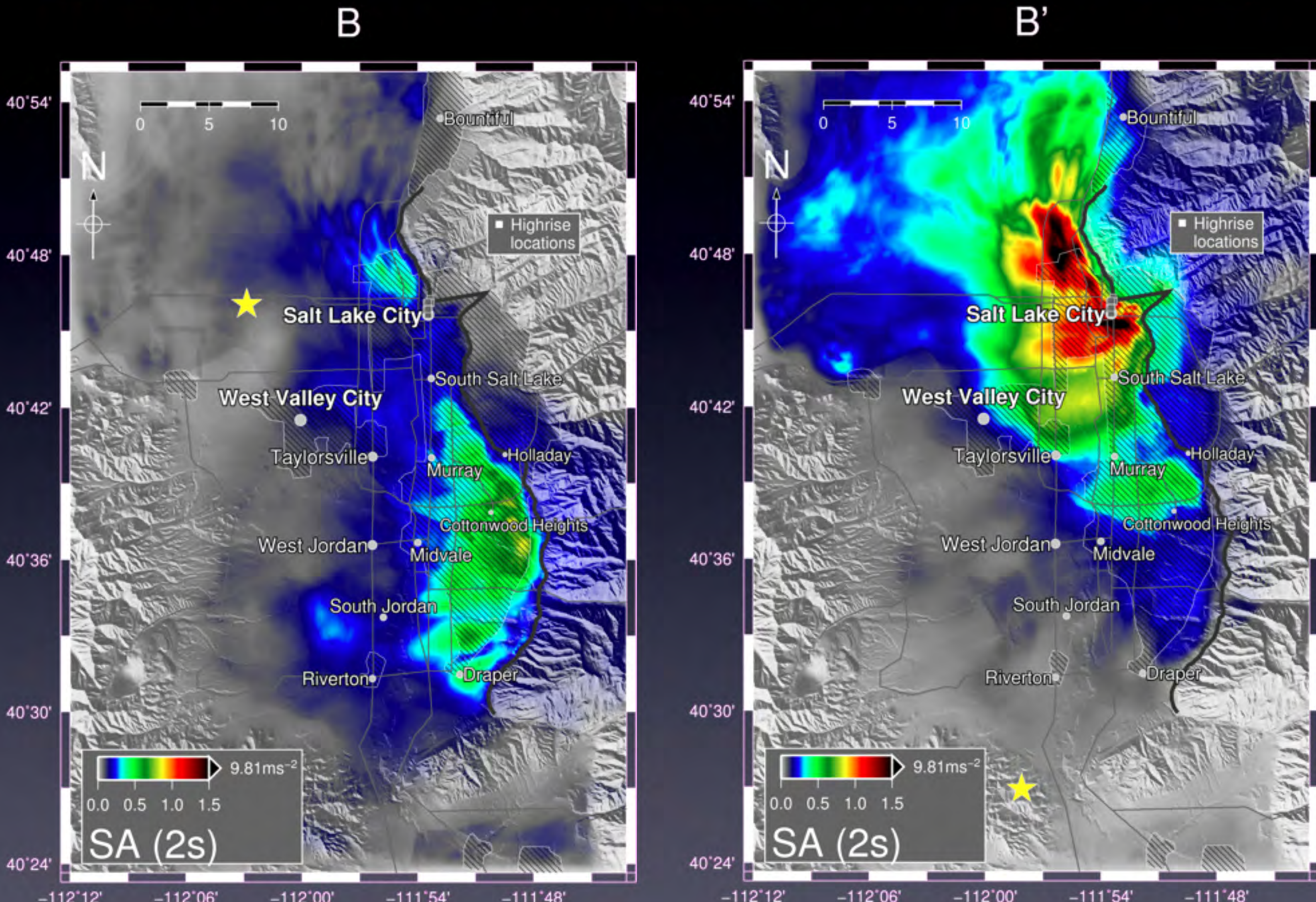

Spectral Accelerations at 2s (2s-SAs)

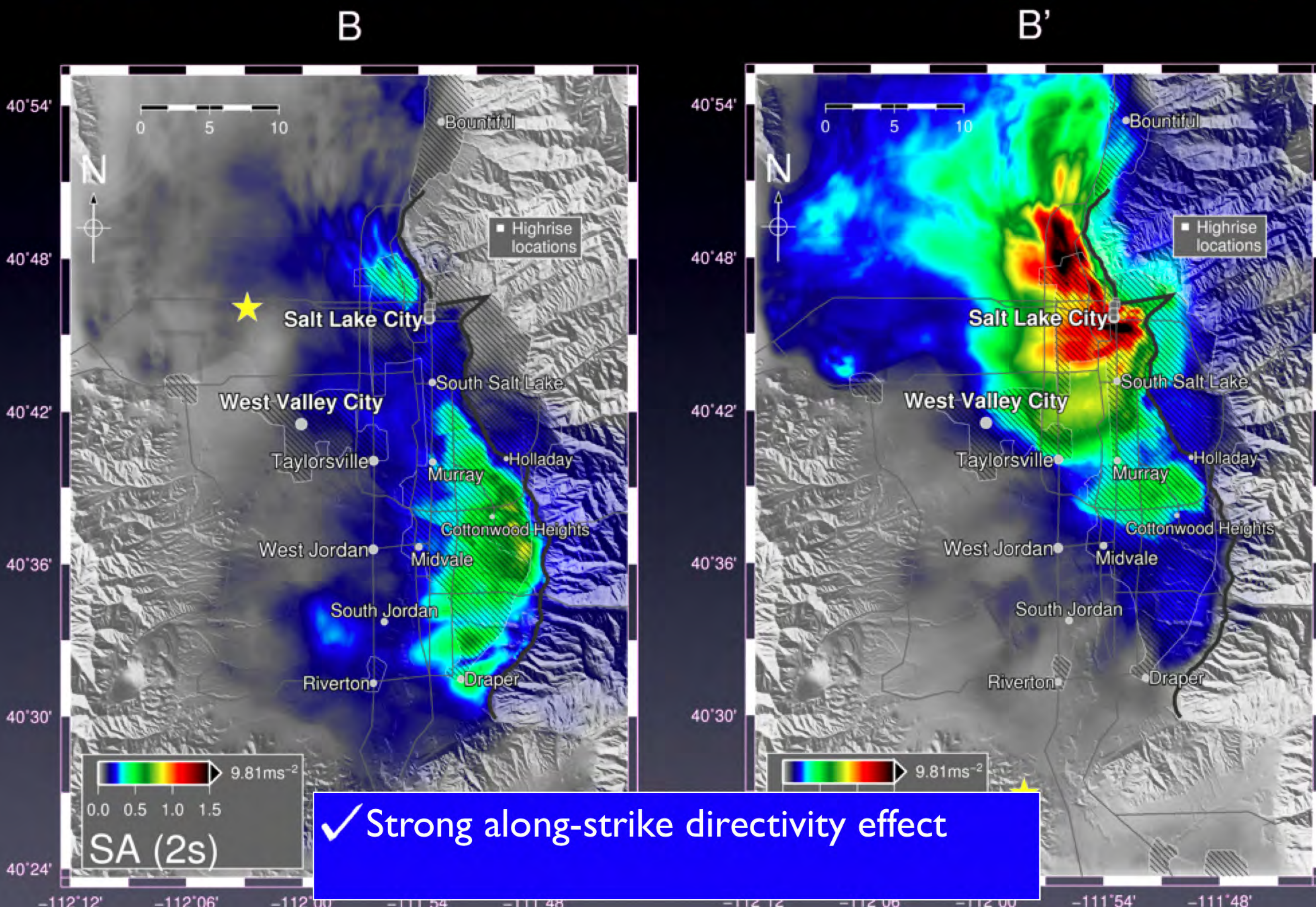

✓Strong along-strike directivity effect

Spectral Accelerations at 2s (2s-SAs)

A

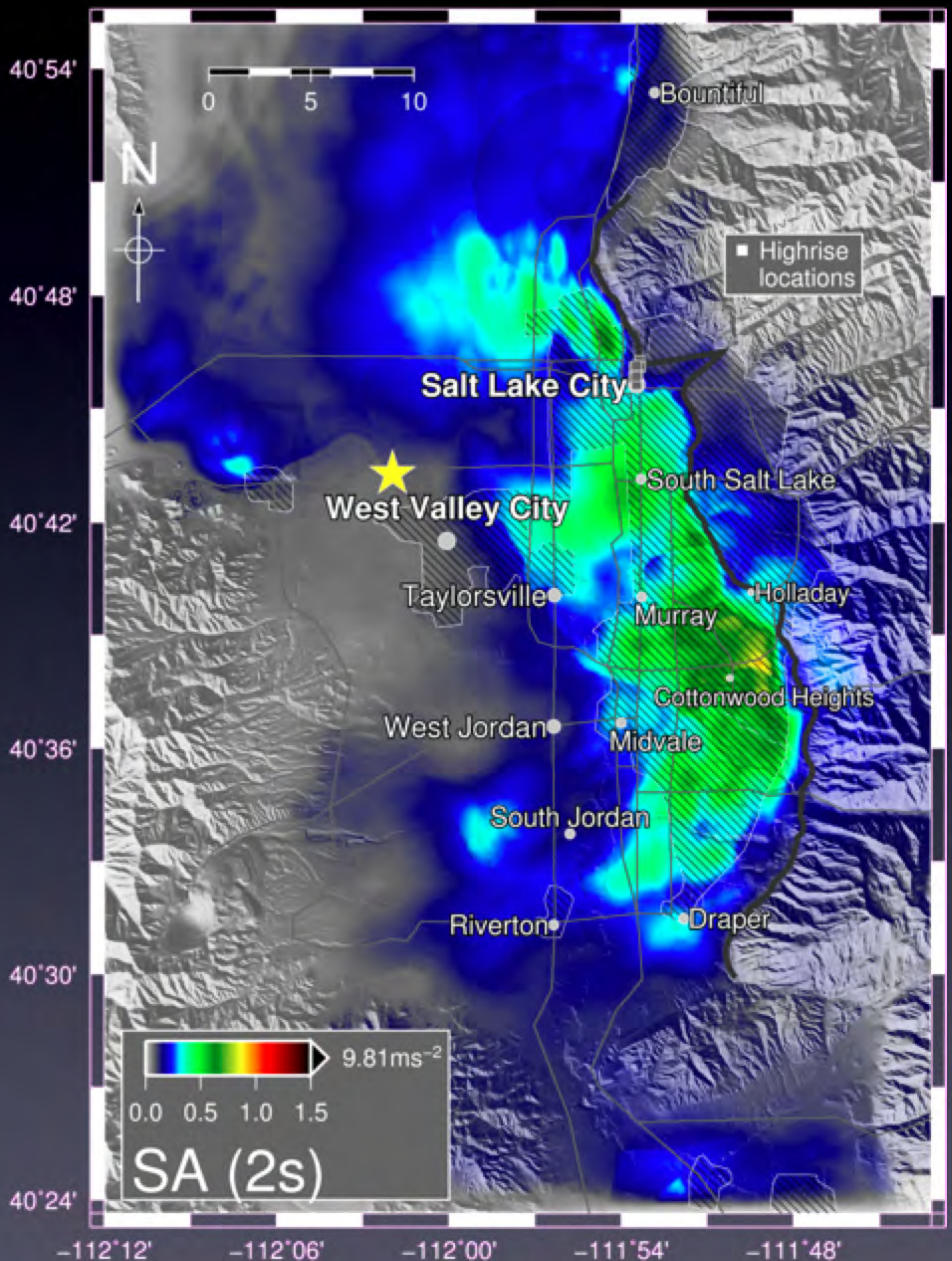

Spectral Accelerations at 2s (2s-SAs)

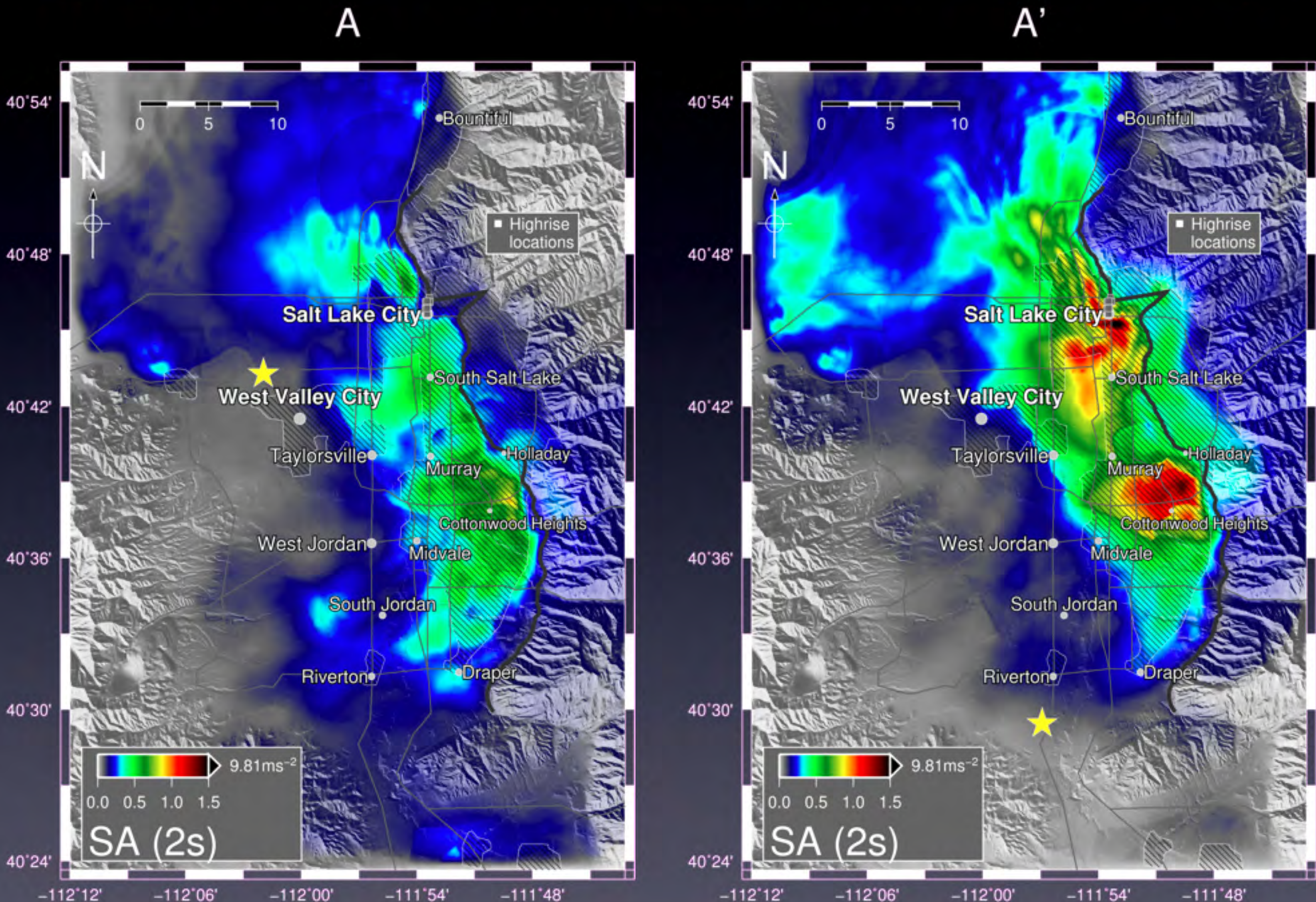

Spectral Accelerations at 2s (2s-SAs)

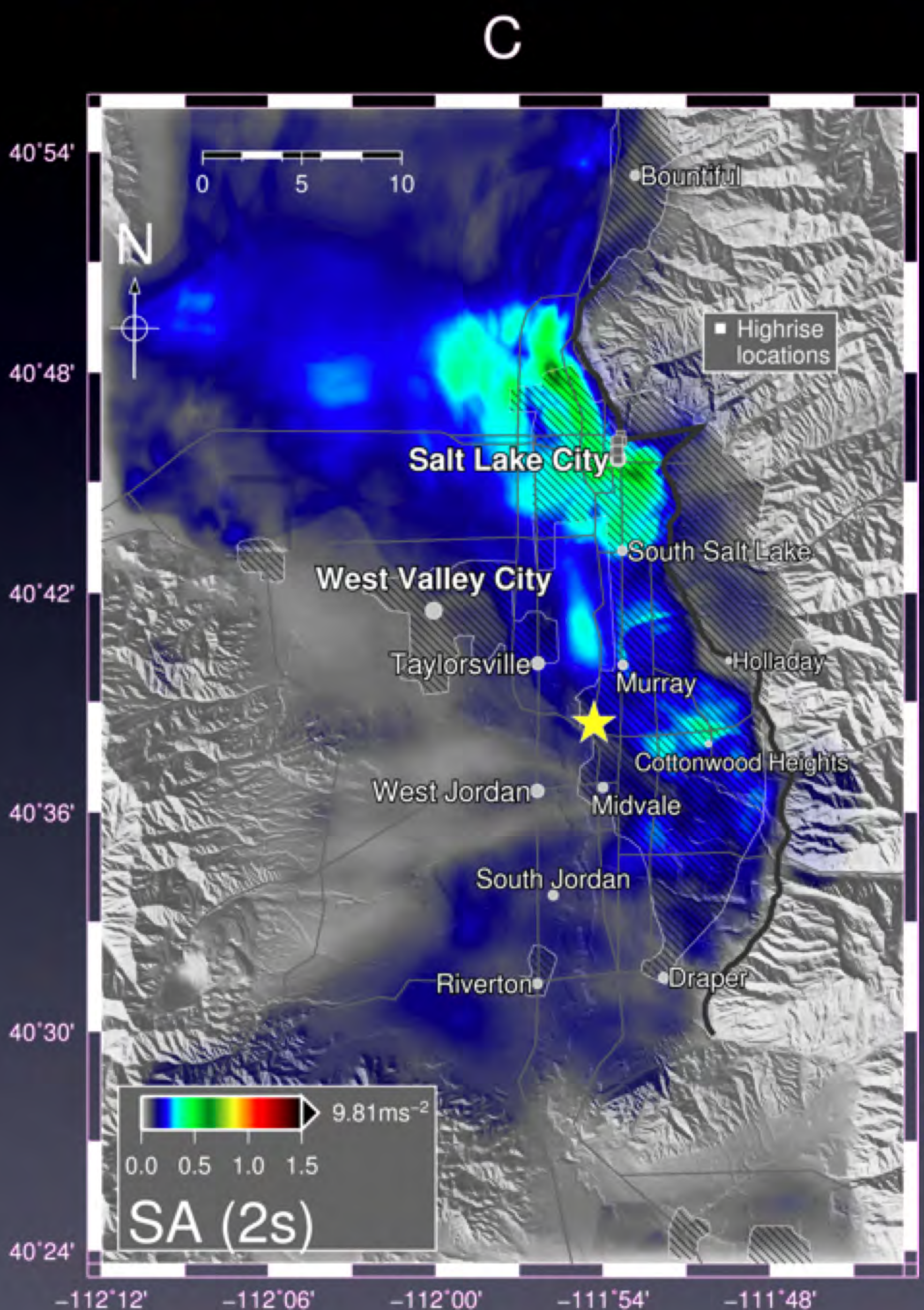

Spectral Accelerations at 2s (2s-SAs)

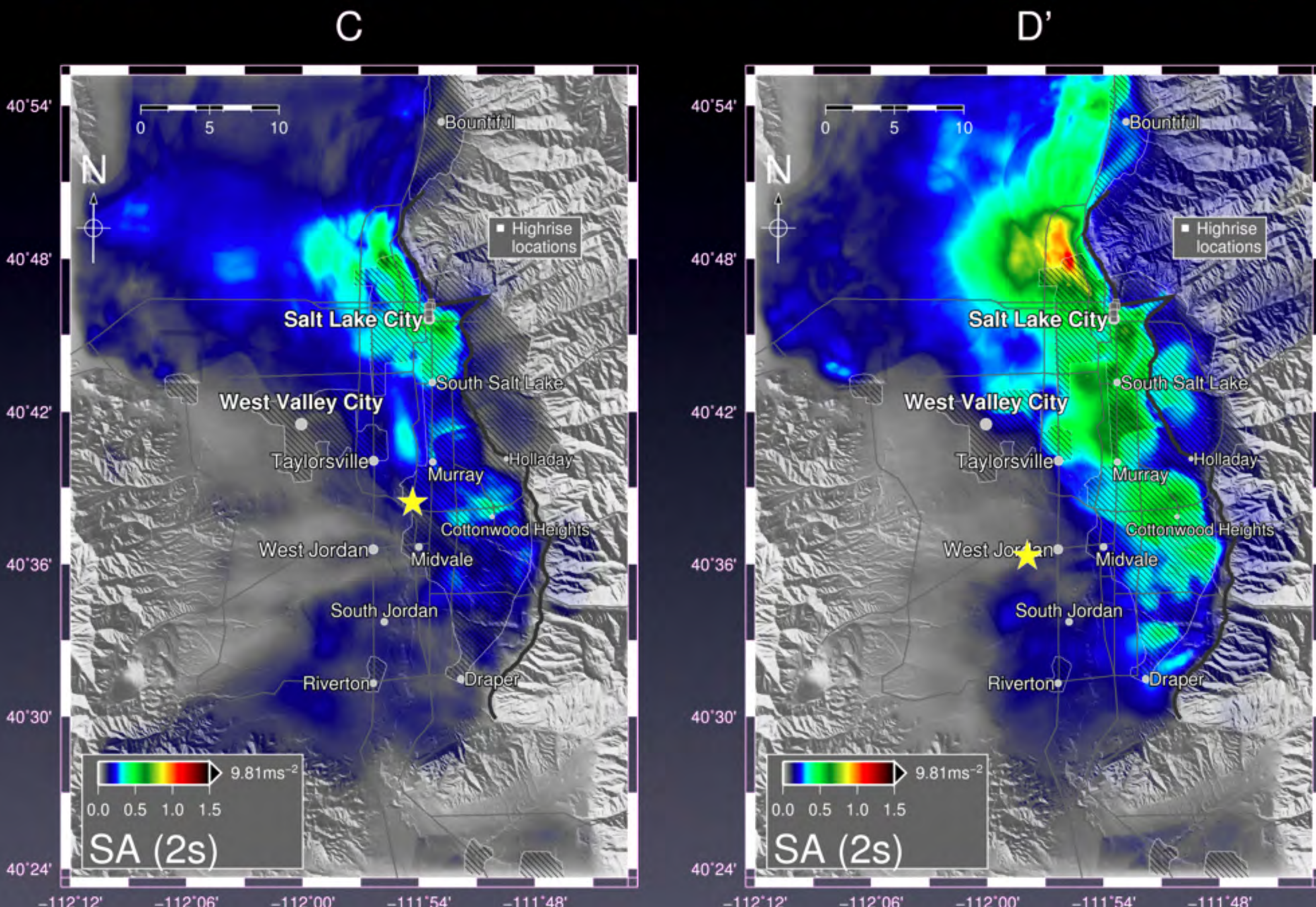

Spectral Accelerations at 2s (2s-SAs)

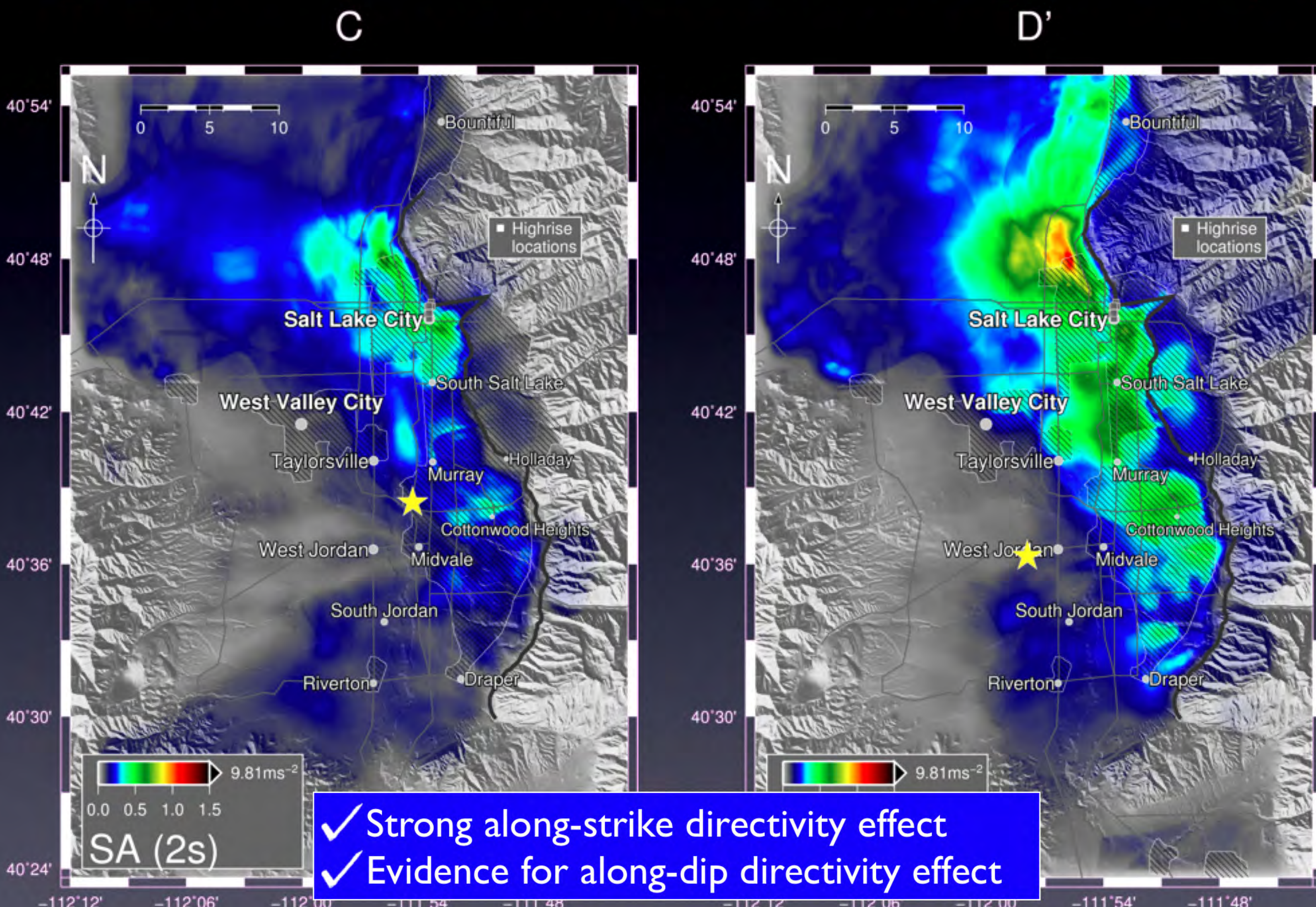

✓ Strong along-strike directivity effect
✓ Evidence for along-dip directivity effect

Average 2s-SAs

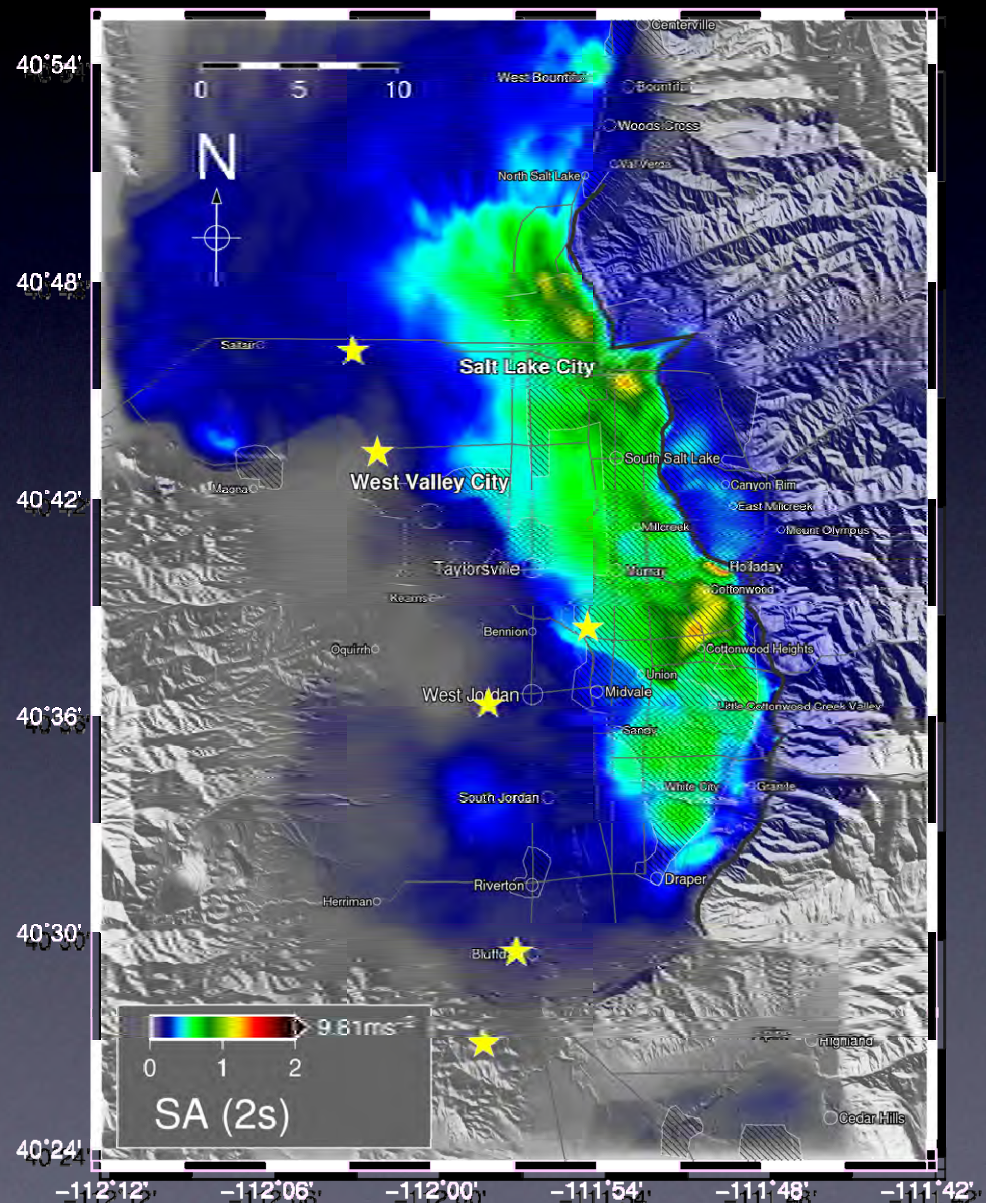

Broadband Synthetics

Combining low-frequency FD synthetics with high-frequency scattering operators

- Scatterograms are computed using **multiple scattering theory** with scattering parameters based on site-specific velocity structure (*Mai et al., 2010*)
- Scatterograms are convolved with dynamically consistent source time function
- **Extended fault** approximation (*Mena et al., 2010*) by subdividing WFSLC into 925 subfaults of 1 km^2 area each
- LF and HF synthetics are combined into broadband seismograms in the frequency domain using a simultaneous **amplitude and phase matching algorithm** (*Mai & Beroza, 2003*)

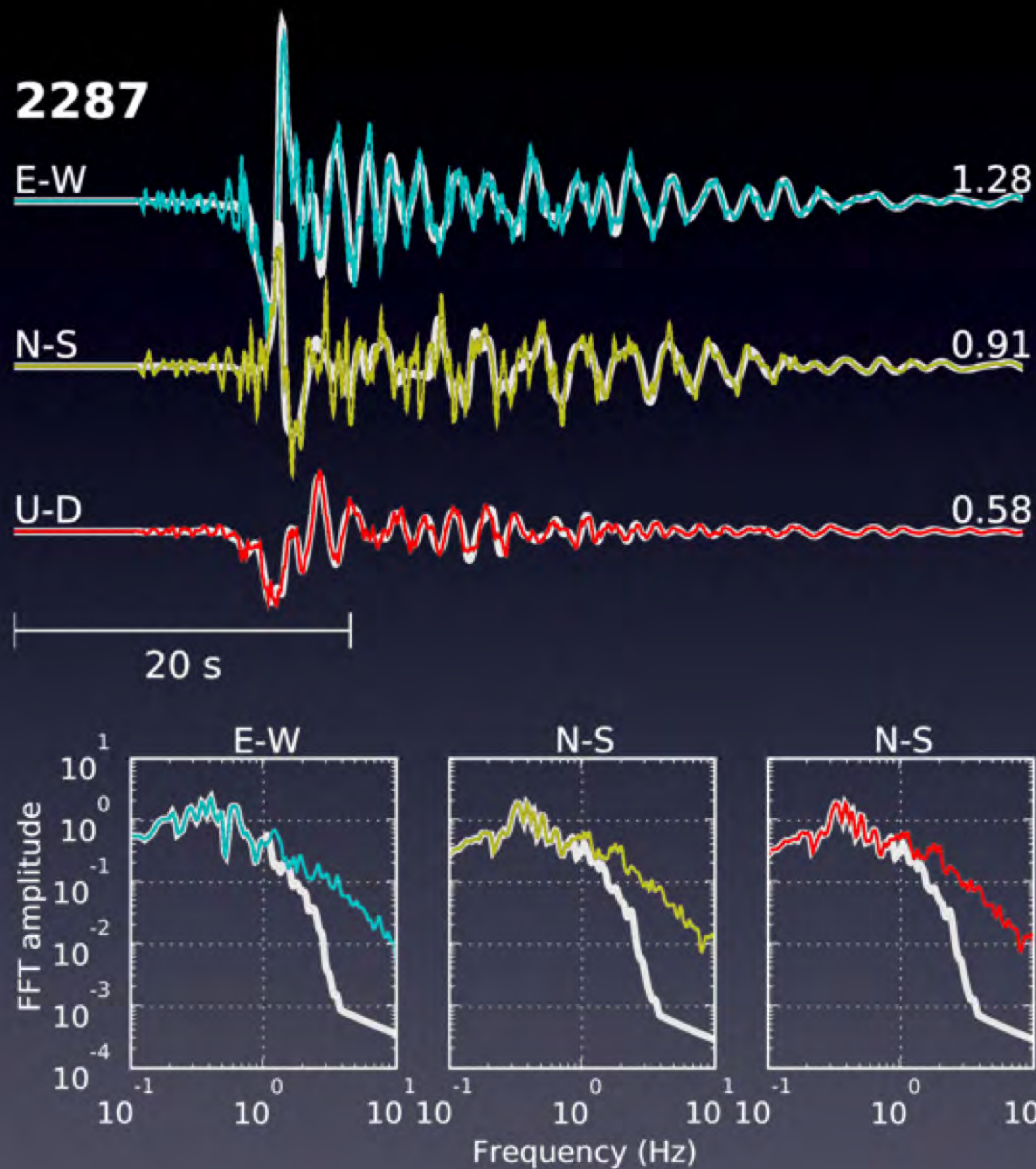

Broadband Synthetics

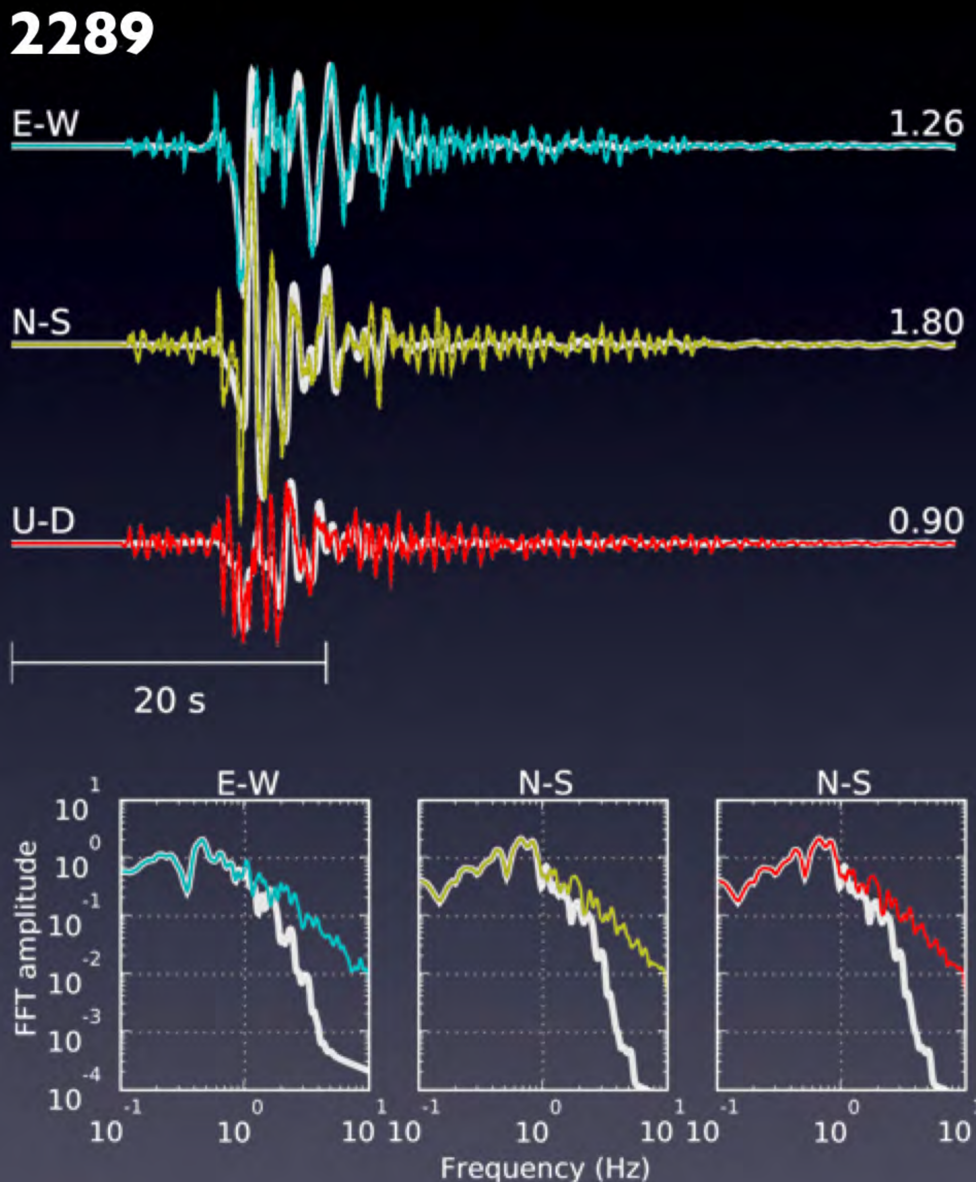

Broadband 5Hz-SAs (Scenario B')

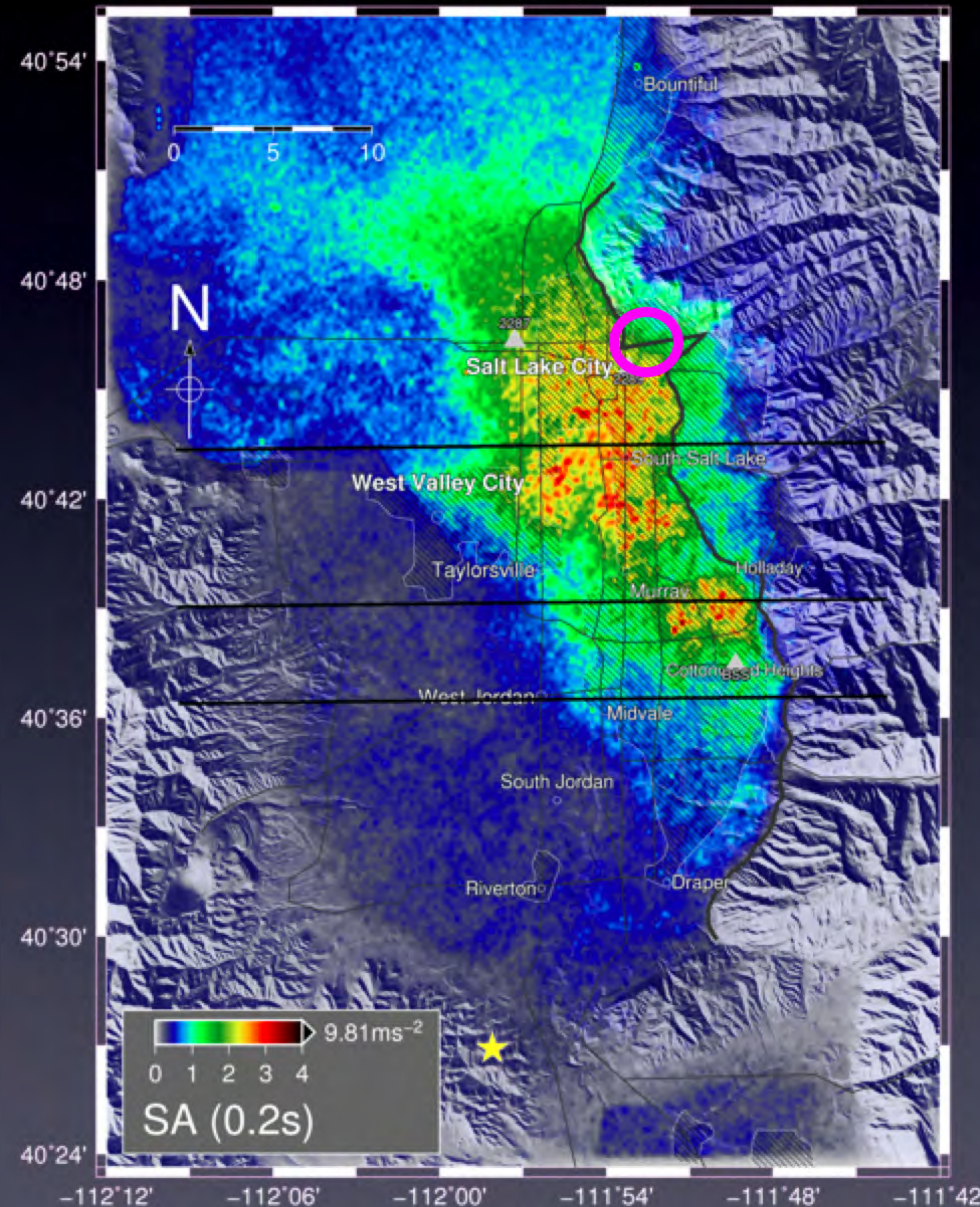

Comparison to NGA

Campbell & Bozorgnia (2008)

- 200 ms^{-1} < $V_s(30)$ < 300 ms^{-1}
- r_{jb} = 0 (above the fault)

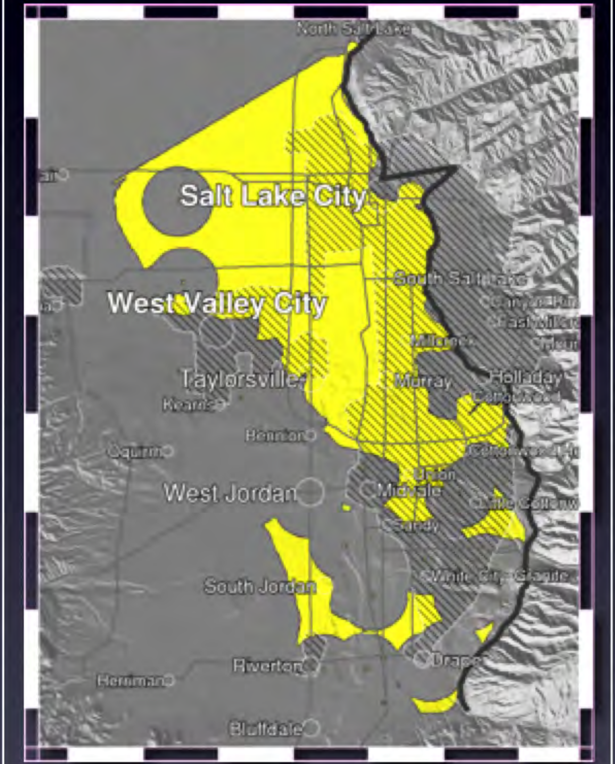

Average Spectral Accelerations (SAs) derived from Broadband synthetics of six scenarios

Values predicted by C&B (2008) for $V_s(30)$ = 250 ms^{-1}

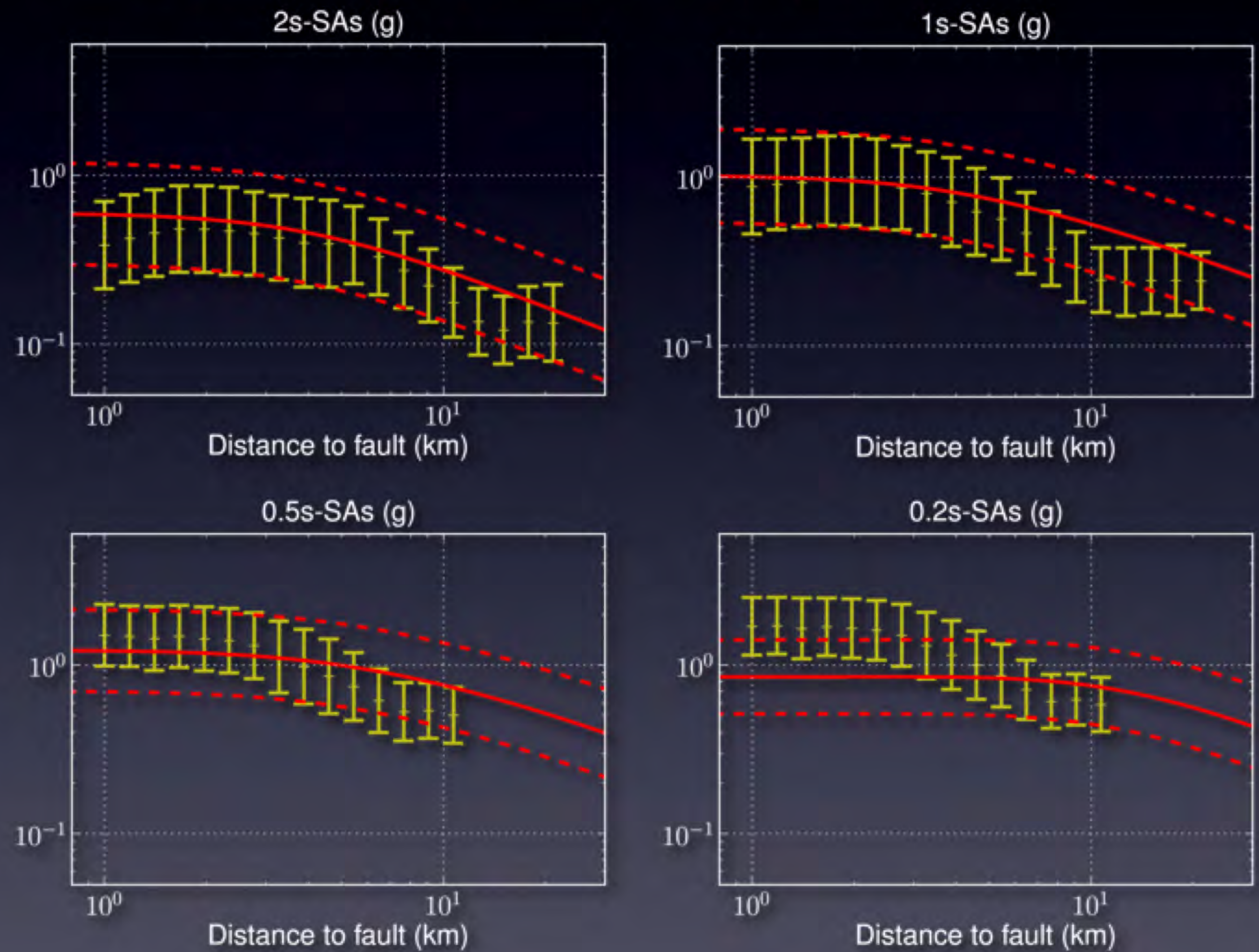

Comparison to NGA

Campbell & Bozorgnia (2008)

- $200\ ms^{-1} < V_s(30) < 300\ ms^{-1}$
- $r_{jb} = 0$ (above the fault)

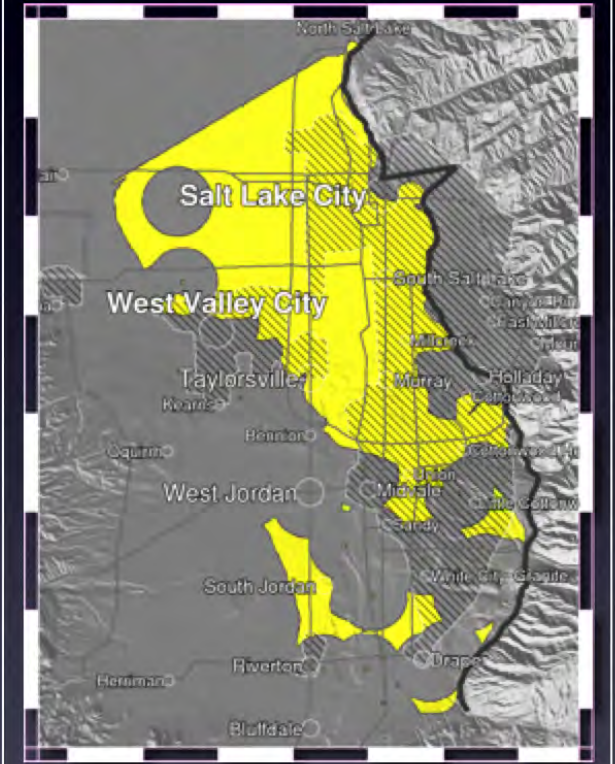

Average Spectral Accelerations (SAs) derived from Broadband synthetics of six scenarios

Values predicted by C&B (2008) for $V_s(30) = 250\ ms^{-1}$

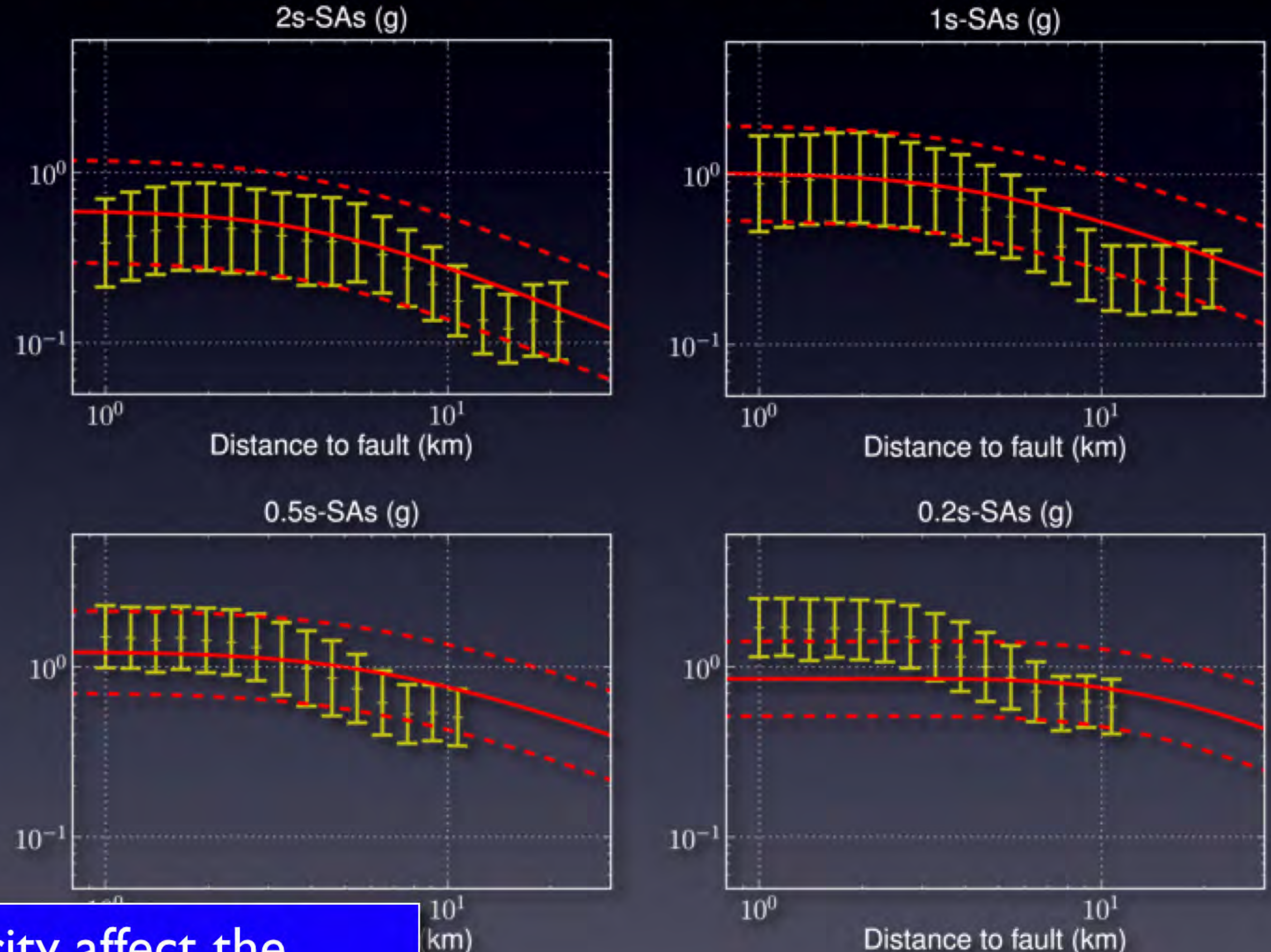

How would soil nonlinearity affect the ground motion at higher frequencies?

Simulation of Nonlinear Soil Response

- Nonlinear 1-D propagator *NOAH* (Bonilla et al., 2005) to model SH propagation in top 240m
- Not modeling pore water pressure or soil dilatancy (parameters are not available)
- Shear modulus reduction is controlled by reference strain γ_r:

$$\frac{G}{G_{\max}} = \frac{1}{1+\frac{\gamma}{\gamma_r}}$$

- *Reference strain* γ_r is derived from an empirical relationship (Darendelli, 2001), modified to take results of recent laboratory test of Bonneville clays into account (Bay & Sasanakul, 2005):

$$\gamma_r(\mathrm{PI}, \mathrm{OCR}, \sigma_v)$$

- Hysteresis dissipation is controlled by maximum damping ratio at large strains ξ_{max}, which we also estimate from Darandelli (2001):

$$\xi_{\max}(\mathrm{PI}, \mathrm{OCR}, \sigma_v, N, f)$$

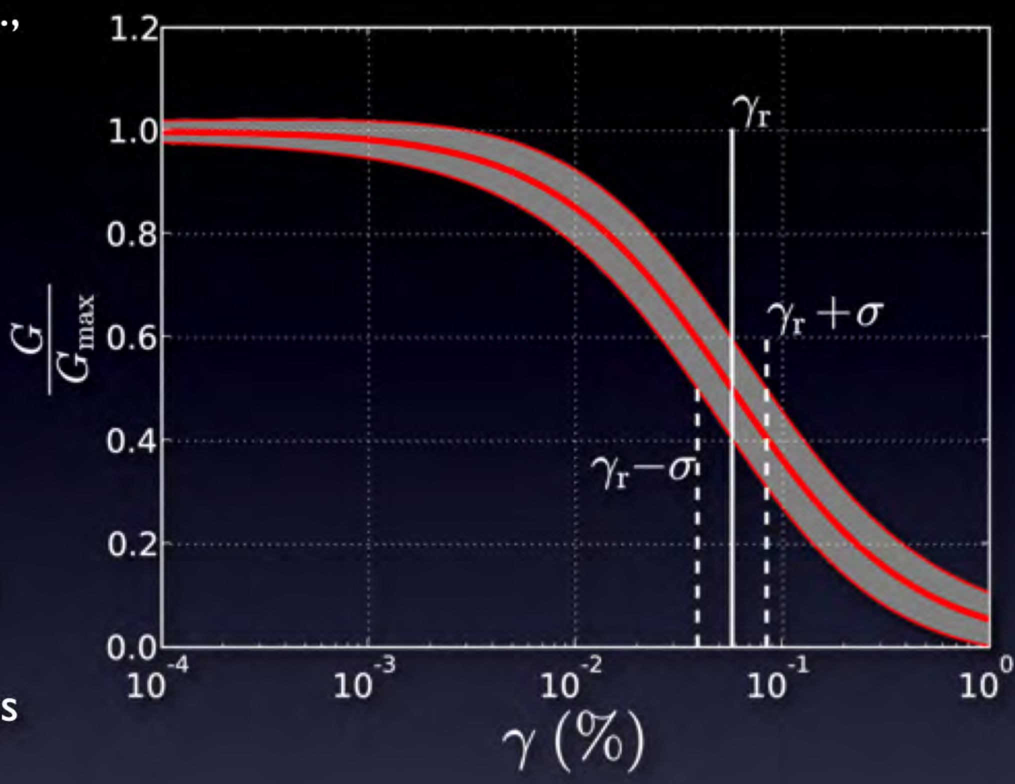

	Parameter	Value
PI	Plasticity Index	0 - 40
OCR	Overconsolidation ratio	1
σ_v	Confining pressure	f(z)
N	Number of cycles	10
f	Frequency	1 Hz

Nonlinear soil parameters

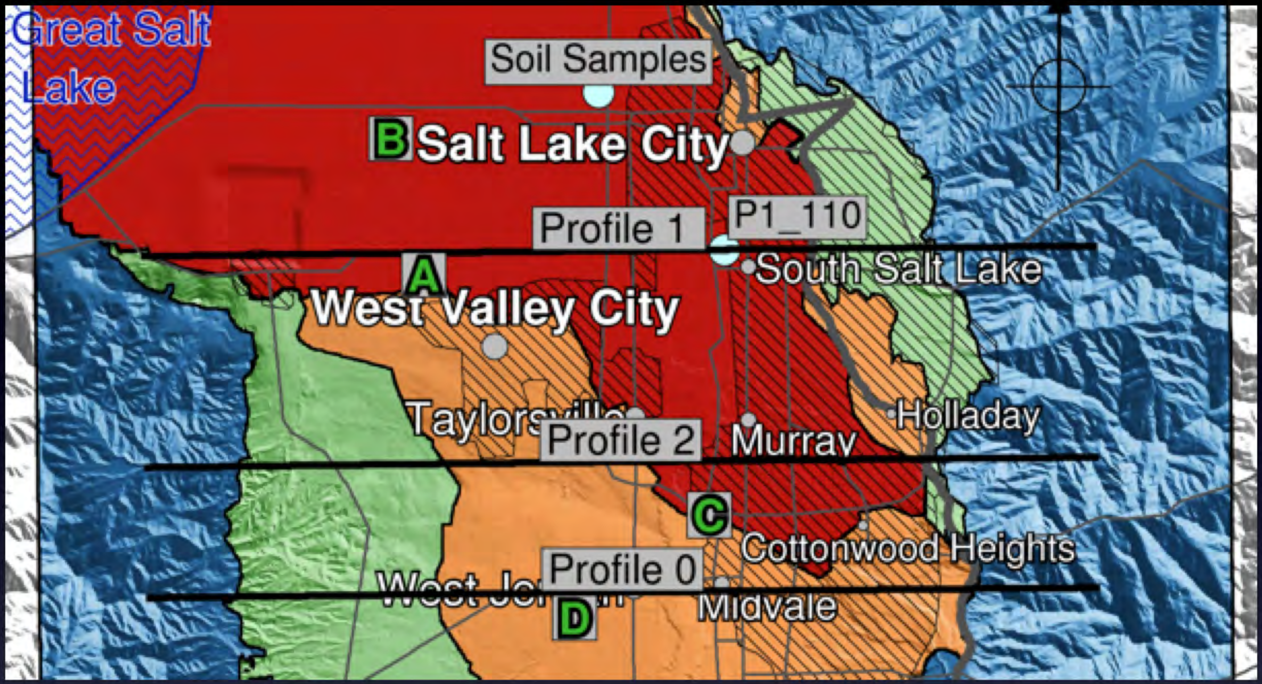

- Plasticity index (PI) depends on local site response unit (McDonald and Ashland,2008)

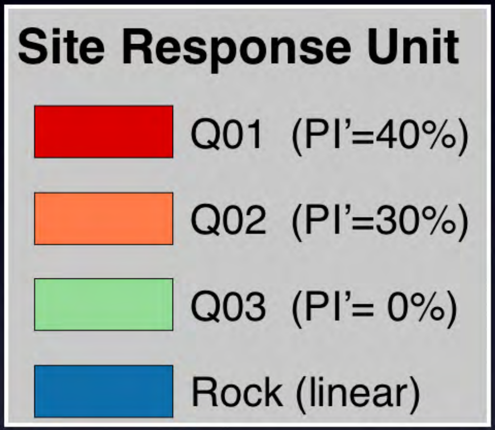

Nonlinear soil parameters

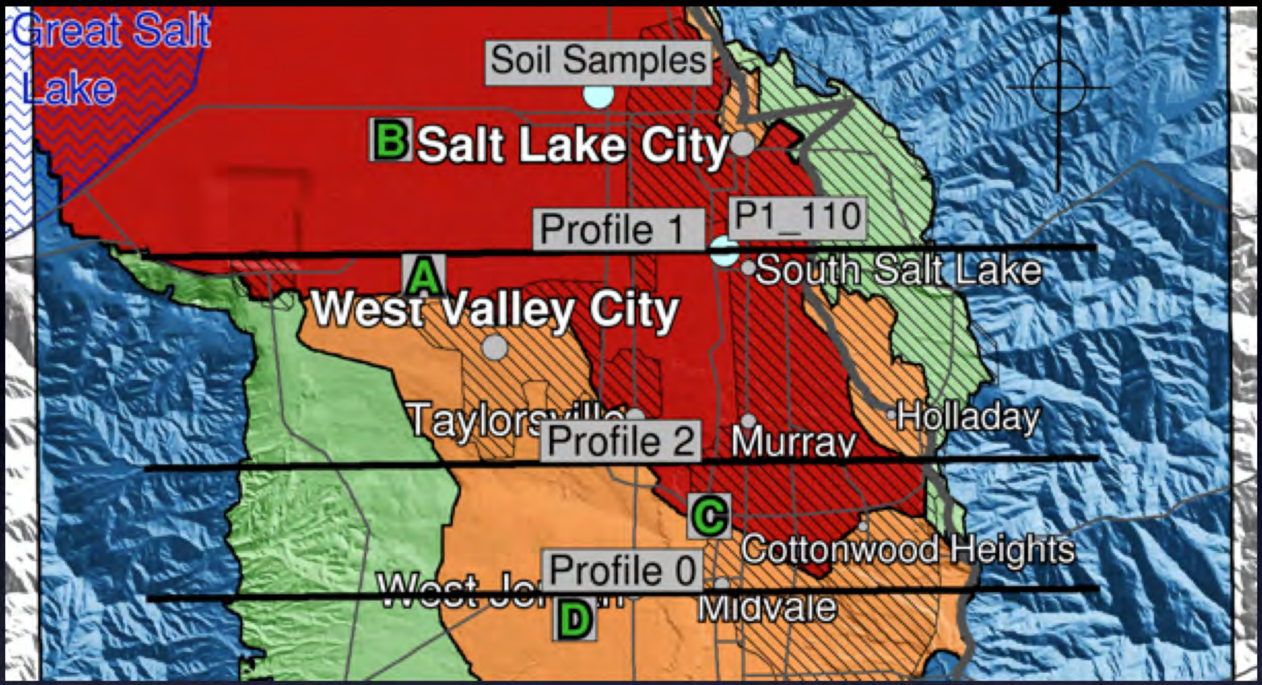

Plasticity index (PI) depends on local site response unit (McDonald and Ashland,2008)

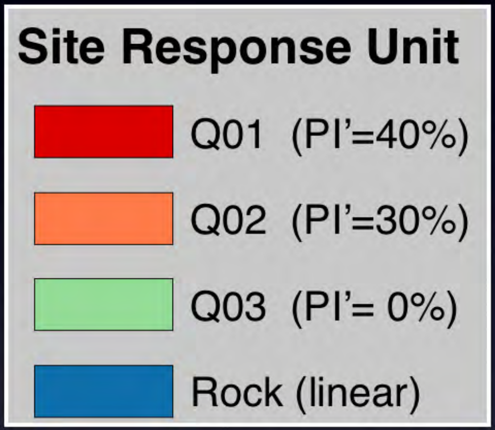

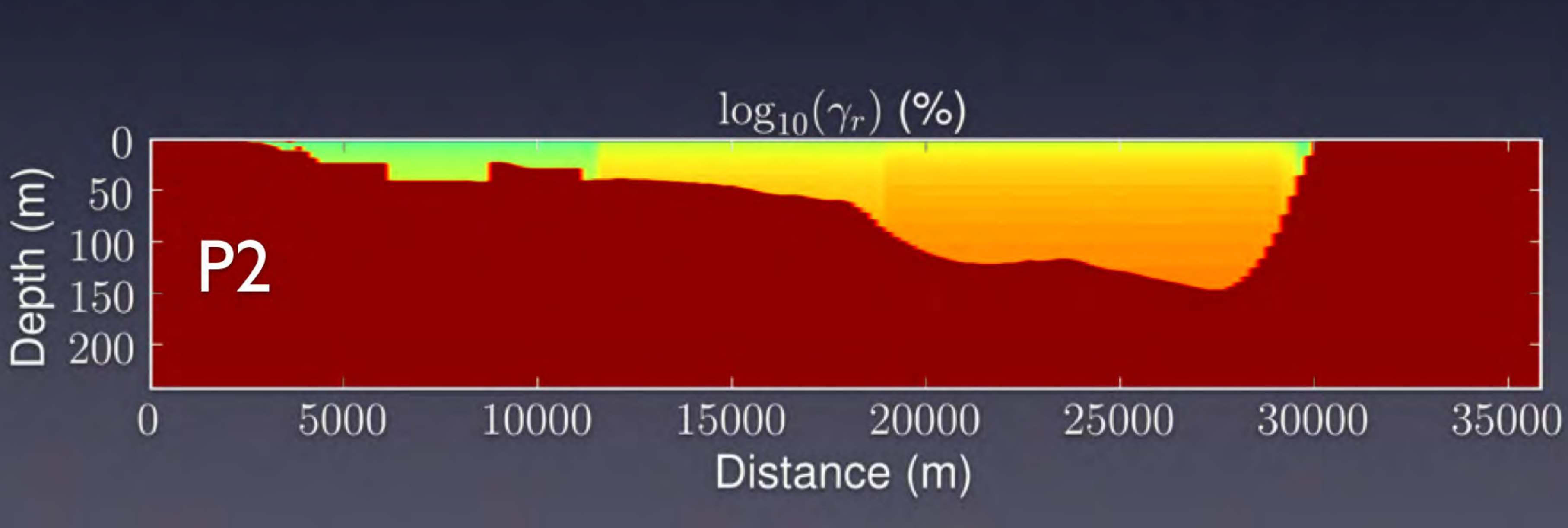

Nonlinear soil parameters

Example site on P1 (South Salt Lake):

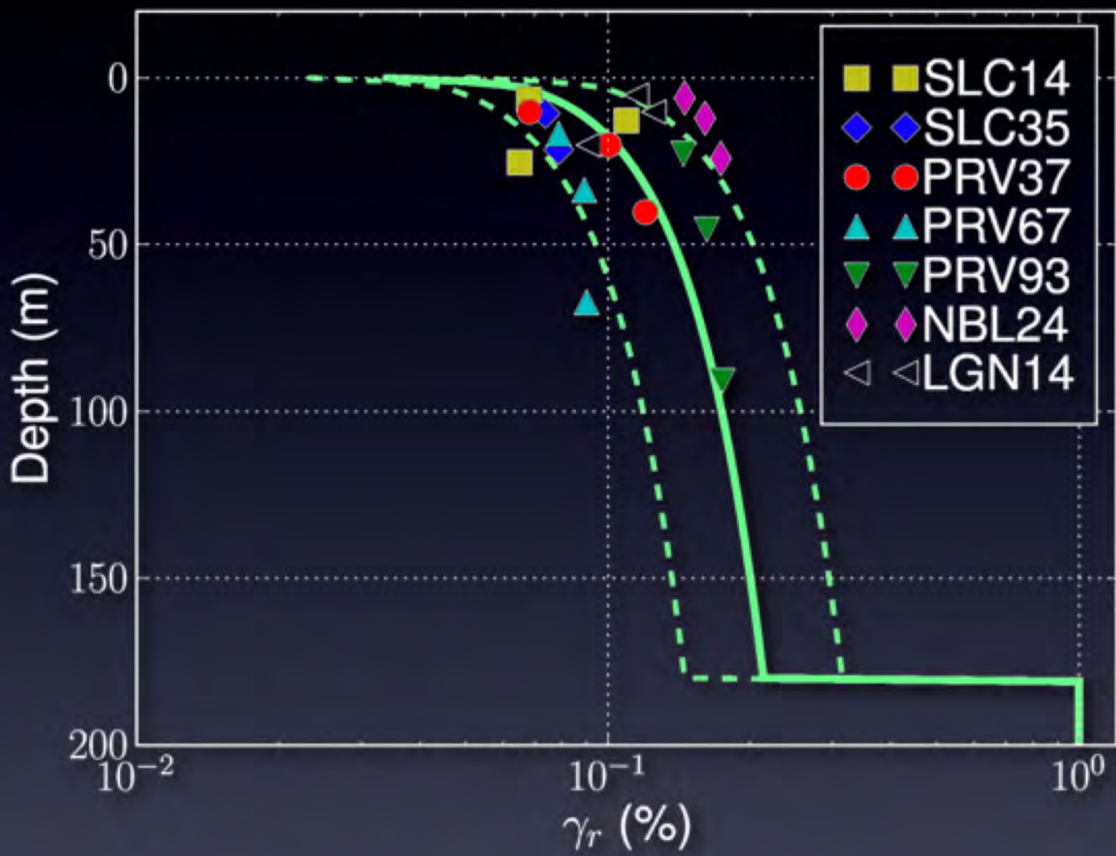

reference strain γ_r

$\gamma_r \pm \sigma$

Three 1D models for each site:

Model	Reference strain	Damping ratio
Nonlinear	γ_r	ξ
More nonlinear	$\gamma_r - \sigma$	$\xi + \sigma_d$
Less nonlinear	$\gamma_r + \sigma$	$\xi - \sigma_d$

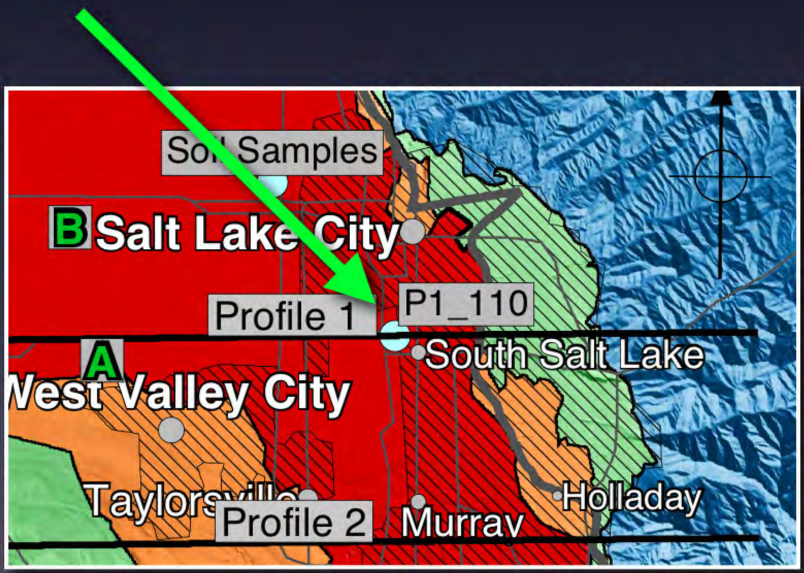

Simulation of Nonlinear Soil Response

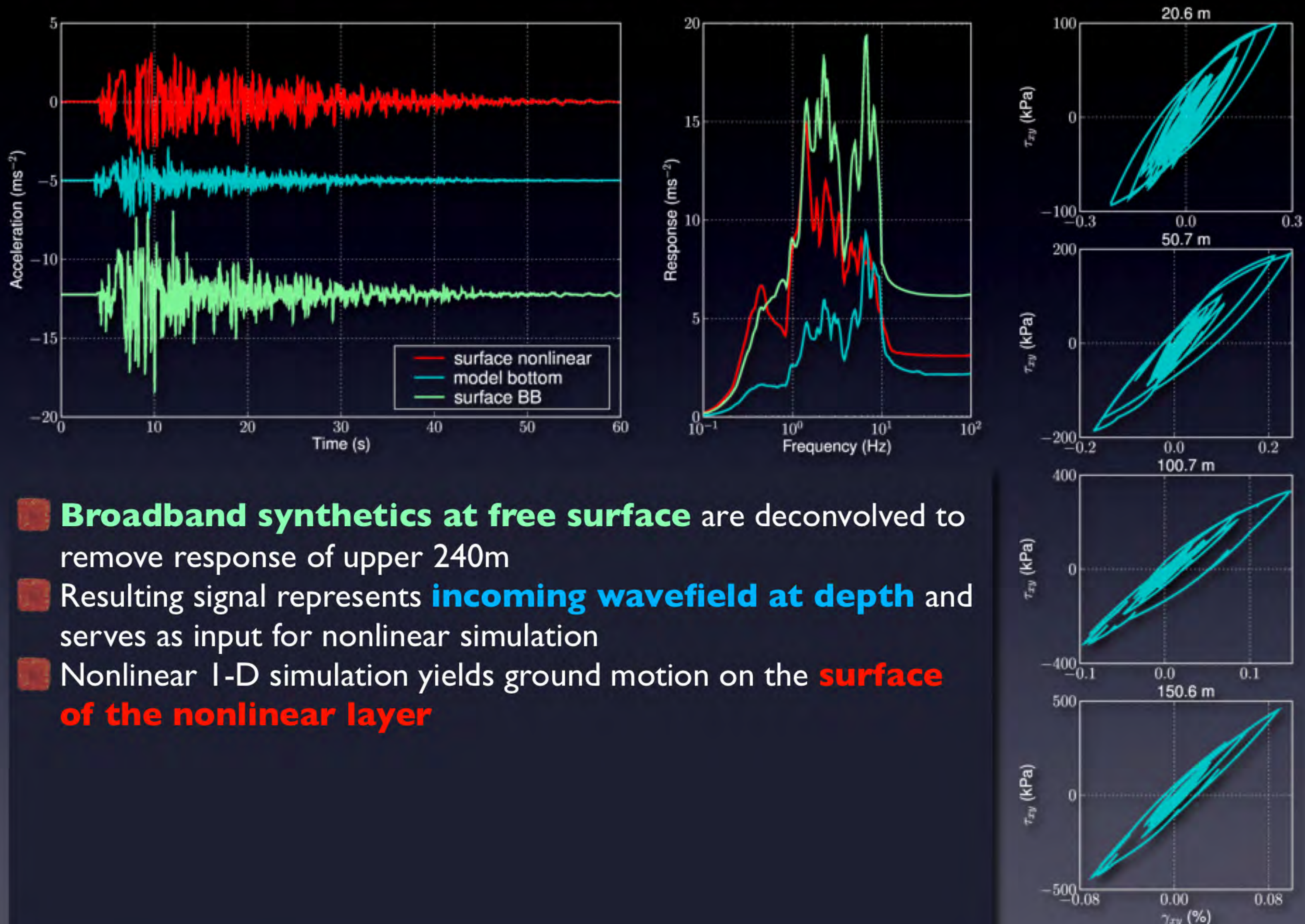

- **Broadband synthetics at free surface** are deconvolved to remove response of upper 240m
- Resulting signal represents **incoming wavefield at depth** and serves as input for nonlinear simulation
- Nonlinear 1-D simulation yields ground motion on the **surface of the nonlinear layer**

Simulation of Nonlinear Soil Response

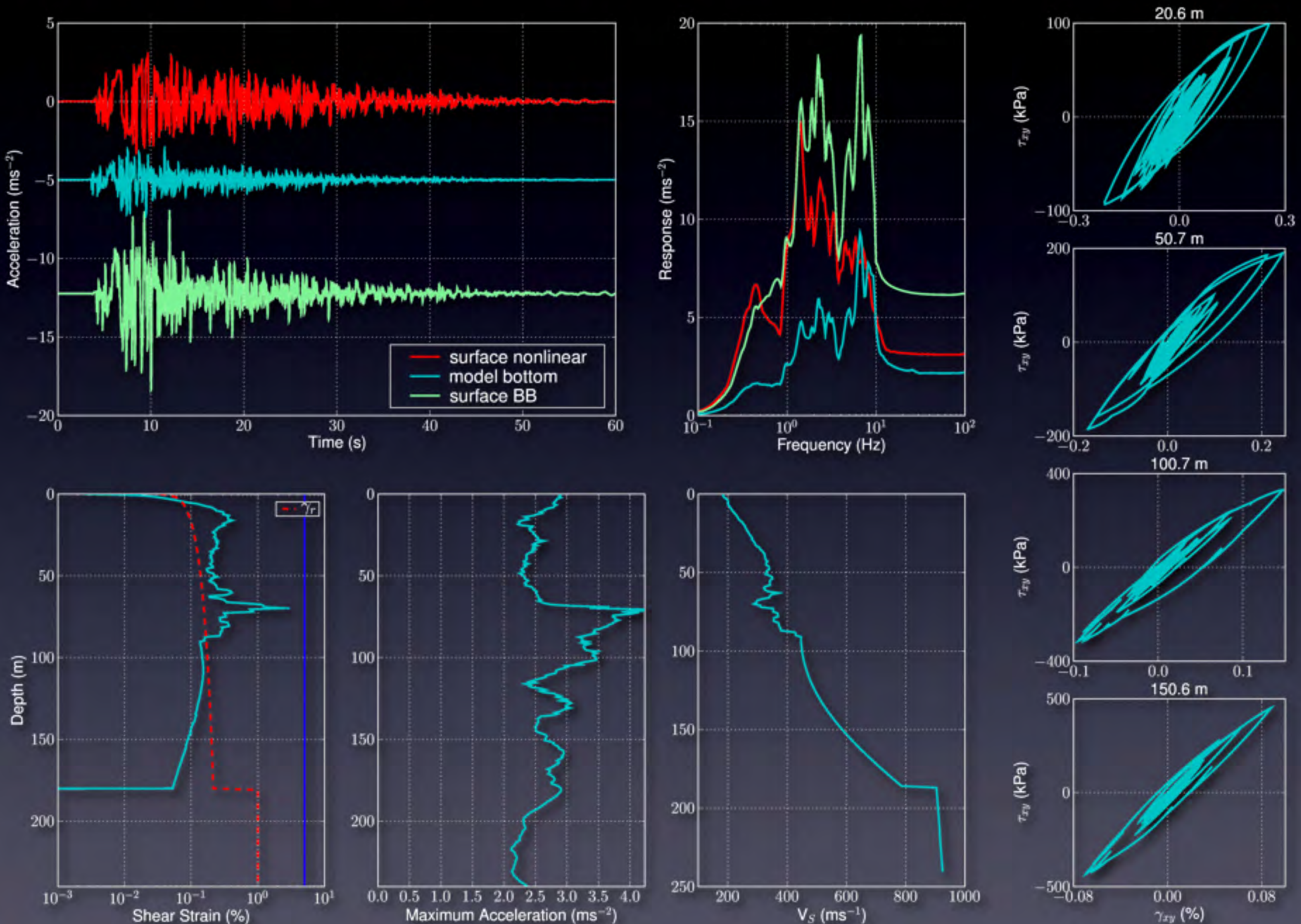

Linear (Broadband) vs. Nonlinear

Broadband 5Hz-SAs (Scenario B)

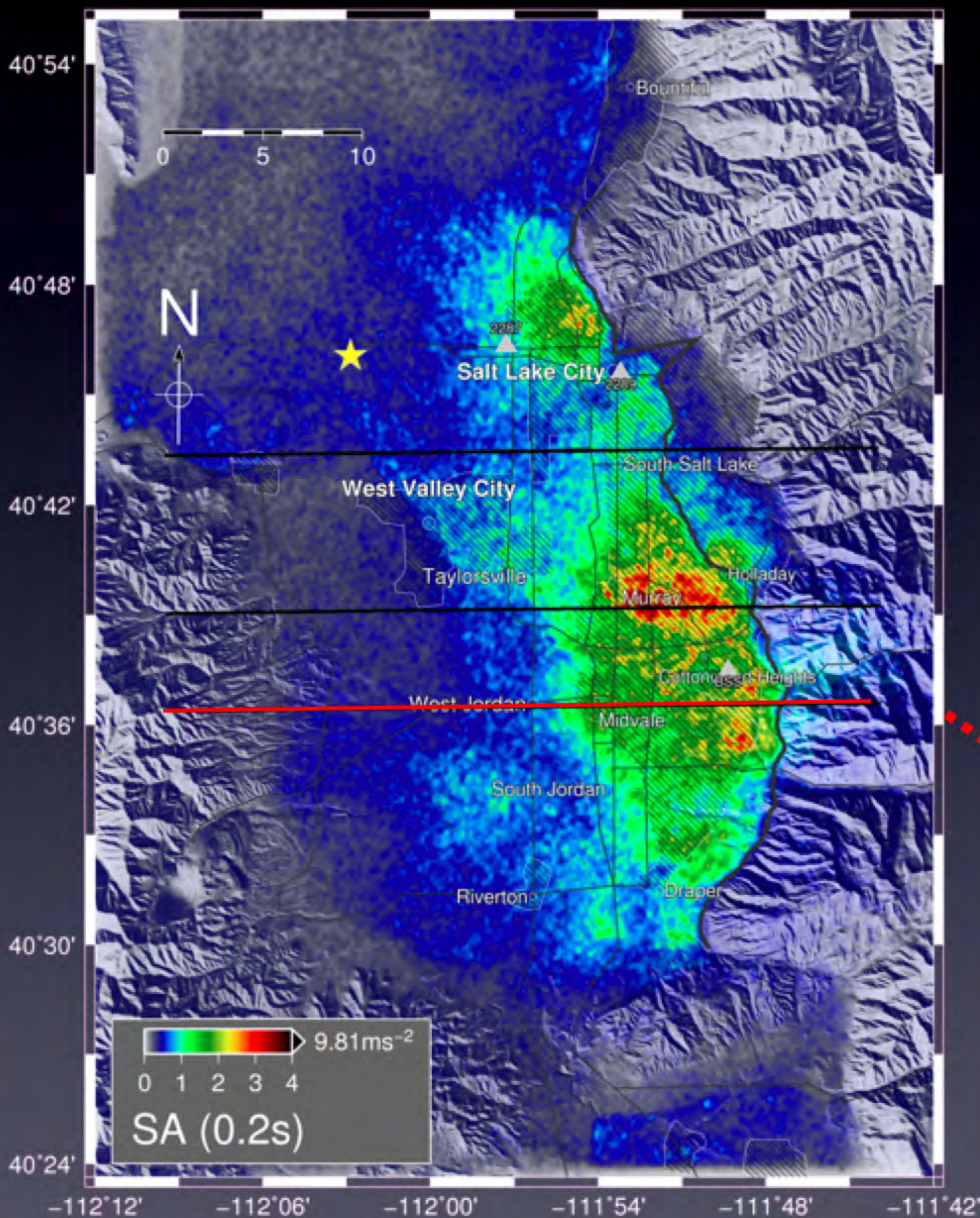

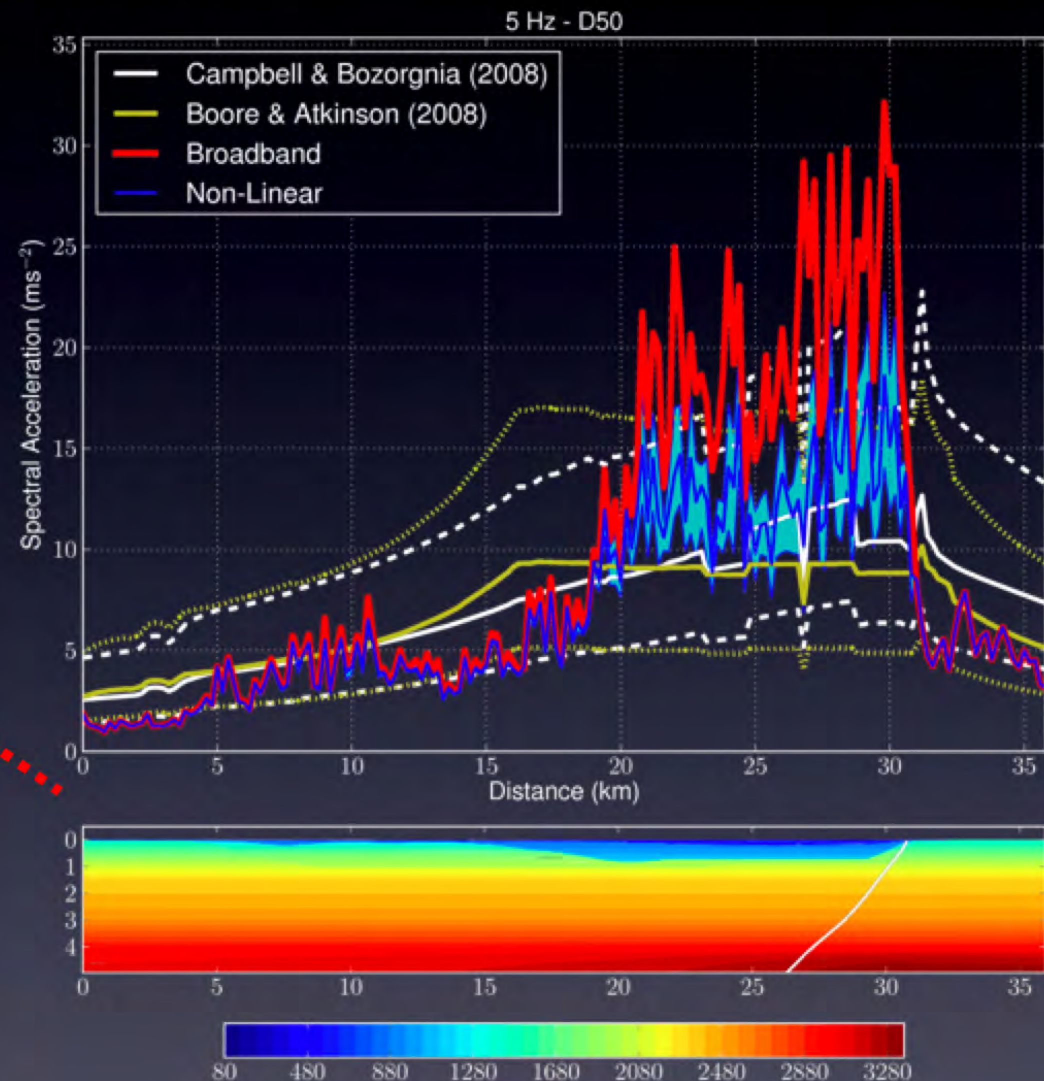

Linear (Broadband) vs. Nonlinear

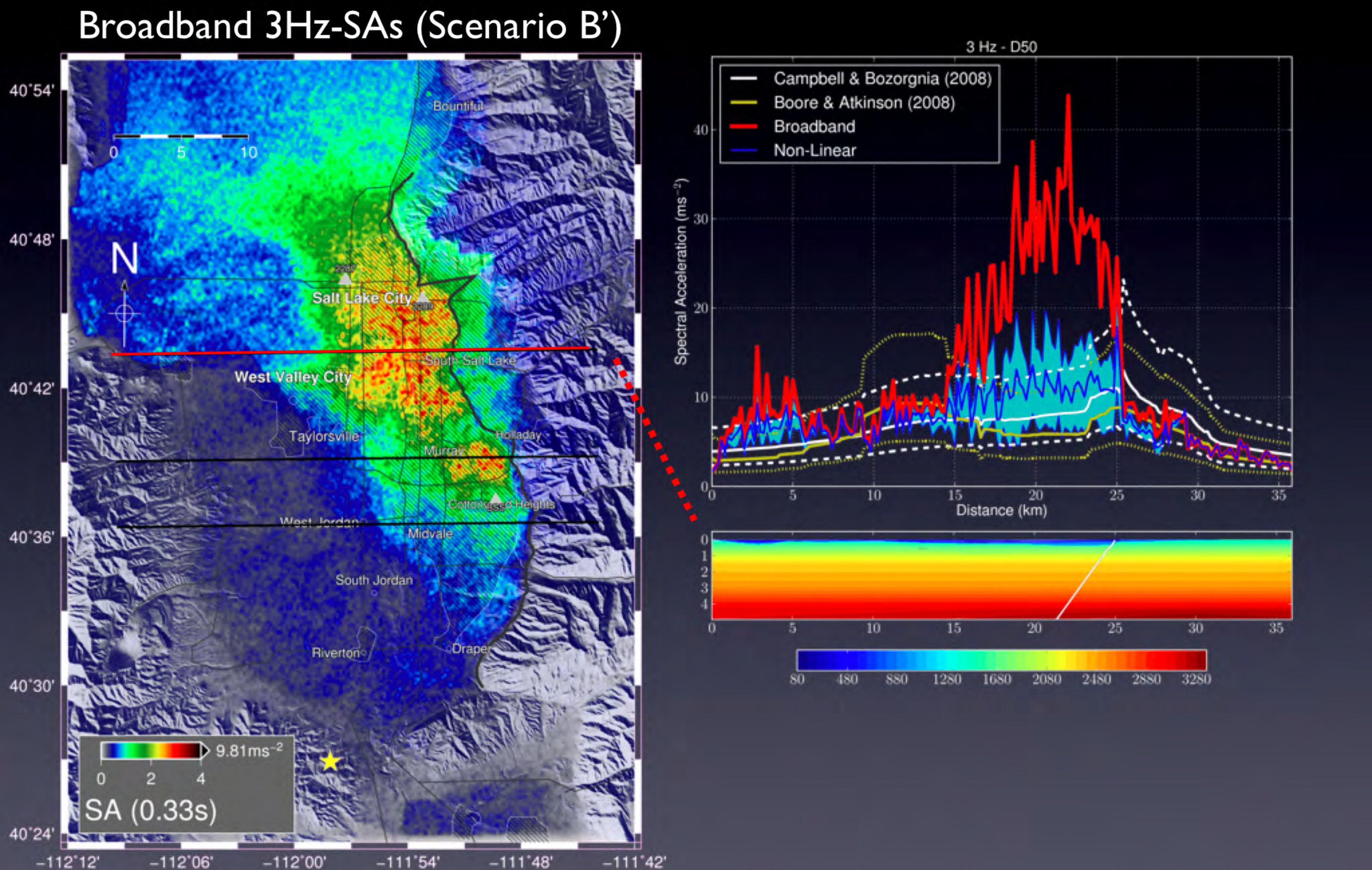

Correction Factors for BB SAs

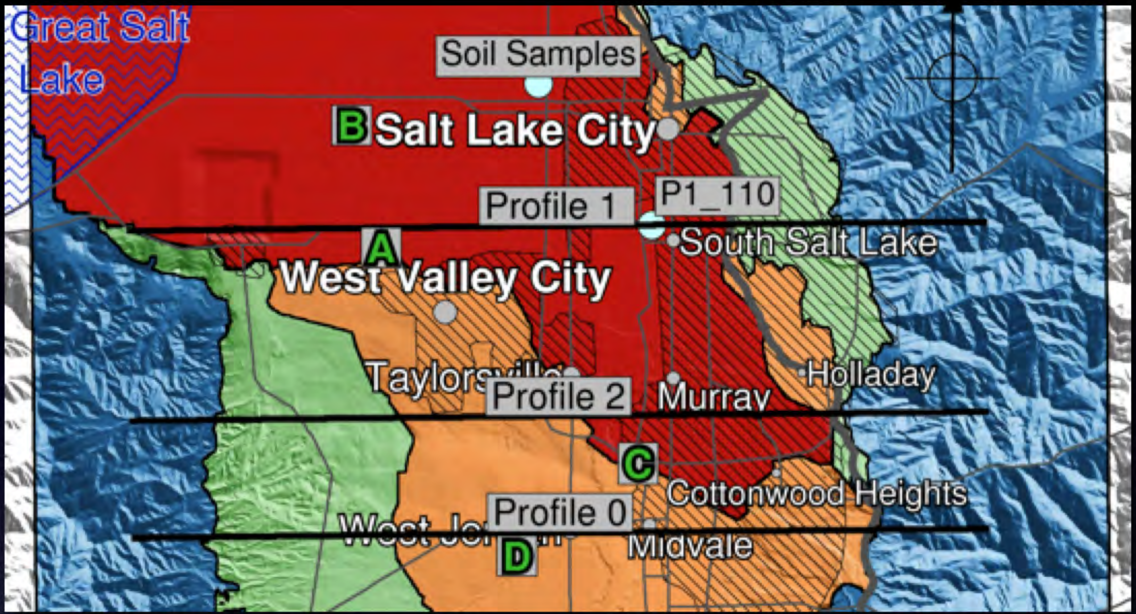

- Definition of amplitude-and site-dependent correction factors
- Coefficients of 3rd order polynomial are determined for each SRU and frequency
- L2 norm using ~2,500 NL 1-D simulations

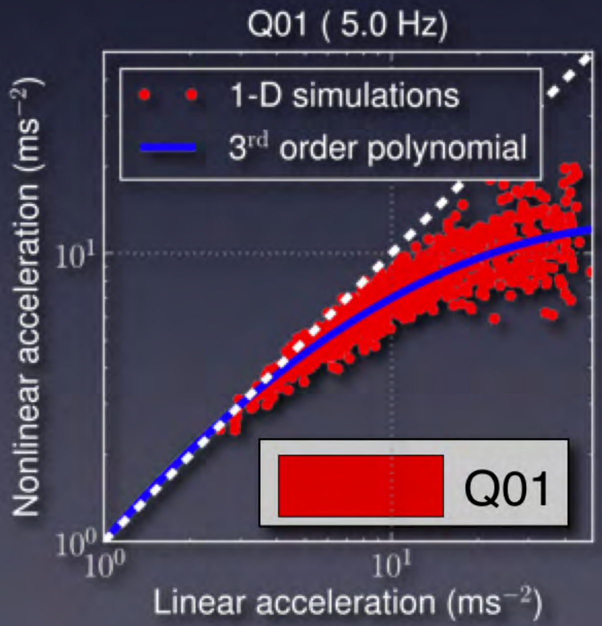

Correction Factors for BB SAs

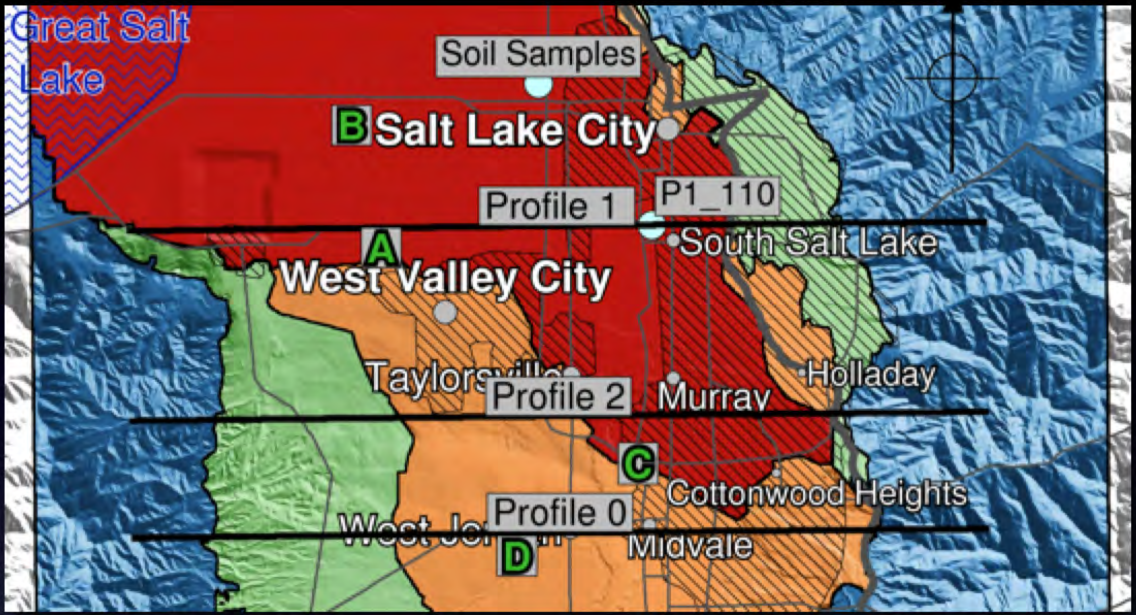

- Definition of amplitude-and site-dependent correction factors
- Coefficients of 3rd order polynomial are determined for each SRU and frequency
- L2 norm using ~2,500 NL 1-D simulations

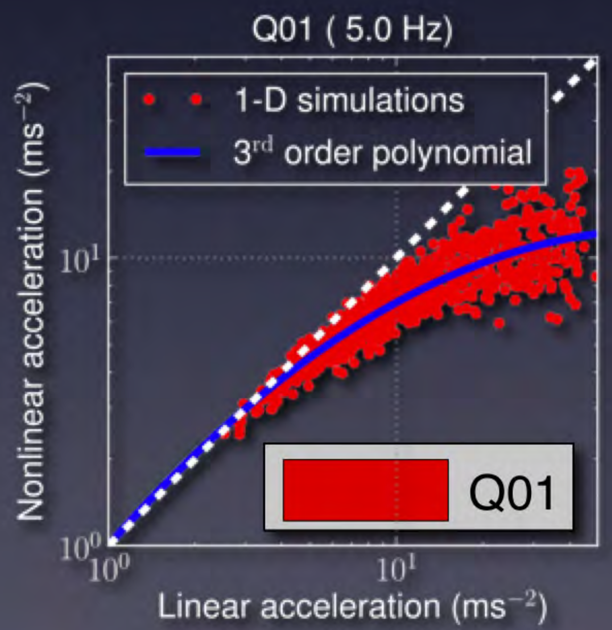

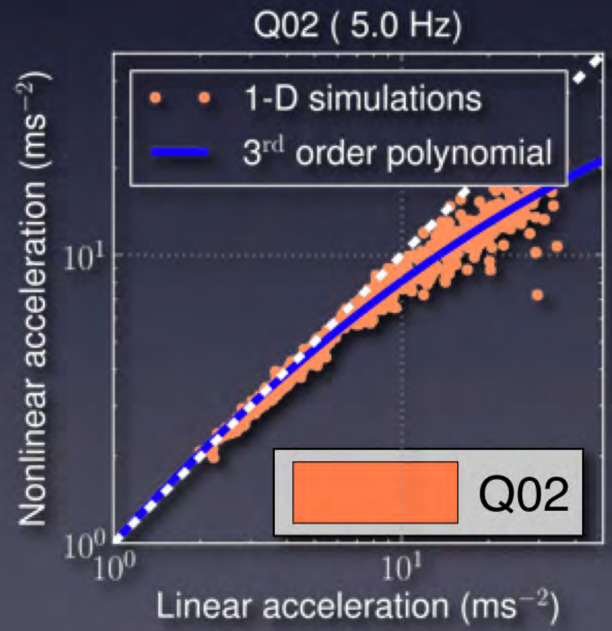

Correction Factors for BB SAs

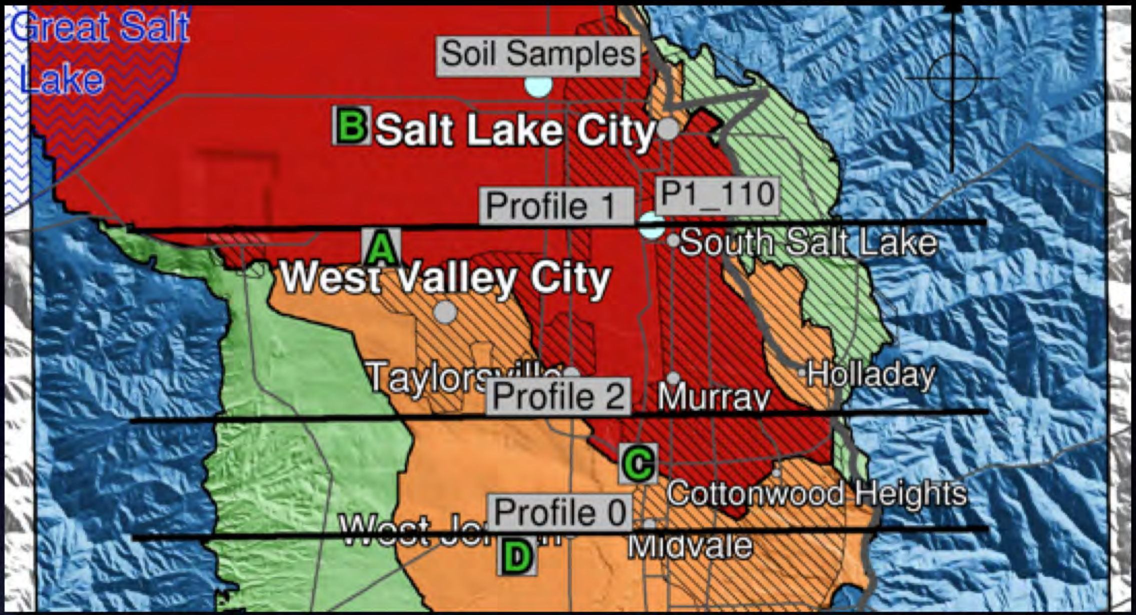

- Definition of amplitude-and site-dependent correction factors
- Coefficients of 3rd order polynomial are determined for each SRU and frequency
- L2 norm using ~2,500 NL 1-D simulations

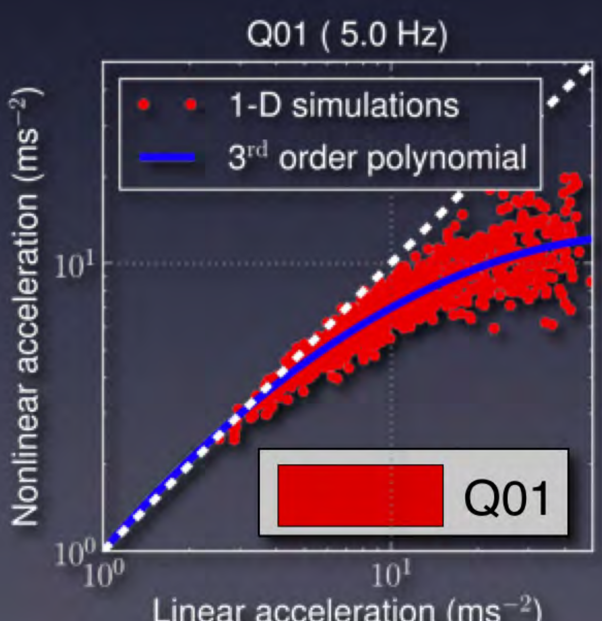

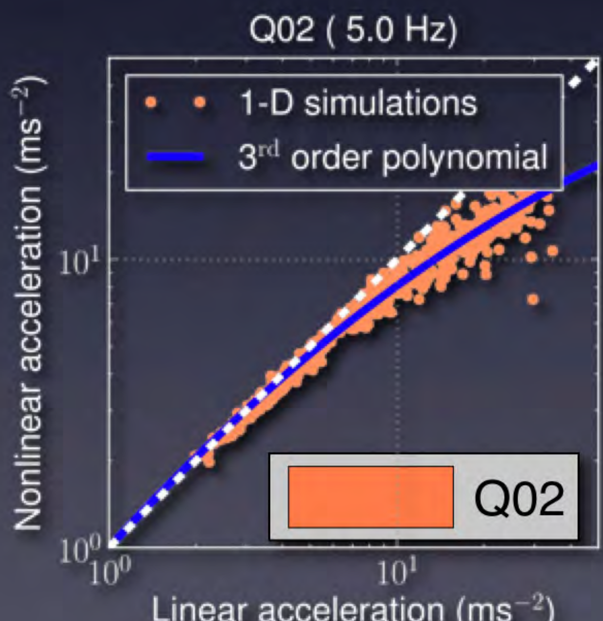

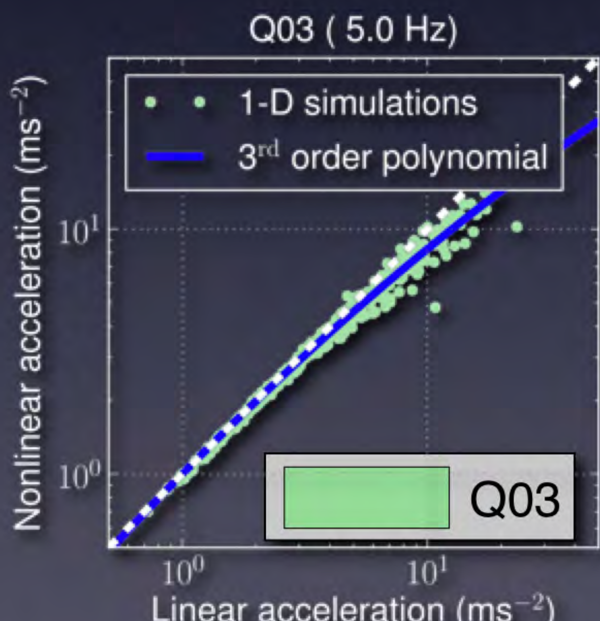

Correction Factors for BB SAs

BB 5Hz-SAs (Scenario B')

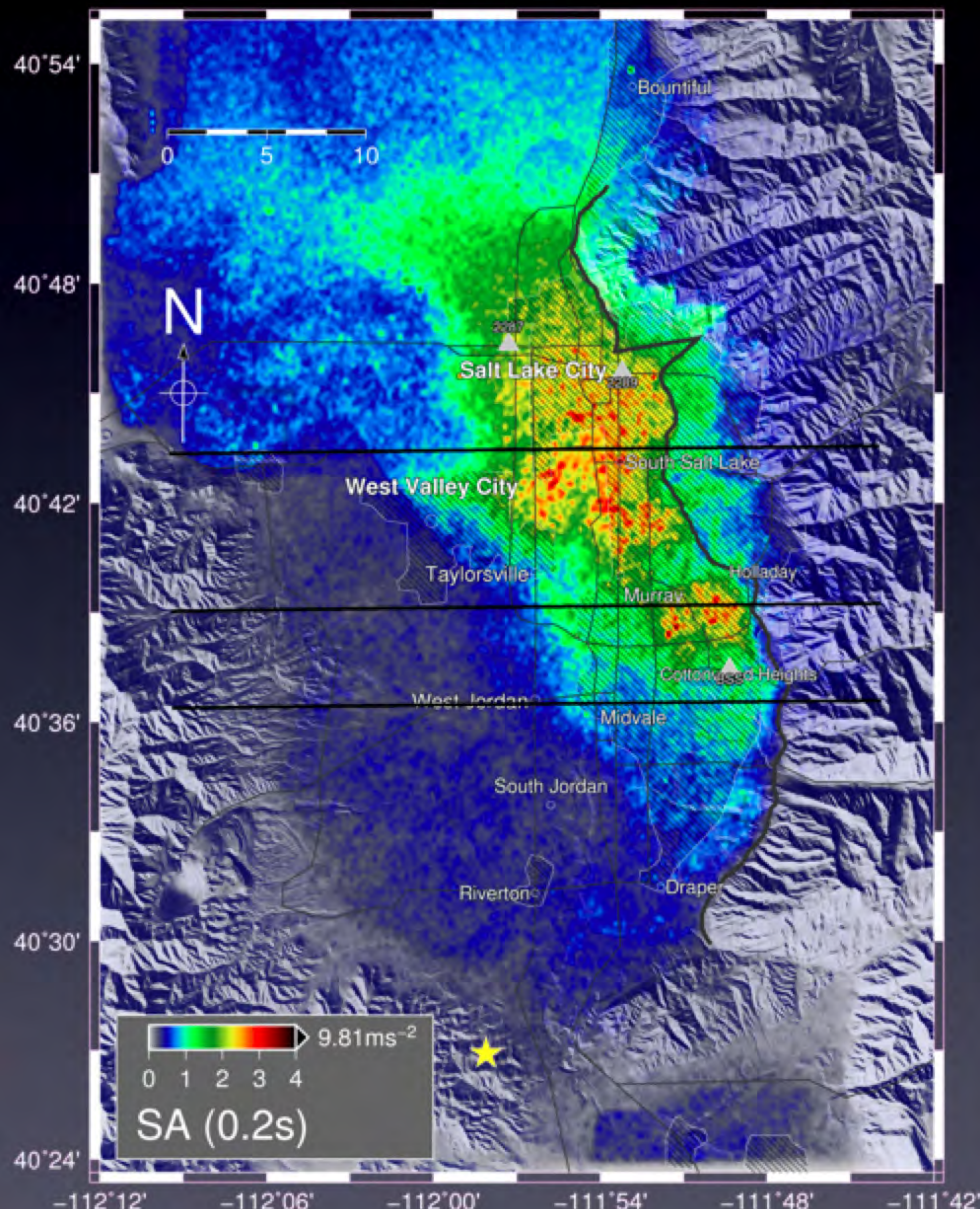

BB-NL 5Hz-SAs (Scenario B')

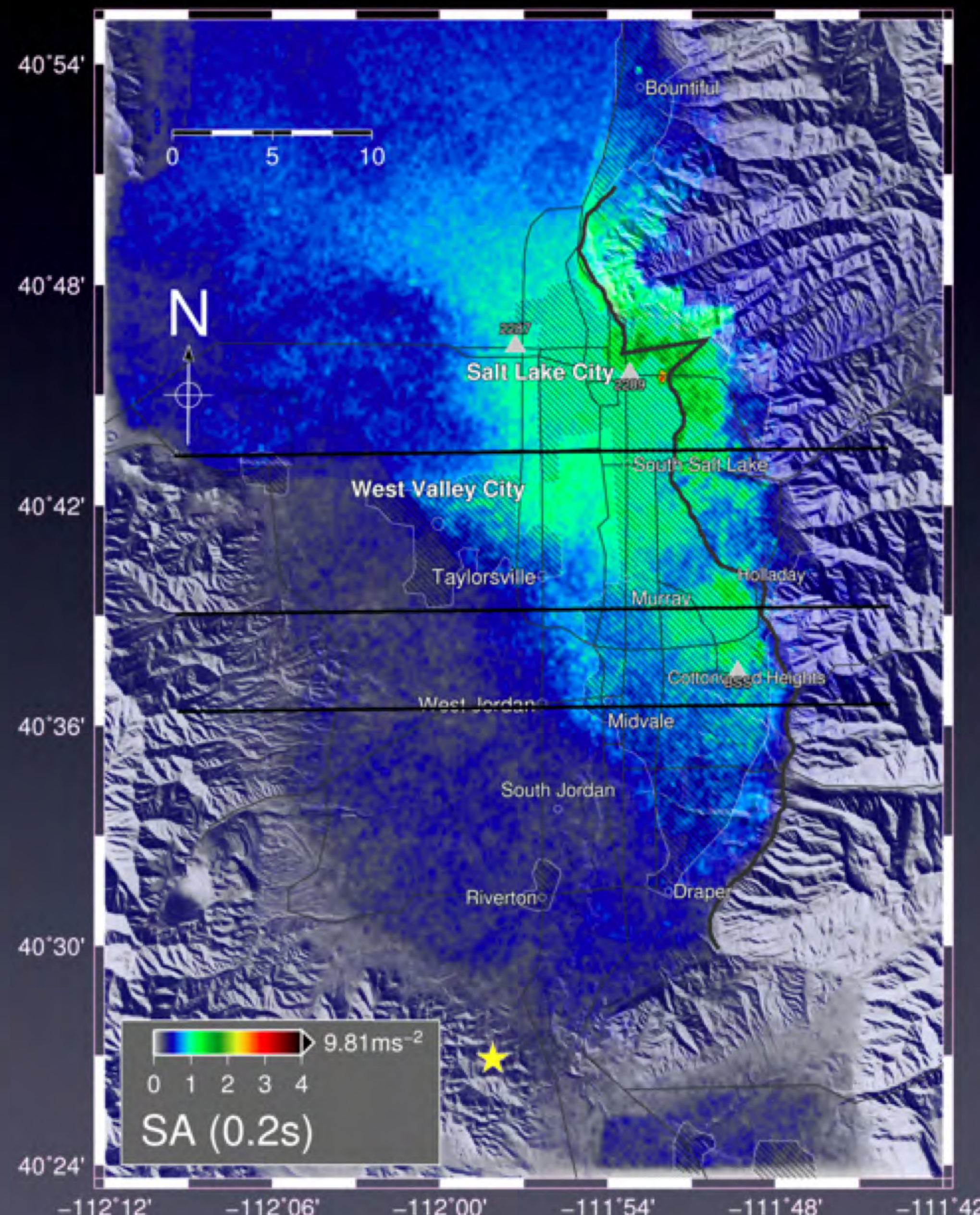

Correction Factors for BB SAs

BB 5Hz-SAs (Scenario A)

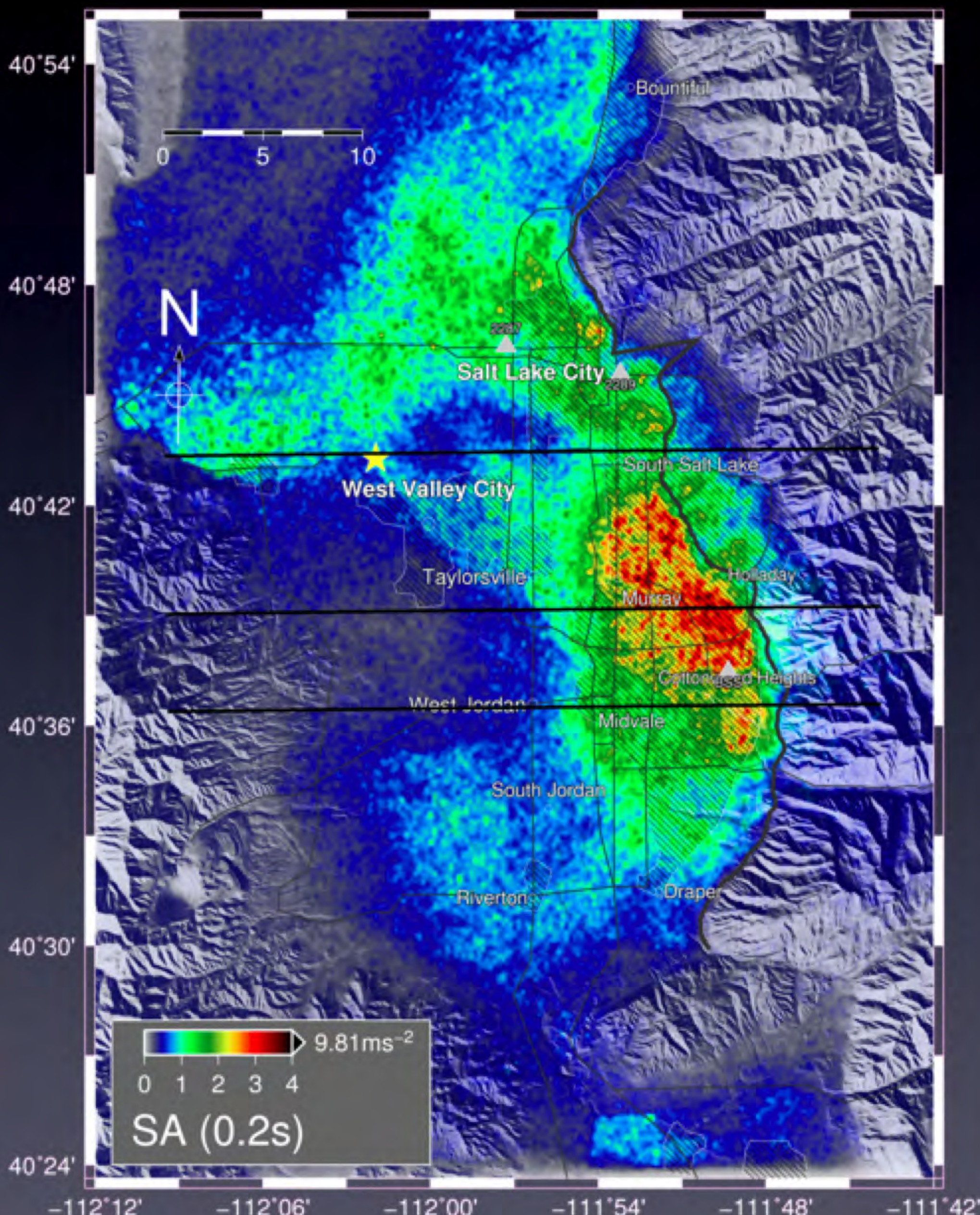

BB-NL 5Hz-SAs (Scenario B)

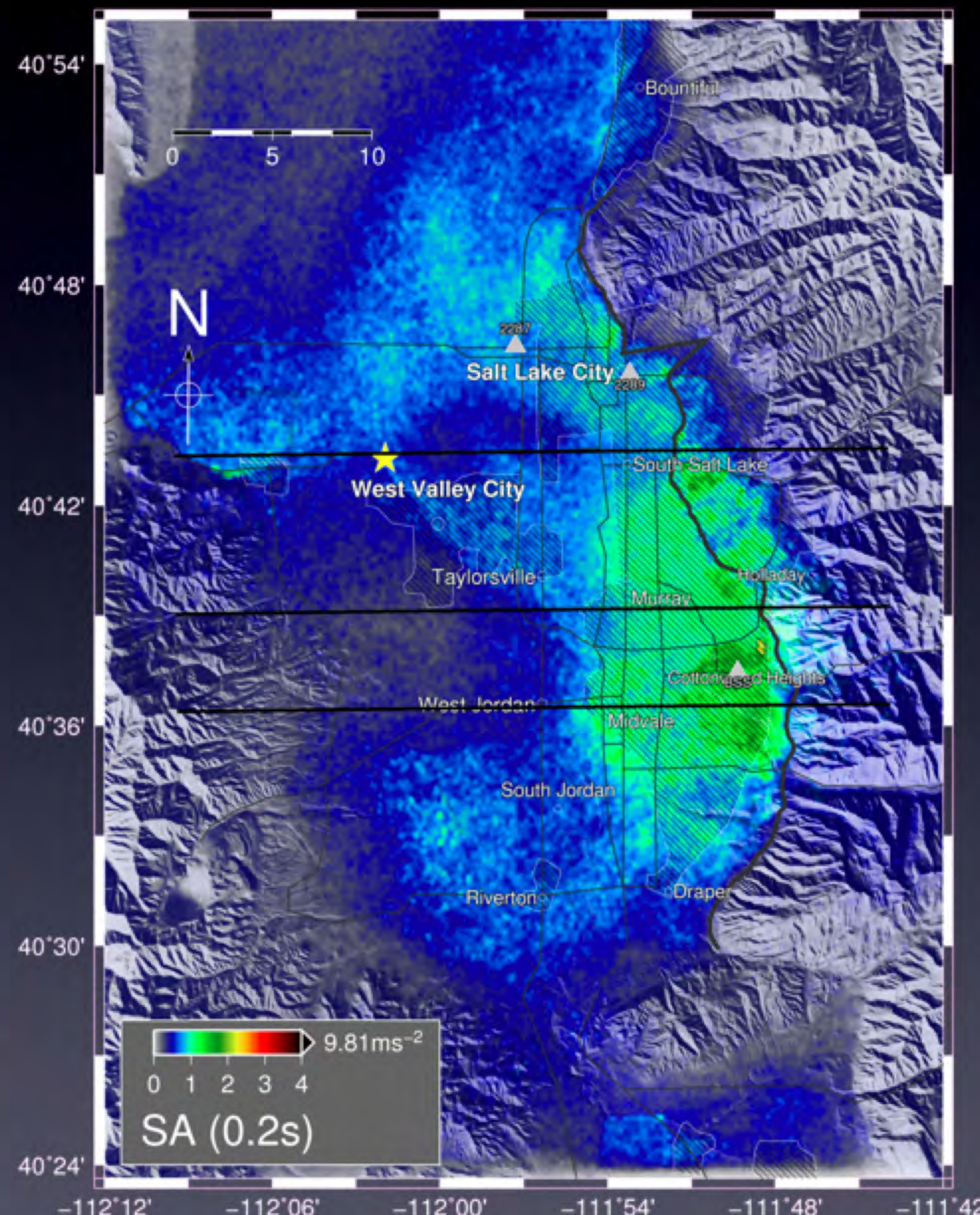

Comparison to NGA

Average BB+NL 5Hz-SAs

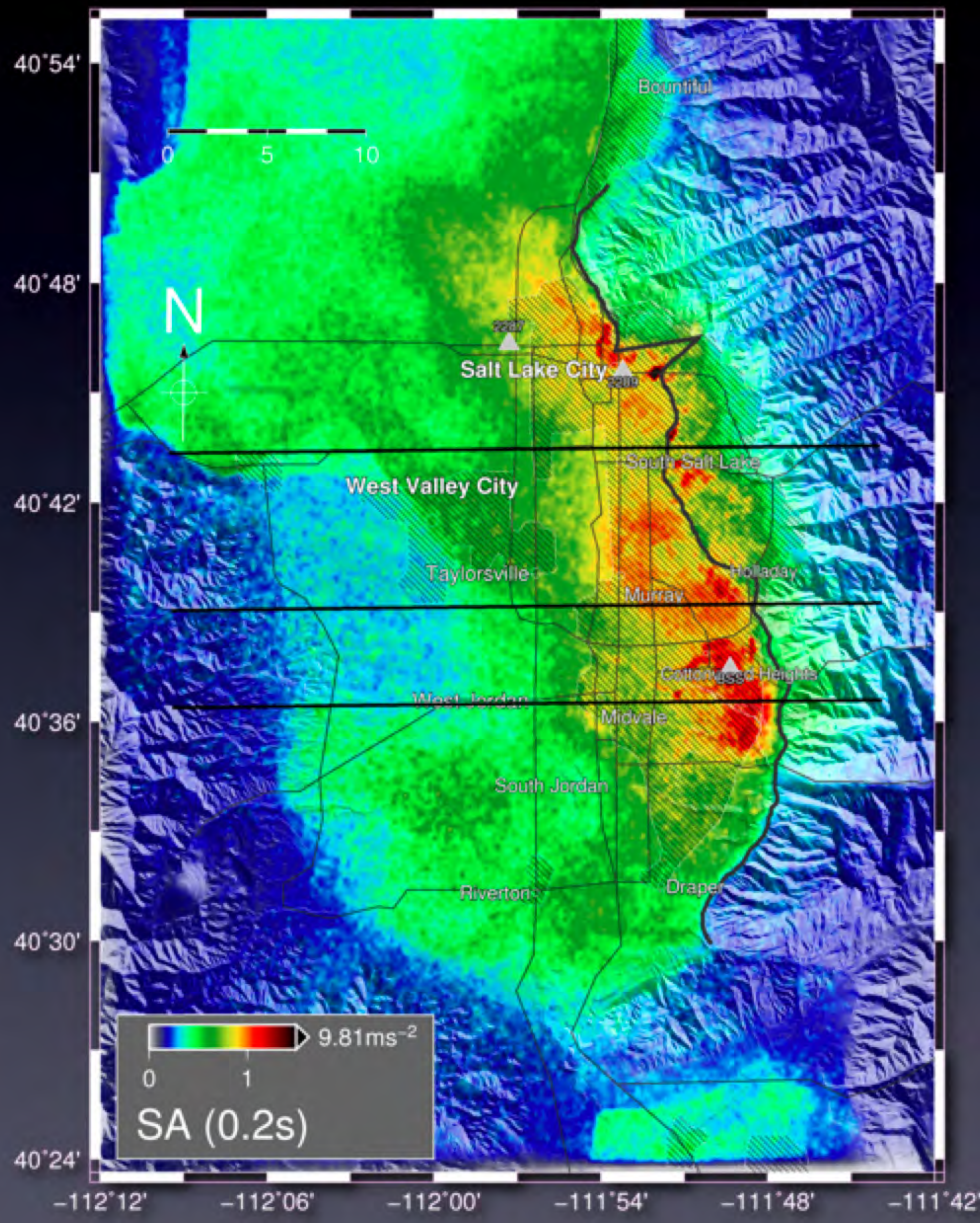

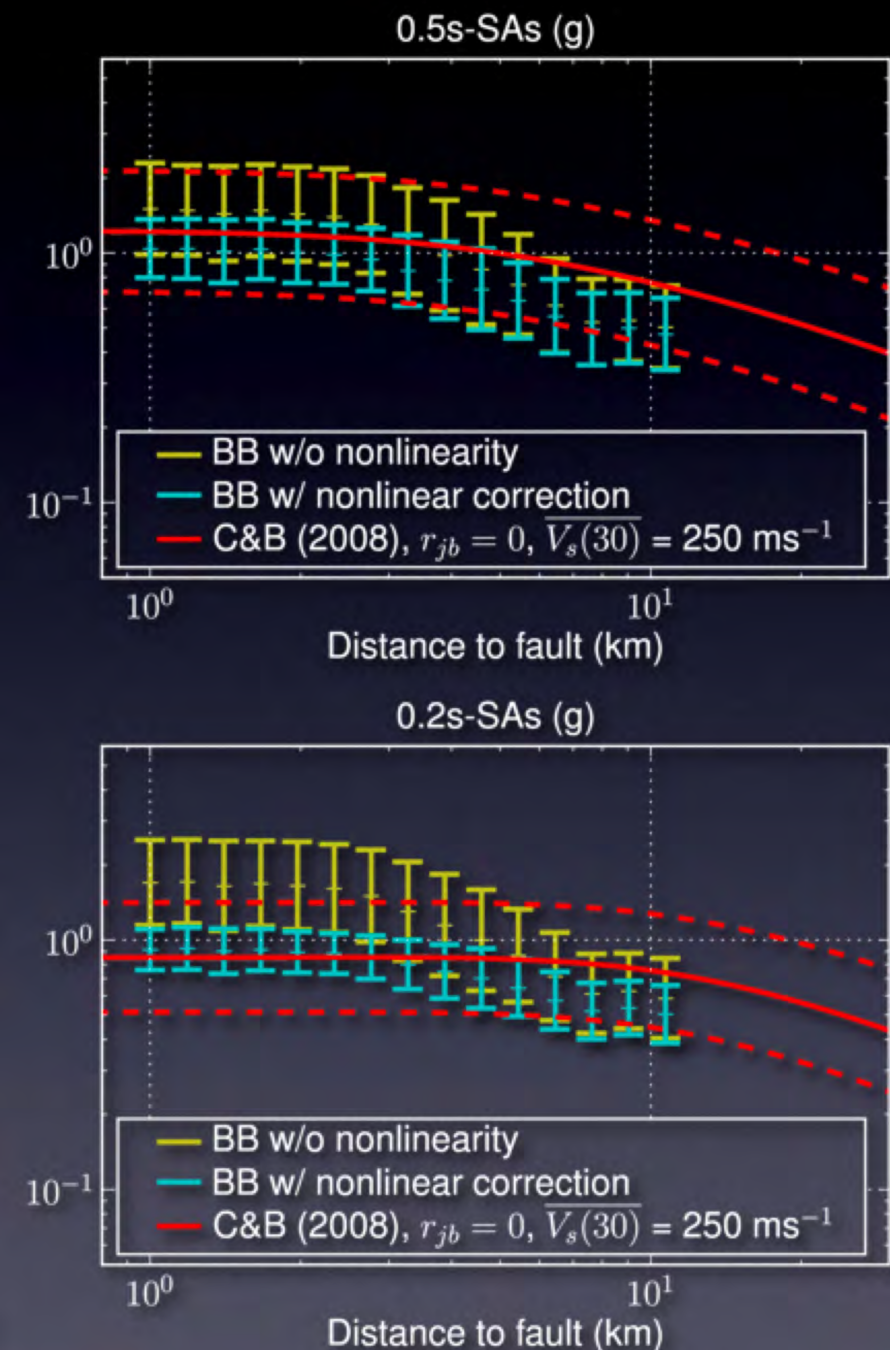

Average 1s-SAs

Wong et al. (2002)

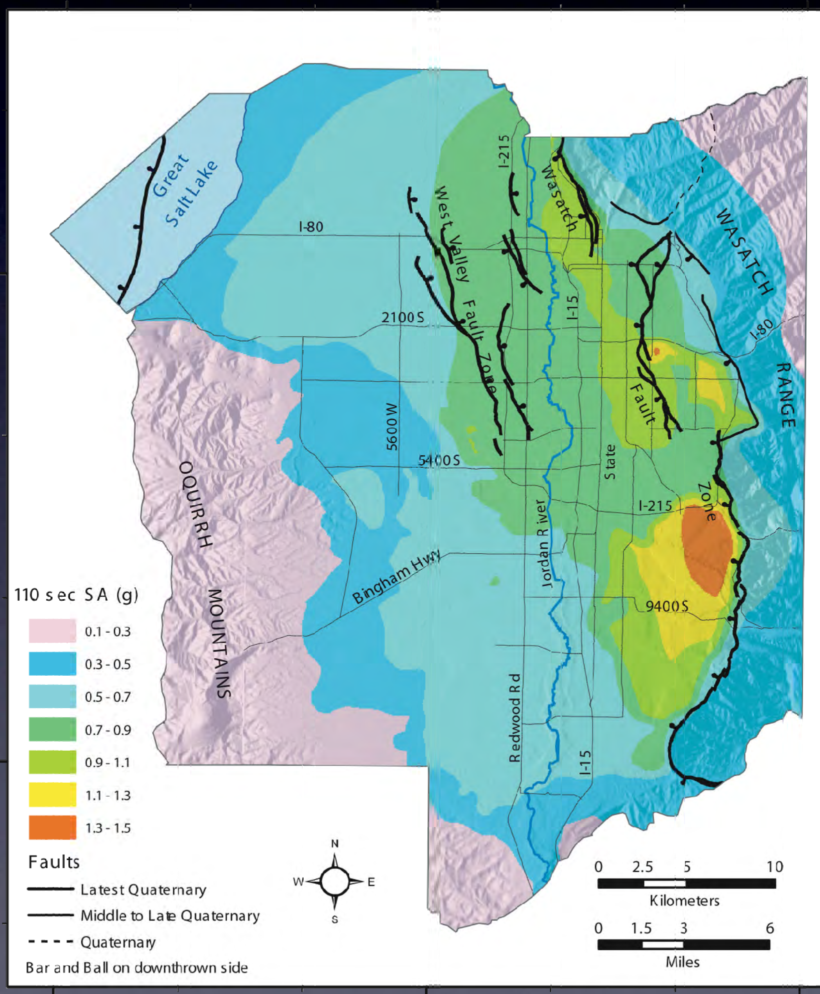

Roten et al. 3-D simulations

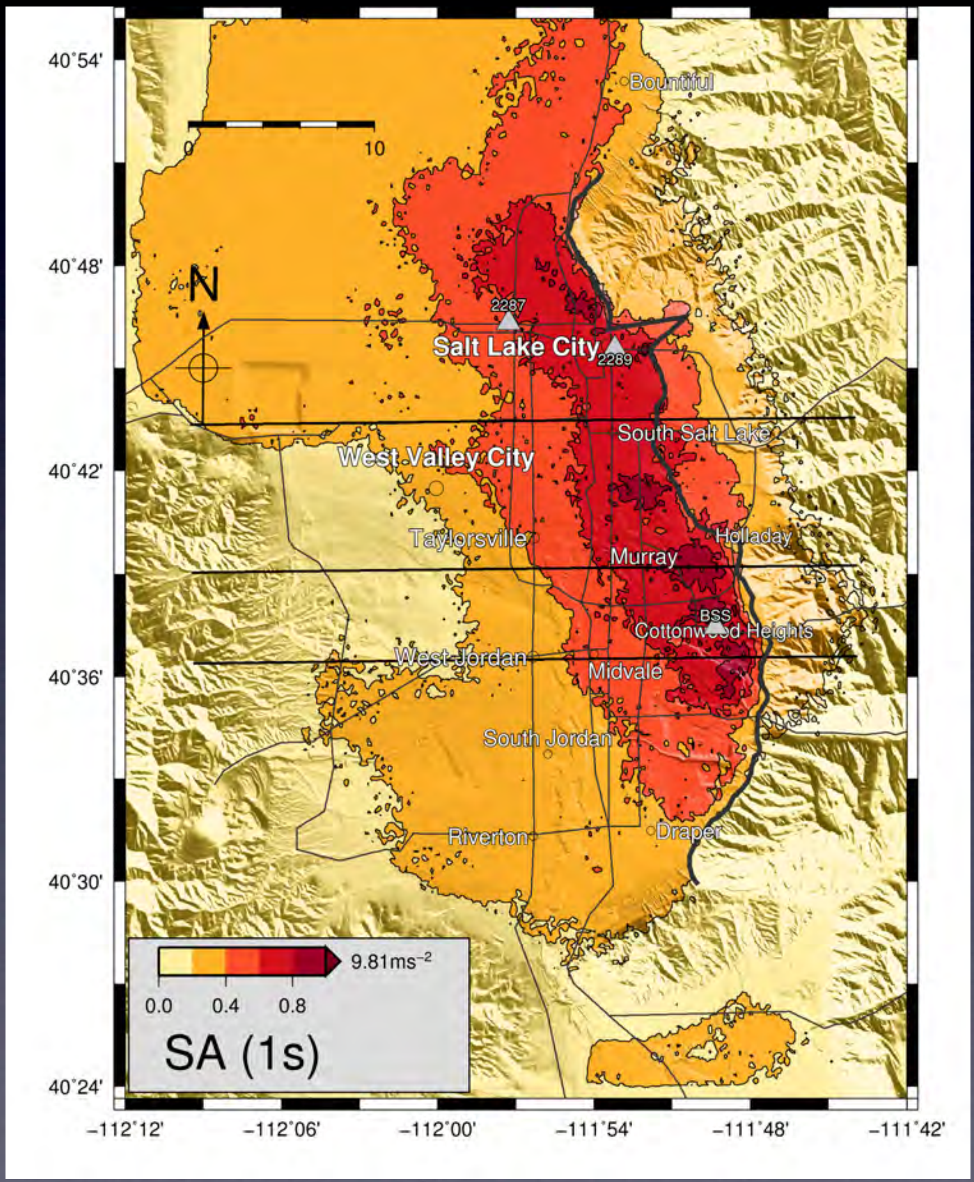

Average 0.2s-SAs

Wong et al. (2002)

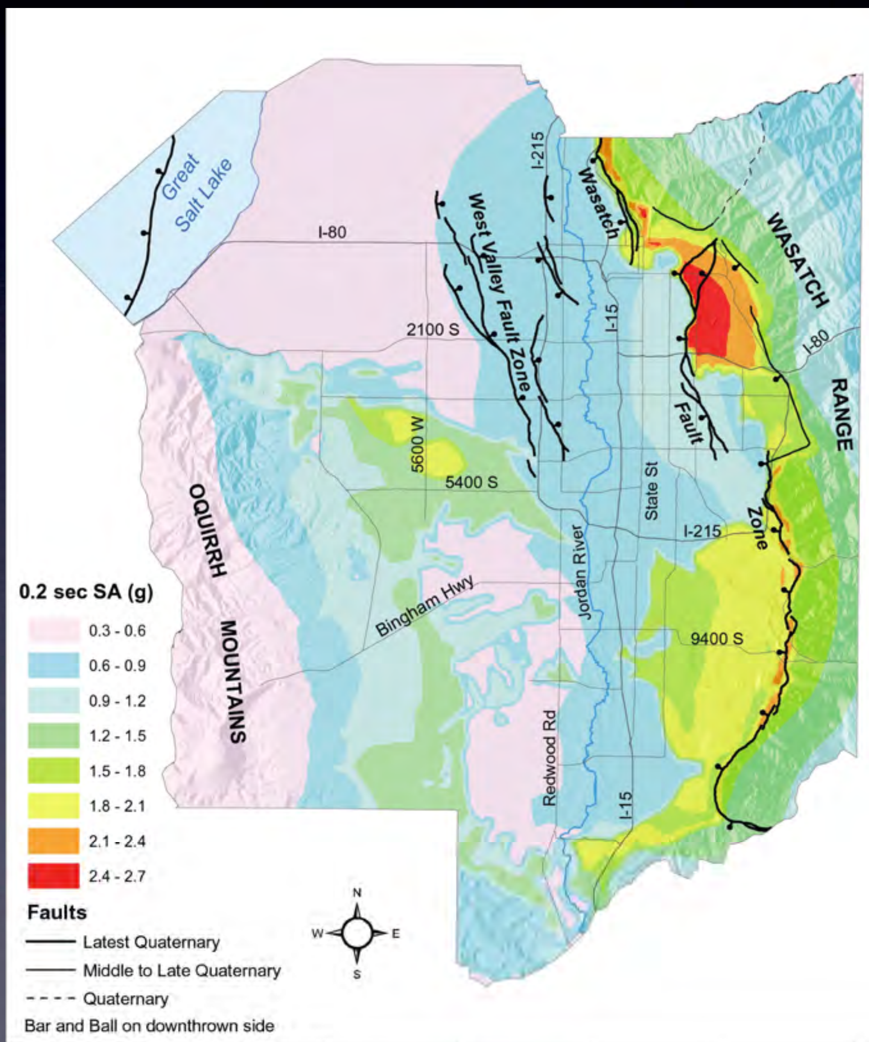

Roten et al. 3-D simulations

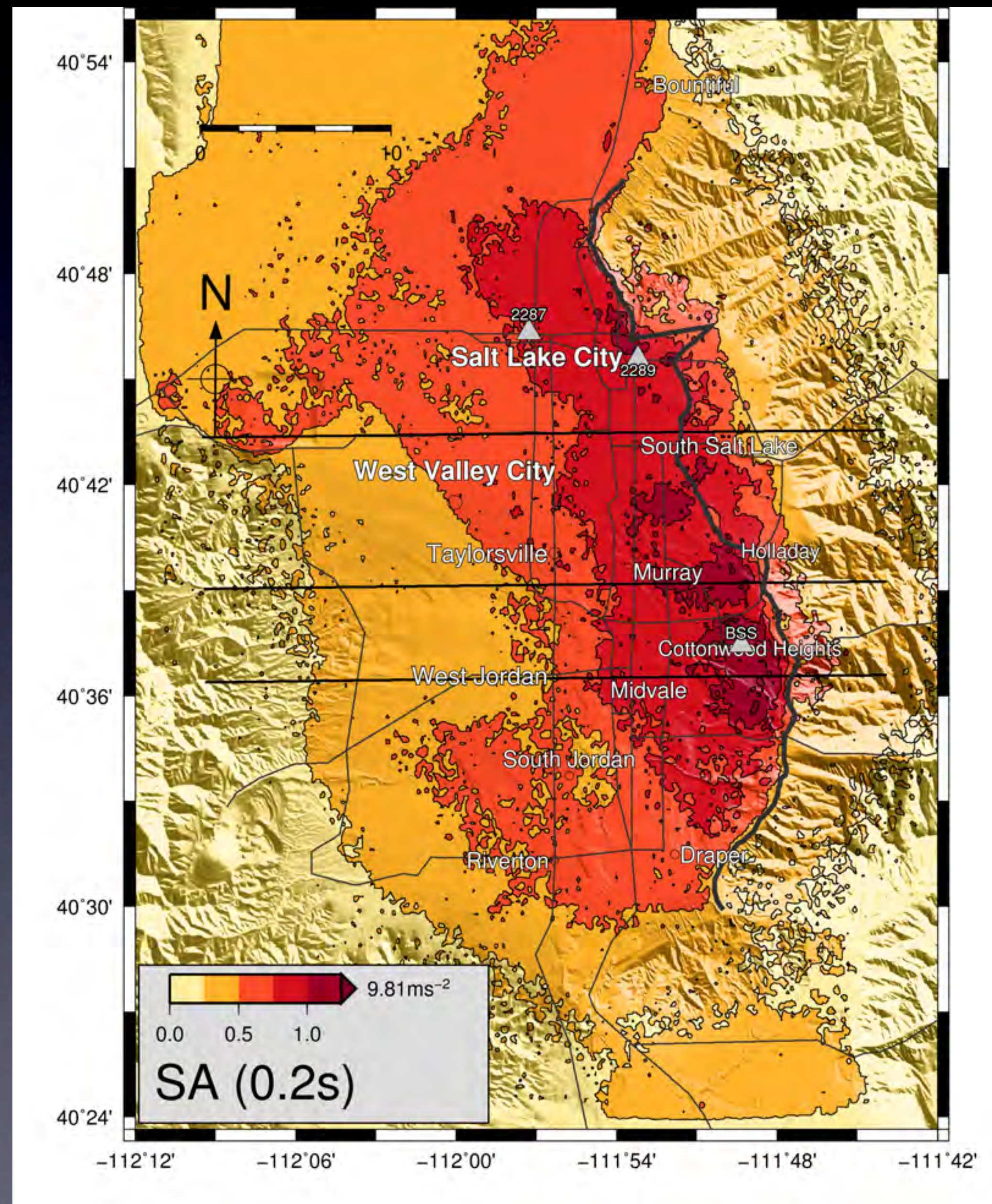

PGAs

Wong et al. (2002)

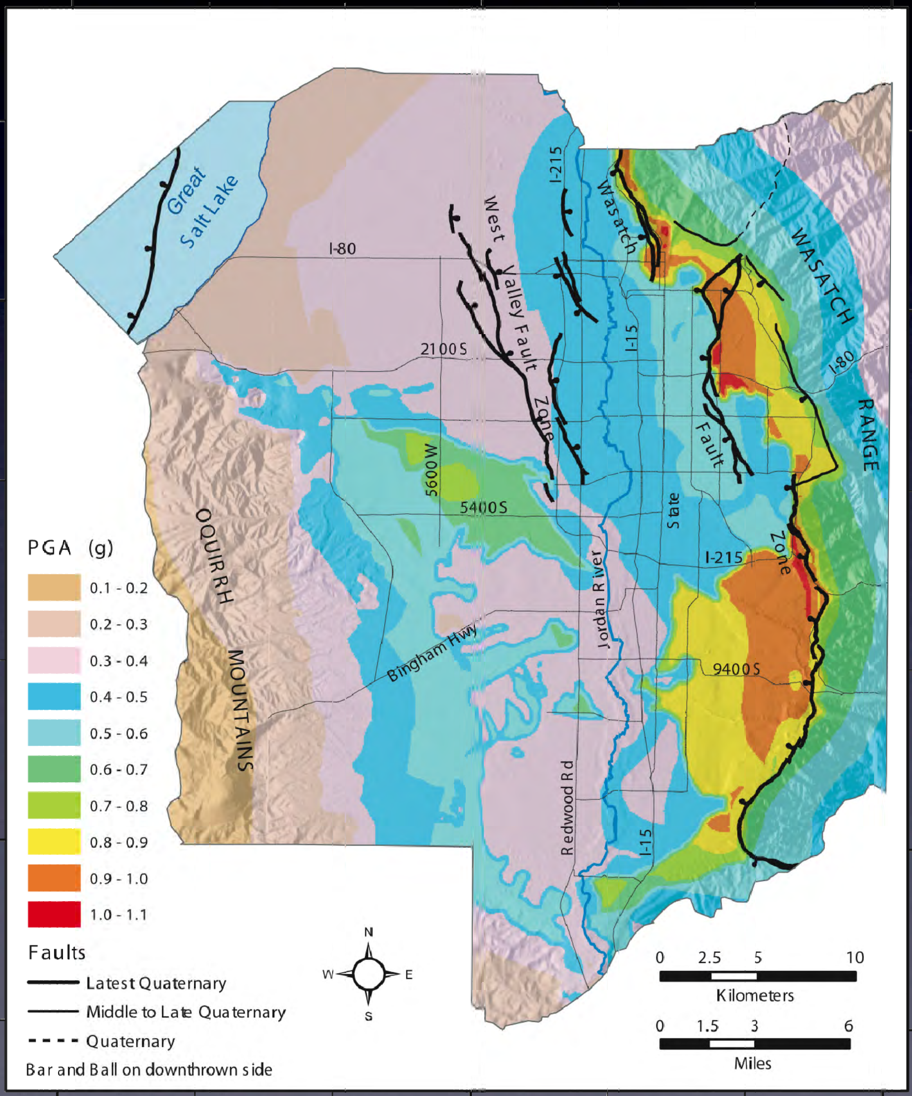

Roten et al. 3-D simulations

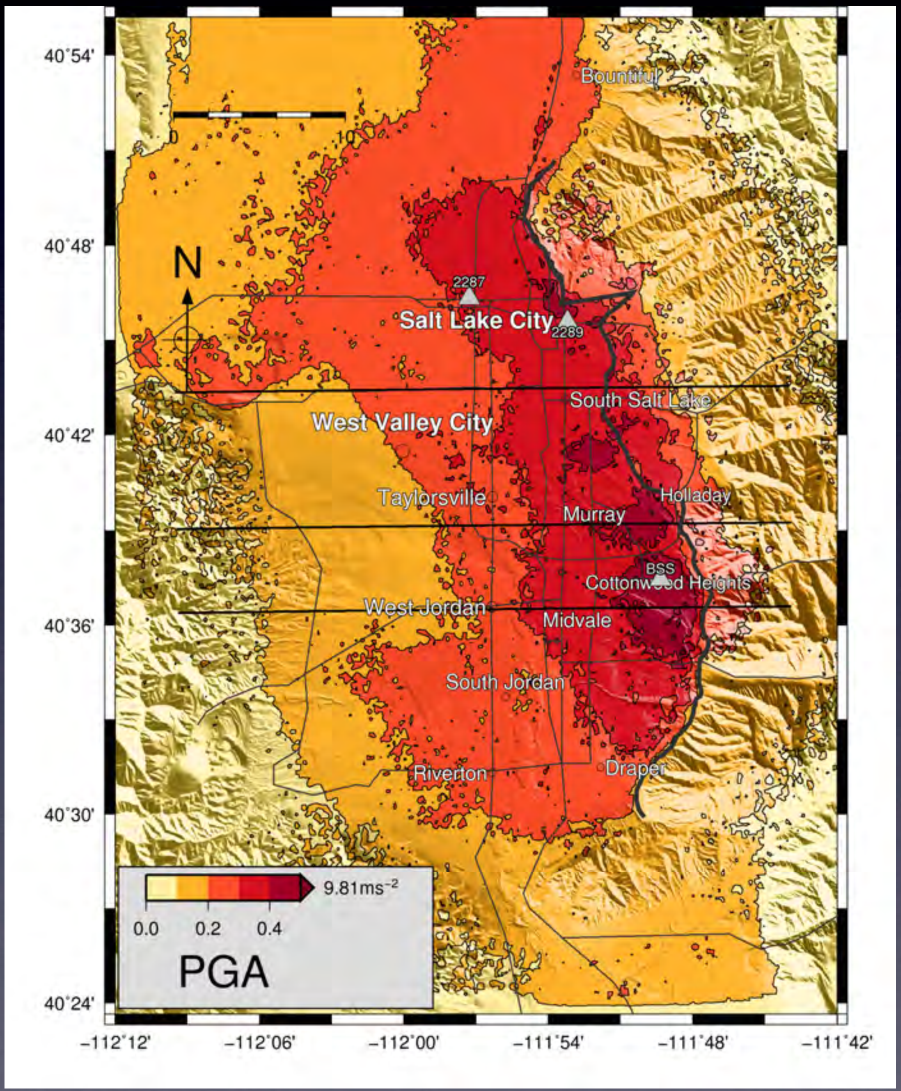

PGVs

Roten et al. 3D simulations

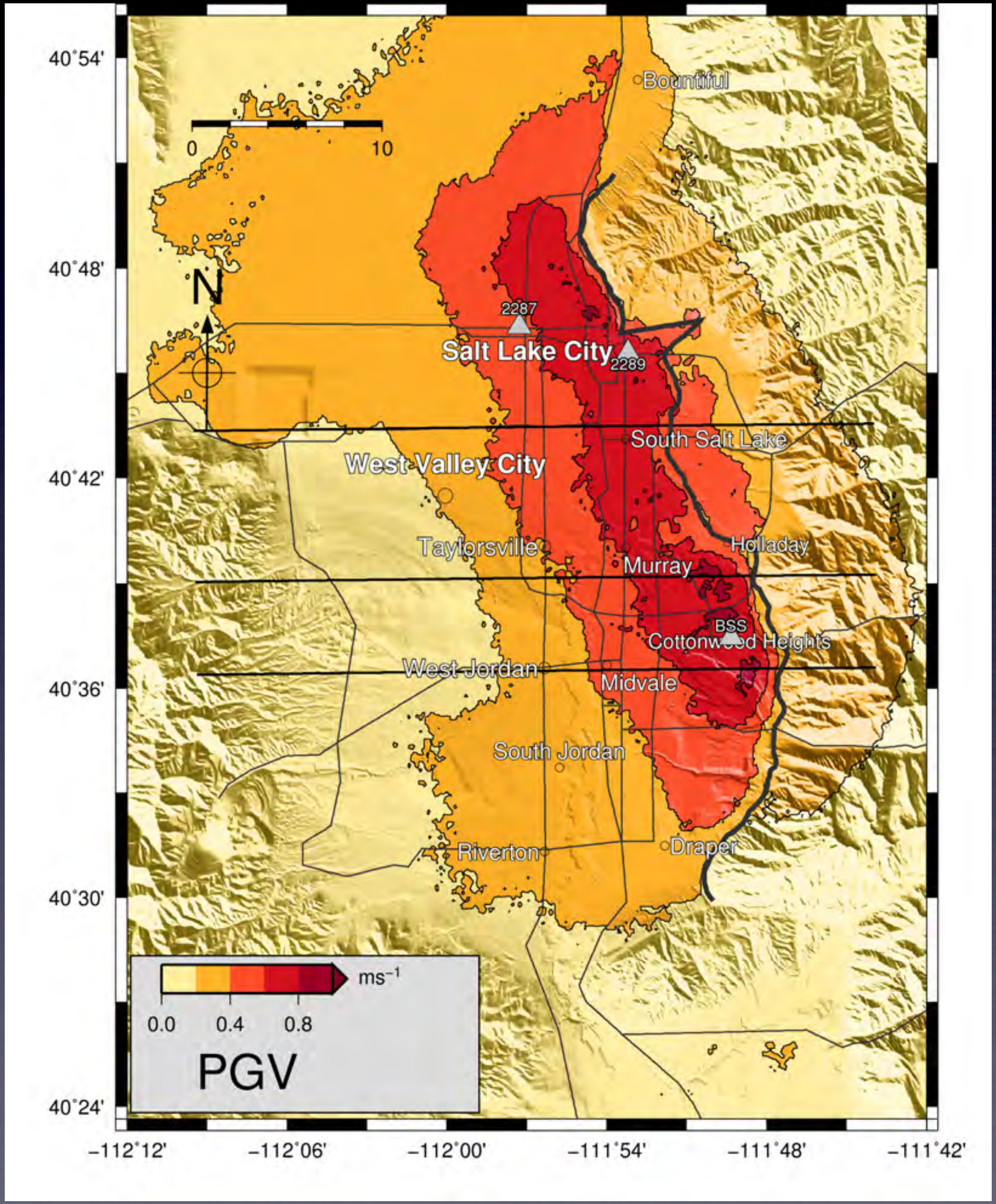

Conclusions I

0-1 Hz 3-D FD simulations of scenario earthquakes

- Ground motion tends to be larger on the low-velocity sediments on the hanging wall side of the fault than on outcropping rock on the footwall side, confirming results of previous studies on normal faulting EQs (O'Connell et al., 2007)
- The simulated ground motions reveal strong along-strike and along-dip directivity effects
- Our simulations suggest that the highest average 2s-SAs occur at ~2-3 km distance from the surface trace of the fault
- 2s-SAs and 1s-SAs are in agreement with values predicted by NGA models

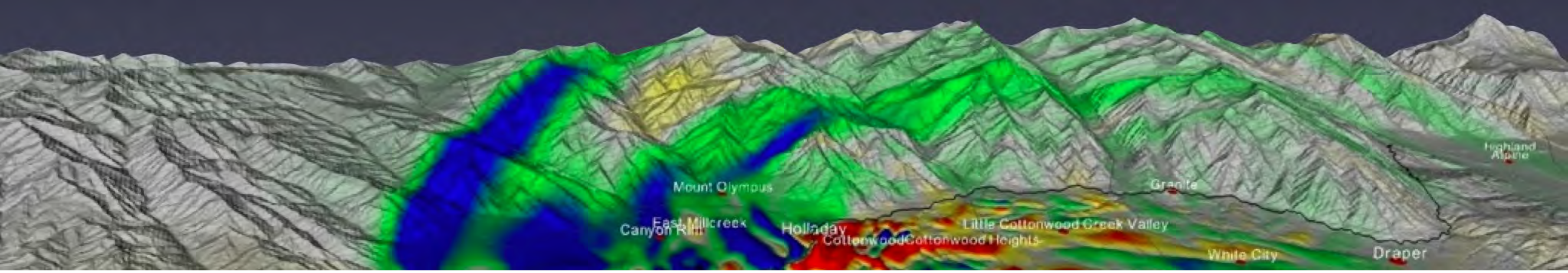

Conclusions II

Broadband (0-10Hz) synthetics:

- 0.2s-SAs derived from broadband synthetic seismograms are exceeding those predicted by NGA models by more than one standard deviation at near-fault locations on the hanging wall side, but agree well at some distance from the fault
- Compared to Solomon et al. (2004), our 3-D FD simulations predict lower 1s-SAs on the footwall wall side of the fault

Nonlinear soil response:

- Synthetic ground motions obtained from a fully nonlinear 1-D propagator exhibit PGAs and SAs that are consistent with values predicted by NGA models, even when taking into account the uncertainty in the nonlinear soil parameters
- Higher-frequency (> 2Hz) ground motion is controlled by nonlinear site response, with larger SAs on the shallow sediments on the footwall side than on the deep sediments on the hanging wall side

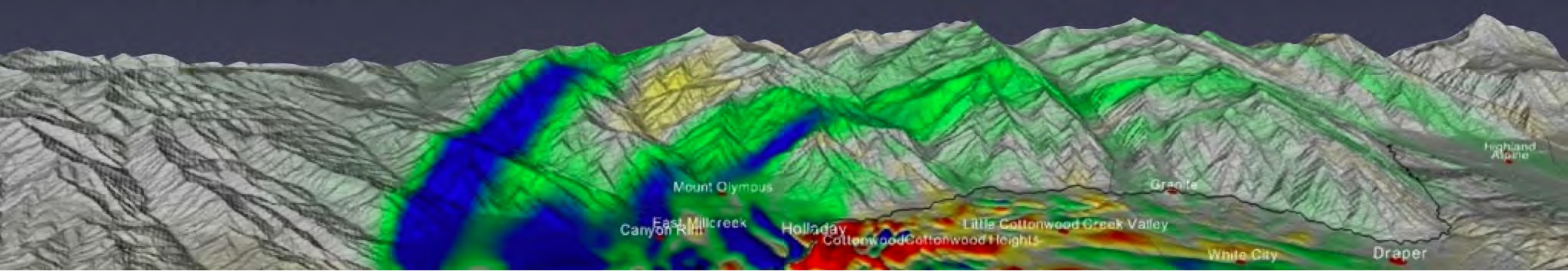

Average 1s-SAs

Solomon et al. (2004)

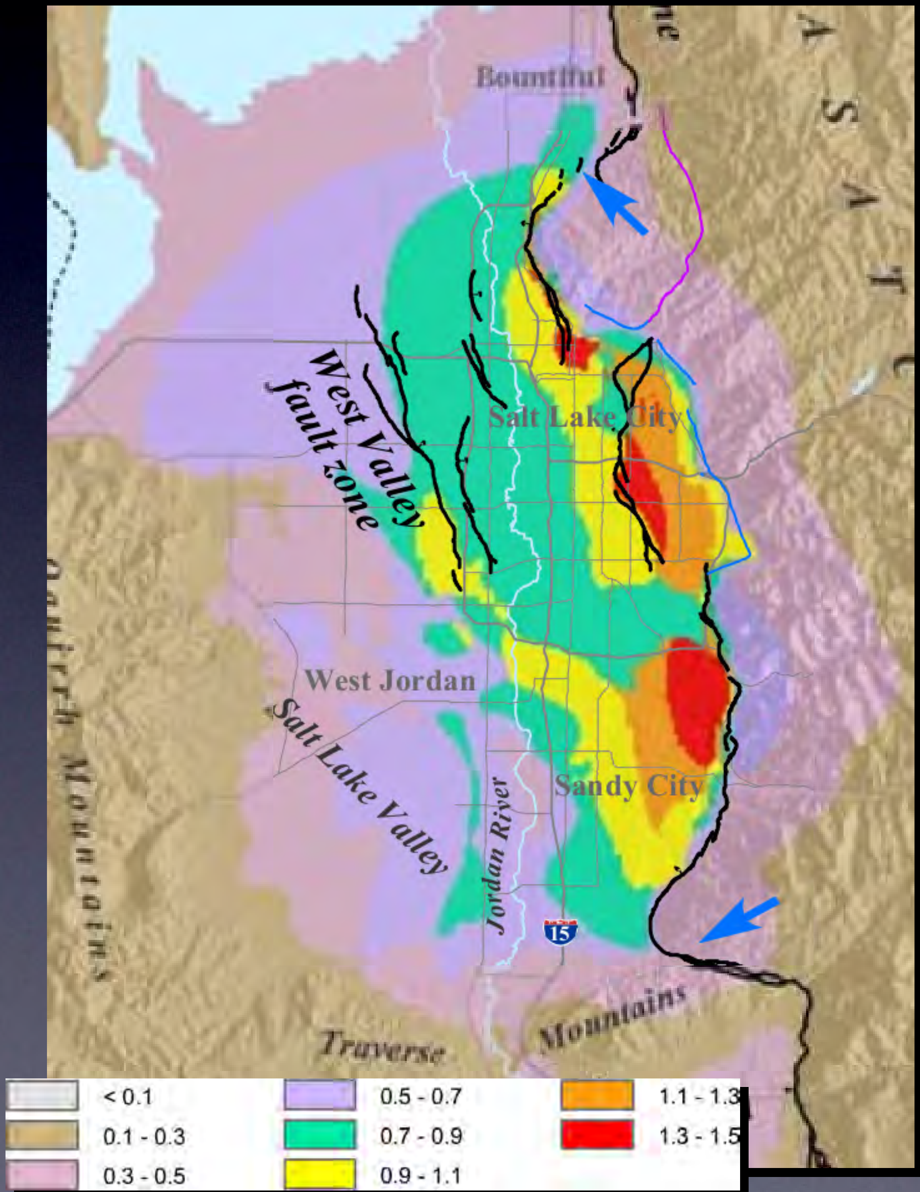

3-D FD simulations

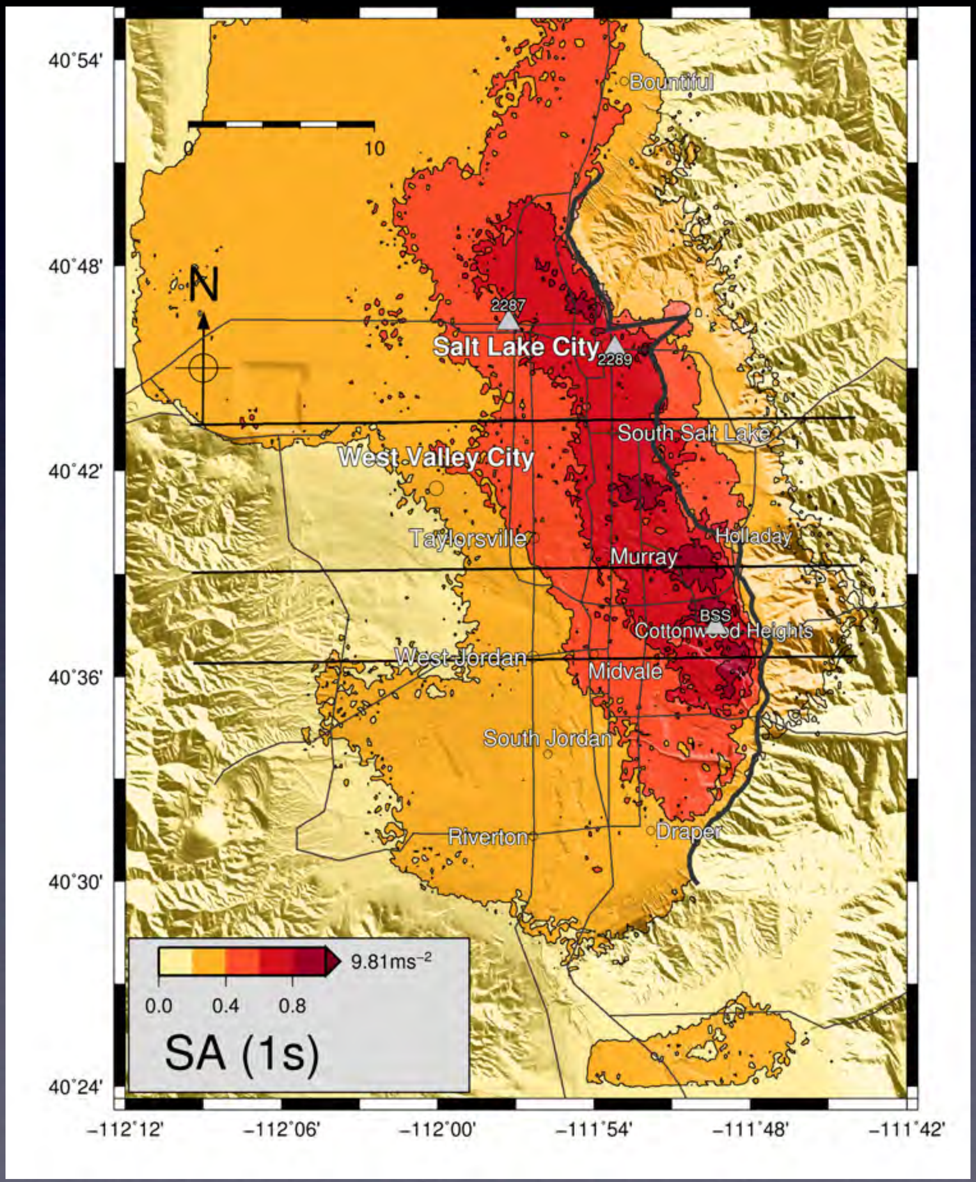

Comparison to BLWN-RVT

1s-SAs by Solomon et al. (2004)

(finite EQ source modeling, band limited white noise GM model, random vibration theory, equivalent linear soil)

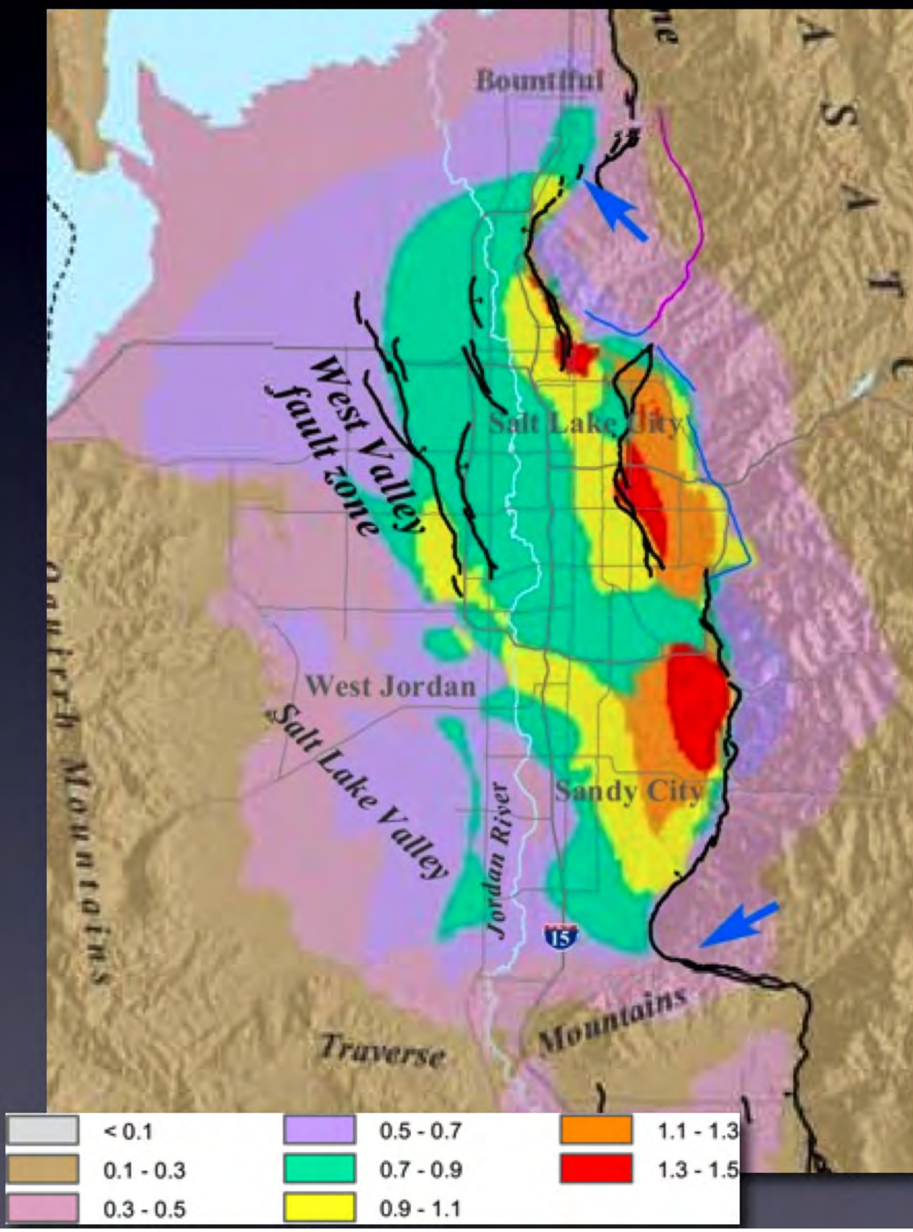

1s-SAs from 3-D FD+BB simulations

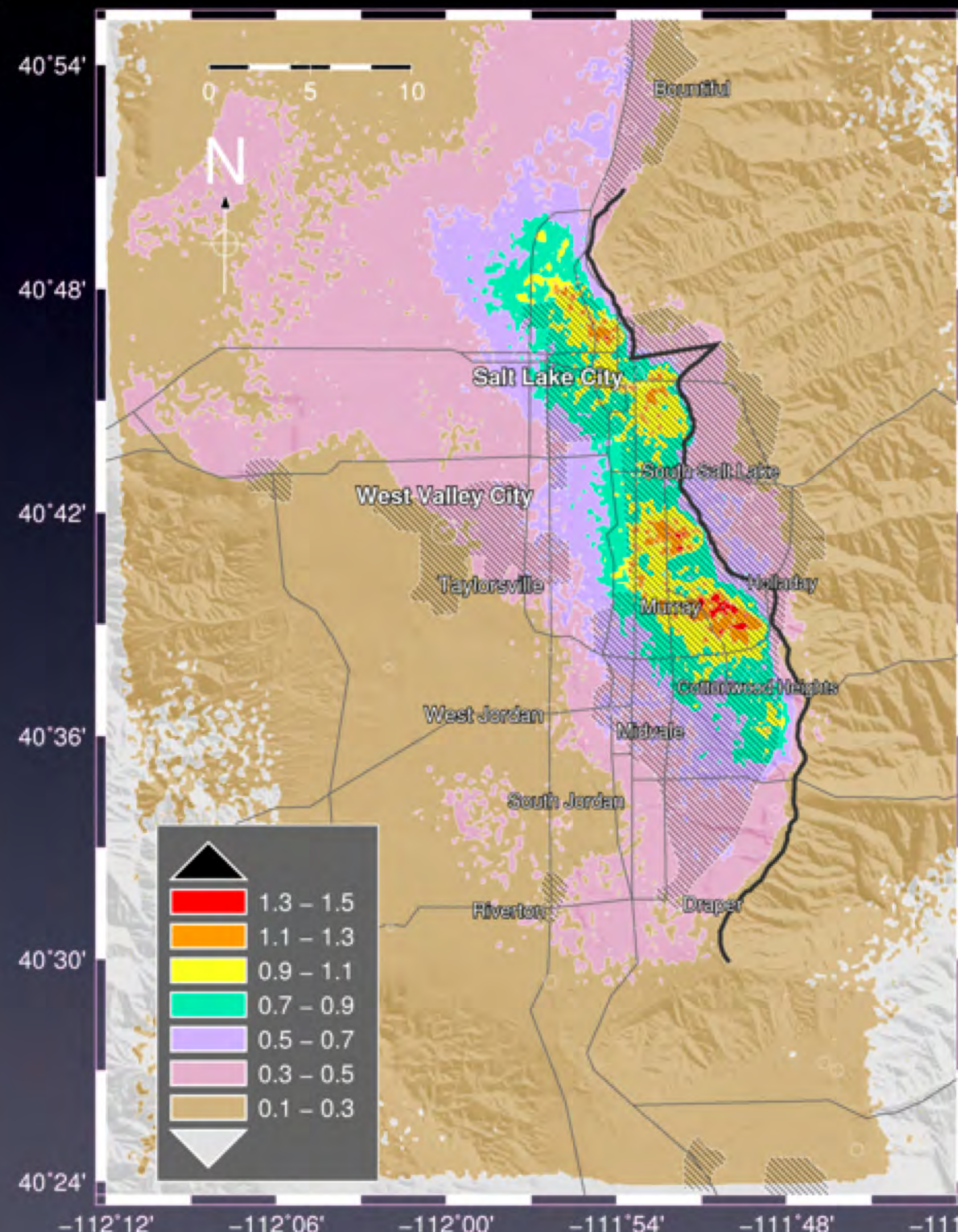

Long period (T > 1-s) earthquake simulations for the evaluation of the WCVM

Morgan Moschetti and Leo Ramirez-Guzman
USGS, Golden, CO
Utah Ground Shaking Meeting
2/14/2011

Motivation

- In preparation for earthquake ground motion modeling with kinematic source models, compare synthetic and observed seismograms using the WCVM to identify any characteristic misfits and bias
- Test effect of simple perturbations to the material model to assess impact on various goodness-of-fit parameters (PGV, spectral acceleration, surface wave speeds)

Outline

- Misfit to synthetic seismograms
- R1-kriging
- Simple perturbations to WCVM for synthetic seismograms
  - Regional model
  - R3
  - GTL

Simulated earthquakes

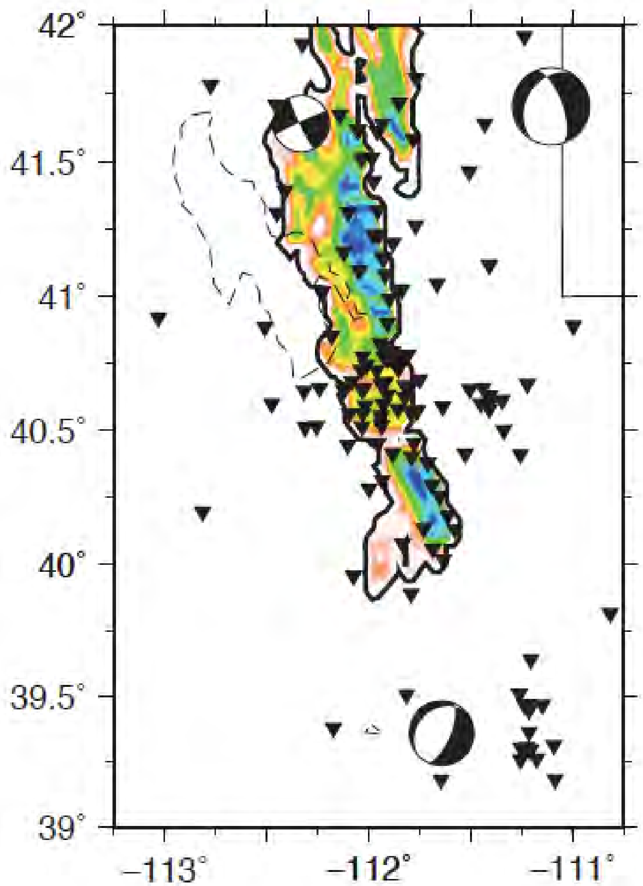

- Set of simulated earthquake selected from catalog based on magnitude, proximity to Salt Lake Basin and number of broadband stations
- Ephraim EQ occurred during TA deployment in Wasatch Front

EQ	Date	Lat	Lon	Strike	Dip	Rake	Depth	Mw
Randolph	4/15/10	41.7	-111.1	210	35	-45	5	4.51
Ephraim	11/5/07	39.36	-111.64	230	25	-65	15	3.76
Tremonton	9/1/07	41.64	-112.33	245	85	5	9	3.66

Earthquake ground motion modeling

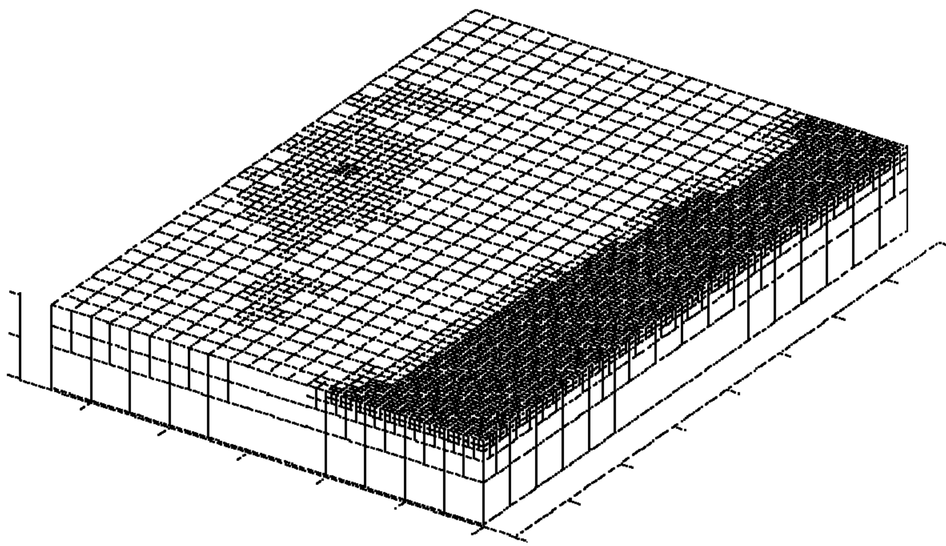

- CMU-Hercules FE toolchain (Tu et al., 2006)
- Simulations run to 0.5-Hz (Regional model, geotechnical layer) and 1.0-Hz (R1 and R3 perturbations – all future simulations to 1-Hz

PGV Comparisons

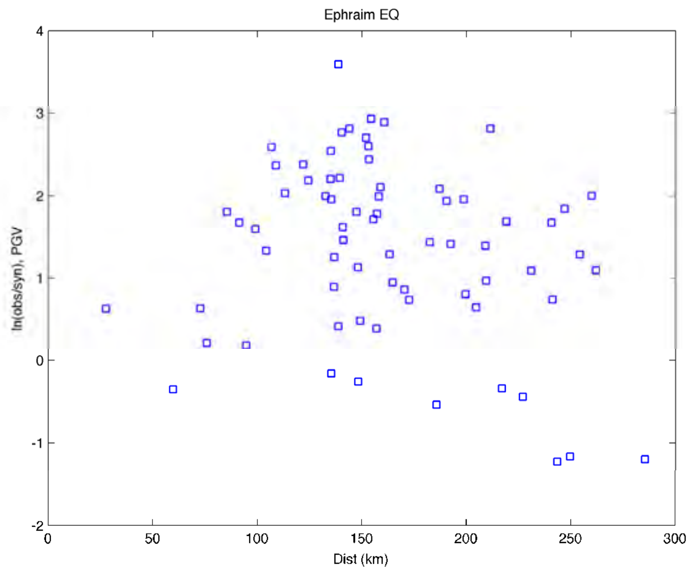

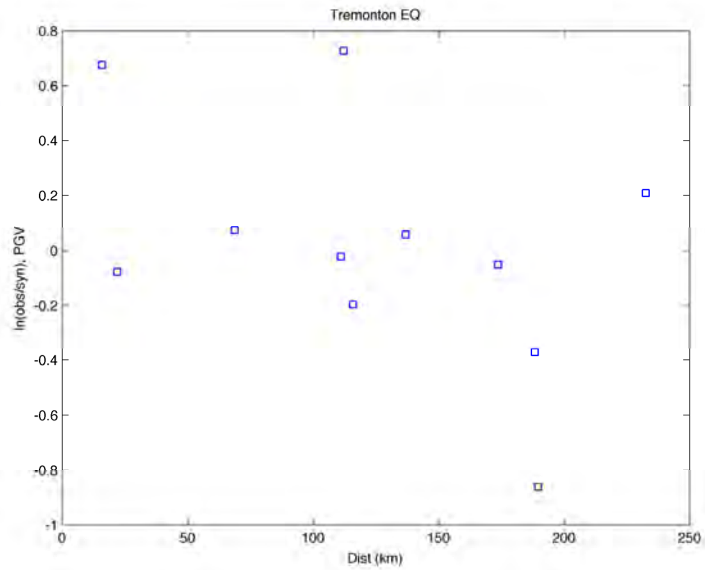

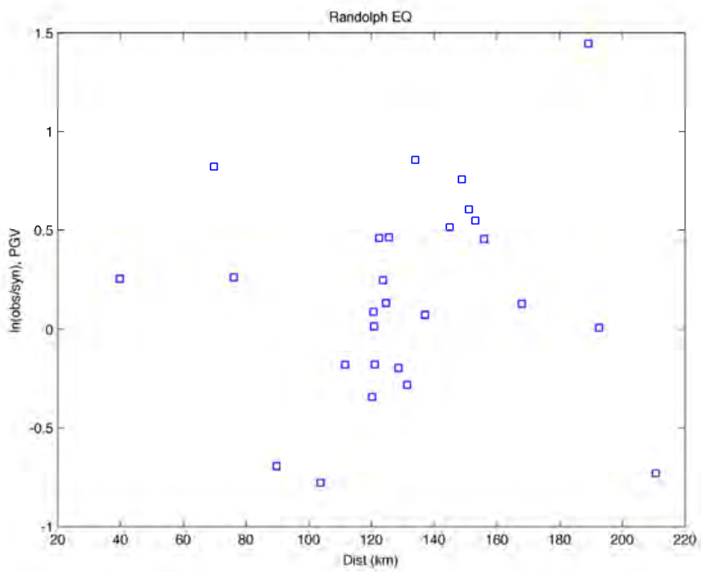

PGV Comparisons

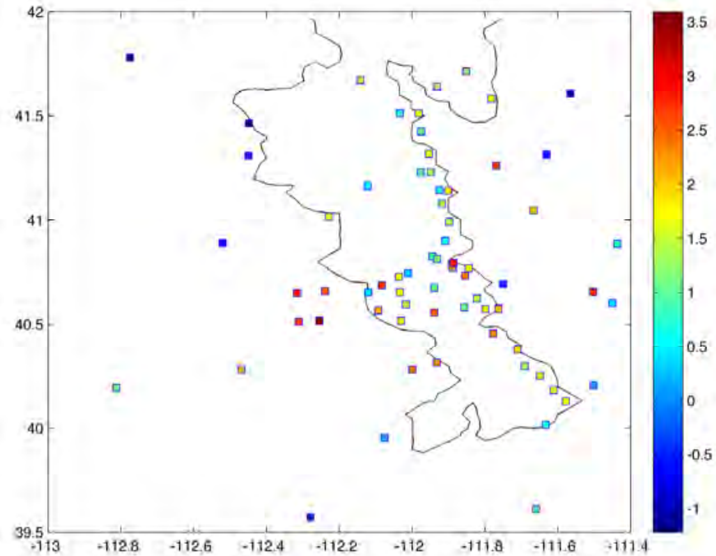

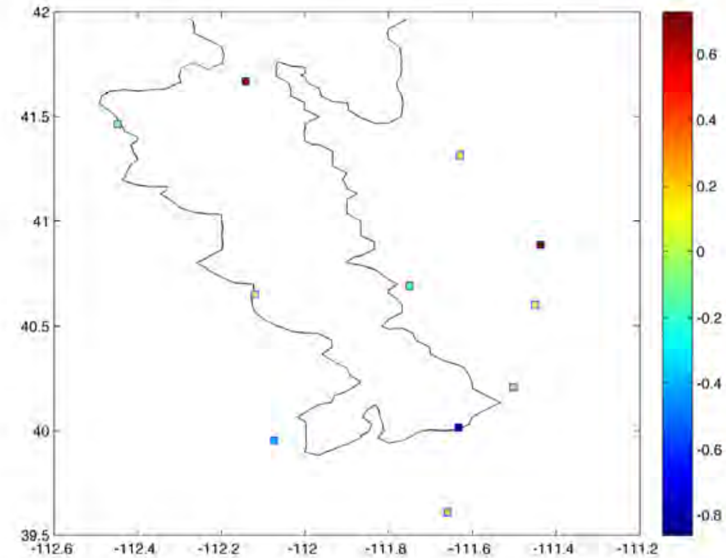

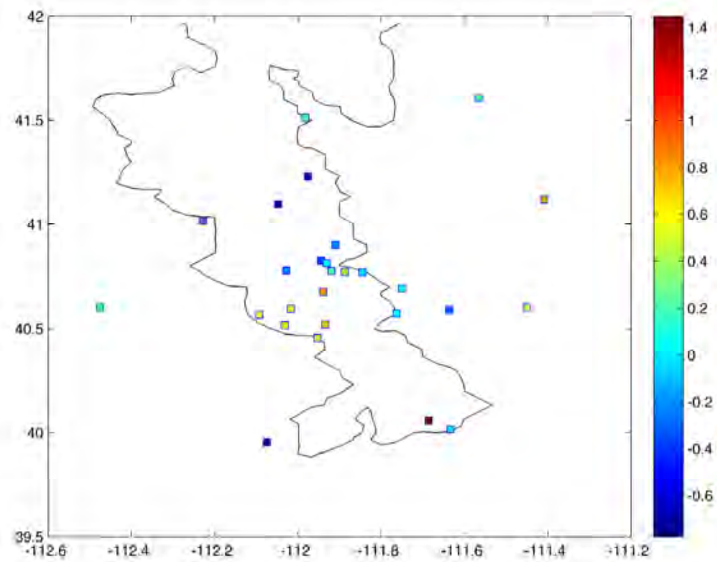

Rayleigh wave group speeds, Randolph EQ

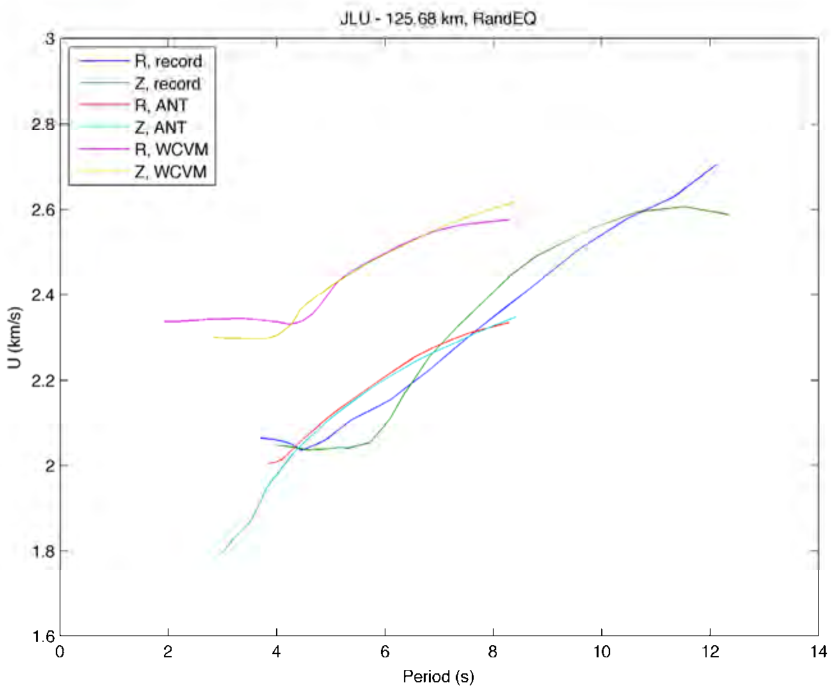

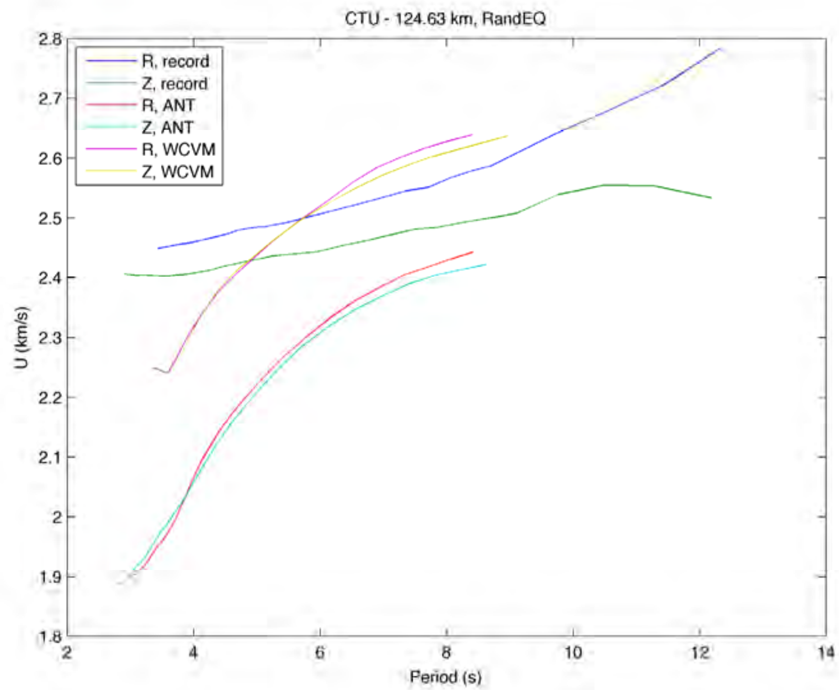

Group speed differences (3-s), Randolph EQ

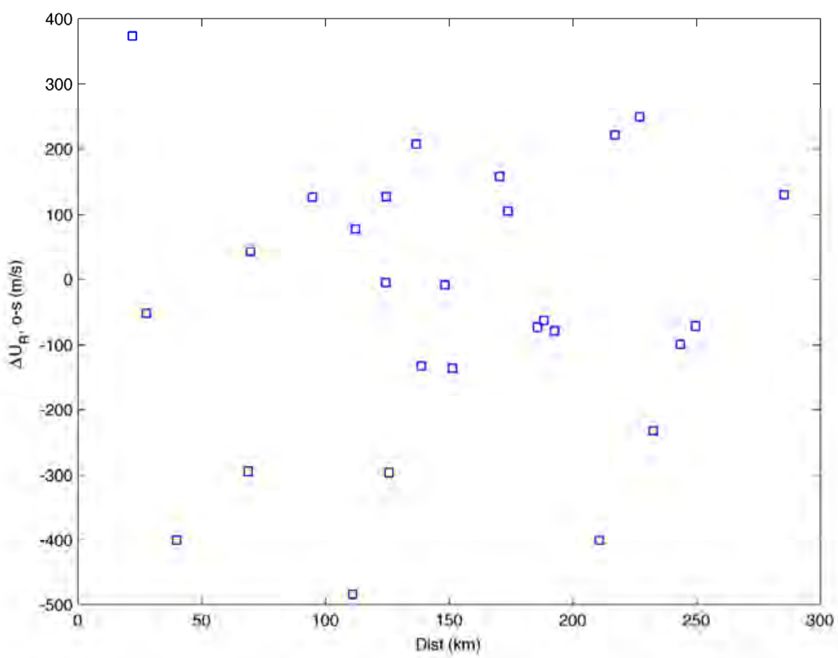

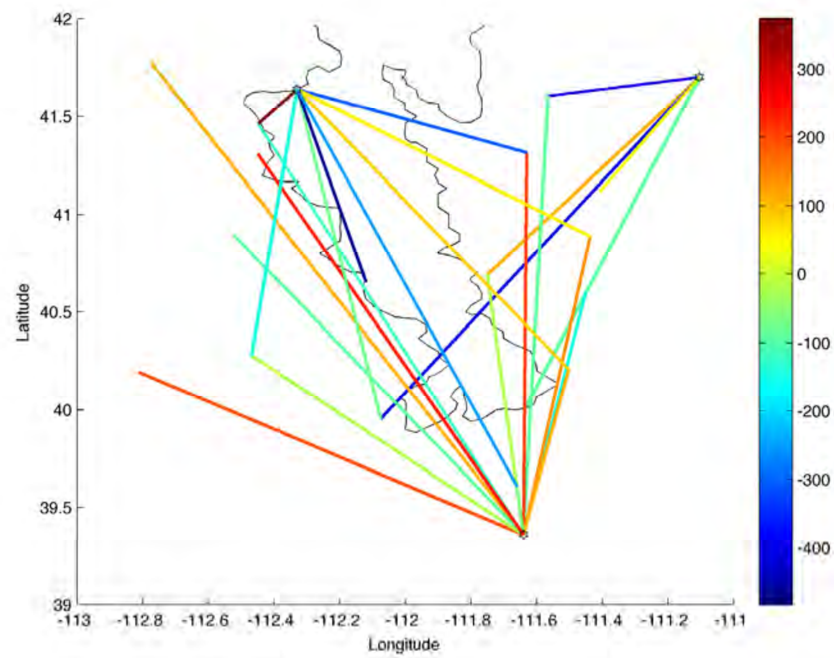

Krigging borehole data in R1

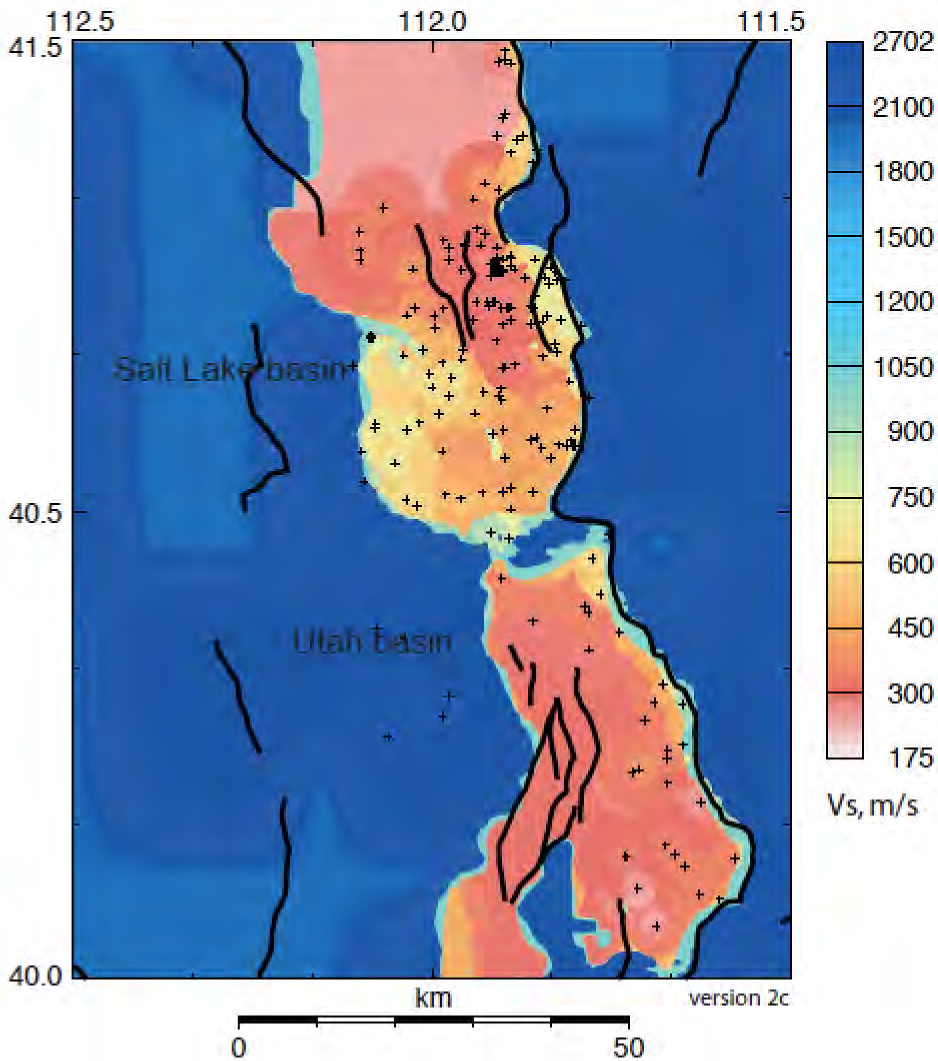

-Test effect of kriging borehole data

- Supplement borehole data with profiles through the CVM

Response spectra ratios, Randolph EQ

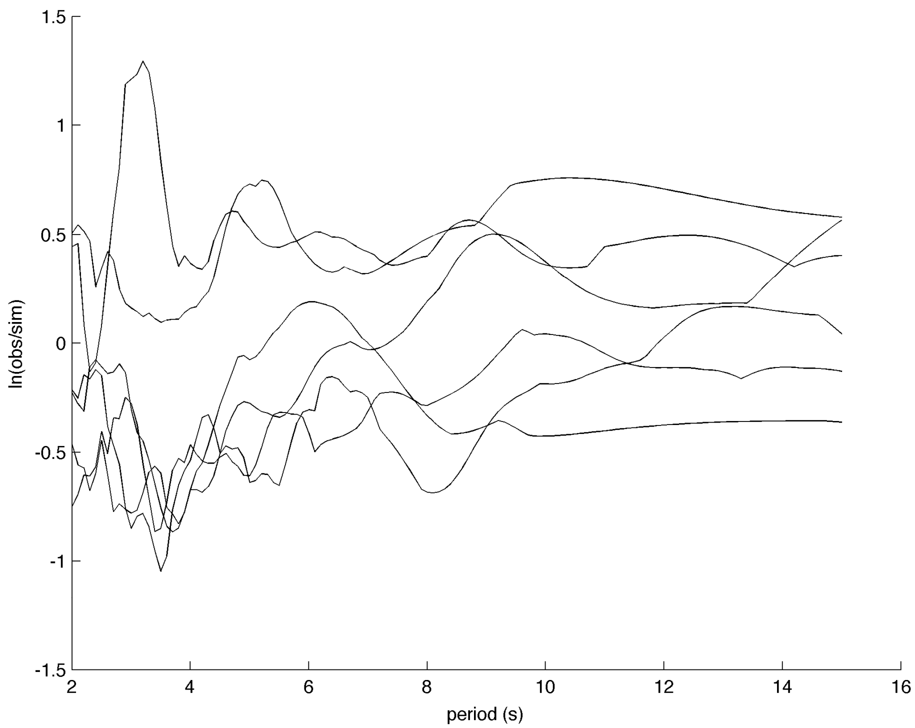

- Response spectra plotted are mean values of all station spectra calculated.

Response spectra ratios, Randolph EQ

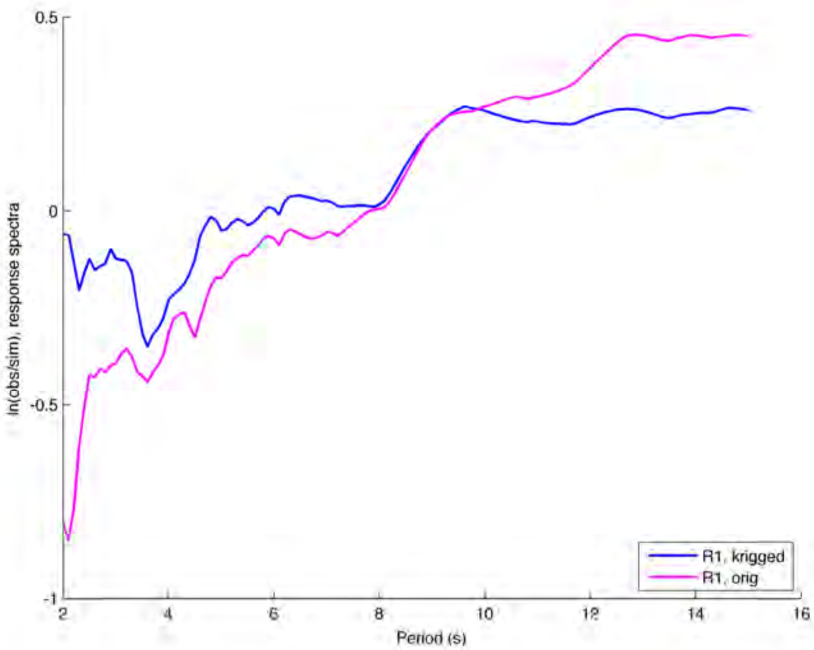

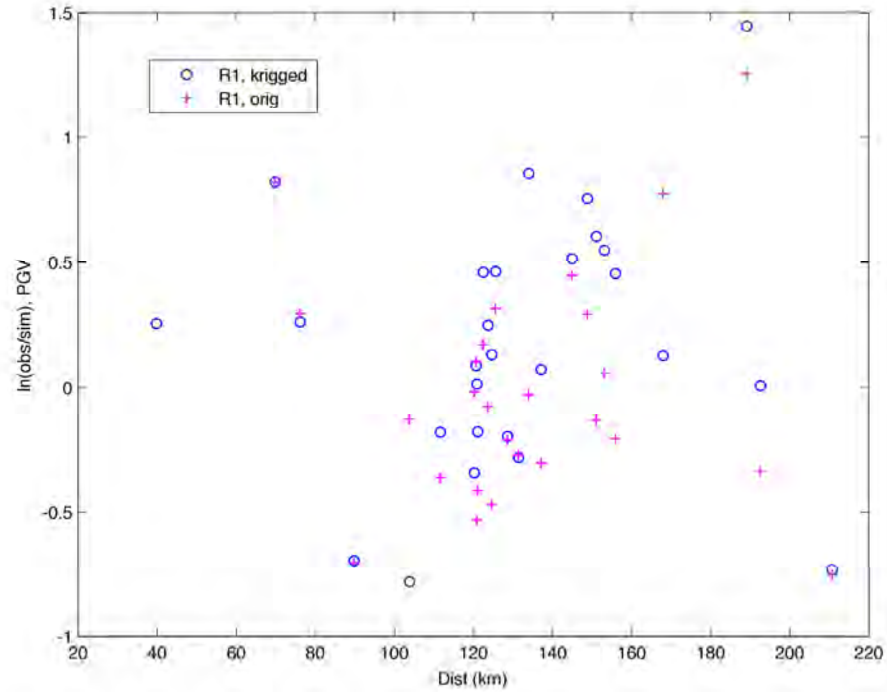

- 15% decrease in mean response spectra ratio
- 6% increase in mean PGV ratio

Testing effects of regional Vs models

5 km

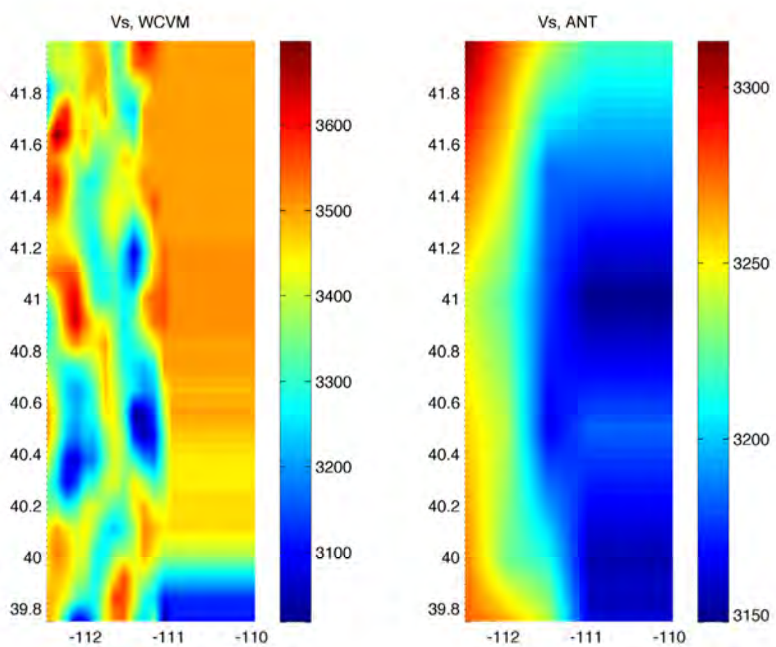

10 km

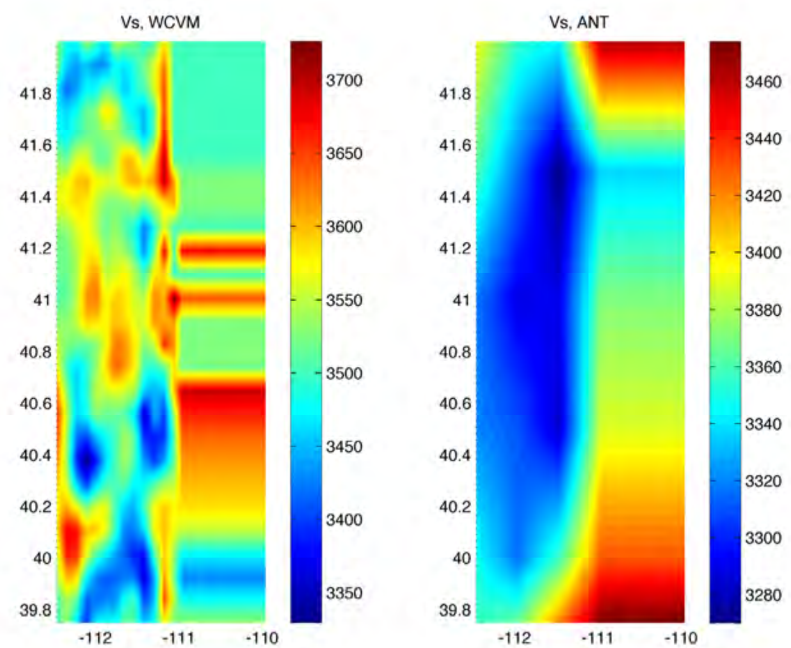

ANT Vs model

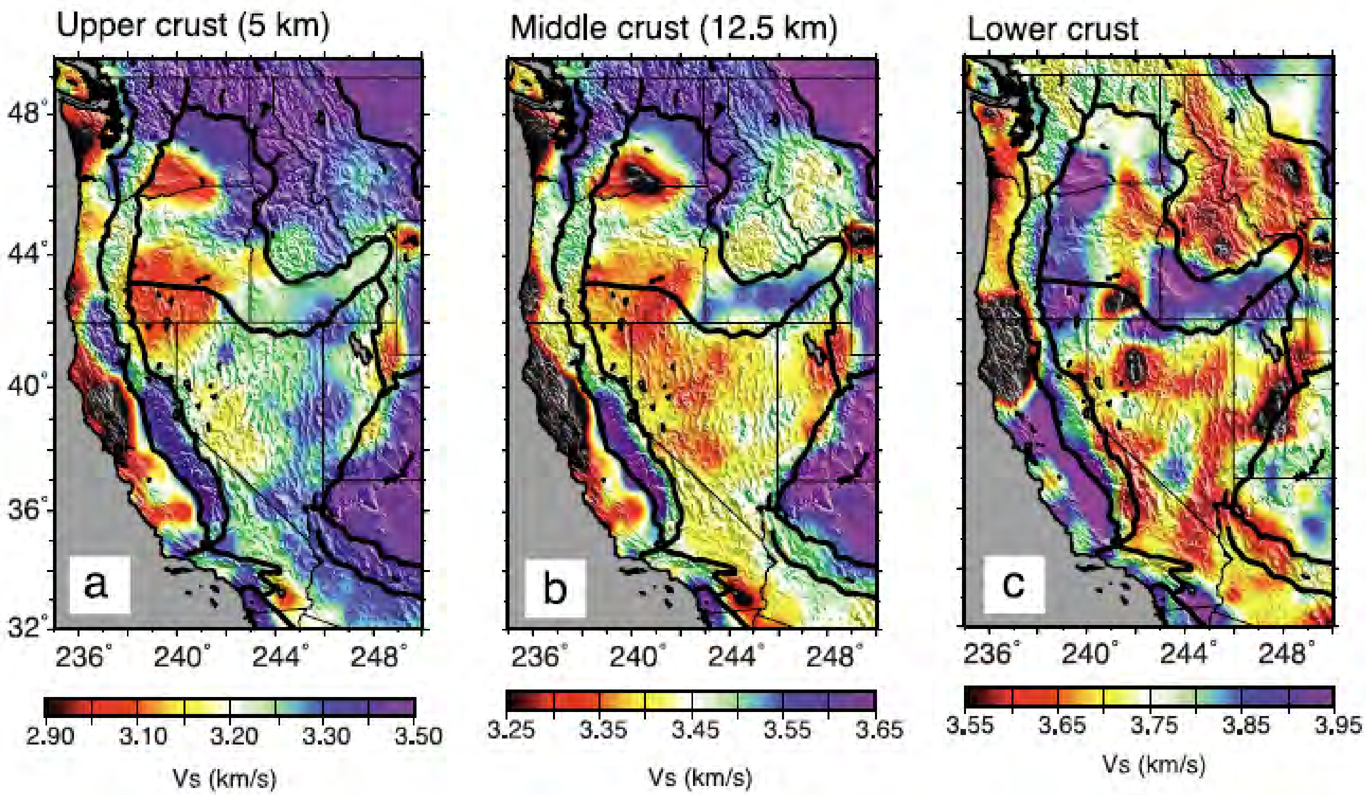

Moschetti et al. (2010) JGR

Randolph EQ simulation

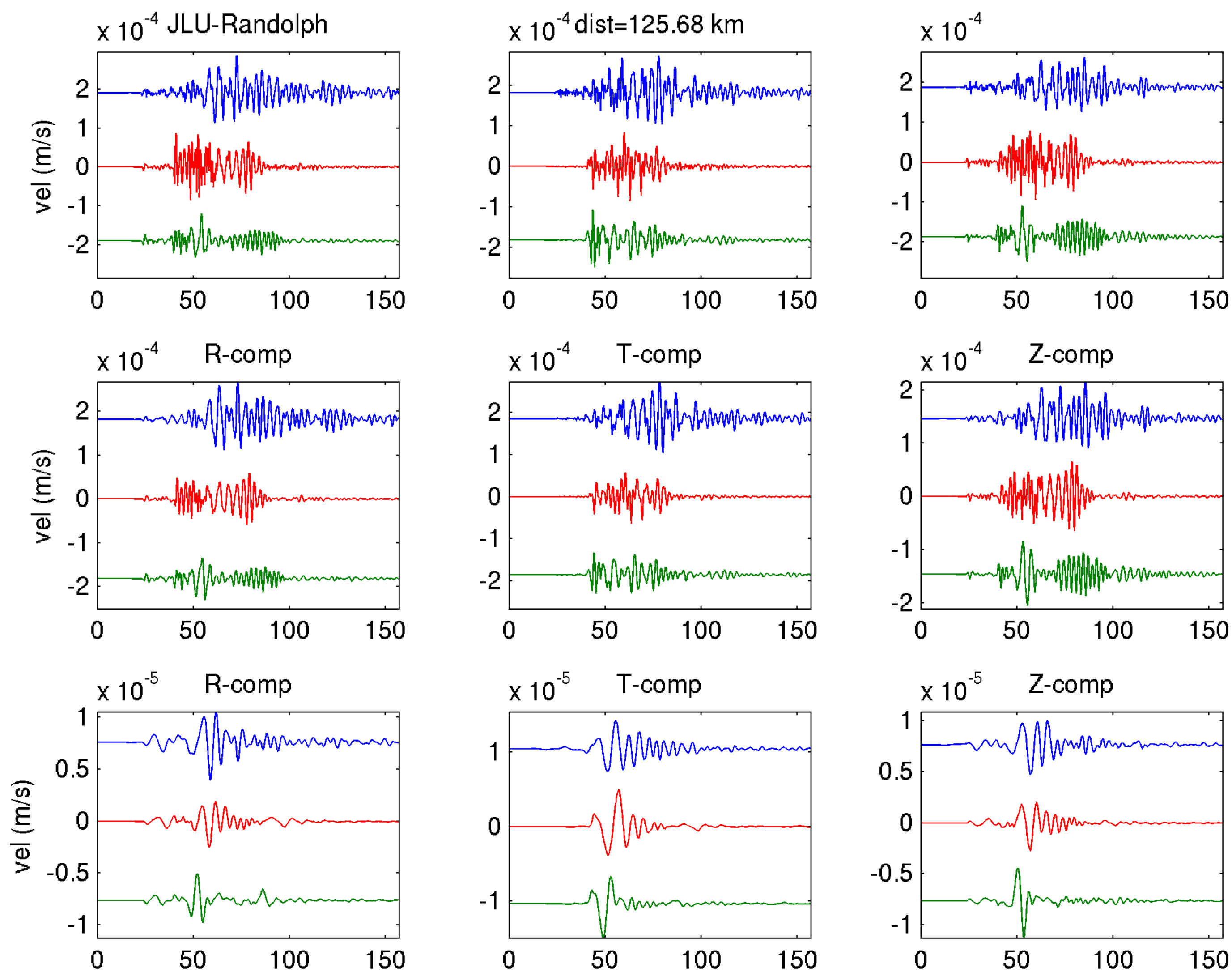

Ephraim EQ simulation

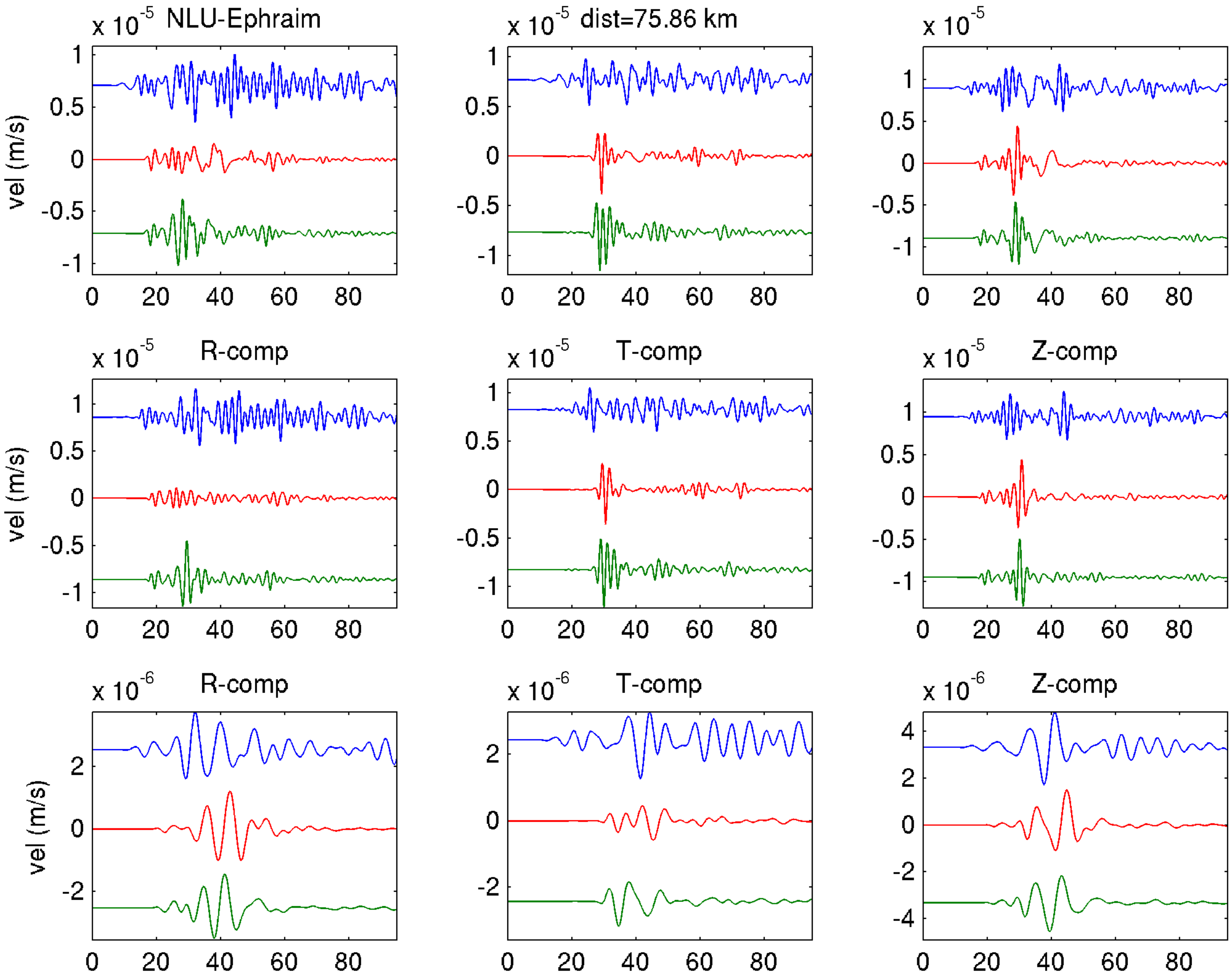

PGV comparisons – Regional Model

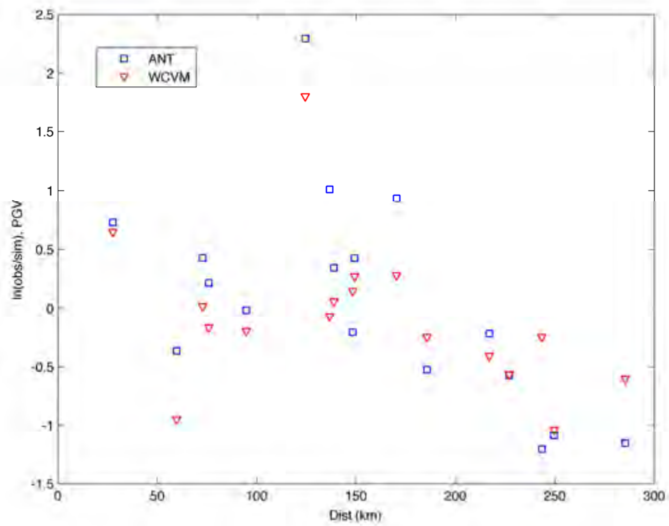

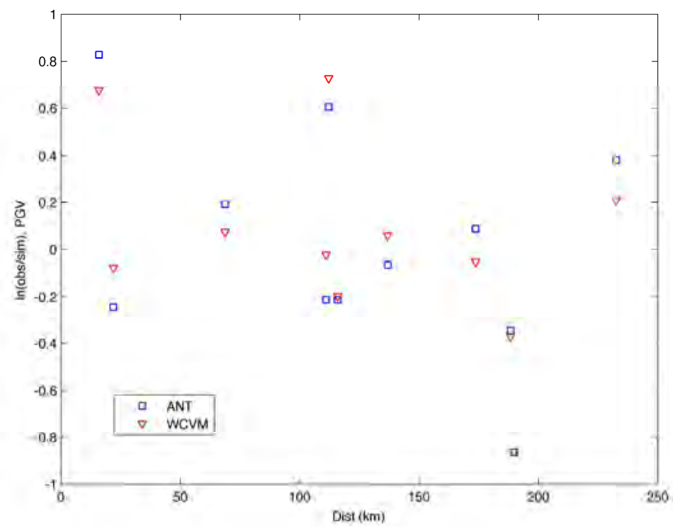

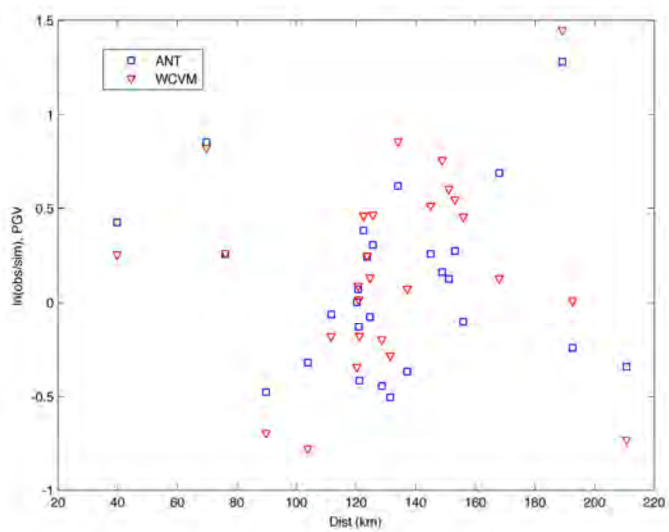

Effect on mean PGV of regional model:

- Ephraim: WCVM 40% better
- Randolph: ANT 11% decreased
- Tremonton: WCVM 8% better

Response spectra, changes in mean values with regional model testing

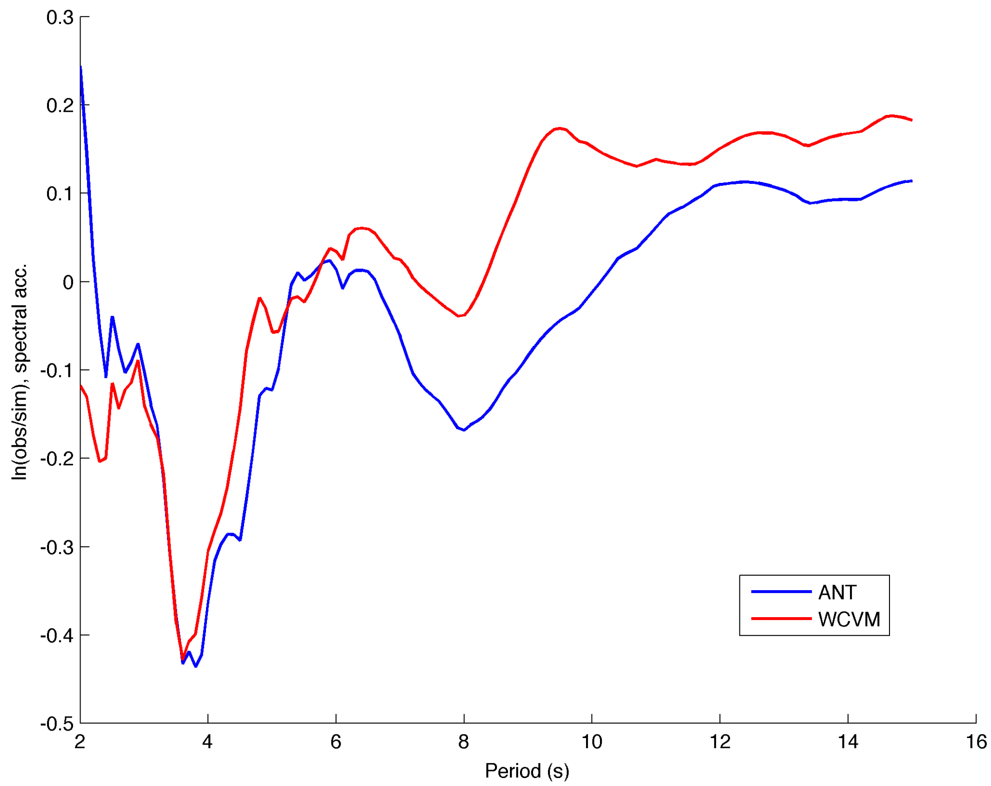

-Several percent decrease in mean response spectral value with ANT regional model

Testing effect of geotechnical layer (GTL)

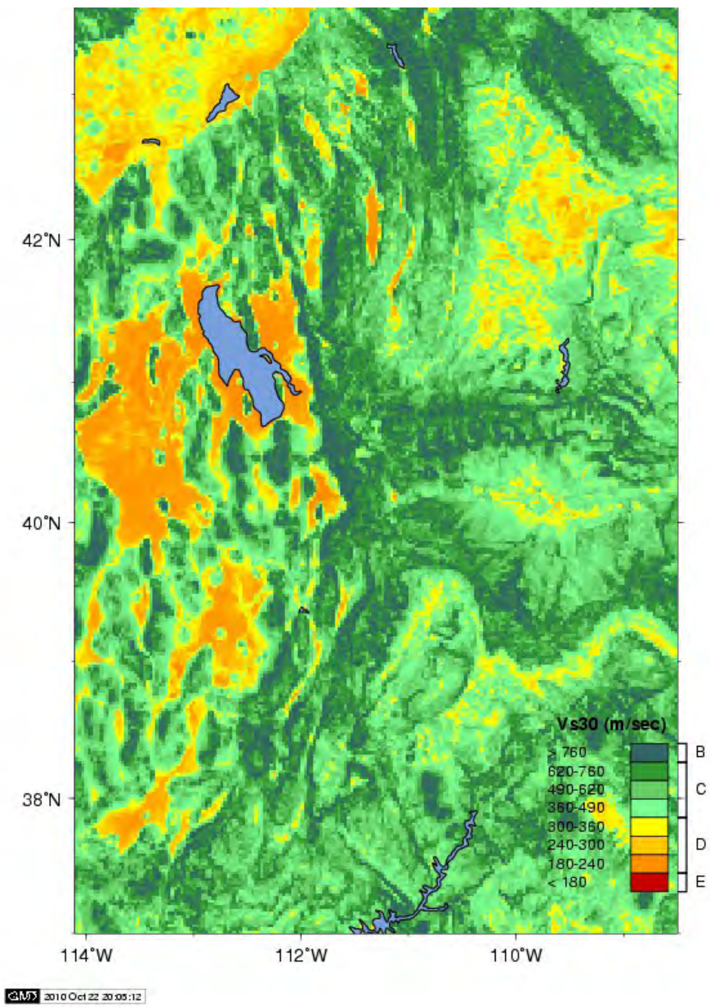

Allen and Wald-derived Vs30

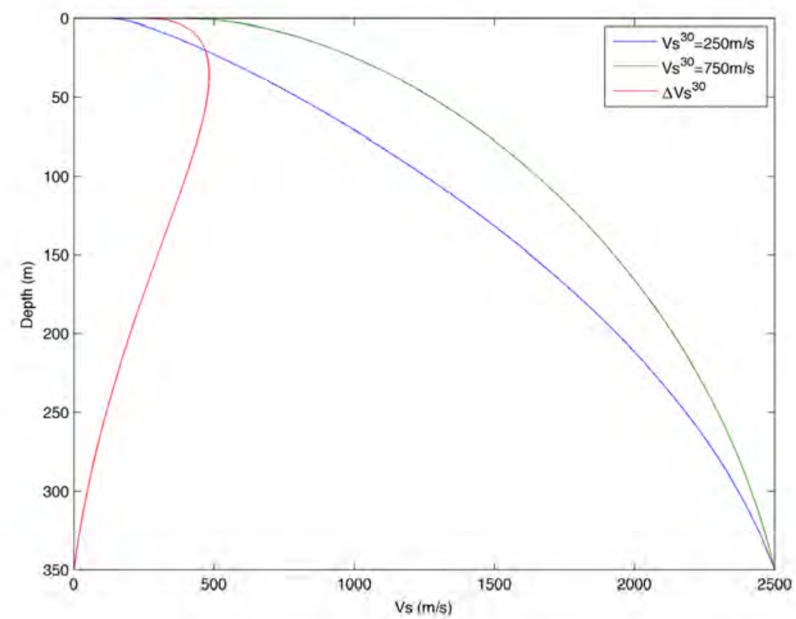

Method for generating GTL velocity profile is based on Ely et al. (2010)

Vs model comparison, 50 m depth

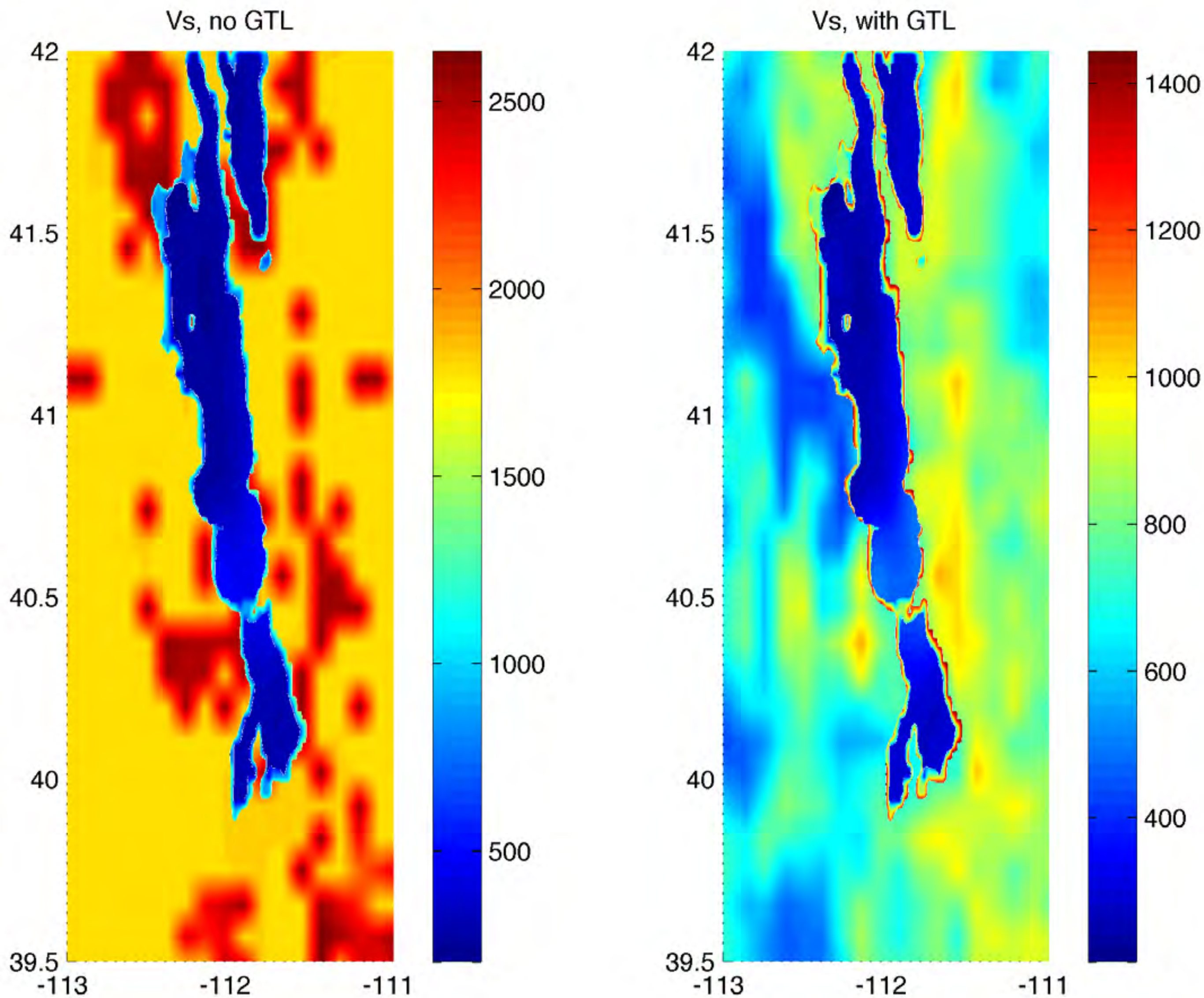

Response spectra ratios, GTL, Randolph EQ

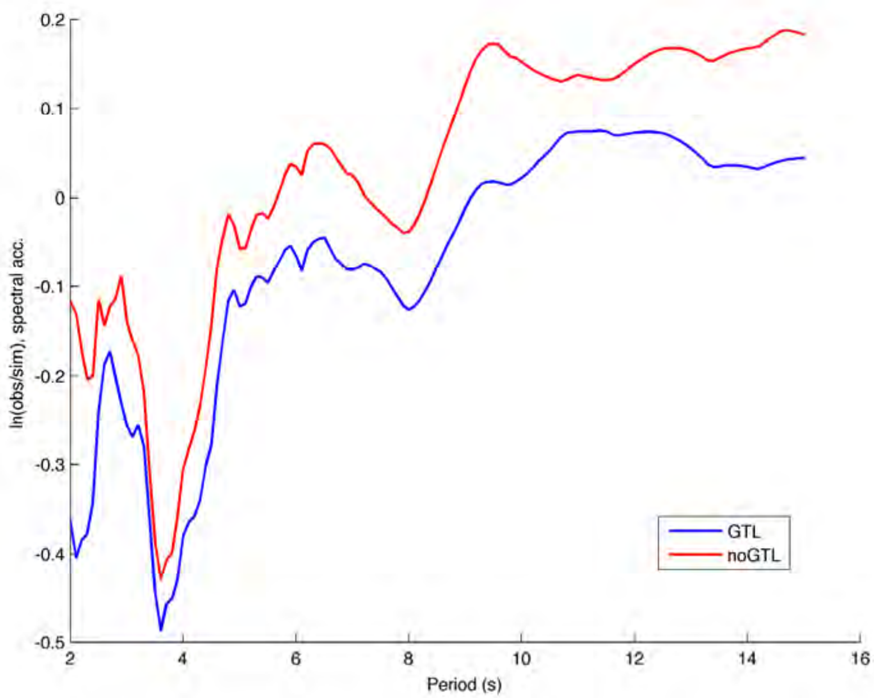

- Several percent improvement in mean response spectra ratio

PGV comparisons - GTL

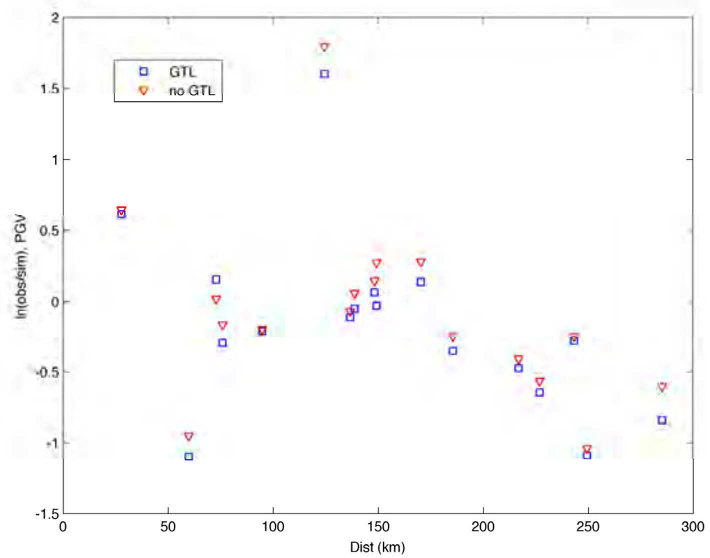

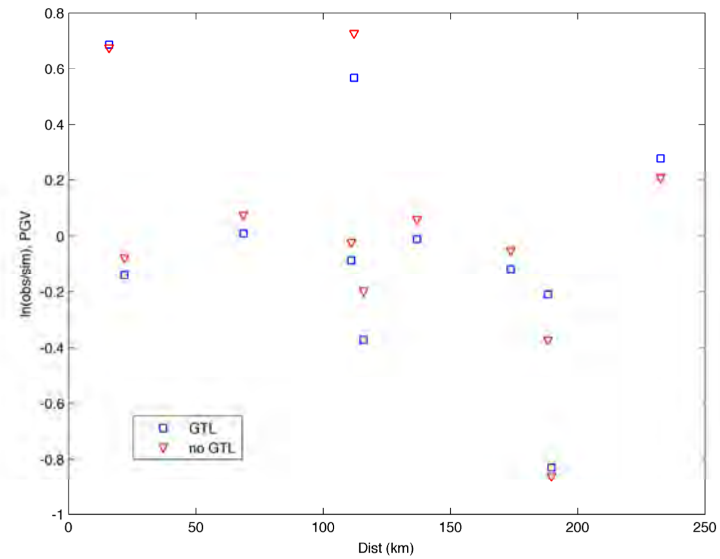

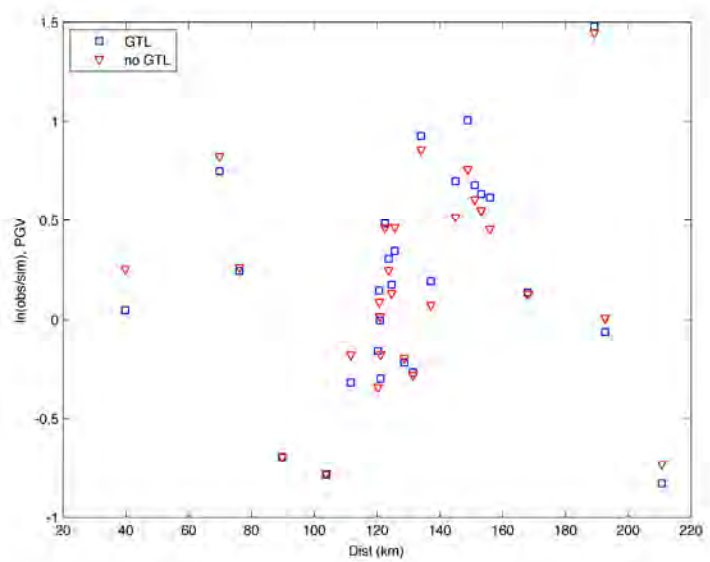

Effect on mean PGV of adding GTL:

- Ephraim: 3% increase
- Randolph: 5% decrease
- Tremonton: negligible

Changes to PGV with ANT Vs model

Ephraim

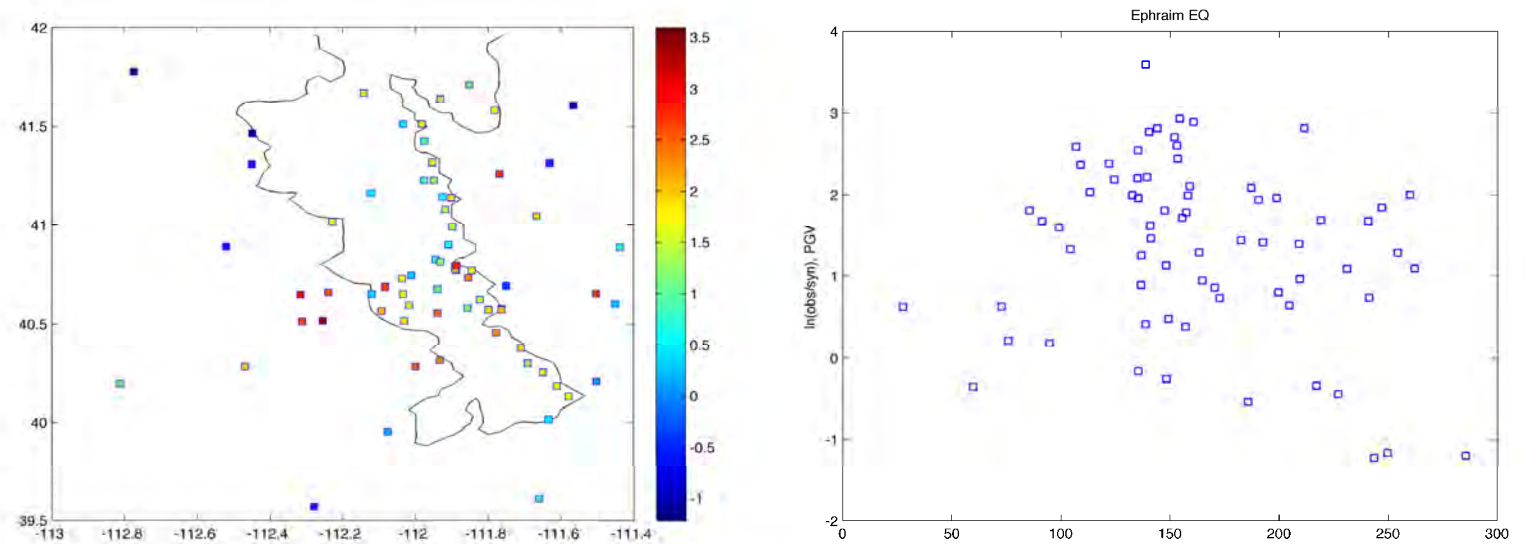

Randolph

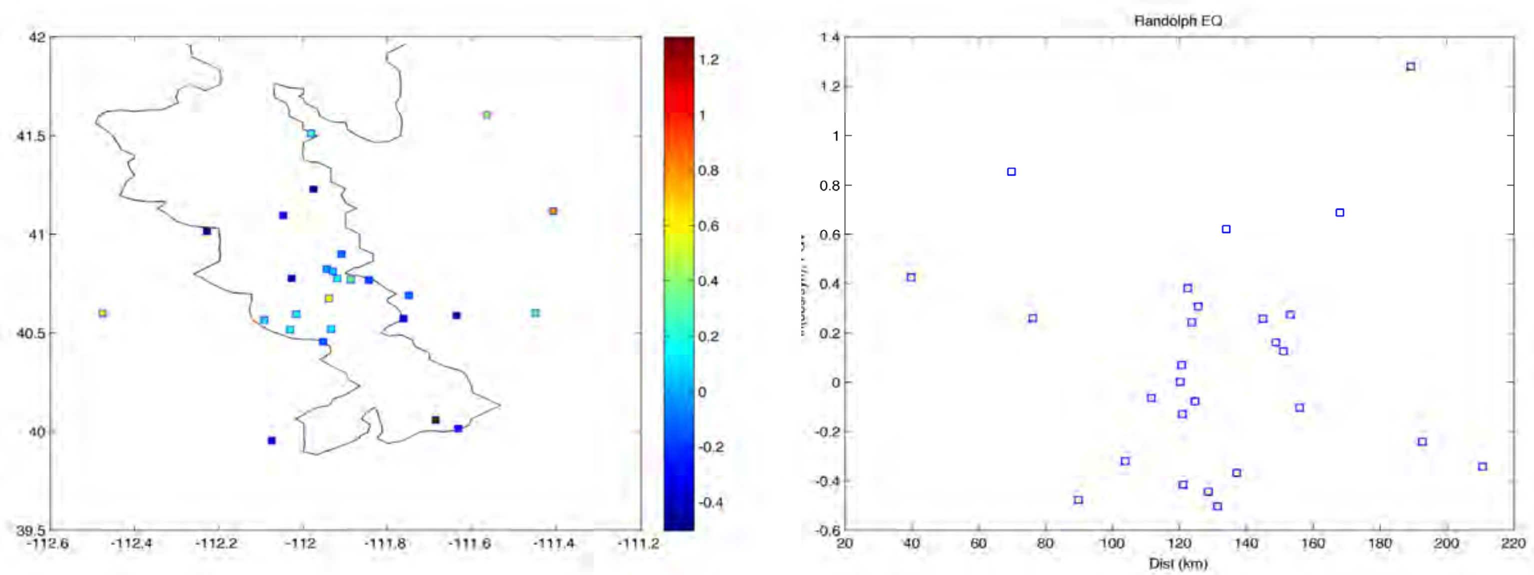

Perturbations to R3 volume

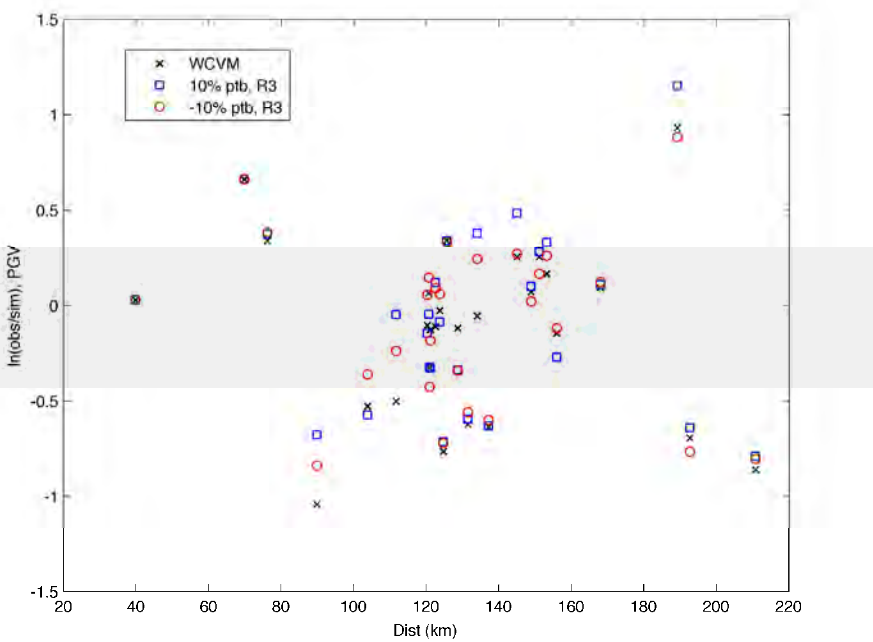

-1-Hz simulation, currently only for Randolph EQ

- +/- 10% perturbation to R3 volume

- PGV ratios identify those stations strongly affected by R3 – both negative and positive values.

Perturbations to R3 volume

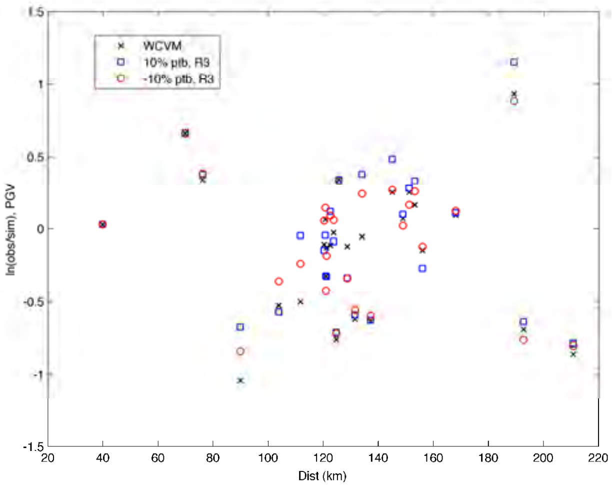

-1-Hz simulation, currently only for Randolph EQ
- +/- 10% perturbation to R3 volume
- PGV ratios identify those stations strongly affected by R3 – both negative and positive values.

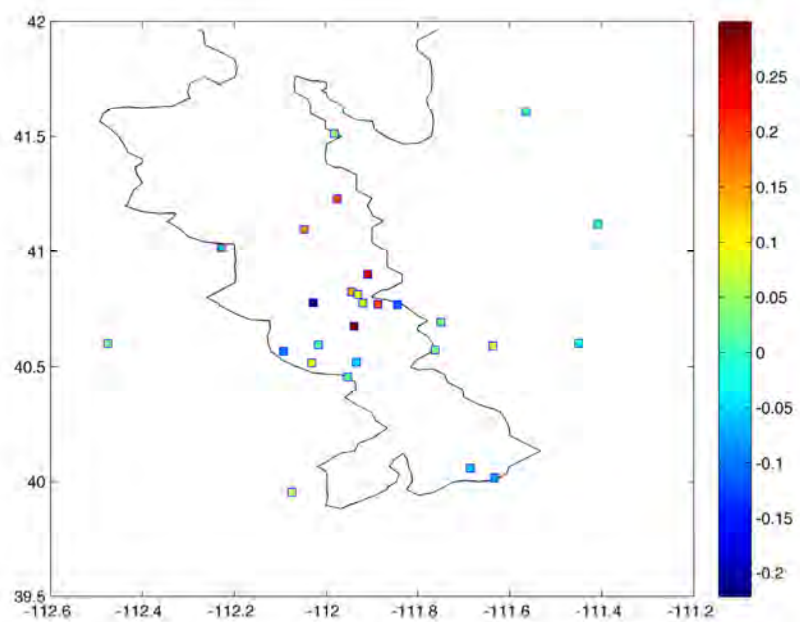

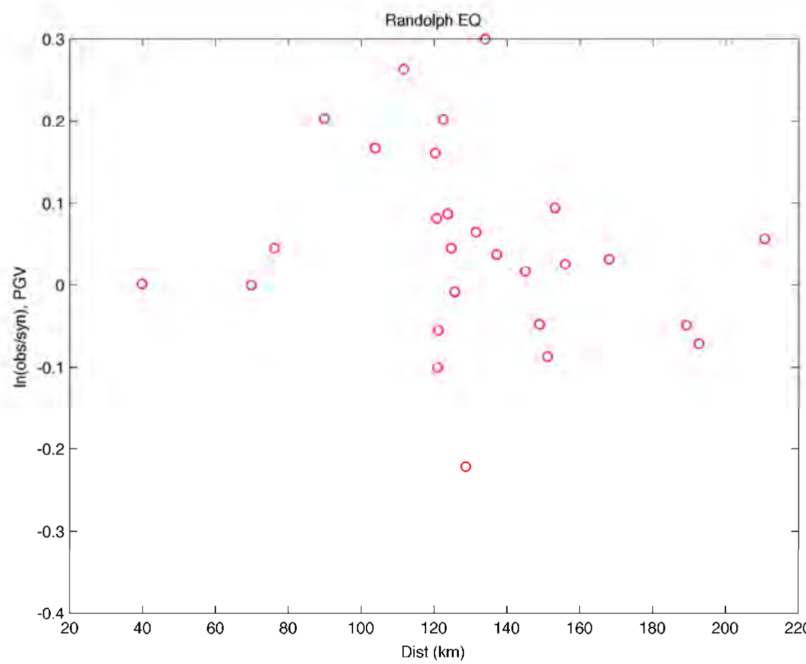

Future directions

- Continued sensitivity testing for simulations at 1-Hz – duration, PGV, PGA (from 1-Hz) simulations, spectral accelerations (1-Hz)
- Additional parameter tests
- Ground motion modeling – Salt Lake Segment of Wasatch Fault (kinematic models from UCSB and/or developed on SCEC platform)

Material model and source uncertainties

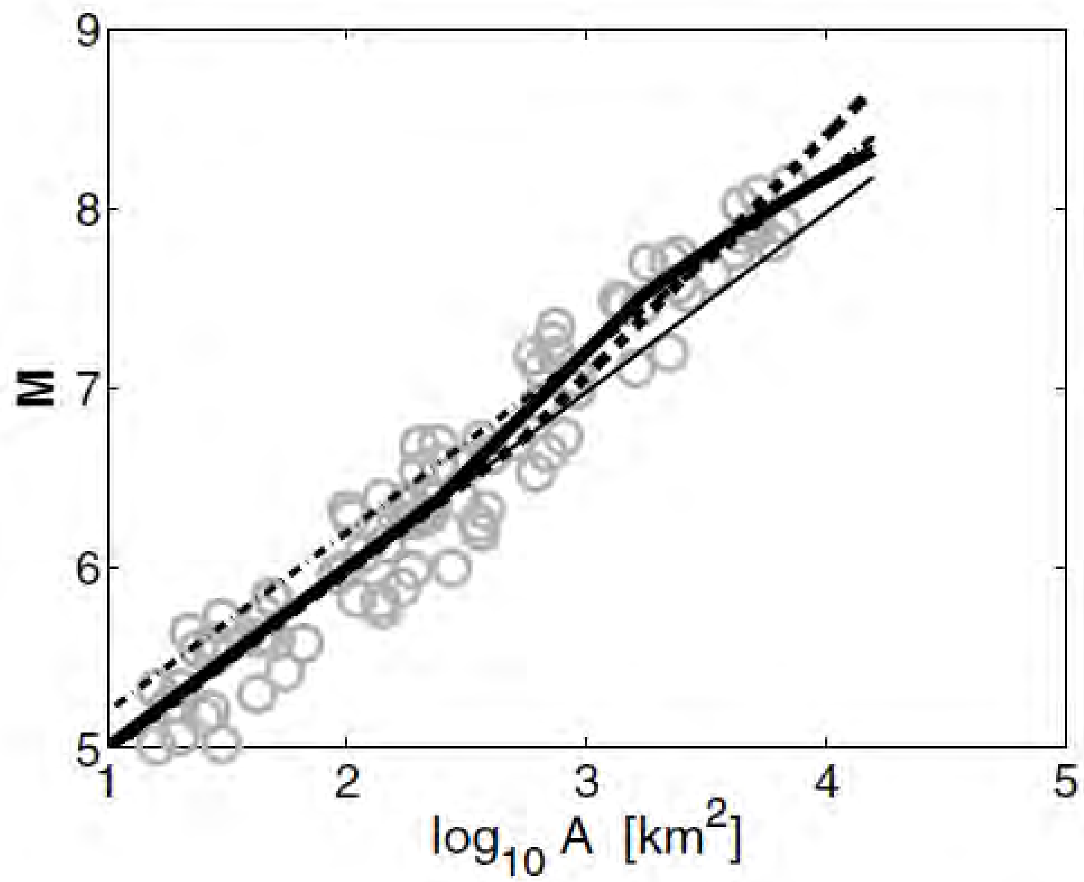

WCVM basin surfaces